Robust Controller for Delays and Packet Dropout Avoidance in Solar-Power Wireless Network

Waleed Al-Azzawi

This thesis is submitted in partial fulfilment
of the requirements of De Montfort University
for the award of Doctor of Philosophy

Faculty of Technology
De Montfort University, Leicester, UK
May 2013

Abstract

Solar Wireless Networked Control Systems (SWNCS) are a style of distributed control systems where sensors, actuators, and controllers are interconnected via a wireless communication network. This system setup has the benefit of low cost, flexibility, low weight, no wiring and simplicity of system diagnoses and maintenance. However, it also unavoidably calls some wireless network time delays and packet dropout into the design procedure. Solar lighting system offers a clean environment, therefore able to continue for a long period. SWNCS also offers multi Service infrastructure solution for both developed and undeveloped countries. The system provides wireless controller lighting, wireless communications network (WI-FI/WIMAX), CCTV surveillance, and wireless sensor for weather measurement which are all powered by solar energy.

The focus of this thesis proposes a SWNCS with stochastic wireless communication network time delay and packet dropout. The wireless communication network time delays and packet dropouts are varying in a stochastic approach. This stochastic approach of the wireless network time delays and packet dropouts are characteristic for commercially used wireless networks, such as Wi-Fi & WiMAX wireless networks. Models for stochastic wireless communication network time delays and packet dropouts are developed, using Markovian chains. Based on such a model, two novel methodologies for delays and packet dropout avoidance in SWNCS are established. The Robust Model Predictive Controller (RMPC) method for the SWNCS is discussed using the linear matrix inequality (LMI) technique. The time delays of the SWNCS are considered as stochastic variables controlled by a Markov chain. A discrete-time Markovian jump system with norm unbounded time delay is presented to model the SWNCSs. Based on the SWNCS model, the RMPC (a full state feedback controller) can be constructed via a set of LMIs. The efficiency of the proposed design is demonstrated by means of modeling and simulation. Further this thesis gives contribution by adding IEEE802.16e to the SIMULINK library of “TrueTime” for the SWNCS simulation techniques. A numerical example is given to validate the proposed control algorithm and to illustrate the effectiveness of the obtained results. Conditions for $H_\infty \; and \; H_2$ norms are used to evaluate stability and stabilization of the fundamental systems and are derived via LMIs formulation. Furthermore, an illustrative numerical example is given to demonstrate the effectiveness of the robust stability analysis.

Another method presented is a Neural Network Predictive Control (NNPC) technique for a SWNCS. A SWNCS model is created by using Back-Propagation Neural Network (BPNN). A learning algorithm adopting an adaptive learning rate approach is used to identify the stochastic time delays in BPNN. The performance of the NNPC controller is based on minimization of the Mean Square Error (MSE). A numerical example is given to demonstrate the effectiveness of the proposed method. Further, the SWNCS based NNPC simulation techniques using MATLAB/SIMULINK are carried out to validate the proposed control algorithm.

The simulation results demonstrate that the proposed design methodologies can achieve the prescribed performance requirements.

Acknowledgements

First of all, my first debt of gratitude must go to Allah and my supervisor, Prof. Marwan Al-Akaidi. He patiently provided the vision, encouragement and advice necessary for me to proceed through the PhD program and complete my thesis. It is difficult to overstate my gratitude to my Ph.D. supervisor, Prof. Marwan Al-Akidi. With his enthusiasm, his inspiration, and his great efforts to explain things clearly and simply, he helped to make mathematics fun for me. Throughout my thesis-writing period, he provided encouragement, sound advice, good teaching, good company, and lots of good ideas. I would have been lost without him. I want to thank Prof. Marwan for his unflagging encouragement and serving as a role model to me as a junior member of academia. He has been a strong and supportive adviser to me throughout my PhD study.

I am grateful and thank all of those who assisted me in my PhD study at faculty of technology.

Also I would like to thank the Iraqi Ministry of Higher Education and scientific Research for granting a PhD Scholarship.

Most importantly, I would like to thank my family (mother, father, brothers, wife, and my sons) and friends for their support throughout all the years.

Contents

List of Tables

List of Figures

Abbreviations and acronyms

SWNCS	Solar Wireless Network Control System
Wi-Fi	Wireless Fidelity
WiMAX	World-wide Interoperability for Microwave Access
RMPC	Robust Model Predictive Control
LMIs	Linear Matrix Inequalities
NNPC	Neural network Predictive Control
BPNN	Back-Propagation Neural Network
MSE	Mean Square Error
WNCS	Wireless Network Control System
QoS	Quality of Service
ZOH	Zero-Order-Hold
WLANs	Wireless Local Area Networks
APs	Access points
OFDM	Orthogonal Frequency Division Multiplexing
TDD	Time Division Duplex
FDD	Frequency Division Duplex
MANs	Metropolitan Area Networks
BWA	Broadband Wireless Access
MPC	Model Predictive Control
LED	Light Emitted Diode
MJLS	Multi Jump Linear System
NCS	Network Control System
SRM	Static Rate Monotonic
DFS	Dynamic Feedback Scheduling
HMM	Hidden Markov Model
PID	Proportional-Integral-Derivative
SMPC	Stochastic Model Predictive Controller
RTD	Round Trip Delay

MIMO	Multi Input Multi Output
RNN	Recurrent Neural Network
ALR	Adaptive Learning Rate
RBFNN	Radial Basis Function Neural Network
RTT	Round Trip Time
PoE	Power-over-Ethernet
CAN	Controller Area Network
AQM	Active Queue Management
IP	Internet Protocol
TCP	Transmission Control Protocol
UPD	User Datagram Protocol
SNR	Signal to Noise Ratio
BLER	Block Error Ratio
MAC	Medium Access Control
AGN	Additive Gaussian Noise
ISI	Inter symbol Interference
RRC	Root Raised Cosine
ADC	Analogue-to-Digital Converter
DAC	Digital-to-Analogue Converter
CSMA/CD	Carrier sense Multiple Access with Collision Avoidance
CSMA/AMP	Carrier sense Multiple Access with Arbitration on Massage Priority

List of Publication

1. Waleed Al-Azzawi, Marwan Al-Akaidi,” **Modelling and Simulation of Solar Wireless Network Control System Based on Robust Model Predictive Controller”,** *Proceeding 10th MESM Conference*, Al-Exandria, Egypt, 1-3 December, 2010.
2. Waleed Al-Azzawi and Marwan Al-Akaidi,” **Solar-Powered Wireless Network Control System Based on “TRUE-TIME” Simulator”,** *Proceeding of 11th Salford Postgraduate Annual Research Conference*, University of Salford, UK, 8 and 9 June 2011.
3. Waleed Al-Azzawi, Marwan Al-Akaidi,” **Simulation Methods for Delays and Packet Dropout Avoidance in Solar-Power Wireless Networks”,** *Proceeding 11th MESM Conference, Amman, Jordon,* November 14-16, 2011.
4. Waleed Al-Azzawi, Marwan Al-Akaidi,” **Robust Stability of Solar-Power Wireless Network Control System with Stochastic Time Delays Based on H_2 Norm”,** *Proceeding of 1st IET Wireless Sensor System Conference,* 18 - 19 June 2012, RIBA, London, UK.
5. Waleed Al-Azzawi, Marwan Al-Akaidi, “**Robust Stability of Solar-Power Wireless Network Control System with Stochastic Time Delays Based on H_∞ Norm**”, *Taylor & Francis Group, International Journal of Systems Science,* DOI: 10.1080/00207721.2013.801092, 28 May 2013.
6. Waleed Al-Azzawi, Marwan Al-Akaidi,” **Robust Model Predictive Controller for Solar Wireless Network Control System”,** *Journal of Intelligent Learning Systems and Applications (JILSA), Accepted 12 September 2012.*
7. Waleed Al-Azzawi, Marwan Al-Akaidi,” **Solar Wireless Network Control System Based on Neural Network Predictive Control”,** *Submitted to European Journal of Control*, 3 May 2012.

CHAPTER 1 ..
INTRODUCTION

1.1 INTRODUCTION TO SOLAR WIRELESS NETWORK CONTROL SYSTEM (SWNCS)

The point-to-point structural design is the conventional communication construction for control systems, that is, sensors and/or actuators are connected to controllers through wires. In recent years, because of the growth of physical setups and functionality, a conventional point-to-point structural design is no longer able to meet new requirements, such as modularity, integrated diagnostics, quick and easy maintenance, and low cost. Such requirements are particularly demanding in the control of complex control systems [1- 3] and remote control systems [4-7]. To satisfy these new requirements, SWNCS architectures have been introduced. The SWNCS architectures can improve the efficiency, flexibility and reliability of integrated applications, and reduce installation, reconfiguration and maintenance time and costs. In recent years, thus, it gives rise to the so-called wireless network-based control systems, or Wireless Networked Control Systems (WNCSs) [8-12].

In general, SWNCSs are a form of distributed control systems where sensors, actuators, and controllers are interconnected through wireless communication networks which are powered by solar energy as shown in Figure 1.1. Sensors compute states of the plant and transmit these states over the wireless communication network to controllers. The controllers receive these states, and compute suitable control signals and send them to actuators over the wireless communication network. Actuators receive control actions and control the plant suitably. Many benefits which can be offered by SWNCS, such as simple installation and maintenance, low cost, no wiring, flexibility, clean environment, and high reliability. Therefore the SWNCS is appropriate to many applications, for examples, remote process control, altitude measurement for airplane and manufacturing automotive [2].

It can be seen from the block diagram in Figure 1.1 that in SWNCSs the closed-loops are closed via wireless communication networks. The insertion of the wireless communication network in the feedback control loop makes the analysis and design of systems more complex than the conventional point-to-point structural design. The wireless network can establish undependable and time-dependent levels of service in terms of, for example, time delays, jitter, or packet dropouts. Quality-of-Service (QoS) can improve the real-time wireless network performance, but the wireless network performance is still subject to interference, routing transients, to aggressive flows. It is also noteworthy that protocols providing QoS are not common in all industrial networks [13].

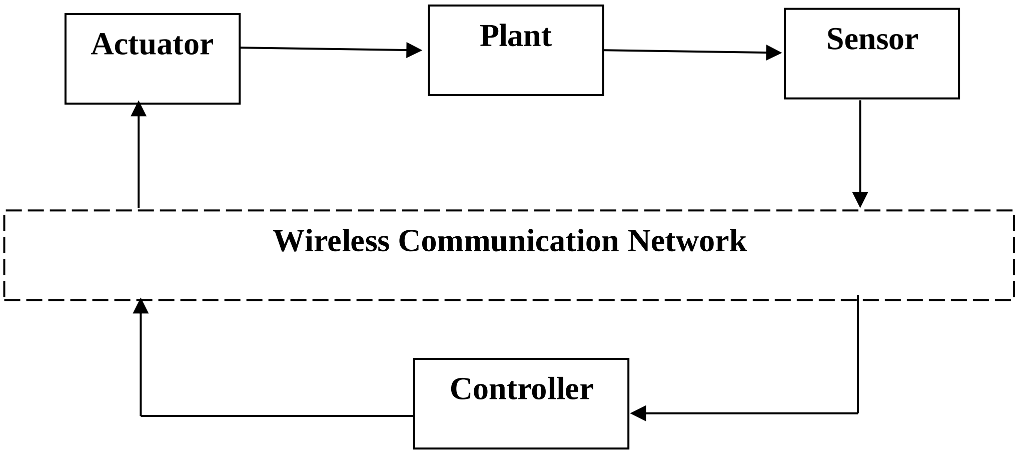

Fig.1.1. Typical Setup of Wireless Network Control System

1.2 FUNDAMENTAL ISSUES IN SWNCS

The following two issues are the most challenging problems with SWNCSs that require to be correctly addressed to guarantee the stability and performance of the closed-loop systems.

1.2.1 Network Time Delay

The first issue is the network time delay, counting sensor-to-controller (forward channel) delay and controller-to-actuator (feedback channel) delay, which occurs when data swap occurs among devices linked by the wireless communication network, which will deteriorate the system performance as well as stability. This time delay, depending on the wireless network characteristics for example network load, topologies, routing schemes, etc., can be constant, time varying, or even random.

Network time delays can vary extensively according to the transmission time of data and the overhead time. The network time delay in SWNCSs takes place when sensors, actuators, and controllers exchange data across the wireless network. In general, the controlled plant in Figure 1.1 is assumed to be continuous-time, and therefore the actuator implements zero-order hold (ZOH), holding the last control signal until the next one arrives or until the next sample time. Since networks are employed for transmitting the calculations from the plant output to the controller, the plant has to be sampled (sample time h), which motivates the use of discrete-time controllers. SWNCS are distributed real-time control systems consisting of the plant, sensors, controllers, actuators, and a shared data wireless network that is employed for communication between the elements of the system. A universal SWNCS design is described in Figure 1.2. The controller may be physically located in a different location from the plant, actuators and sensors, resulting in a distributed control system. The controller can be time-driven or event-driven, so it can compute the new control signal at discrete time instants with a constant sample time or it can compute the control signal immediately once it gets a new measurement from the sensor. Further, the actuator can be time or event-driven. The network time delays in the signals: τ_k^{sc}in Figure 1.2 indicate the sensor-to-controller delay and τ_k^{ca} the controller-to-actuator delay at time k.

1.2.2 Network Packet Dropouts

As mentioned above the first issue, now we must consider the second issue which is the data packet dropouts. In the SWNCS, data is transmitted via the wireless network in packets. Due to this wireless network characteristic, any continuous-time signal from the plant is first sampled to be carried over the wireless communication network. It is possible that those packets can be dropped during transmission because of uncertainty and disturbance in wireless communication channels. It may also happen at the destination when out of order delivery takes place. It is straightforward to study that the hardness of the wireless network time delays is aggravated when data packet dropouts happen during a network transmission. Additionally, in the case of multiple-packet transmission, chances are that part of the packets could reach your destination by the time of control computation, which creates the analysis and control of SWNCS harder, if not impossible.

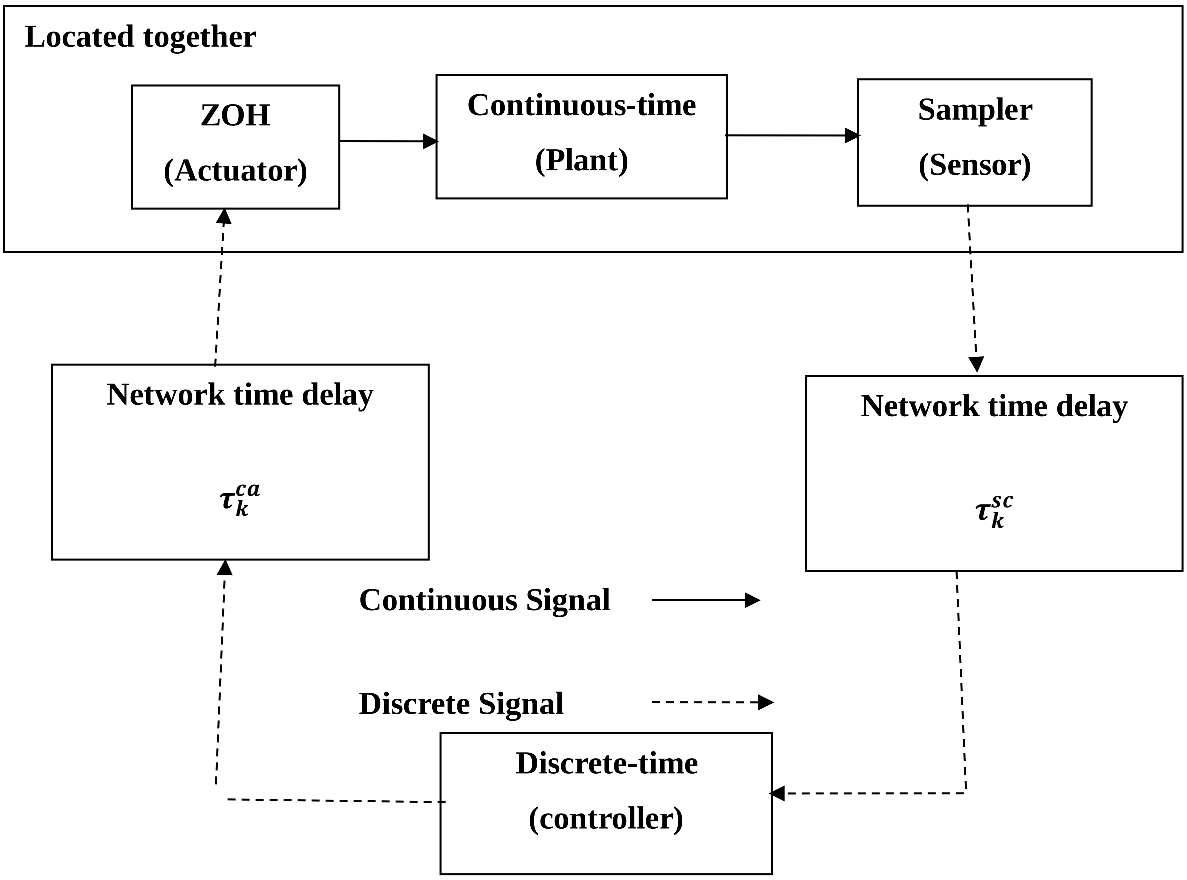

Fig.1.2. SWNCS Model

The timing mechanism plot of this type of construction of SWNCS is illustrated in Figure1.3. we assumed that each data can arrive at its destination within one sampling period $T_s = t_k - t_{k-1}$, that is, wireless network time delay τ_{k-1}^{sc} and τ_k^{ca} is less than T_s. The process of the SWNCS which is runs as follows. At the previous time instant t_{k-1}, the response signal *x(t)* is calculated by a clock-driven sensor.(This is highlighted in green colour on the timing plot below. The sampled signal arrives at the ZOH at the controller side at time $t_{k-1} + \tau_{k-1}^{sc}$. The controller is also clock-driven and at time t_k it creates a control action using the most recently arrived signal. This control action is received by the ZOH at the actuator side after τ_k^{ca} will be held awaiting the new control action (blue one) which arrives at the instant $t_{k+1} + \tau_{k+1}^{ca}$. Which means a control action is held for the period $(t_k + \tau_k^{ca}, t_{k+1} + \tau_{k+1}^{ca})$. We can also learn from the system formulation that the system includes both continuous-time and discrete-time signals, where a hybrid methodical synthesis approach is needed.

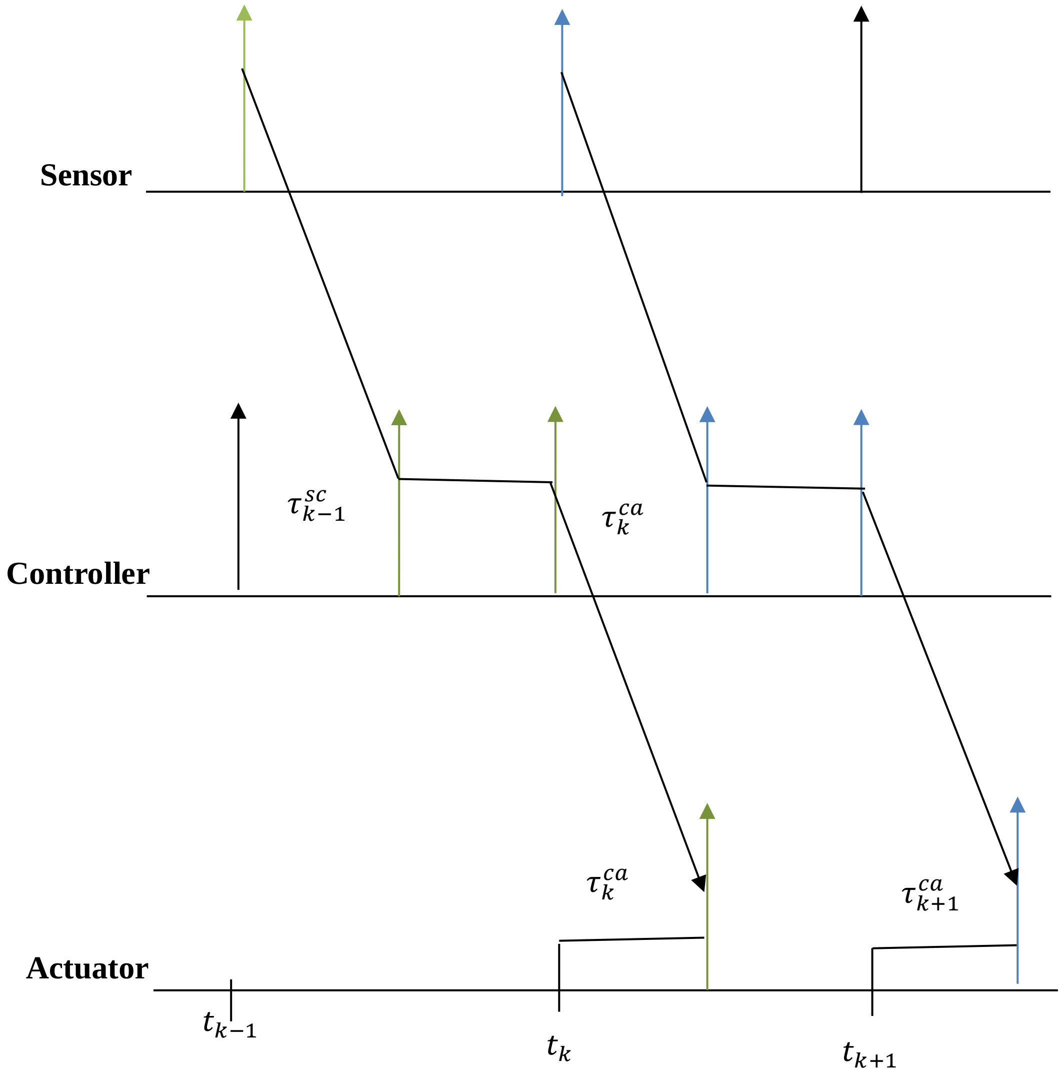

Fig.1.3. Timing Mechanism Plot of a SWNCS

1.3 WIRELESS NETWORK ACCESS

Wireless technology has helped to simplify networking by enabling multiple computer users to simultaneously share resources in a home or business without additional or intrusive wiring. Wireless network access techniques are continuously expanding their transmission bandwidth, coverage, and QoS support. With the huge market success of Wireless Local Area Networks (WLANs) governed by the Wi-Fi standard, the new generation wireless technique, WiMAX, has now been standardised and deployed [14-17]. The following sections provide detailed information on Wi-Fi & WiMAX.

1.3.1 Wi-Fi Access Point

Wi-Fi is a brand of the Wi-Fi Alliance (Wireless Ethernet Compatibility Alliance), which is in charge of testing and certifying the interoperability of devices based on the IEEE 802.11 standard. Wi-Fi permits Access Points (APs) a coverage radius, or hotspot, of approximately 100m in interior spaces. Meanwhile, Wi-Fi external coverage can cover a radius of approximately 300m, depending on environmental conditions [18]. The transmission speed of the various Wi-Fi standards ranges from 11Mbps to 54Mbps [19]. Wi-Fi offer many benefits for example; its use of a non-licensed frequency band, its less international regulatory constraints, its infrastructure less structural design that allows for ubiquitous functioning and dynamic growth, its low cost, and its mobility without network connection breaks. Meanwhile, Wi-Fi difficulties include; its use of the 2.4GHz spectrum, which is susceptible to interference and its higher energy consumption when compared to other standards.

1.3.2 WiMAX Access Point

WiMAX is stand for Worldwide Interoperability for Microwave Access and its architecture is based on broadband point-to-multipoint wireless access. WiMAX was produced in 2001 to endorse the IEEE 802.16 standard. This standard was finally approved in June 2004 [20]. The 802.16 standard relates for fixed and mobile WiMAX in 802.16d and 802.16e, respectively [21]. Several significant characteristics of WiMAX comprise: its use of the microwave frequency band for wireless data transmission, its high transmission speed over long distances, its use of OFDM (Orthogonal Frequency Division Multiplexing) to enable non-line-of-sight communication, its multi-channel support for TDD (Time Division Duplex) and FDD (Frequency Division Duplex), its flexible treatment with channels in the 3.5MHz, 5MHz and 10MHz frequencies. While, challenges for WiMAX comprise: reaching a coverage area of up to 10 miles providing wireless broadband and consecrated links, making the technology more reasonable and permitting access from more remote areas.

1.3.3 Wi-Fi vs. WiMAX

Wi-Fi or WLAN is the name with which the IEEE 802.11 standard-based products are recognised. It comprises the 802.11a requirement, able to present data rates of 54 Mbps working in the frequency band of 5.2 GHz; and the 802.11b requirement, in the 2.4 GHz frequency band, which provides clients with data rates of 11 Mbps. This technology has usually a coverage area of 100 meters and fixed channel bandwidths of 20 MHz [18]. WiMAX fulfils the need for delivering wireless access to Metropolitan Area Networks (MANs). It was designed to present Broadband Wireless Access (BWA) services to metropolitan areas providing clients with larger coverage ranges and higher data rates. WiMAX systems are capable of supporting clients in ranges up to 50 km with a straight visibility to the base station and ranges from 1 to 7 km where no visibility is available. Rates from 70 to 240 Mbps are presented and can be accomplished with this technology. However, there is no contradiction between WiMAX and the mentioned Wi-Fi, because they are complementary technologies. WiMAX offers a low cost way to backhaul Wi-Fi hot-spots and WLAN points in businesses and homes, presenting a wireless last mile extension for wire and DSL infrastructures. Table.1.1 gives an overview on the comparison between the Wi-Fi and WiMAX.

Table 1.1. Overview Comparison between Wi-Fi and WiMAX

Specification	Wi-Fi	WiMAX
Standard	**IEEE802.11**	**IEEE802.16**
Channel Width	**Fixed 20MHz**	**Variable ≤ 20MHz Variable ≤ 28MHz**
Spectrum	**2.4/5.2GHz**	**2-11GHz 10-66GHz**
Data rate	**2/54Mbps**	**70Mbps 240Mbps**
Range	**100meter**	**1-7kilometer 12-15kilometre**
Multiplexing	**TDM**	**FDM/TDM FDM/TDM**
Transmission	**SS[15]/OFDM**	**OFDM/OFDMA SC**
Mobility	**Pedestrian**	**Vehicular no**
Benefits	**Throughput and costs**	**Throughput and range**
Challenges	**Short range**	**Interference issues**

1.4 ROBUST CONTROL THEORY

Robust control can be defined as designing a controller such that certain behaviour of the controlled system is obtained cater for variations in the process dynamics within a predetermine period. Consider a simple representation of a controlled system in Figure 1.4. The controller block Gc is to be calculated as the subsequent targets and conditions can be recognised in a certain optimum methods [22]:

- Stability: the feedback control system must be stable
- Tracking: the actual output C must track the input signal R
- Disturbance elimination: the output C must be free of the effects of noise.
- Measurement (sensor) noise elimination: the noise presented by the measuring device (sensor) must not influence the output C.
- Escaping of actuator overloads: the actuator, not obviously haggard at this point, occupied the main part of process G, but must not to be overloaded however has to work as a direct transmission.
- Robustness: if the actual dynamics of the process alter by a quantity ΔG, the behavior of the scheme, namely completely preceding desiderata, must not worsen to an unsatisfactory stage.

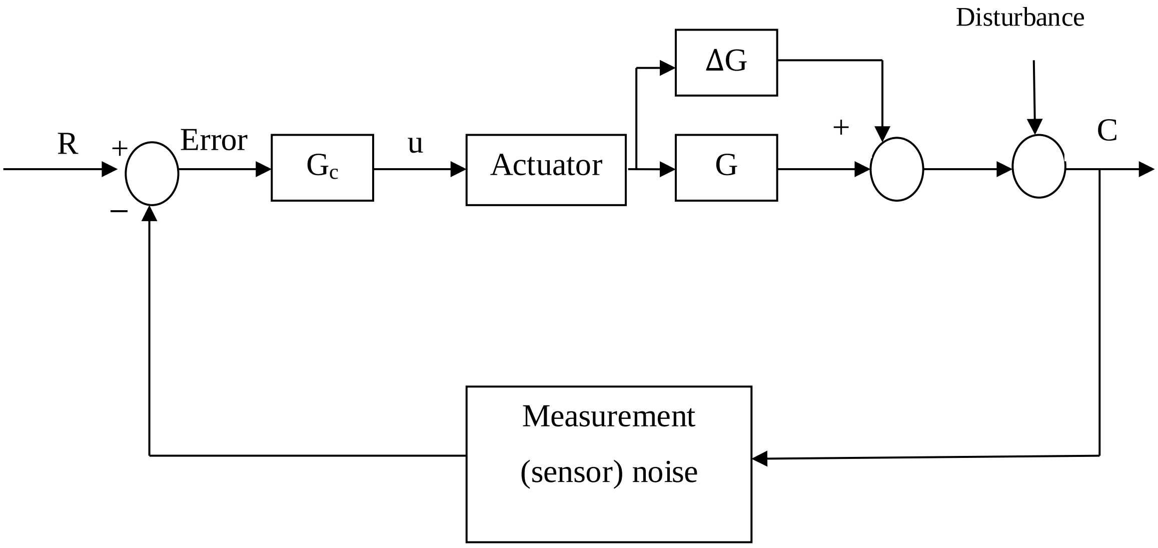

Fig.1.4. Elementary Block Diagram Structure of a Controlled System

It can be described how several constraints place same requests on the controller G_c, though others need inconsistent activities, and as an outcome the last controller can be only a form of cooperation. To that drive it is significant that we can calculate the several objects and thus weight all requests in contrast to the others. In such a case, applying a higher weight on a certain constraint will inevitably cause the robustness attached to the other realisable constraints to deteriorate [23]. The behavior must not only hold for an actual exact process G, wherever the control action can be adjusted exactly for different dynamics. The correct process kinetics is at that moment assumed by

$$\boldsymbol{G_t = G + \Delta G} \ldots\ldots\ldots (\mathbf{1-1})$$

Where, at the present G proceeds the purpose of the nominal model though ΔG characterises the incremental model disturbance. There is no manner to evade ΔG in view of the following reasons.

- **Unmodelled kinetics**: the nominal process G will be usually occupied by linear, time invariant and of minimum action. In this case, the actual performance is automatically approximated. However, actual processes cannot be fixed in this mode demonstration.
- **Time alteration**: unavoidable due to the actual dynamics of real process variation in time. For example, the effect of high temperature, or pressure, and humidity variations.
- **Variable loads:** dynamics can significantly vary. If the load is changed the mass and the moment of inertia of an agent arm can significantly change the dynamics.
- **Industrial modification:** a model process may be categorized exactly. if industrial modification is made, then the manufacture sequence is great. A small industrial modification manufacturing can be greatly expensive.
- **Moderate diagnoses:** even if the actual processes were linear and time invariant, we still have to calculate or recognize its diagnostics and this cannot be complete without a fault. Calculating instrument and diagnoses techniques, employing bounded information groups of finite sample time, will unavoidably be hampered by uncertainties.
- **Measuring devices (sensors) and (actuators):** what has been assumed for the process can be applied also to sensors and actuators that are form a part of the controlled system. One might want a smallest stage of behavior for instance stability of the controlled system in situations of perhaps sensor and actuators failure or degradation [24].

1.4.1 Robustness

Robustness is a significant characteristic of control systems and it describes how demonstrating errors, perturbation and noise or additional differences influence the behavior. If the control system provides same performance when exposed to differences than it would under insignificant conditions, the control system is robust. Robustness investigation of linear structures is usually achieved by employing the sensitivity functions.

Consider the closed loop system shown in Figure 1.5, where the control system is unprotected to output disturbance (w) and measurement noise (v). The response of the system may be written as:

$$\boldsymbol{C = \frac{G_c G}{1 + G_c G}(R - v) + \frac{1}{1 + G_c G} w \ldots\ldots\ldots (1 - 2)}$$

Subsequently, the sensitivity and complementary sensitivity functions are outlined and characteristics discussed [16].

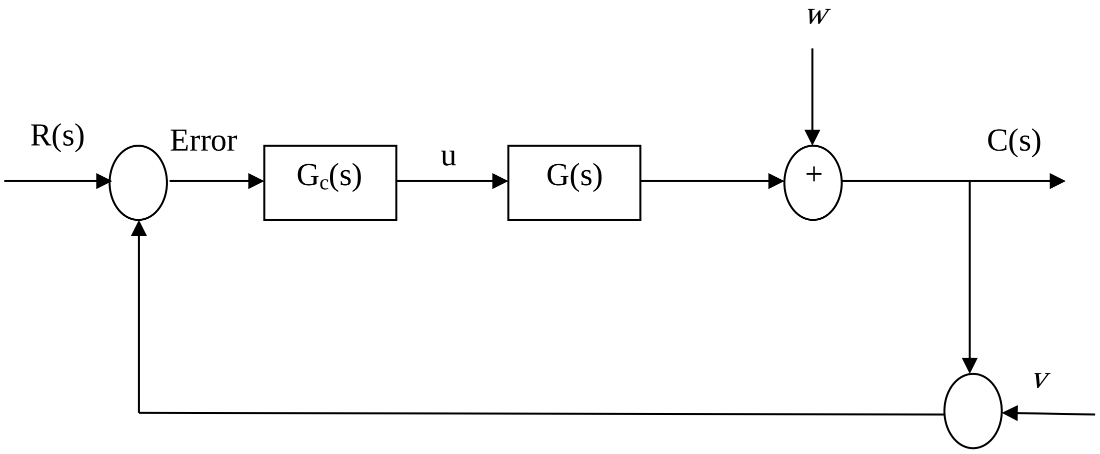

Fig.1.5. Control System by Means of Output Disturbance (w) and Measurement Noise (v)

1.4.2 Sensitivity Functions

Let the cascade transfer function be H(s) = G(s)C(s). Then the sensitivity function S(s) and the complementary sensitivity function T(s) are defined as

$$\boldsymbol{S(s) = \frac{1}{1 + H(s)} \ldots\ldots\ldots (1 - 3)}$$

$$\boldsymbol{T(s) = \frac{H(s)}{1 + H(s)} \ldots\ldots\ldots (1 - 4)}$$

Note that *S(s)+T(s)* = 1 for all frequencies. Using the S(s) functions, the response of the system in Figure 1.5 may be written as:

$$\boldsymbol{C = T(s)(R - v) + S(s) w \ldots\ldots\ldots (1 - 5)}$$

It can be realised from equation (1-5) that so as to have best desired tracking behavior, *S(s)* must be zero for all frequencies to avoid the output disturbances *w* affecting the output response *C*. The complementary sensitivity function would be one, because *S(s)+T(s)=1*. This collection would produce perfect control (*C* = *R*), if measurement noise was not existing (*v=0*).

Actually, however, measurement noise continuously exists in certain mode. Usually, measurement noise arises at comparatively high frequencies, which means that *T(s)* can be prepared large at low frequencies, however it has to be reduced at higher frequencies to reduce the influence of noise. This has the influence that *S(s)* has to develop at higher frequencies and therefore the output disturbances (*w)* will have a hard influence here. But, this output disturbance usually arises at low frequencies, where *S(s)* may be small. Currently reflect the control signal in the form

$$\boldsymbol{u = \frac{T(s)}{S(s)}(R - v - w) \ldots\ldots\ldots (1-6)}$$

Generally, the control signal must be kept as small as possible to evade extreme use of energy. This target may be achieved according to the above equation by calculating such a controller that makes *T(s)* a small value for all frequencies. In brief, the control design and modification technique of every linear controller must produce the equation of sensitivity function S(s) and equation of complementary sensitivity function *T(s)* that have small values for all frequencies to reduce the influence of output disturbances and measurement noise on the output response and control signals. But, the sensitivity function and the complementary sensitivity function cannot be kept very small at the same time, because the summation of their values at any frequency is equal to one, by definition [22-25].

1.4.3 Norm

A norm is a distance-computing tool that can be practical on functions, vectors and matrices. A norm is denoted as|| ||, a norm of *x* can be characterized by the subsequent statements.

I. $\boldsymbol{||x|| \geq 0, and\ ||x|| = 0}$ **if and only if** ***x=0***

II. **Used for whatever scalar** $\boldsymbol{\beta}$ **and vector** ***x*** $\boldsymbol{||\beta x|| = |\beta|||x||}$

III. $\boldsymbol{||x + z|| \leq ||x|| + ||z||}$

Subsequently any manipulator that achieves the above statements is named a norm, there are numerous descriptions for norms. For instance, in the event $x\in \Re^n$ is a vector, the ρ norm is outlined by

$$\|\boldsymbol{x}\|_{\boldsymbol{\rho}} = \left(\sum_{\boldsymbol{i}=\mathbf{1}}^{\boldsymbol{n}} |\boldsymbol{x}_{\boldsymbol{i}}|^{\boldsymbol{\rho}}\right)^{\frac{\mathbf{1}}{\boldsymbol{\rho}}} \ldots\ldots\ldots (\mathbf{1-7})$$

Frequently ρ has single of the values $\rho = 1$ (l_1-norm) or $\rho = 2$ Euclidean or l_2-norm. Furthermore, the norm $\|x\|_\infty$ (l_∞-norm) is often utilised in calculations. $\|x\|_\infty$ is outlined in [26].

$$\|\boldsymbol{x}\|_\infty = \max_{\boldsymbol{i}} |\boldsymbol{x}_{\boldsymbol{i}}| \ldots\ldots\ldots (\mathbf{1-8})$$

1.4.4 Robust Stability

Take a prototypical $\overline{G}$ of the real process G and assume that the undemonstrated dynamics may be defined by additional disturbances $\Delta\overline{G}$ so as to

$$\boldsymbol{G} = \overline{\boldsymbol{G}} + \Delta\overline{\boldsymbol{G}} \ldots\ldots\ldots (\mathbf{1-9})$$

Observe that the control strategy is depending on the prototypical $\overline{G}$ instead of the process G, and therefore the cascade transfer function is not $\overline{H} = G_c\overline{G}$, but rather $H = G_c\overline{G} + G_c\Delta\overline{G}$. To have a stable feedback control system, the cascade transfer function must enclose (counter clockwise) the critical point (-1, 0) as many times as the cascade transfer function has unstable poles, according to the Nyquist stability norm. At this point the process disturbances are expected to be stable, so that there are no extra right-half (s-plane) poles that would need extra encirclements of the critical point. The distance amid the cascade transfer function $\overline{H}$ and the critical point is $\left|1+\overline{H}\right|$. Until with the disturbances, stability is preserved, if

$$\left|\boldsymbol{G}_{\boldsymbol{c}}\Delta\overline{\boldsymbol{G}}\right| < \left|\mathbf{1}+\overline{\boldsymbol{H}}\right| \ldots\ldots\ldots (\mathbf{1-10})$$

This suggests

$$\left|\Delta\overline{\boldsymbol{G}}\right| < \left|\frac{\mathbf{1}+\boldsymbol{G}_{\boldsymbol{c}}\overline{\boldsymbol{G}}}{\boldsymbol{G}_{\boldsymbol{c}}}\right| \leftrightarrow \left|\frac{\Delta\overline{\boldsymbol{G}}}{\overline{\boldsymbol{G}}}\right| < \frac{\mathbf{1}}{\overline{\boldsymbol{T}}(\boldsymbol{s})} \ldots\ldots\ldots (\mathbf{1-11})$$

Because the above equation necessarily holds for all frequencies on the Nyquist curve, the status for robust stability may be scripted in the formula

$$\left|\frac{\Delta\overline{\boldsymbol{G}}(\boldsymbol{jw})}{\overline{\boldsymbol{G}}(\boldsymbol{jw})}\right| = \left|\frac{\boldsymbol{G}(\boldsymbol{jw})-\overline{\boldsymbol{G}}(\boldsymbol{jw})}{\overline{\boldsymbol{G}}(\boldsymbol{jw})}\right| < \frac{\mathbf{1}}{\overline{\boldsymbol{T}}(\boldsymbol{jw})} \ldots\ldots\ldots (\mathbf{1-12})$$

The status of robust stability regulates how much the prototype process may diverge from the real process. Great differences are acceptable in the scope where the complementary sensitivity function is small and only minor differences are acceptable in the scope where $\overline{T}(s)$ is large. Remark that a traditional estimate of allowable process differences that will not produce instability is acquired by [27]

$$\left|\frac{\Delta\overline{\boldsymbol{G}}(\boldsymbol{jw})}{\overline{\boldsymbol{G}}(\boldsymbol{jw})}\right| < \frac{\mathbf{1}}{\boldsymbol{M_t}} \ldots\ldots\ldots (\mathbf{1-13})$$

$$\boldsymbol{M_t} = \boldsymbol{Sup_w}\left|\overline{\boldsymbol{T}}(\boldsymbol{jw})\right| = \left\|\frac{\boldsymbol{G_c}\overline{\boldsymbol{G}}}{\mathbf{1}+\boldsymbol{G_c}\overline{\boldsymbol{G}}}\right\|_{\infty} \ldots\ldots\ldots (\mathbf{1-14})$$

1.4.5 Robust Model Predictive Control (RMPC)

The model predictive control (MPC) method is a feedback approach that has been broadly accepted in manufacturing and academia. The cause for its achievement is its skill to deal with contribution constraints then multi-variable schemes. Therefore, to utilise the MPC process, MPC needs the recursive answer of the upper-lower bounded problem, which can be resolved through a quadratic package or semi-certain package [28]. MPC has shown distinguished care in the control of active systems and significant performance improvements in control action. The knowledge of MPC can be summarised as follows:

- Predict the upcoming performance of the future state and output through the limited time period
- Calculate the upcoming input signals on-line on every stage by minimising a performance index based on variation constraints on the handled (manipulated) one or both measured variables.
- Implement only the primary trajectory control vector to the controlled process then iterate the preceding stage with modern controlled input-state-output vectors.

Thus, the availability of the process model is an essential status for the progress of the predictive control. The achievement of MPC is based on the grade of accuracy of the process model. Demonstrating actual processes characteristically comprises of uncertainties that need to be treated with care in this control technique. This technique, guarantees stability, behavior and robustness belonging of feedback control systems in the complete uncertainty field. Dual characteristic types of uncertainty, state space unbounded and limited unorganized uncertainty are widely reported in the arena of robust model predictive control [29].

There are two techniques to RMPC. The basic technique is robust complete state feedback MPC with an estimator, as presented in Figure 1.6. This specifies the output feedback control, taking in to account uncertainties and delay time in state data. The other technique shown in Figure 1.7 is appropriate once the stage of uncertainty is not well identified. It is a method of adaptive control, taking information in to account to estimate the unbounded parameter and adapting the MPC controller to suit. RMPC controller ensures robust possibility and constraint fulfillment assumed complete state data. The modern consequences in this approach develop from the skill to change additional constraints to this method and employ the similar consequence. The system taken for this study is a linear-time invariant and demonstrated using the discrete-time state-space equation as in appendix A. This category of concluding constraint is a general characteristic of MPC constructions, comprised to guarantee stability [30].

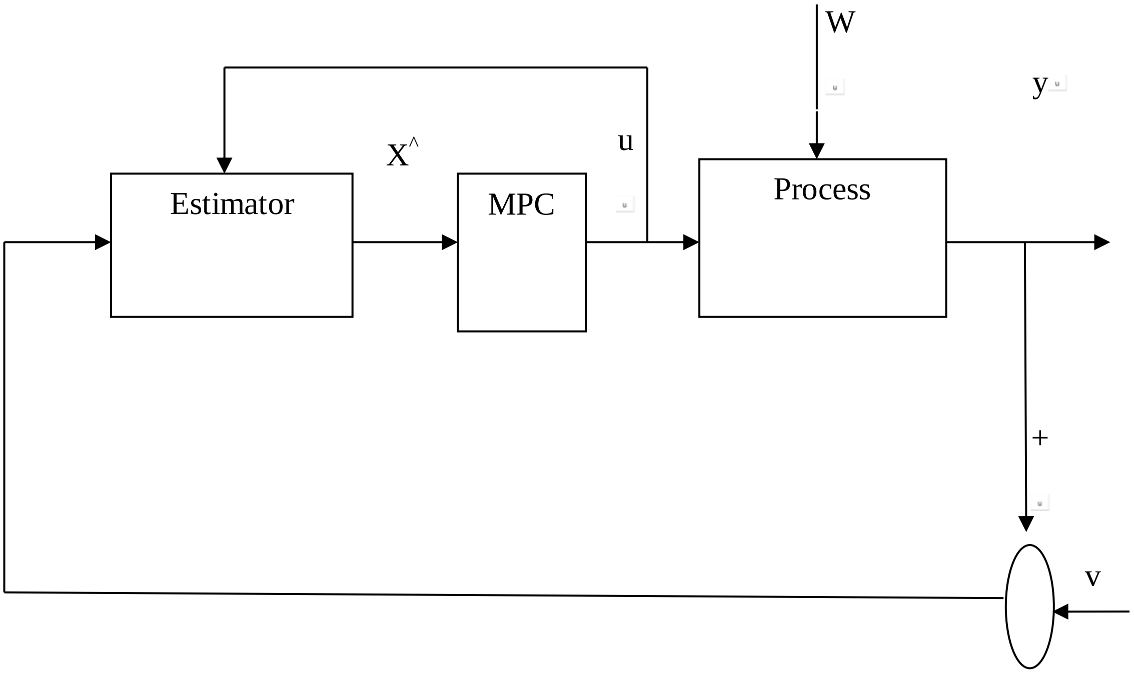

Fig.1.6. MPC with Output Feedback through Estimator by Means of Constant Error Set

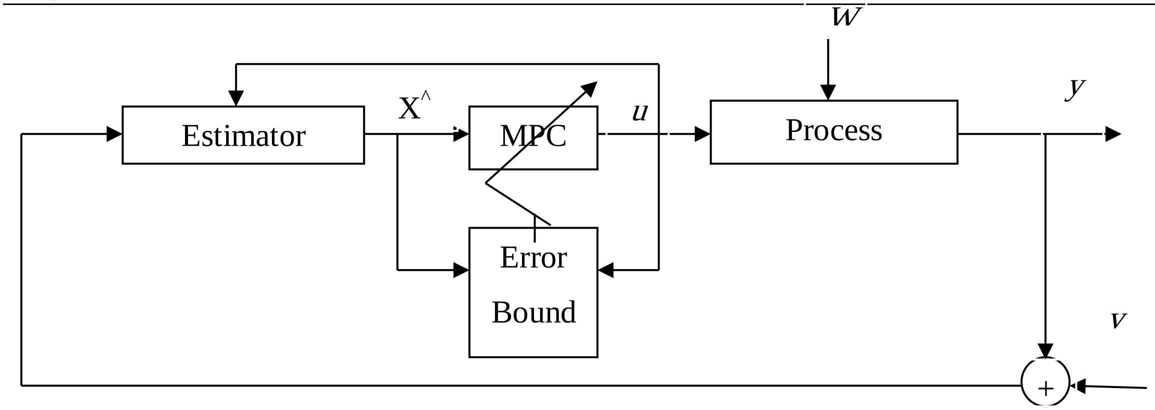

Fig.1.7. MPC with Output Feedback through Estimator by Means of Adaptive Error Bounding

1.5 MOTIVATION AND OBJECTIVES OF THE RESEARCH

Based on the aims of the work outlined above, we find overall mathematical modelling methods for SWNCS powered by solar energy. The SWNCS mathematical model must include the mathematical for wireless networks Wi-Fi & WiMAX, mathematical model for solar cell power system, and mathematical model for matrix (LED) lighting control. Consequently, the objective is to design and develop RMPC scheme such that it could manage and control the SWNCS from any disturbance or uncertain parameters. Furthermore, the requirement is to preserve the stability of the SWNCS even when confronted with challenges such as time delays, and packet dropout. Alternatively, the performance of the control system must be kept acceptable despite the robust controller modification. Hence the selected RMPC construction for SWNCS must be validated through examining the performance from the desired signal tracking, robustness to jitters (delays time), robustness to packet dropouts, and robustness to perturbation and uncertain signals viewpoints. For comparison purposes, we implement a Neural Network Predictive Control (NNPC) technique for a SWNCS so that reducing the effect of wireless network time delay and packet dropout take place in SWNCS.

1.6 STATEMENT OF THE RESEARCH PROBLEMS

The main research theme of this thesis is: the improvement of RMPC and NNPC that can reduce the impact of SWNCS employing Wi-Fi & WiMAX standard on the real-time and control performance of SWNCS. The main problems addressed in this thesis are:

- How to obtain the mathematical model for both Wi-Fi &WiMAX wireless networks.

- How to implement the SWNCS in real-time control performance, in the presence of network time delay and packet dropout.
- How to develop a mathematical technique for maintaining and enhancing the real-time performance of Wi-Fi & WiMAX for real-time control applications.
- How to design an optimal controller for removing and reducing the effect of network time delays and packet dropouts in SWNCS.
- How to use the WiMAX wireless network in a simulation environment. Due to many co-simulation tools such as, "TrueTime" use only Wi-Fi and ZigBee wireless networks.

1.7 THESIS CONTRIBUTIONS

The contributions of the thesis demonstrated in this work can be summarized as follows:

1. In the related work, most RMPC for SWNCSs are also mode independent (the controller does not depend on time delays) or one mode dependent (the controller depends on sensor-to-controller time delaysτ_k^{sc}). Only little research covers the mode dependent controller design (the controller depends on both sensor-to-controller $\tau_k^{sc}$and controller-to-actuator time delaysτ_k^{ca}). In this thesis, a full state feedback mode dependent controller is designed and developed. Mutually, the control structure problems and stabilization are measured.
2. The method is used to compensate for the network time delays is an interesting matter for SWNCS strategy. A normal method is to use a robust predicted indicator to substitute the delayed time out. At every period stage, the RMPC not only generates the present control signal but rather a sequence of upcoming control signals. This sequence of upcoming control signals can be employed to reduce the effect of stochastic time delay in SWNCSs. An adaptive RMPC technique for SWNCSs with stochastic time delays in both (sensor-to-controller and controller-to-actuator channels has been designed.
3. Development of RMPC techniques for robustly stable mixing SWNCS with stochastic time delays and packet dropouts. RMPC techniques highlight robustness to uncertain signals, and place an emphasis on supplying the desired time delay. The investigation take in to account both of the network time delay and packet dropout, and then controller

performance index allows RMPC optimally in the performance sense such that a specified network time delay and packet dropout is satisfied.

4. Based on the SWNCS model, the RMPC (a full state feedback controller) can be constructed by using the Lyapunov functional method. Both sensor-to-controller and controller-to-actuator time delays of the SWNCS are considered as stochastic variables controlled by a Markov chain. A discrete-time Markovian Jump Linear System (MJLS) with norm bounded time delay is presented to model the SWNCSs. Sufficient conditions for stochastic stability based on H_∞-norm & H_2-norm and stabilization of the fundamental systems are derived via LMIs formulation.
5. Introduction of a NNPC technique for a SWNCS. A SWNCS model is created by using a Back-Propagation Neural Network (BPNN) and a learning algorithm adopting an adaptive learning rate approach is used to identify the stochastic time delays in BPNN. The performance of the NNPC controller is based on minimization of the Mean Square Error (MSE).
6. Design of a SWNCS with specific communications and control parameters using TrueTime co-simulation tools. TrueTime provides apparatuses for confirming the performance of the established RMPC approaches and instructions in an accurate SWNCS situation with actual methods. Furthermore, development of the TrueTime co-simulation tools has been carried out according to the following:
    - Adding the IEEE802.16e standard to wireless network on SIMULINK library in TrueTime.
    - Inserting the RMPC parameters on the TrueTime co-simulation tools.

1.8 NOTATION

The most important notation is summarised in the list of Acronyms and in the notation and symbols at the end of this thesis. We have employed lower-case letters for vectors and signals such as u, y, r, e and capital letters for matrices, transfer functions, norms and systems for exampleP, S, K, A, W, B, C. Furthermore, the notation $P > 0 \ and \ S > 0$ means that P, S are real symmetric and positive definite matrices.

1.9 THESIS OUTLINE

The outline of the thesis is given below, together with references to the related publications:

Chapter 2 is dedicated to reviewing the previous background studies related to SWNCS modeling and simulation environment, SWNCS model based time delays, SWNCS model based on packet dropouts, SWNCS modeling for both network time delay and packet dropout. Control methods dealing with network time delays and packet dropouts in using both RMPC & NNPC techniques are also reviewed. An overview of Wi-Fi/WiMAX communication protocols and transport communication protocols in SWNCS is presented. The chapter end up with an overview of the robust stability analysis based on $H_\infty \, and \, H_2$ norms is presented.

Chapter 3 constructs the SWNCS as follows; the complete solar-power system design is introduced, wireless access points in SWNCS for both Wi-Fi/WiMAX wireless networks, Network Management Centre, followed by solar street lighting with broadband wireless internet access, analysis of transport protocol over Wi-Fi/WiMAX with Simulation scenario. Then, SWNCS is considered for maintenance.

Chapter 4 covers the mathematical model for; Wi-Fi (IEEE802.11b) wireless network, WiMAX (IEEE802.16e) wireless network, Photovoltaic PV system, followed by development of a SWNCS simulation environment based on TrueTime simulator tools that effectively integrates state-space model of physical plant processes and wireless communication networks.

Chapter 5 presents the first techniques for avoidance of network time delay and packet dropout for SWNCS. This deals with problem formulation of the SWNCS with Markov time delay and packet dropout models, full state feedback controller design, MPC and RMPC design based on LMIs, construction of the SWNCS in TrueTime simulator tools. An illustrative numerical example is given to validate the proposed control algorithm and to illustrate the effectiveness of the obtained results. Furthermore, the power consumption in SWNCS is simulated for situations with/without power control system.

Chapter 6 covers the robust stability analysis for SWNCS, defines the robust stability analysis for SWNCS based on H_∞ norm and identifies the robust stability based on H_2 norm, followed by the general definition to Product Reduction Algorithm (PRA).

Furthermore, an illustrative numerical example is given to demonstrate the effectiveness of the proposed techniques.

Chapter 7 presents another technique for avoidance of network time delay and packet dropout for SWNCS. This deals with system identification of the SWNCS based on Back Propagation (BP) algorithms, model predictive control techniques based on neural networks. Furthermore, stochastic network time delay of SWNCS architecture based on NNPC. A numerical example is given to demonstrate the effectiveness of the proposed method. Further, the SWNCS based NNPC simulation techniques using MATLAB/SIMULINK are carried out to validate the proposed control algorithm.

Chapter 8 is dedicated for the discussion and review of the results.

Chapter 9 presents concluding comments and suggestions for future research work. Finally, some mathematical background knowledge that is used during this research is given in the **Appendix.**

CHAPTER 2 ..

PREVIOUS AND RELATED WORK

2.1 INTRODUCTION

The use of wireless communication networks in control systems has received increasing attention in recent years due to its cost effectiveness, high transmission speeds and flexible uses. Considerable research has been carried out on the design and analysis of SWNCSs regarding the wireless network effects in control systems, due to transmission time delay and packet dropouts. The WNCS community has addressed a wide range of research matters, for example modelling time delays, optimal control techniques and stabilization analysis of WNCS. More recently, standard wireless communication protocols such as Zig-Bee and the Wi-Fi families are also making their way into the area of control systems. However, there has been little research study and analysis of employed WiMAX protocol family in the area of control systems.

In this thesis, we focus on adoption of SWNCSs appropriate for real-time control applications. This chapter presents a literature review of recent developments in Wi-Fi and WiMAX wireless networks relating0 to SWNCSs; specifically with regard to SWNCS modelling and simulation environments, simulation methods for network time delays and packet dropout avoidance in SWNCS, stability analysis of SWNCS based on $H_\infty \& H_2$ norms. Further, analysis of communication protocols for SWNCSs is also carried out.

2.2 SWNCS MODELLING AND SIMULATION ENVIROMENT

The rapid evolution of WNCS in the industrial environment has encouraged growth of new control algorithms and wireless communication protocols for changing control and networking conditions in SWNCS for example Quality of Service (QoS) support. The calculating and wireless communication resources in SWNCS applications are frequently limited, making co-design approaches significant. Co-design methodologies recognize interconnects between the control system and wireless communication network, and aim to optimise the performance of both. Another ordinary characteristic of SWNCS is that their control systems interrelate with wireless communication network. For example, Li and Wang [31] summarised the basics and some recent results of Networked Control

Systems (NCS). The recently established synthesis of communication, control in addition to data processing techniques means that not only the information is delivered through the networks. However, also the intelligence, basically knowledge, is joint and evolves over the networks. Tipsuwan and Chow as well as Mittal Siddiqui [32-33] study one of the major challenges in NCS that is the network time delay effect in the feedback control system. Network time delays degrade the NCS control performance and destabilize the system. An important emphasis has been on developing control analysis methods to manipulate the network time delay effect that happens in NCS. Shuang-Hua and Millam [34-35] establish the fundamental ideas of networked control and wireless sensor networks then introduce the challenges in these fields. In reference [36] NCS and its various structures are presented and discussed by Gupta and Chow. The history and evolution of NCS are demonstrated. Furthermore, Gupta and Chow focus on various areas and research fields such as: networking technology, network time delay, network reserve allocation, scheduling, network security in real-time NCS, combination of elements on network, fault tolerance, etc. The application of the methods for enhancing the QoS over NCS may consider the behavior of the network and its underlying characteristics. The existence of a wireless network source of the time delay and packet dropouts so that the QoS of the controlled system is poorly affected are introduced in work by Boughanmi et al [37].Zhao et al [38] suggest a co-design technique to handle the communication constraints for a set of NCSs which are linked to a shared network. To decrease the effect of the network time delay and packet dropout, predictive control theory is applied to construct future control signals to the systems. The scheduling theorem, both the static algorithm Static Rate Monotonic (SRM) and dynamic Feedback Scheduling (DFS) which obtains gain of the feedback data of the system performances, is applied to schedule the transmissions of the predictive control sequences of all the systems. Naghshtabrizi and Hespanha [39] demonstrate that time delay impulsive systems are a usual structure to model wired and wireless NCSs with variable sampling periods and time delays in addition to packet dropouts. Further, they employ a discrete-time Lyapunov functional to illustrate acceptable sampling periods and time delays such that exponential stability of NCS is guaranteed.

This section has looked at the fundamentals and challenges for such simulations and reviewed the available options for a WNCS that can meet these needs. A brief introduction had been made to the significant emphasis that has been made in the research on developing control architectures to control the network delay and packet dropout effect in WNCS.

2.2.1 Modelling for time delay

The manner of the communication medium plays a very important role in the working of SWNCSs. Different work has been carried out in the past by researchers to analysis this issue. Time delay characteristic of the network is the most critical behavioural characteristic of such closed-loop control systems. The manner of time delays is random as observed by numerous researchers. Due to these random time delays, stability of the system is negatively affected. Different studies have been made to analyse, estimate or compensate for such time delays to stabilize the SWNCSs.

The Kumar et al [40] focus on modelling of network time delays as a **probability distribution**. Liu and Yao [41] presented a new method for modeling and analysis of NCSs with network time delay using **Hidden Markov Models (HMM)**. Stochastic optimal controllers of NCSs whose networked time delay controlled by an inherent Markov chain with unidentified probability distribution are designed. The HMM consists of a number of hidden states, which might correspond to network load states belonging to networked time delay. Each state produces observations according to observation emission probabilities, and the states are interlinked by state transition probabilities. Starting from some initial state, a sequence of states is created by moving from one state to another according to the transition probabilities until an end state is reached. Each state then produces observations according to that state's emission probability distribution, generating an observable sequence of observations. A HMM is a twice stochastic process with one inherent process that is not observable but may be estimated via a set of processes that produce a sequence of observations. The structure of HMM is illustrated in Figure 2.1.

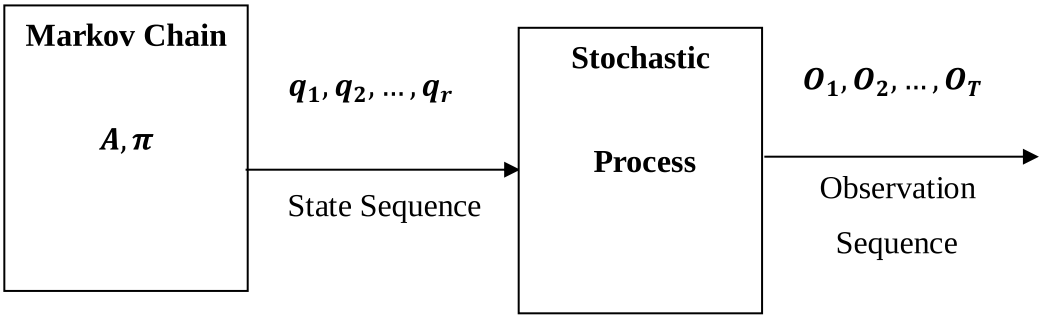

Fig. 2.1 Basic Structure of HMM

Vatanski et al [42] presented the upper bound delay algorithm which applies schemes from network calculus theory. For the enhancement of quality of performance, two delay compensation approaches; the Smith predictor based and the robust control based delay compensation approaches, are presented and compared. Furthermore, in reference [43] modelling and stabilization of NCSs are discussed by Jinna et al. Their approach takes into account the presence of packet distracting in data transmission. A new mathematical model is suggested to describe the dynamical characteristics of NCSs with bounded network time delay. Different from the present models, the number of delay items is time-varying in the model obtained. However, in work by Yang et al [44], the stochastic time delays are modelled as a linear function of the stochastic variable satisfying **Bernoulli random binary distribution**. The observer-based controller is calculated to exponentially stabilise the NCS in the sense of mean square, and also accomplish the appointed H_∞ perturbation attenuation level. In contrast, Jian et al [45] model the stochastic time delays presented by WNCS by an Inverse Gaussian distribution obtained from experiments on an IEEE 802.11b wireless network.

It is noted that in all references cited above [40-45], the networked time delay is supposed to be constant, arbitrarily distributed and bounded, or even identified by the controller. However, in SWNCS applications network time delays are stochastic due to three issues these are: communication architecture, the network devices adopted and communication protocols employed. Thus, it is very difficult to express transmission time delays with mathematical formulations in SWNCS with arbitrary access network. In the NCS with random network time delay in both forward and backward channels, a type of controller based on Smith compensator and signal neuron incomplete differential forward PID is introduced by Haitao and Zhen [46].

In this thesis, we assume that the time delays of the SWNCS are considered as stochastic variables controlled by a Markov chain. A discrete-time Markovian jump system with norm unbounded time delay is presented to model the SWNCSs.

2.2.2 Modelling for Packet Dropout

An information packet travelling via a wireless network suffers from not only transmission time delays but also, perhaps, packet dropout. Packet dropouts infrequently occur in SWNCS when there are node failure or communication collisions. Though most network protocols are provided with transmission redo method, they can resend packets for only a limited time. After this time has expired, the packets are failed. Moreover, for real-time closed-loop control data, for example sensor measurement and control actions, it is frequently useful to remove packets that are extremely delayed since a new sensor or control packet is more important than an old one. Because new packets are created each sampling period, it is reasonable to remove packets that are older than one sampling period. Thus, User Datagram Protocol (UDP) is desired for real-time control system over Transmission Control Protocol (TCP), chiefly when the control period of the closed-loop control system is very short, though UDP is subject to much more than TCP on regular [47]. As a result, packet dropout is another significant issue that affects SWNCS performance.

Sun and Qin and Dexiao et al [48-49] discuss the modelling and control for a category of NCSs with packet dropouts. In cases where there may be packet dropouts in both forward and feedback channels in a communication network, NCSs are modelled as a discrete-time switched system with four subsystems. By employing the average **dwell** time technique, adequate conditions for the exponential stability of the NCSs are introduced, and the relationship between the packet dropout rate and the stability of the NCSs is clearly recognized. Yu et al [50] have proposed an iterative method to model NCSs with random but finite data packet loss as switched linear systems. This allows the implementation of wealthy theory of switched systems to analysing such NCSs. Sufficient conditions are introduced on the stability and stabilization of NCSs with packet dropout and network delays. Stabilizing state output feedback controllers can be created by employing the feasible solutions of some LMIs. Tian and Levy [51] propose to compensate for the control packet dropout at the actuator using past control actions. Three model-free strategies for control packet dropout compensation, namely, PD (proportional plus derivative), PD2 (proportional plus up to the second-order derivative), and PD3 (proportional plus up to the third-order derivative) are formulated. They are appropriate for a large number of NCSs without the want to adjust the compensator parameters. The packet drop sequences in the WNCS are characterised as states of a Markov chain. A new discrete Markov chain switching system model integrating 802.11 protocol and new scheduling method for wireless networks with control systems were introduced by Chang-Chun et al and

Seiler and Raja [52-53]. However, the insertion of a shared communication network between plant and controller by Christopher et al [54] certainly leads to infrequent random data loss. The authors present new results concerning to the probability of such system being globally asymptotically stable or input to state stable. Wu and Chen [55] are concerned with stability and controller design of NCSs with packet dropouts. New NCS models are designed based on both single- and multiple-packet transmissions. Both backward and forward channels packet dropouts are modelled and their previous behaviour is expressed by various independent Markov chains. Mehrdad et al [56] analyse the problem of H_∞filtering in NCSs with multiple packet dropouts. By using the new formulation, random dropout rates are transformed into uncertain parameters in the system's statement. Huang and Dey [57] have proposed Kalman filtering in a network with packet dropouts, and in their method, utilise a two homogenous state Markov chain to demonstrate the normal working state of packet delivery and transmission failure. Furthermore, they analyse the behaviour of the estimation error covariance matrix and establish the idea of peak covariance, which demonstrates the upper bound of the sequence of error covariance matrices $\{Pt, t \geq 1\}$ for the case of an unstable scalar model. Finally, Vijay et al [58] have observed two special cases of the problem of optimal Linear Quadratic Gaussian (LQG) control of a system whose state is being calculated by sensors that interact with the controller over packet dropping connections. This design is optimal among all fundamental algorithms for any random packet drop pattern.

2.2.3 Modelling for Network Time Delay and Packet Dropouts

The majority of previous researchers have attempted to create controllers that are robust to only one of the possible communication faults in an NCS. Thus, the compensation methods are not well suited to investigating a practical NCS since the effect of network time delays and packet dropouts need to be addressed simultaneously. Therefore, the control techniques have been extended for compensating for both network time delays and packet dropouts at the same time. However, these techniques are based on some assumptions about network time delays or packet dropout performances which perhaps are not proper in practice. For example, Van et al [59] presented three discrete-time modelling methods for NCSs that integrate time-varying sampling periods, time-varying delays and dropouts. The core of this research centred on the addition of two existing algorithms to describe dropouts, that is dropouts modelled as prolongation of the delay and, dropouts modelled as prolongation of the sampling period. Further, the demonstration of a new method based on explicit dropout modelling utilising automata. Meanwhile, Yu-Long et al [60] are concerned with quantitative analysis and combination for continuous-time NCSs with packet dropouts and interval time-varying sampling period. A new packet dropout separation approach is suggested to separate packet dropouts from the amount of network time delay and packet dropouts, and an interval time-varying sampling period method is introduced to model the variation of sampling period. Then, a new packet dropout decay based Lyapunov functional is created, and the quantitative associations between packet dropout probability, stability and stabilization of NCSs are proved.

a new mathematical model of NCS whose network time delay is longer than one sampling period is achieved by Liabc et al [61], which can fully describe packet reordering and effectively reduce the impact of packet reordering on the performance of NCS such that the newest control action can be implemented by the actuator. Based on this model, the time-varying NCS is transformed into an uncertain discrete linear system with multi-step delay in terms of matrix theory. Considering the size of network time delay, the NCS with packet dropout is modelled as an asynchronous dynamical system with rate constraints. A new linear discrete time model which converts the uncertainty of network time delay into the uncertainty of parameter matrix is proposed by Wang et al [62].

The NCS with time-varying network time delays and data packet dropouts in the transmission is modelled as a discrete-time system with time-varying delays in the state. The network time delays are supposed to have both an upper bound and a lower bound. Subsequently, an asymptotic stability condition for the NCSs is created, which depends on the upper and lower bounds of delay times. Further, three methods to the static output-feedback controller are suggested, where the effect of both network time delays and data packet dropouts has been considered. Moreover, the robust stability condition and controller design technique for such NCSs with structured uncertainties are introduced in work by Hao and Zhao [63]. Xie and Xia [64] addressed the robust fault tolerant controller design of uncertain NCSs with both time-varying network time delay and data dropout. Based on Lyapunov stability theory and using LMI method, new criteria were considered for the controller design. The new criteria were unrelated to the bound of the derivative of the delay; no constraint is compulsory to the matrix construction.

Gabel and Litz [65] presented a simulation method for QoS adaptive control in NCS that takes into account random network time delays and packet losses simultaneously. The proposed idea is based on calculating the QoS by adding numbers to the transmitted packets and computing new control signal values with reference to these QoS parameters that are calculated online. The results demonstrate that control performance can be enhanced if delays and packet losses between sensor and controller take place. To reduce the negative effects of communication constraints counting network time delays, packet dropout and quantization effect, a new approach on the H_∞controller design was suggested by Jin and Zhang [66]. Also, Liu et al [67] discussed a class of NCSs with random network long delay and packet dropouts. The random network time delay is modelled as a Markov chain and the closed-loop NCS is illustrated as a Markovian jump system. By employing traditional optimization theory, the presence of piecewise-constant state feedback predictive controller sequences is introduced in terms of LMIs.

In this thesis, we have a proved that the predictive model for SWNCS with unbounded delay and packet dropouts is robust stable in terms of H_∞& H_2norms, if it’s corresponding switched system is stable when employing the RMPC technique.

2.3 SIMULATION METHODS FOR DELAY AND PACKET DROPOUT AVOIDANCES IN SWNCS

Our discussions about progress of network time delays and packet dropout avoidance strategies are executed in various categories depending on how hard the control processes are. Mainly industrial processes can be well controlled utilising the traditional controller such as, proportional-integral-derivative (PID) control algorithm. For those processes, it does not really make sense to create more modern and sophisticated control strategies from the application opinion though some theoretical analyses are still valuable. This thesis does not deal with the control design for this type of industrial processes. Some processes have hard dynamics, disturbances and uncertainties. Simple control strategies such as PID are inefficient. However, the variables to be controlled can be calculated simply and reliably, and a superior process model can be constructed. Therefore, advanced and model-based control can be improved for the processes. Improving model-based control still attracts important attention. Various schemes have been applied, based on different categories of network configurations, to treat the network time delay and data packet dropout problems. In these schemes, some assumptions have been made to derive generic control techniques for SWNCSs. To name a few: network time delay is less than one sampling time, network traffic cannot be overloaded. Based on such assumptions, different control techniques have been developed for the control of SWNCSs, and some of which are described in the following section.

2.3.1 Robust Controller Techniques Dealing With Time Delays and Packet Dropouts

A RMPC technique to solve the problem of wireless network time delays and packet dropouts that occur in SWNCSs is considered in this thesis. This is recognised to highly degrade the control performance of the controlled system in both continuous-time case and discrete-time case. For example, Bernardini et al [68] presented a Stochastic Model Predictive Control (SMPC) approach for NCSs which are subject to time-varying sampling periods, time-varying network delays, and packet-dropouts in the backward channel. In these networks, uncertain parameters are assumed to be described by random processes, having a bounded support and a random continuous probability density function. Assuming that the controlled plant can be modelled as a linear system, the authors presented a SMPC explicate based on scenario enumeration and quadratic programming which optimises a stochastic performance index and supplies closed-loop stability in the mean-square sense. While, an r-suboptimal H_∞ controller for NCSs with model uncertainty and network time delay is longer than one sampling period. A feedback control system with structured uncertainties and long transmission delay that is asymptotically stable is proposed by Zhanshan et al [69]. Furthermore, Liu et al [70] propose a solution to the NCSs with time delays and packet dropout problem by employing a modified model predictive control. This uses the future control sequence to compensate for the forward network time delay. Also, employing a model predictor, the time delay in the backward channel can be compensated too. Liu et al, Kostas and Lygeros, Gang et al and Ulusoy et al [71-74] proposed a networked predictive controller consisting of a networked control predictor and a traditional predictive controller. The networked control predictor compensates for the network time delay.

The traditional predictive controller obtains the required control performance. Chen et al [75] introduces a packet-based RMPC approach in a co-design framework for Wireless WNCS. Lyapunov stability is guaranteed if the optimization problem is reasonable. An Inverse Gaussian model which characterises the statistical distribution of the Round-Trip-Delay (RTD) in an IEEE802.11 WNCS was applied to support a simulation study. Xiao-Hua and Jian [76] presented a RMPC algorithm for polytope uncertain NCSs with arbitrary time delay and constrained input considering the Min-Max infinite horizon cost function. While, the network time delay is assumed as Markov chain, the mode-dependent state feedback controller is suggested, all the results are given by LMI. The state predictive model following control system with network time delay is considered by Wang et al [77]. The bounded property of the interior states for the control is given, and the utility of this control design is guaranteed. Peng and Yue [78] have also worked on controller design of NCSs. The continuous-time plant with parameter uncertainty and state delay is analysed. A new model of the NCS is presented under consideration of the non-ideal network conditions. In terms of the specified model, a controller design scheme is suggested based on a delay dependent approach. In contrast, an event-based model predictive control approach for nonlinear continuous time systems under state and input constraints is investigated by Varutti et al and Li et al [79-80]. This scheme is able to work against bounded delays, data dropouts, as well as handle event triggering caused by sensors and actuators. Wang and Yang as well as Tavassoli and Maralani [81-82] have studied the problem of designing H_∞controllers for NCSs with both network time delay and packet dropout by employing an active altering sampling period scheme, where the sampling period switches in a finite set. A new linear estimation-based scheme is suggested to compensate packet dropout. H_∞ Controller design is also introduced by employing the multi-objective optimization methodology. Naskali and Onat [83] introduced a model based predictive NCS architecture extended by counting stochastic time delay in the communication network. The network time delays and packet dropouts due to the communication network are compensated for by employing the computational power of the computer nodes of the NCS. The construction is independent of the control algorithm and employs a model to predict the plant states into the future to create equivalent control outputs. This approach permits the system to be controlled in a pre-simulated behaviour and stability can be maintained even with high packet dropout probabilities. In other work, the network time delay-dependent robust stability criterions for uncertain discrete time-varying singular systems are considered by Du et al [84]. An enhanced network time delay-dependent stability criterion is recognized in terms of Lyapunov functional and severe LMIs, which guarantees the nominal singular network time-varying delay systems to be accepted, causal and asymptotically stable. Wang and Yang [85] have suggested a technique which can avoid the high calculation difficulty of the network time delay switching-based method and present less conservatism than the factor uncertainty-based method. In other research, Wang and Yang [86] tackle the problem of robust H_∞controller design for NCSs with time delay, packet dropout and variable sampling period. The devised NCSs may collect over one control action during a sampling period. A multi-objective optimization algorithm in terms of LMIs is presented to deal with H_∞ performance optimization for NCSs with variable sampling period. The problem of designing a H_2 controller for a NCS with network time delays from the sensor to the controller and/or from the controller to the plant to accomplish a sub-optimal H_2 performance is the effect of possible network time delays. Further, the stabilisation of the system will be achieved by Lu et al [87]. In this thesis, an RMPC is designed to avoid unbounded random network time delays and packet dropouts that occur in SWNCS.

2.3.2 Neural Network Predictive Control (NNPC) Dealing with Time Delays and Packet Dropout

In this work, for networked control systems in which network time delay is time-varying and less than one sample time, a NNPC method is presented to avoid the random network time delays. Lu et al [88] presented a neural-network-based predictive control scheme for a class of discrete-time multi-input multi-output (MIMO) systems. A discrete-time mathematical model utilising a Recurrent Neural Network (RNN) is described and a learning algorithm adopting an Adaptive Learning Rate (ALR) approach is utilised to recognize the indefinite parameters in the RNN model. The NPC controller is obtained based on a modified predictive performance index, and its convergence is guaranteed by implementing an optimisation algorithm with an adaptive optimal rate method. An output error prediction model is built using a Back Propagation (BP) neural network to manage the network time delay between sensor node and controller node. The standard of this model is to modify the predictive output of general predictive control model employing predictive error signal; if the rate of network time delay exceeds the upper limit, the controller nodes will directly create the control approaches adopting the modified predictive output, and hence the compensation for network time delay between sensor nodes and controller nodes would be achieved [89-90].

Yi et al [91] consider NCSs with variable network time delay. A feed-forward multi-layered neural network is first correctly developed to estimate the time delay at each sampling period. Subsequently, this predicted network time delay is taken as the sampling period between the present and the future sampling steps. Also, Antunes et al [92] presented a network time delay compensator to decrease the variable sampling to actuation time delay effects in NCSs and used neural networks. The compensator achievement is based on the information of the sampling to actuation time delay affecting the system and the control action. A novel strategy that uses a new Smith predictor aggregated with single neural adaptive control for the WNCS has been presented in research by Du and Du [93]. Also, a neural predictive controller that is able to control non-linear systems and achieve good tracking and robustness features has been presented by Kara et al [94]. In other work, Du and Du [95] proposed a novel approach using a new Smith predictor integrated with Radial Basis Function Neural Network (RBFNN) control for the NCS. It approaches accurate compensation network time delays on construction. This new Smith predictor hides predictor models of the network time delays into real network packet transmission methods, then the network time delays no longer require to be calculated, identified or estimated on-line. In work by Schnitman and Fontes [96], the application of NNPC has been introduced. The design demonstrates the construction of the predictive controller and the optimization functions that are usually employed to update the control action, then apply the NN method. The NN equations and their gradient equations are improved. A recursive NNPC algorithm was suggested for NCSs by Pang and Liu [97]. This generally consists of two parts: a control prediction generator and a network time delay compensator. For NCSs in which network time delay is variable and less than one sample period, a NNPC technique has been introduced by Chao et al to compensate for the random time delays [98]. A genetic algorithm is utilised to optimize parameters. A Neural network is established to achieve prediction and optimization computation and the uncertainty of the time delay is transformed to parametrical uncertainties. Sharmila and Devarajan [99] focused on the feasibility of neuro-fuzzy controller for NCSs. The neuro-fuzzy controller has been developed for controlling the speed of the networked DC motor by using the integrated characteristics of neural networks and fuzzy logic theories.

2.4 ANALYSIS OF COMMUNICATION PROTOCOLS IN SWNCS

With the rapid progress of wireless communication technologies, there has been an increasing demand for SWNCS. NCSs use a packet switching network to accomplish hard control actions without cumbersome point-to-point wiring infrastructures. However, their performances are greatly affected by variable network time delays and packet dropouts due to the communication system. Therefore, real-time control systems are usually used at NCS nodes to timely serve events scheduled by control applications. The following sections demonstrate that it is possible to adopt WNCSs in industrial environments for supporting these applications.

2.4.1 Analysis of the Wi-Fi and WiMAX MAC and Physical Scheme

Boggia et al [100] proposed a real-time communication construction based on the standard wireless 802.11 technology and on the real-time networking framework RTnet. The QoS presented by the suggested system, in terms of packet dropout ratio and network time delay, has been experimentally estimated by varying protocol parameters. A scheme of adapting the sampling period based on an ‘a priori’, static sampling strategy has been demonstrated by Colandairaj et al [101] and, more considerably, guaranteeing stability in the mean square performance criteria employing discrete-time Markov jump linear system theory. Applied topics taking in to account present constraints of the 802.11b protocol, the sampling strategy and stability are highlighted. On the other hand, the non-beacon permitted mode of IEEE 802.15.4/ZigBee does not guarantee the stability for the closed-loop control because no mechanism can avoid the disturbance coming from other application contribution to a similar network [102]. Chen et al [103] presented practical performance results for WNCS employing the IEEE 802.11b standard. A practical policy employing an echo chamber is summarised, which enables for repeatable multipath conditions. Results for a cart-mounted inverted pendulum case study are evaluated and the experimentally recorded RTD is characterised for use in Monte Carlo models of a network predictive controller. In the meantime, Rafael et al [104] introduced a model that executes six various methods focused on the estimation of the Round Trip Time (RTT) delay in a network. The RTT delay rates are created based on characteristics previously experimental in Wi-Fi networks. The model comprises three algorithms based on arithmetical rules, namely; Mean Value Estimation Algorithm, Median Value Estimation Algorithm and Max Value Estimation Algorithm. The algorithm proposed is based on the Kalman Filter algorithm. Rafaat et al [105] consider a WNCS which uses the IEEE 802.11b protocol without modifications to communicate between sensors and actuators in a production line environment. Ulusoy et al [106] demonstrated a WNCS that can realise adequate control even under unbounded delay, bursts of packet dropout and ambient wireless traffic. Ambient wireless traffic is dealt with modified IEEE 802.11b MAC parameters providing the suggested system with a greater medium access priority. Packet targets defined at each node of system decrease unbounded packet delay to packet dropouts. Performance degradation due to packet dropouts is maintained at a minimum utilising the predicted plant states and control actions. Combining the Ethernet, the control area network (CAN), and the wireless 802.11b in the present NCS has been studies by Cheng et al [107]. An experimental optimization of a wireless IEEE 802.11b communication method, two scenarios to the tuning process of the controller parameters, for real-time control applications has been introduced by Nikolakopoulos et al [108]. In crowded WNCS, there are significant packet dropouts in the transmission process between the client and server parts. However, Jia et al [109] focused on the design of IEEE 802.11-based wireless network. Especially, the authors presented a MAC controller that dynamically regulates the retransmission limit to track the optimal comparison between network time delays and packet dropouts and hence optimises the overall control system performance. Onat et al [110] calculated network time delay and time synchronization of local and remote system. Then, they proposed to employ a synchronization function of IEEE 802.11 based wireless network. They also carried out simulation studies on identification and network time delay compensation.

In contrast, WiMAX have appeared as promising broadband access solutions for the newest generation of wireless MANs. Their complementary characteristics allow the use of WiMAX as a backhaul service to connect multiple distributed Wi-Fi hotspots to the Internet. Li et al [111] summarised the characteristics of a WiMAX channel and its operation on a simulator. As well, limitations on present models for simulating fixed WiMAX channels are known and an approach to expand those models to a mobile scenario is also proposed. Lin et al and Ibanez et al [112-113] proposed an integrated construction using a new WiMAX & Wi-Fi Access Point (AP) device to effectively merge the WiMAX and Wi-Fi technologies. In the suggested construction, the protocol action of the Wi-Fi hotspots is similar to that of the WiMAX system. Therefore, the Wi-Fi network can provide connection-oriented transmissions and QoS in a similar style to the WiMAX system, and as a result a significant enhancement in the delay performance is achieved. However, in publication [114] Jindal et al focused on models of WiMAX technology, which utilise microwave for to transmit data wirelessly, and it also introduces its trade-off with Wi-Fi, and 3G technologies.

Recently, the real-time performance of Wi-Fi & WiMAX wireless networks has been investigated in different ways. Such as, Markov chain theory. An analytical model which utilises two homogenous Markovian chains for Wi-Fi &WiMAX wireless networks are formulated in this thesis.

2.4.2 Transport Communication Protocols for SWNCS

Over the past two decades, research concerning the closed-loop control problem over networks has focused on two main parts: one part is the progress of protocols for network communications, while the other is proposed and is the investigation of network controllers. In both parts, the research has mainly used wired networks. Regarding network protocols, there has been much research on deterministic performance of control networks employing token passing bus and CAN bus constructions. Data network constructions for example, fast Ethernet, which are not designed to guarantee time of data delivery, have also been considered for network control signals. Relatively, considerable work has analysed protocols for the more newly developed Wi-Fi, WiMAX, and Bluetooth wireless network standards. Further application relates to transport communication protocols. Lai and Hsu [115] combined the IEEE 802.11g ad-hoc wireless network and the CAN in the present NCS or WNCS. Both the TCP and the CNA protocols are implemented as the communication gateway in a closed-loop control system. The network time delay between the application layer of the client and the application layer of the closed-loop control target has been calculated and analysed. In other work, Feng and Nelson [116] are concerned with enhancing an H_∞ approach, from a control theoretic opinion, to the design of an active queue management (AQM) based congestion controller for wireless networks providing Internet Protocol (IP). The authors further analysed networks in which the backbone is a conventional wired network providing Internet Transmission Control Protocol (TCP), while end client access is through wireless. The characteristics of the routing protocol together with lower-layer network mechanisms give increase to a network time delay process with high divergence and stepwise varying mean. A new predictive control method with a delay estimator was demonstrated by Witrant et al [117]. NCS, based on the merged utilisation of MPC with a network time delay compensation approach in the framework of non-recognised UDP-like networks, has been considered by Pin and Parisini [118]. The target of this work was to stabilize in the direction of an equilibrium a constrained nonlinear discrete-time system, affected by unidentified disturbances and subject to network delayed packet-based communications in both sensor-to-controller and controller-to-actuator channels. Vardhan and Kumar [119] assumed the prediction based network time delay compensation method by the use of a Smith Predictor. Stability analysis has been carried out for various plant transfer functions. Transport layer protocol User UDP has been employed for communication. Yafeng and Shaoyuan [120] have considered a novel control problem for networked systems with quantization and arbitrary packet dropouts, where the packet dropouts are modelled as Markov chains. For the various category communication links, the H_∞ packet dropout dependent jump controller for TCP category link and the H_∞ packet dropout independent time-invariant controller for UDP category link have been considered to accomplish a required H_∞ disturbance rejection level, correspondingly. While, Fontaine and Laurencot [121] established a mathematical model articulating the maximum throughput in infrastructure based wireless network using TCP and UDP over distributed coordination function as a function of the number of stations in competition to access the base station, the packet size and the transmission rate of the stations. This mathematical model is then confirmed by experimentation and provides satisfactory accuracy. In this thesis, TCP/IP is designed to transmit/receive data host to host via Wi-Fi & WiMAX wireless networks. Next, related work on the analysis of robust stability is reviewed.

2.5 ROBUST STABILITY ANALYSIS IN SWNCS

Stability is is very significant in system analysis and design. Numerous results have appeared in previous work to analyse the robust stability in the presence of network time delays and packet dropouts in SWNCS. For example, Wu et al [122] proposed to design a robust state feedback guaranteed cost controller so that the resulting closed-loop system is robustly stable, and a specified quadratic performance index is upper bound for all allowable uncertainties under network time delays and packet dropouts. A model of NCSs is established which includes two additive delay elements, one being an identified constant, and the other an unidentified constant. However, employing the Lyapunov-Krasovskii functional method, the sufficient conditions on stochastic stability and H_∞ performance for the faulty NCS were analysed by Xie et al, Figueredo et al and Zhang et al [123-125]. The stability and stabilization problems of a class of NCSs with bounded packet dropout were considered in research by Sun and Qin [126]. Both sensor-to-controller and controller-to-actuator packet dropouts have been taken into account. Ge et al, Ge and Jiang and Li et al [127-129] all presented work on robust stability criteria of NCSs with the influences of both the variable network time delay and packet dropout taken into consideration. A less conservative delay-dependent stability condition is expressed in the structure of a LMI based on a Lyapunov–Krasovskii functional. In another publication, Seuret [130] proposed a new approach to measure the stability of linear systems with network time delayed and sampled-data inputs. The author considered both asynchronous sampling and input time delay based on an expansion of present results on the stability of sampled-data systems to the case where a time delay is established in the control loop. The stability properties of discrete-time networked linear systems with Markovian packet dropouts were considered Xie and Xie [131]. A binary Markov chain were utilised to describe the packet dropout fact of the network. Required and sufficient conditions for the stochastic stability properties were recognized. Those conditions are based on the associations of stability properties between the systems developing in deterministic continuous-time, deterministic discrete-time, and arbitrary discrete-time. Furthermore, Ko et al [132] deal with the problem of stability analysis for NCSs through the network time-delayed system approach. The network time delays are modelled as two additive variable time delays in the closed-loop system. To verify the stability of such special characteristic systems, a suitable Lyapunov-Krasovskii functional is suggested and the Jensen inequality lemma is applied to the integral terms that are derived from the derivative of the Lyapunov-Krasovskii functional. A robust stabilization problem of a class of uncertain nonlinear systems employing output measurements through a finite data-rate communication channel are discussed. Cheng [133] assumed that there exist an observer and a control law for the systems in the absence of any finite data-rate communication channel. Based on the observer and the control law, the author constructed an encoder/decoder pair and supplied a sufficient condition, counting appropriate sampling time and data-rate, which will guarantee the stability of the closed-loop system when a finite data-rate communication channel is presented. Azimi-Sadjadi [134] demonstrated the conditions under which undisturbed NCSs are mean square stable. These conditions can be verified rather simply if the parameters of the non-NCS and the packet dropping rate in the network are given. If the dropped packets are not re-transmitted these conditions are required and sufficient for stability. The model of MIMO NCS with state feedback is demonstrated in works by Liu and Li [135]. The delay-independent stability condition is derived according to Lyapunov stability theory. Peng et al [136] described the NCS with a network time delay and packet dropout. With this model, a less conservative stability condition has been recognized, which is dependent on the lower and upper bounds of the corresponding network time delay to guarantee the asymptotic stability of the NCS with parameter uncertainties. The stability analysis results have been more applied to the output feedback stabilization of the NCS. Hao and Zhao [63] were concerned with the static output-feedback stabilisation problem of discrete-time NCSs. If the controlled plant is a discrete-time system, the NCS with time-varying network time delays and data packet dropouts in the transmission is modelled as a discrete-time system with variable time delays in the state.

In contrast, little research employs H_∞ and H_2 to analyse robust stability. For example, Jiang et al and Wang et al [137-138] looked at robust H_∞ control of linear NCSs with time-varying network time delay and data packet dropout. A new Lyapunov–Krasovskii functional, which formulates the utilisation of the data of both the lower and upper bounds of the time-varying network time delay, is proposed to drive a new delay-dependent H_∞stabilization criterion. The criterion is formulated in the form of a non-convex matrix inequality, of which a reasonable solution can be achieved by solving a minimization problem in terms of LMIs. Then, Jia et al [139] proposed an estimation technique to compensate the packet dropout. Furthermore, the design of H_∞ control is considered for the available and unavailable states, respectively, and several sufficient conditions are derived such that the closed-loop control systems are exponentially mean-square stable with prescribed H_∞ perturbation decrease level. The problem of H_∞ control for a class of network predictive control systems has been considered by Wang et al [140]. An enhanced compensation strategy based on the average **dwell-time** technique was combined with a new controller design approach to construct the equivalent closed-loop control system exponentially stable with the H_∞ performance bound. Xia et al [141] consider the design of NCSs with random network time delay in the sensor-to-controller channel and H_2 of closed-loop networked predictive control systems. A new networked predictive controller is suggested to overcome the effects of network time delay and packet dropout. The necessary and sufficient conditions on the stability of the closed-loop NCS and the performance of H_2 are derived. The NCS with both multiple measurement and control packet dropouts are first modelled as a random parameter system. This includes two independent Bernoulli distributed white sequences, and an observer-based feedback H_2 controller based on a LMI to guarantee the NCS to be asymptotically mean-square stable and to maintain a guaranteed H_2 performance. This work is presented by Wang et al [142]. In this thesis, we analyse the robust stability based on both H_∞ and H_2 norms.

2.6 CHAPTER SUMMARY

In this chapter, research on the adaptation of Wi-Fi & WiMAX wireless networks in WNCS covering the last few decades has been reviewed.

Real-time communication is one of the most significant requirements for an SWNCS. Wi-Fi & WiMAX wireless networks are usually considered inappropriate for SWNCS due to the network time delays and packet dropouts. However, with the development of Wi-Fi & WiMAX wireless networks towards high QoS, the real-time performance of Wi-Fi & WiMAX wireless networks have been evaluated and some transport protocols have been developed to provide the real-time requirements of SWNCS.

From the control theory viewpoint, the effect of network time delays and packet dropouts on the system performance is avoidable by using some predictive controller techniques. Such schemes have been designed to enhance the system performance. Also, robust stability analysis has been measured. Furthermore, to validate communication and control methods for SWNCS, some simulations have been proposed to simulate SWNCS.

In this chapter, the research gaps in the adaption of Wi-Fi & WiMAX wireless networks in SWNCS have been highlighted as:

- For evaluating the real-time performance of Wi-Fi & WiMAX wireless networks, the traffic features in an SWNCS, for example periodic traffic, were not analysed by most present analytical models.
- To remove or reduce the effect of network time delays and packet dropouts from SWNCS, some predictive controller methods have been designed. However, they are based on some assumptions such as Markovian Chain control delays, which may not be accurate in a practical system.

Finally, most present SWNCS simulation solutions employ simplified or static assumptions, so they lack standardisation, flexibility and cloning.

CHAPTER 3 ..

IMPLEMENTATION OF AN SWNCS

3.1 INTRODUCTION

Solar power systems are progressively employed for a variety of applications, for example, new wireless street lighting, wireless surveillance and wireless communication. A solar powered solution for wireless street lighting system is presented, wireless Surveillance and wireless communication. There are numerous motivations why solar power is a good alternative to conventional power sources street lighting and wireless networks. When deploying wireless systems, power is not always available where we need it. It is also cheaper to install solar than using a conventional power line. Solar power is always on in times of emergency when conventional power may have gone down, solar pays for itself over time.

SWNCS is a system which permits the provision of many services comprising wireless internet, wireless street lighting, and wireless surveillance. It merges a unique set of powerful benefits such as solar power, battery back-up, low cost maintenance, access to wireless broadband services and ever-evolving amount of add-on applications. SWNCS offers a sustainable, multi-service infrastructure explanation for the developing world, allows support for wireless controlled allowed, LED street lighting combined with a wireless communications network (Wi-Fi/WiMAX), all powered by solar energy. A SWNCS proposes the following features and benefits; safety and security, wireless internet, Voice over Internet Protocol VOIP telephony, and remote diagnostics.

3.2 ARCHITECTURE OF AN SWNCS

The virtual SWNCS core items consist of three major packages; SWNCS lighting, communication systems, Network Management Centre (NMC). Figure 3.1 illustrates how each pylon in virtual SWNCS appears in the real-world.

1. A SWNCS lighting system consists of a kit that contains several components. This kit is intended to be mounted on one Pylon. The kit contains:
   - A LED being the street light
   - Solar power system that contains the following components:

    - A battery which provides power when the sun has not been available for a period of time.
    - A solar panel as the main power source.
    - Controller unit which integrates the charge controller, radio, CPU and anti-theft into one unit.
2. The communication system contains:
    - A SWNCS access point to connect the street light system to the backhaul system.
    - A SWNCS Wi-Fi & WiMAX controller/backhaul provides the connection to SWNCS backhaul connection on one side, and Wi-Fi & WiMAX subscribers on the other side.
3. Network Management Centre (RMPC)

3.2.1 Solar-Power System Components

Solar-powered systems consist of solar panels, a battery, charge controller, and an inverter. The lifetime of the panels is usually 25 years, which reflects the lifetime of the whole system. The battery saves the power from the sun and is employed when the sun isn't shining or through cloudy weather. The charge controller regulates the current added to and drawn from the battery in order to maximize the battery lifetime and for user safety. Since solar-powered systems create a direct current, the inverter is required especially when the end-user requires an alternating current [143].

3.2.2 SWNCS Access Points

The SWNCS access point presents Ethernet connection and Power-Over-Ethernet (PoE) -48 volt supported to the Wi-Fi /WiMAX based integrated access point and backhaul system. The SWNCS radio is battery powered, and characteristics very low power operation 150 KBPS data rate and it has a 12 volt solar power input and connection to a 12 volt DC battery for night operation [144]. Wi-Fi and WiMAX wireless networks are often deployed in tandem by service providers and municipalities since many mesh deployments require backhaul connectivity, which can be provided efficiently by WiMAX. A WiMAX deployment requires Wi-Fi mesh to provide access to the growing base of Wi-Fi enabled devices and multi-mode Wi-Fi phones. Wi-Fi/WiMAX products used in a typical outdoor broadband wireless network will now be discussed [145].

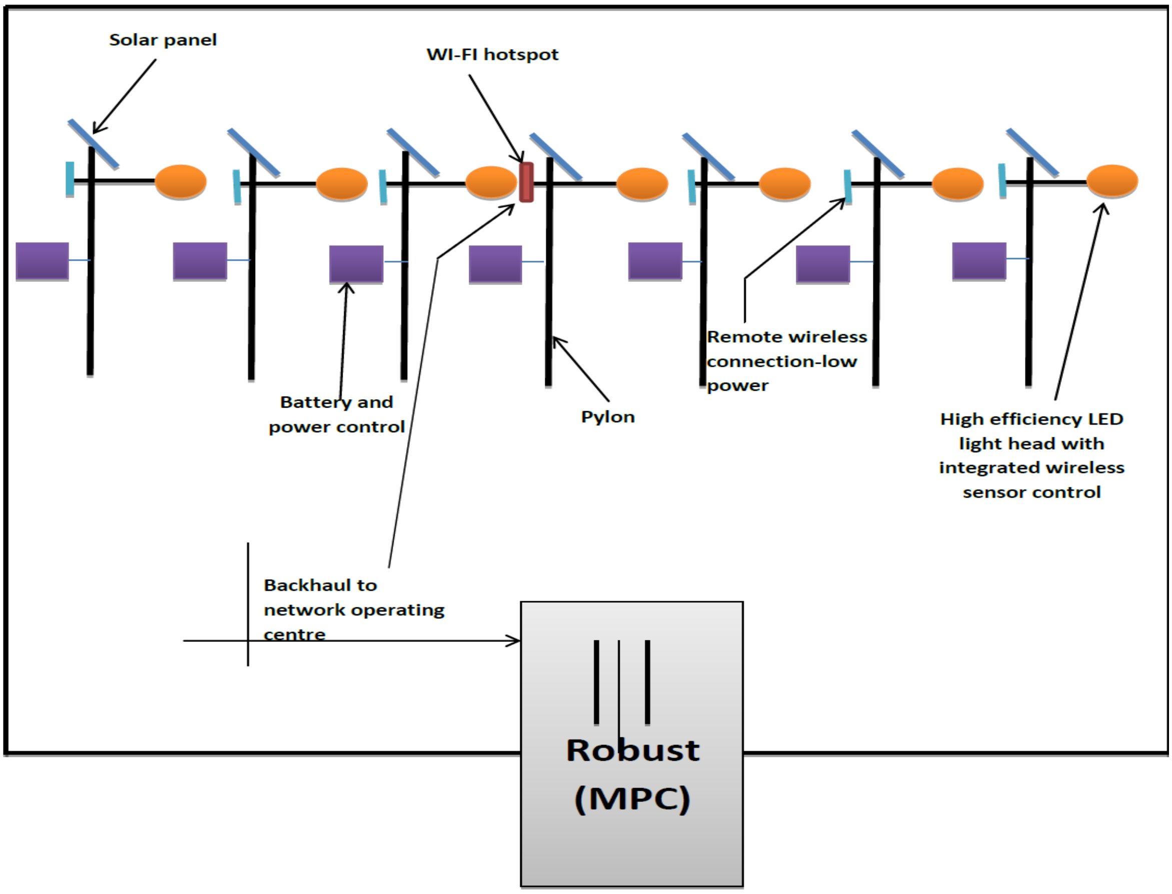

Fig. 3.1. Virtual SWNCS in Real-World Pylons

3.3 NETWORK MANAGEMENT CENTRE

The SWNCS will be government appointed and funded. The SWNCS is implemented in each country by what is called a network operating centre. The network management centre is the robust control centre for operations, hosting network management and management centre for street lighting network control reporting critical information round the clock day and night. The Network management centre provides SWNCSs with a low cost flexible operating centre on which to base their wholesale model. Further, it allows SWNCS to connect to satellite or fibre optic backhaul networks depending on each country’s requirements. The SWNCS management system is a robust controlling, comprehensive, real-time remote system for monitoring and troubleshooting. The SWNCS provides the ability to remotely turn on/off the lights; it also monitors the ongoing status of all nodes. Furthermore, it flags various problems to initiate service calls including missing nodes [146].

3.4 SOLAR-POWERED SYSTEM DESIGN

The Solar-power solution was designed to work continuously for 24/7/365. Some issues were taken into consideration during the design phase, which are as follows [147]:

- Balance of the rate of solar power authentication in an area with the power required by the load.
- Every day peak sun hours, load power requirement, battery storage and discharge efficiencies were considered to achieve the required capacity/number of panels.

In the design example, the power rating of the model SP90 LED street lighting is 28 Watts [148]. The transmission power for Wi-Fi is 30dbm=1000mWatts and receiver threshold is -48dbm=$1.58e^{-005}$mWatts with coverage area approximately 7.69 meters. The transmission power for WiMAX is 23dbm= 200mWatts with coverage area of approximately 1.5 kilometres. The rating power for a wireless network is 5 Watts. The total power in each pylon that consisting of a street lighting system and wireless networks = 28+5=33 Watts. Based on the total power consumption in each pylon, the number and size of solar panels required as illustrated in Table 3.1. In contrast, the battery size and number of batteries required for the developed system is illustrated in Table 3.2 [147]. The maximum power drawn is 100Watts and the system voltage is 12 volts, where I=P/V, therefore: I=100/12=8.33 Amps. This means a charge controller with approximately 10 Amps is required.

3.5 SOLAR STREET LIGHTING WITH BROADBAND WIRELESS INTERNET ACCESS

There may also be numerous applications that require wireless data connectivity in times of emergency that are independent of power or require portability or fast temporary deployment of equipment.

- Public security or disaster improvement where permanent deployments are installed with solar to present network connectivity in times of emergency and temporary communications points can be setup autonomous of vehicle power or a failed or damaged power grid.

- Transportation service and maintenance already uses isolated care and information signs powered with solar energy. Wireless stations can be powered the same way to supply data communications. This is particularly useful for main projects that may comprise a satellite office location for an extended period of time [144].

Table 3.1. Solar Panel Sizing

Solar Panel Sizing	Value
Daily Photo Voltaic (PV) output need	(28+5)W*24h=792Wh
80% effeciency factor	792/0.8=990Wh
Average sun light hours per day	10h
Minimum system size	990Wh/10h=99W
Chosen system module	100W
No. of modules required	99/100=0.99 ≈1of100W module

Table 3.2. Battery sizing

Battery Sizing	Value
System voltage	12Volts
Total Ampere-hours per day	792Wh/12V=66AH
Discharge reserve	40.635AH
Optimum battery size	40.635AH
Chosen Amper-hours per battery	50AH
No. of batteries required	40.635AH/50AH=0.8127≈ 1 battery

All of this provides an almost unmatched level of flexibility in deployment allowing us to produce all in one systems of radios and power source that can be mobile, present temporary service, or be redistributed quickly. Outside Broadband Wireless needs as much line of sight as possible. Also, range constraints and obstacles require that we place multiple APs in a given area. Frequently, the installation point of an AP that gives you the best coverage may not have any power source, or may want modifications to existing power. These include: installation points where power is not available such as rooftops with no egress point, locations without available light pylons, open areas such as parks, light pylons that are only powered at night, remote locations in rural and forest or remote areas in developing countries where power has never been run. A further example is power systems that are not compatible or only have dangerous voltages available that would want alterations such as addition of large transformers.

The explosive universal development of the wireless internet access phenomenon through the propagation of Wi-Fi/WiMAX depends on the distance between each Pylon. Therefore, all urban and rural communities can provide their residents and businesses with a low-cost solution for broadband wireless internet access. SWNCS provides clients a complete wireless broadband solution that brings protected internet access and permits various city government departments such as police, fire and government employees to use the same

SWNCS without mobility limitations. In addition, SWNCS uses the Wi-Fi/WiMAX, allowing clients with Wi-Fi enabled laptop computers or handheld computing devices to access the network without new hardware or software. SWNCS can present the following characteristics as illustrated in Figure 3.2: mobile internet access, multi-radio, multi-channel, multiple hopping to solve the non-line of sight issue, TCP/IP routing to enhance the performance and be decentralized to avoid a central point of failure. Furthermore, the SWNCS can transmit power control to reduce the effect of delays and packet dropouts in often encountered.

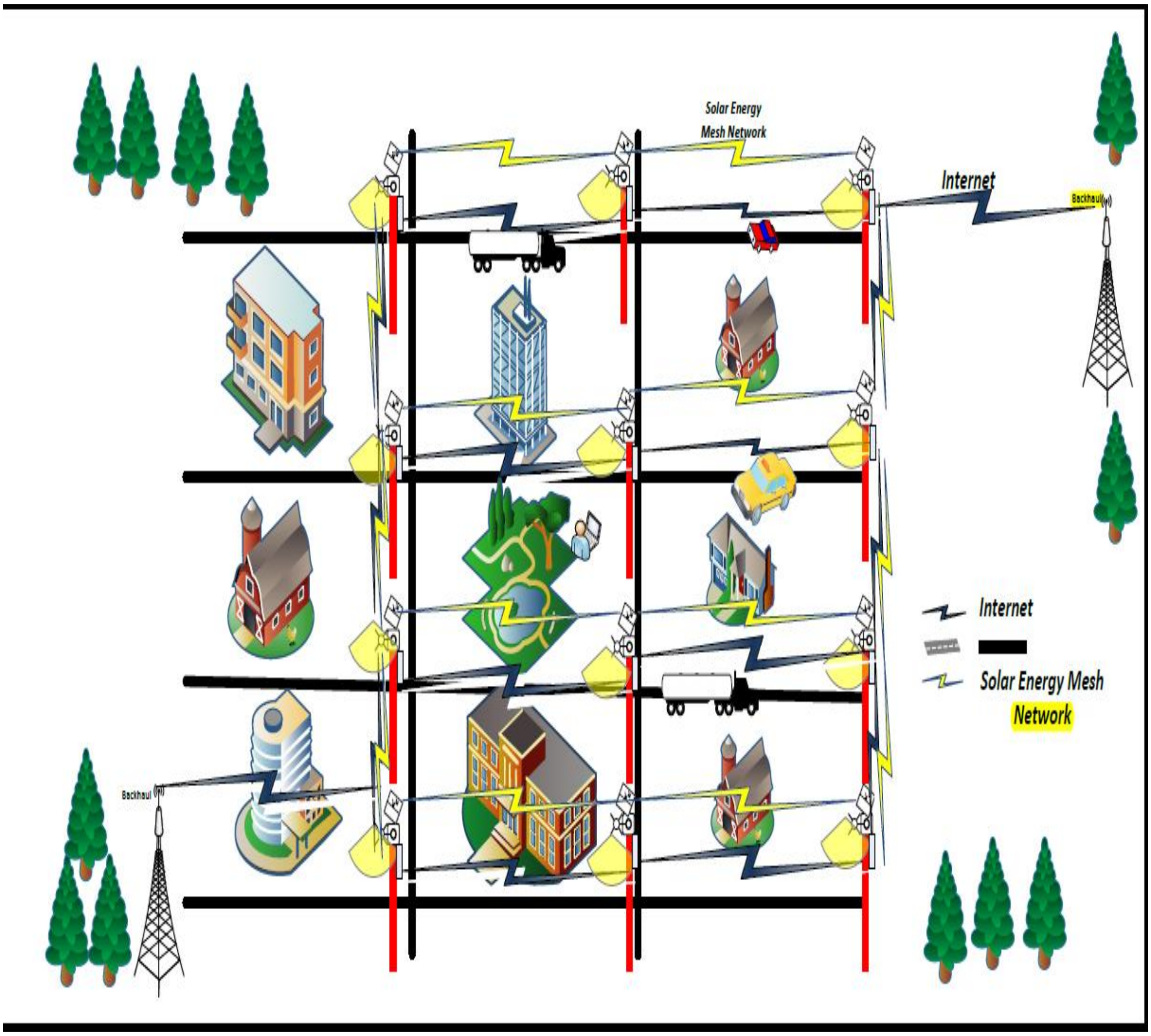

Fig.3.2. The Virtual Solar Street Lighting with Broadband Wireless Internet Access

3.6 TCP/IP PERFORMANCE ON SWNCS

Investigation in transport protocol over IEEE802.11/WiMAX with various signal levels have demonstrated that without retransmission applied at the link layer, dropout rates become unacceptable for any application. It was also shown that the MAC layer retransmissions enhance TCP performance. On the other hand, a high number of frequent retransmissions can cause TCP to timeout anyway and retransmit similar information as the MAC layer. Furthermore, MAC retransmissions can be improved and potentially harmful for time-sensitive applications, for example real-time video or audio over UDP. The Wi-Fi/WiMAX MAC layer protocol tries to face the packet dropout challenge by using its own retransmission method.

In particular, dropped data are retransmitted after a certain period of time without having received any equivalent ack. Successive retransmissions for similar data are repeated equal to a maximum number of times, that is by default set to numbers in the standard Wi-Fi, or until receiving a successful ack [149-151]. This method hides wireless fault losses from the TCP overcrowding control method, therefore avoiding harmful multiple decreases of the data sending window. Conversely, local retransmissions influence packet delivery time delay by increasing its unpredictability and thus affecting time-constrained applications for example audio or video stream. The first TCP executions were employing cumulative positive recognitions and wanted a retransmission timer expiration to send a dropped data throughout the transport. Wi-Fi/WiMAX MAC layer responds via local retransmissions which in turn cause following data to wait in the queue until the scheduled ones or their retransmissions finally reach the receiver. The back off mechanism of the Wi-Fi/WiMAX presents an increasing amount of time before attempting again a retransmission [152].

3.7 SIMULATION SCENARIO

The network design of the simulation scenario that is the subject of the analysis in this thesis is presented in Figure 3.3. MATLAB/SIMULINK has been used in order to simulate point-to-point (one node) the outdoor environment presented in Figure 3.3. Network topology consists of wireless nodes. The distance between nodes is set at 20m and 10km. The wireless nodes are configured to work according to the Wi-Fi (IEEE802.11b) when the distance is 20m and WiMAX (IEEE802.16e) when the distance is 10km.

In mesh wireless networks, each node Wi-Fi/or WiMAX connects to numerous neighbouring nodes and on to a gateway i.e. a WiMAX that collects the mesh wireless network traffic and routes it to be the Internet. The fact that each node has several routes to a gateway makes the mesh wireless network very reliable.

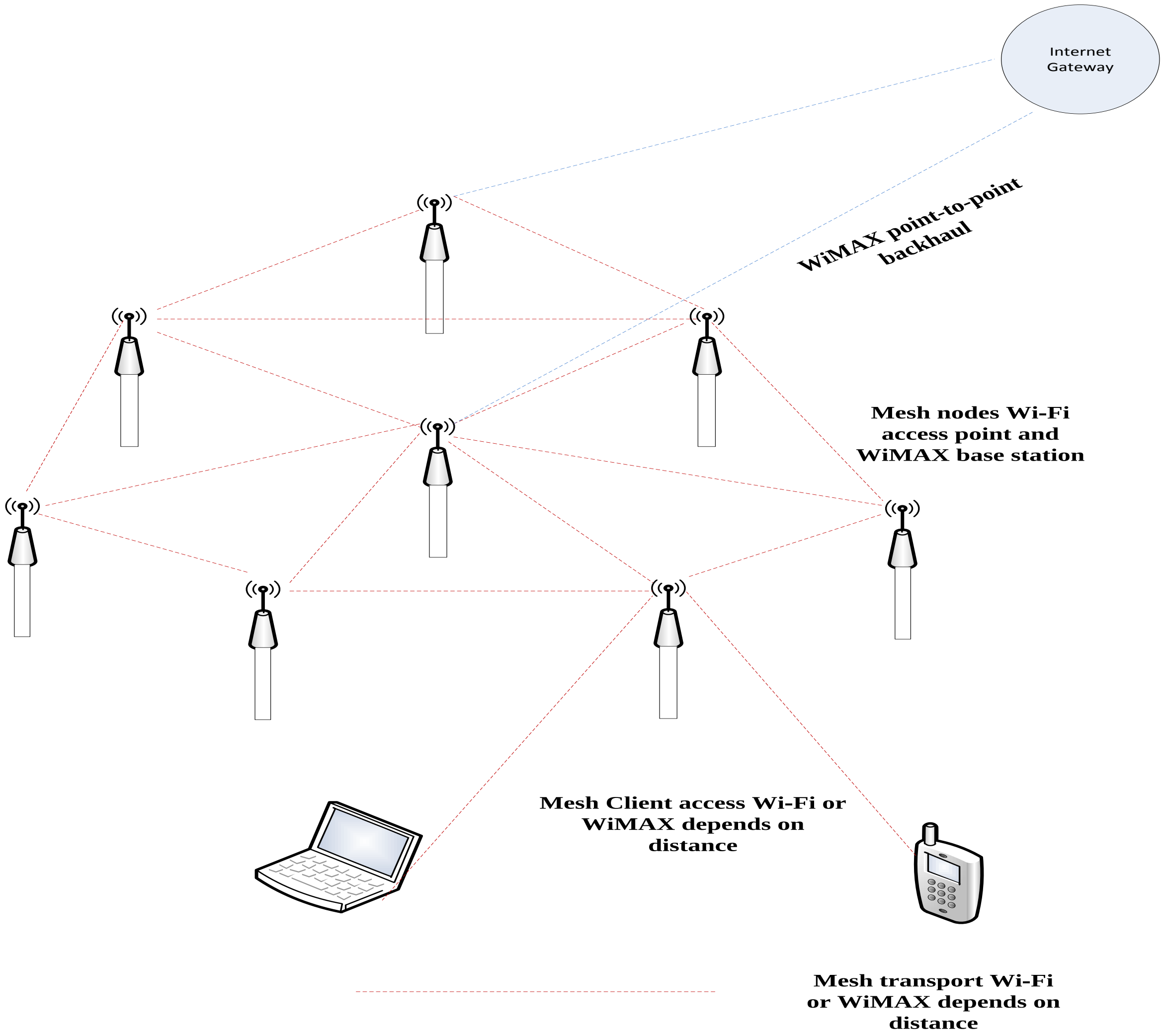

Fig.3.3. Simulation Scenario for the Wireless Network with Wi-Fi/or WiMAX

There are three layers in the present wireless network architecture; mesh access managing clients access to a mesh node, mesh transport linking mesh nodes and routing traffic to mesh gateways, further backhaul connecting a mesh gateway to an Internet point of presence [153]. This scenario constructs a simple model using MATLAB/SIMULINK library and illustrates how to send information to an echo server using TCP/IP and to read that data back into your model. An echo server will be created on a machine that will simulate sending a signal to the TCP/IP send block. The result will be echoed back to the send block to transmit data via Wi-Fi or WiMAX wireless networks and then the TCP/IP receive block will be used to read that same data back into the model in the same way as shown in Figure 3.4. The sending signal and receive signal when using Wi-Fi or WiMAX is shown in Figure 3.5.

3.8 MAINTENANCE OF SWNCS

When comparing solar power against conventional power there are some compelling things to take note of:

- High quality solar panels can have a warranty lifetime of up to 25 years.
- High quality solar battery backup systems can last up to 10 years.
- Incidental maintenance for equipment damage carries different costs between solar and traditional power
  - Utilities generally require the use of certified linesman when working with anything on their pylons.
  - Solar equipment is not linked to the infrastructure allowing utilisation of less expensive labour.
- When connected to the conventional power infrastructure you are subject to any power outages and downtime that the service experiences. Solar can supply in excess of 99.999% uptime.
- Solar power means that the equipment will continue to work even during local or city-wide power breakdown.
- A solar powered system may operate for up to 10 days or more without sun!

Despite a higher initial cost when deploying solar power, the reduced maintenance costs combined with the flexibility to install anywhere allows you to use this type of network for a variety of needs as well as get around obstacles encountered when traditional power is used [154].

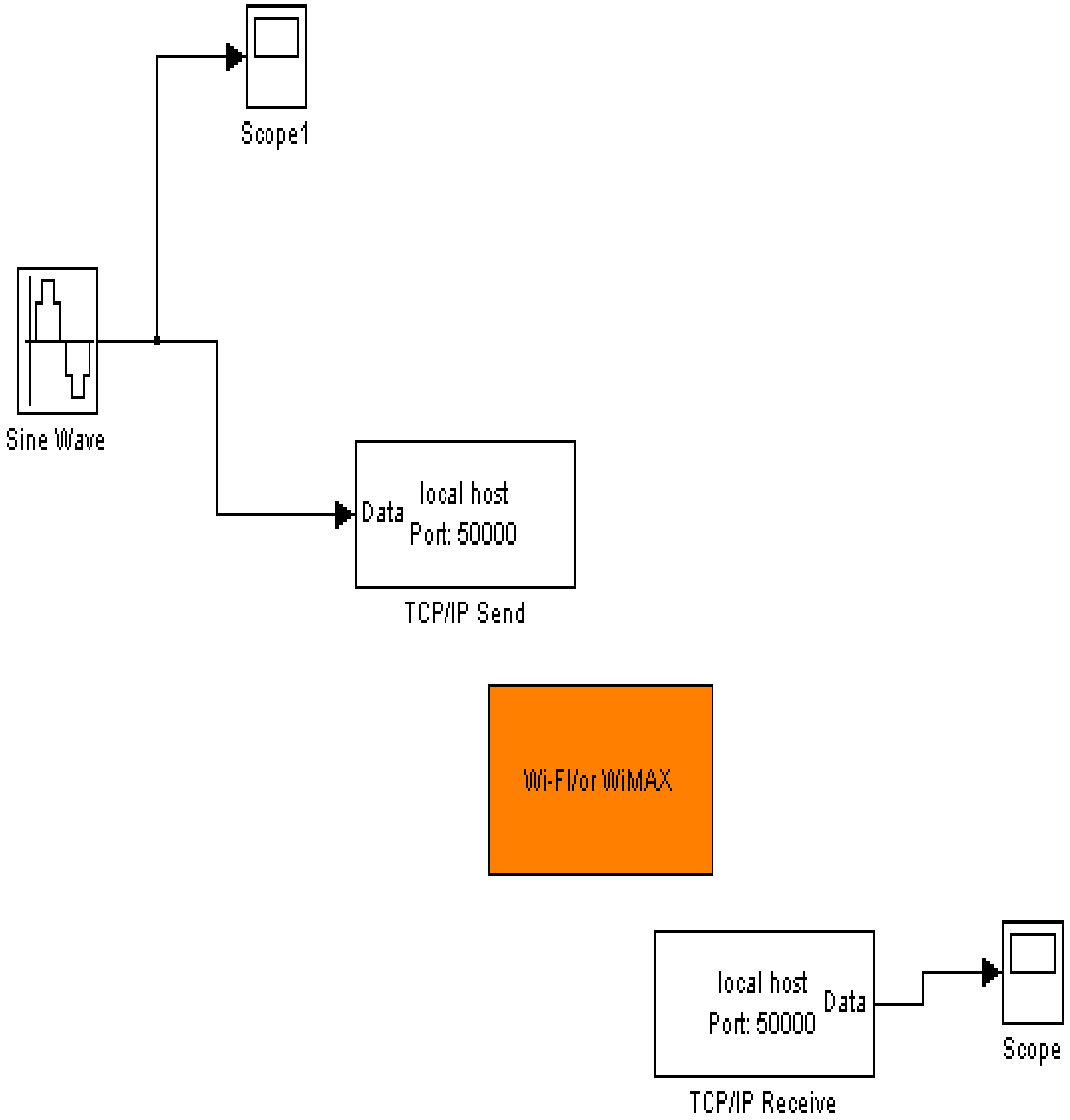

Fig.3.4. SIMULINK Model of Send and Receive Data via TCP/IP Routing

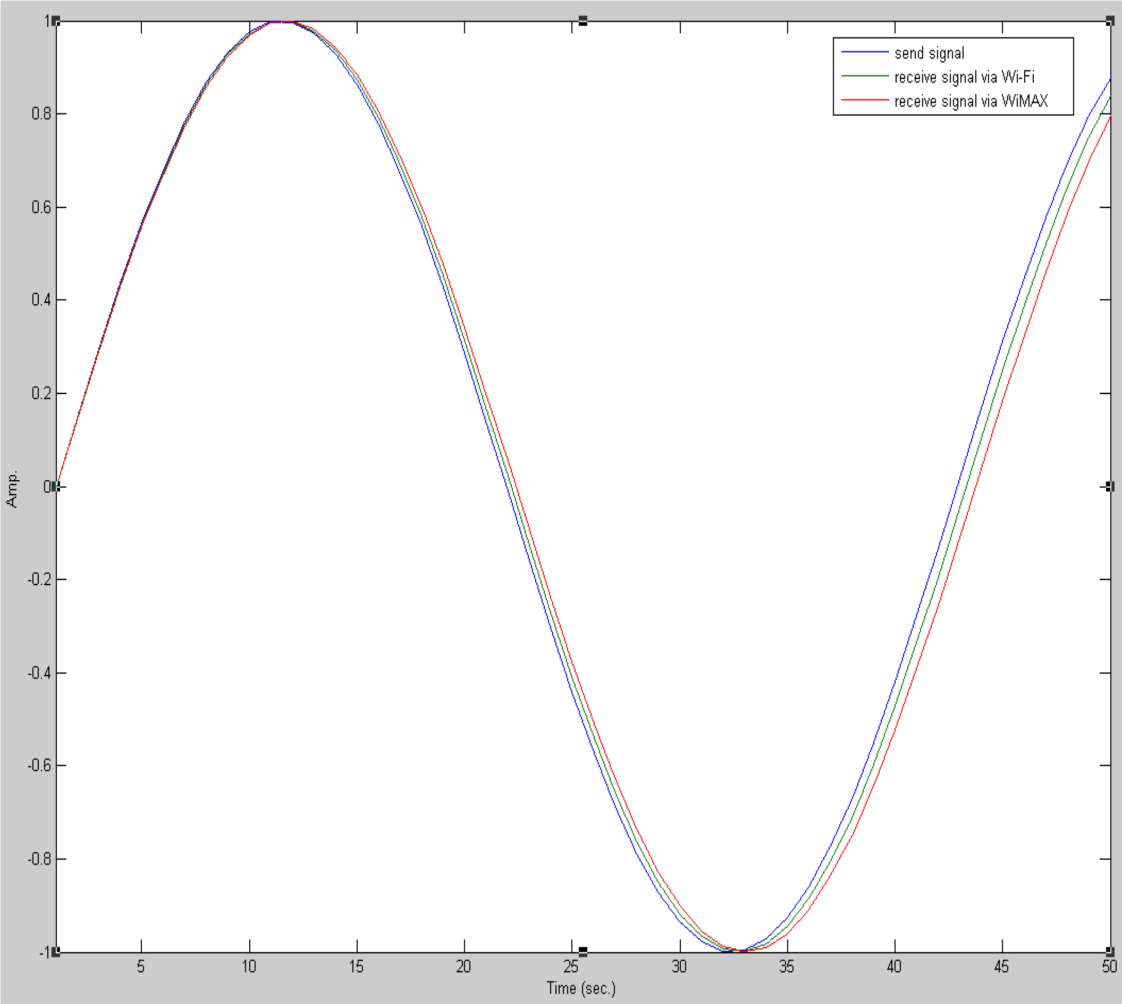

Fig. 3.5. Simulation Output for TCP/IP Routing

3.9 CHAPTER SUMMARY

SWNCS presents a range of services for many cities and rural environments. The highlighted points of the SWNCS are summarized as:

1. **Solar power is both a benefit and a necessity in many areas**

   SWNCS low energy lights use the latest solar and high power LED technologies. Reliable, long life LED lamps are less fragile and save energy compared with conventional street lights. Therefore SWNCS is considered as a pollution free development, no re-occurring energy costs, power where no conventional power exists, portability and fast deployment, flexibility to install nearly wherever, backup even when the conventional electrical grid maybe down for days, and solar powered systems present a deposit benefit of a system that operates when all else has failed.

2. **Low power consumption is critical**

   Reduces the size of the solar power system required and helps maintain availability and reliability.

3. **Wireless broadband products are the best fit for solar power systems**

   Wi-Fi and WiMAX products have the lowest power consumption in the industry. Small form factor radios allow for rapid deployment and redeployment, public safety solutions to take advantage of the flexibility and portability, go green and install where you want with a truly wire-free Outdoor Wireless Broadband network. The SWNCS can be configured to provide QoS that allows priority to be given to different types of traffic from different clients. If configured correctly, the SWNCS can provide voice mobility through VoIP allowing clients to roam across the SWNCS without losing the signal. The SWNCS administrator lowers maintenance costs to a significant extent for example maintenance crews are only sent to faulty fixtures, rather than having to inspect all lights on a regular basis. The SWNCS allows direct CCTV camera connection to remote administrator stations or any authorised enabled PC. Once duly authorised and connected to the network, emergency service vehicles can tap in to local CCTV images and be where and when needed.

CHAPTER 4 ..

SWNCS MODELLING AND SIMULATION

4.1 INTRODUCTION

SWNCSs are a form of distributed control system, where the control system data components such as reference input, plant output, and control input, etc. are exchanged through wireless communication networks. Due to the introduction of communication networks, SWNCSs have numerous smart benefits, such as no system wiring, low weight and space, simplicity of system diagnosis and maintenance, and increased system flexibility. All these attributes have encouraged research in SWNCSs. However; the introduction of communication networks also faces some challenges, for example, network time delays and packet dropouts. In this chapter, the wireless network model based on MATLAB/SIMULINK for both Wi-Fi/WiMAX physical layer models, SWNCS simulation TrueTime tools is presented for dynamics of a SWNCS. Furthermore, the model and design of a photovoltaic and battery power system has been developed and simulations have been achieved so as to supply electricity to a DC load.

The photovoltaic module creates electricity to meet the requirements of a load. When there is sufficient solar emission available, the external load can be powered completely by the photovoltaic source. For continuous-power supply of the load, a battery bank is employed with the photovoltaic module. Throughout the time of low insulation, an auxiliary electricity source is required. All the developed models are based on physical standards, in addition to experimental parameters. The state space model for the whole system is derived.

4.2 WIRELESS NETWORK MODEL

4.2.1 Wi-Fi (IEEE802.11b) Model

In the WI-FI simulation model, a packet broadcast is demonstrated in the following approach. The node that has requirements to transmit a packet verifies to realise if the intermediate is idle. The broadcast may continue, if the intermediate is established to be idle, and has remained consequently for 50µs. If, in contrast, the intermediate is established to be occupied, a stochastic back-off period is selected and decremented in the similar method such as when clashing occurs. When a node begins to transmit, its comparative location to all additional nodes in the similar network is measured, and the signal stage in all additional nodes are measured in relation to the path failure expression $\frac{1}{t^a}$. Where, t is the distance in meters and a is a parameter chosen to model the environment [155].

The signal is supposed to be conceivable to discover if the signal stage in the receiving node is greater than the receiver signal verge. If this is the situation, then the Signal to Noise Ratio (SNR) is measured and used to discover the block error rate. Observe that all additional broadcasts add to the related disturbance when computing the SNR. The proportion of number of incorrect blocks to overall number of blocks received on digital circuit is called the Block Error Rate (BLER) [156]. The BLER collected along with the size of the message, are used to measure the quantity of bit errors in the message and if the fraction of bit errors is smaller than the error encrypting threshold, then it is supposed that the channel encrypting structure is capable of completely restructuring the message. If there are already continuous broadcasts from additional nodes to the receiving node and their various SNRs are smaller than the recent one, then those messages are completely marked as clashed. Similarly, if there are additional continuous transmissions arriving from the submitting node then those messages may be marked as clashed as well.

Note that a transport node does not distinguish if its message is clashing, therefore ACK messages are transmitted on the Medium Access Control (MAC) protocol layer. From the viewpoint of the transport node, missing messages and message crashes are similar, that is, ‘certainly not ACK’ is received. If ‘certainly not ACK’ is received throughout ACK timeout, the message is retransferred subsequently waiting a stochastic back-off period within an argument space. The argument space amount is twice for each re-transfer of a definite message. The back-off regulator is block-off if the intermediate is occupied, otherwise if it has not been idle for at least 50μs [157].

Model of IEEE 802.11b wireless network physical layer, supporting, 1Mbps, 2Mbps, 5.5Mbps, and 11Mbps modes. Model includes framing, long and short preamble, DBPSK and DQPSK modulation, Barker code spreading, Complementary Code Keying (CCK), root raised-cosine pulse shaping, channel number selection (frequency shift) and an AWGN channel. The physical layer parameter simulation is identified as shown in Appendix B [158]. Figure 4.1 illustrates an IEEE802.11b SIMULINK model.

Furthermore, the frequency response for IEEE802.11b as shown in Figure 4.2 (a), the receiver power spectrum and signal constellation of IEEE802.11b are demonstrates in Figure 4.2 (b, c) respectively.

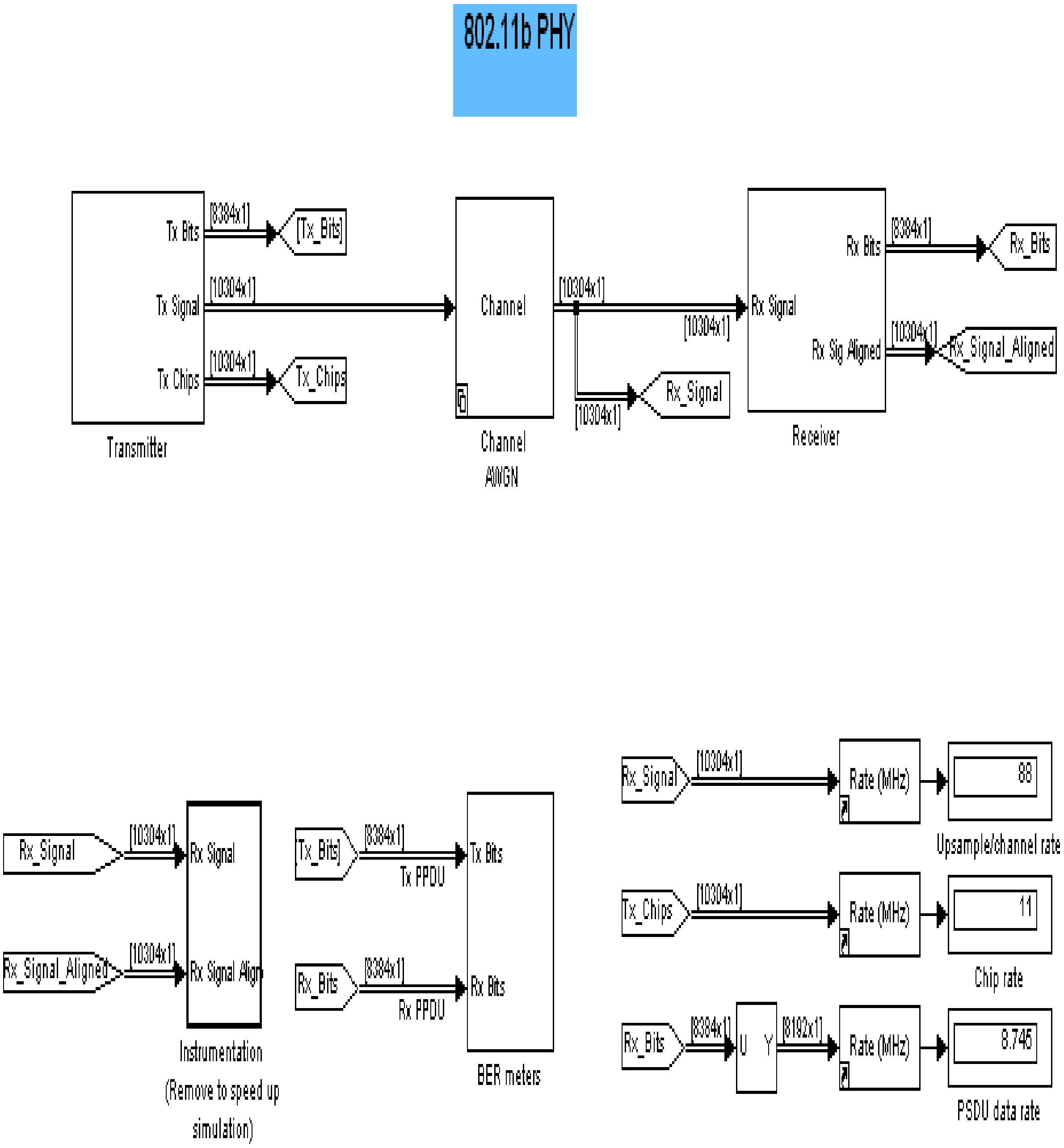

Fig.4.1. SIMULINK Model for IEEE802.11b

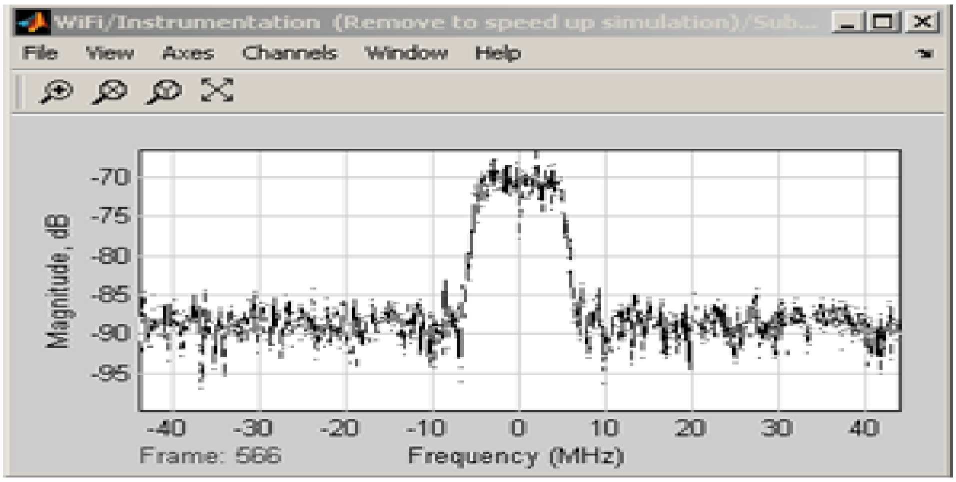

Fig.4. 2 (a). Frequency Response of IEEE802.11b

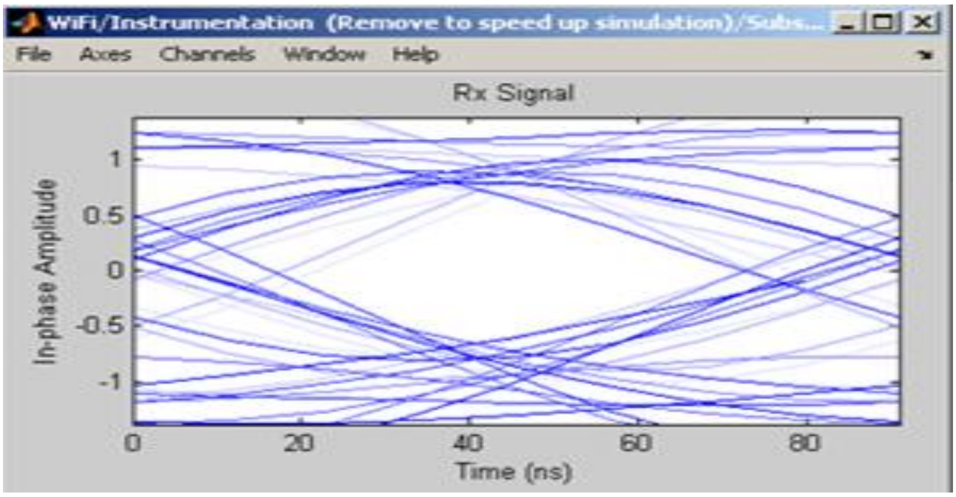

Fig.4. 2 (b). Receiver Power Spectrum of IEEE802.11b

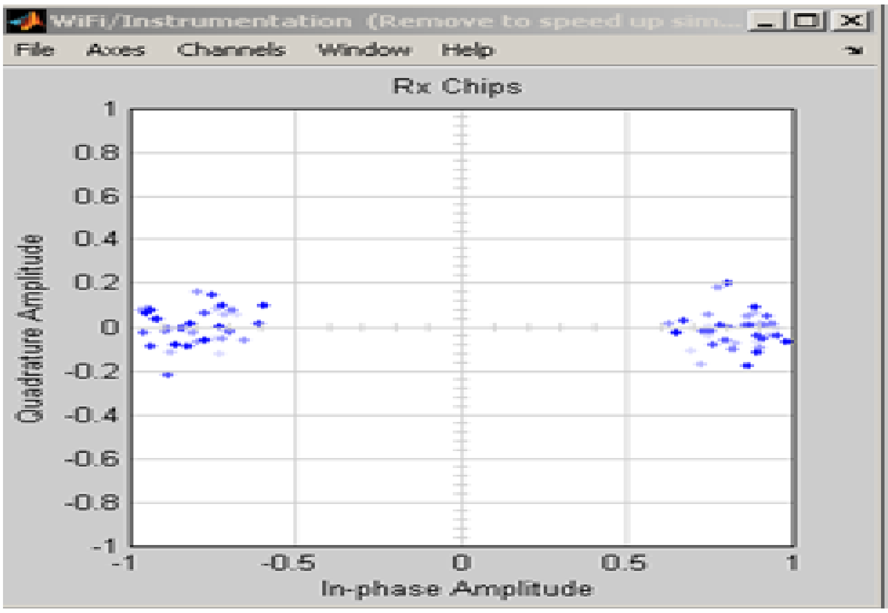

Fig.4. 2 (c). Signal Constellation of IEEE802.11b

Fig.4.2. On-line Simulation for IEEE802.11b

4.2.2 WiMAX (IEEE802.16e) Model

WiMAX has three elementary components; a transmitter, a channel through which the data is sent, and a receiver. The main elements of a WiMAX communication scheme are presented in Figure 4.3. The practical blocks that constitute the transmitter of the WiMAX emulator are described in Figure 4.4. While interactive through a wireless radio set channel, the received signal cannot be just demonstrated as a transcript of the communicated signal degraded by Additive Gaussian Noise (AGN). Alternatively, signal attenuation, though produced by the variant-time appearances of the transmit setting seems, like this, small period oscillations produced by signal dropping of packets in the transmit setting cause a phenomenon identified as multipath transmit. The period scattering in a multipath setting produces the signal to experience either flat or frequency-choosy attenuation. Moreover, the period scattering is established by the scattering in time of the controlled codes directing to Inter Symbol Interference (ISI). So as to evade ISI in OFDM schemes, the recurring preface period has to be selected greater than the extreme delay feast of the channel. Furthermore, Root Raised Cosine (RRC) filters, typically employed for band bounding the communicated signal, are used as extrapolation filters in the trainer. The receiver fundamentally achieves the inverse process as the transmitter in addition to channel estimation essential to uncover the unidentified channel factors as demonstrated in Figure 4.5 [159]. The WiMAX SIMULINK model and SIMULINK library are illustrated in Figure 4.6. Transmitted and received signals constellation with DQPSK modulation of WiMAX are illustrated in Figure 4.7 (a, b). Figure 4.7 (c, d) demonstrates the transmitted and received power spectrum of WiMAX.

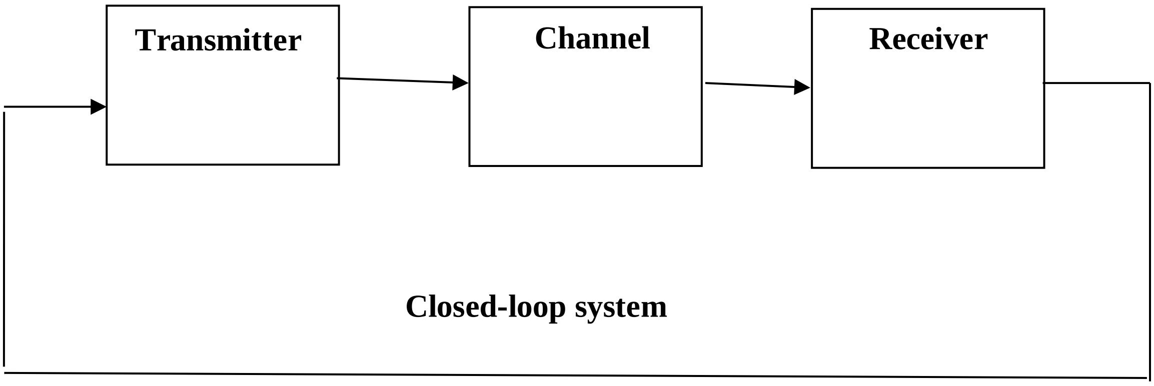

Fig.4.3. WiMAX Basic Communication System

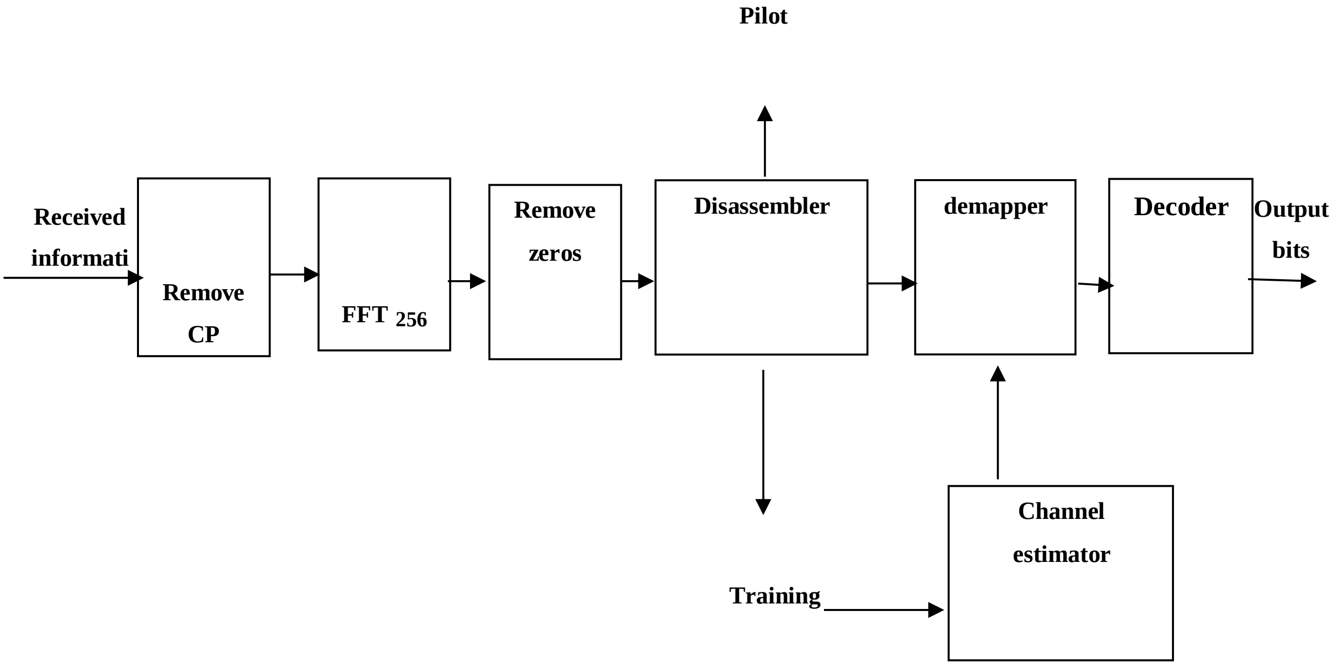

Fig.4.4. Transmitter Structure of WiMAX for 256 Subcarriers

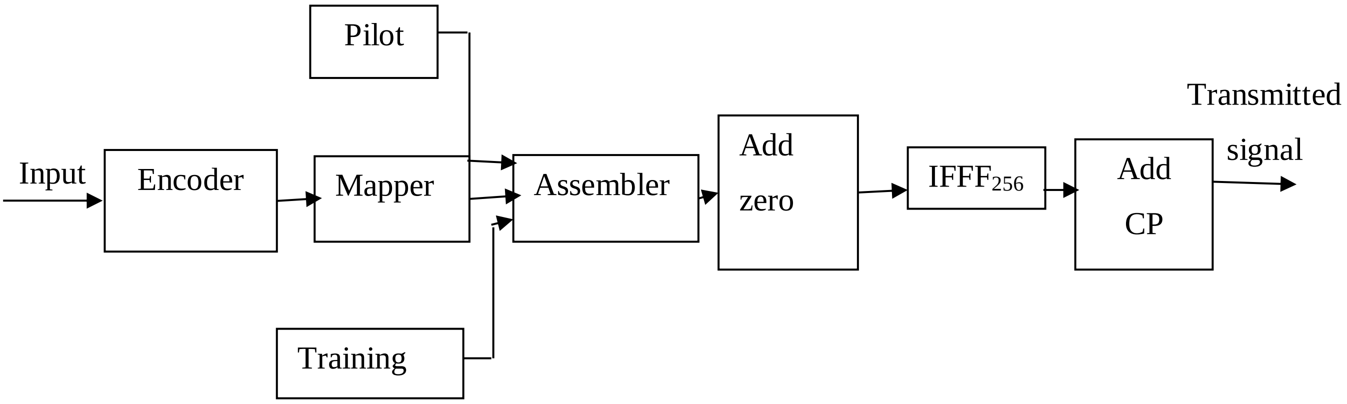

Fig.4.5. Receiver Structure of WiMAX

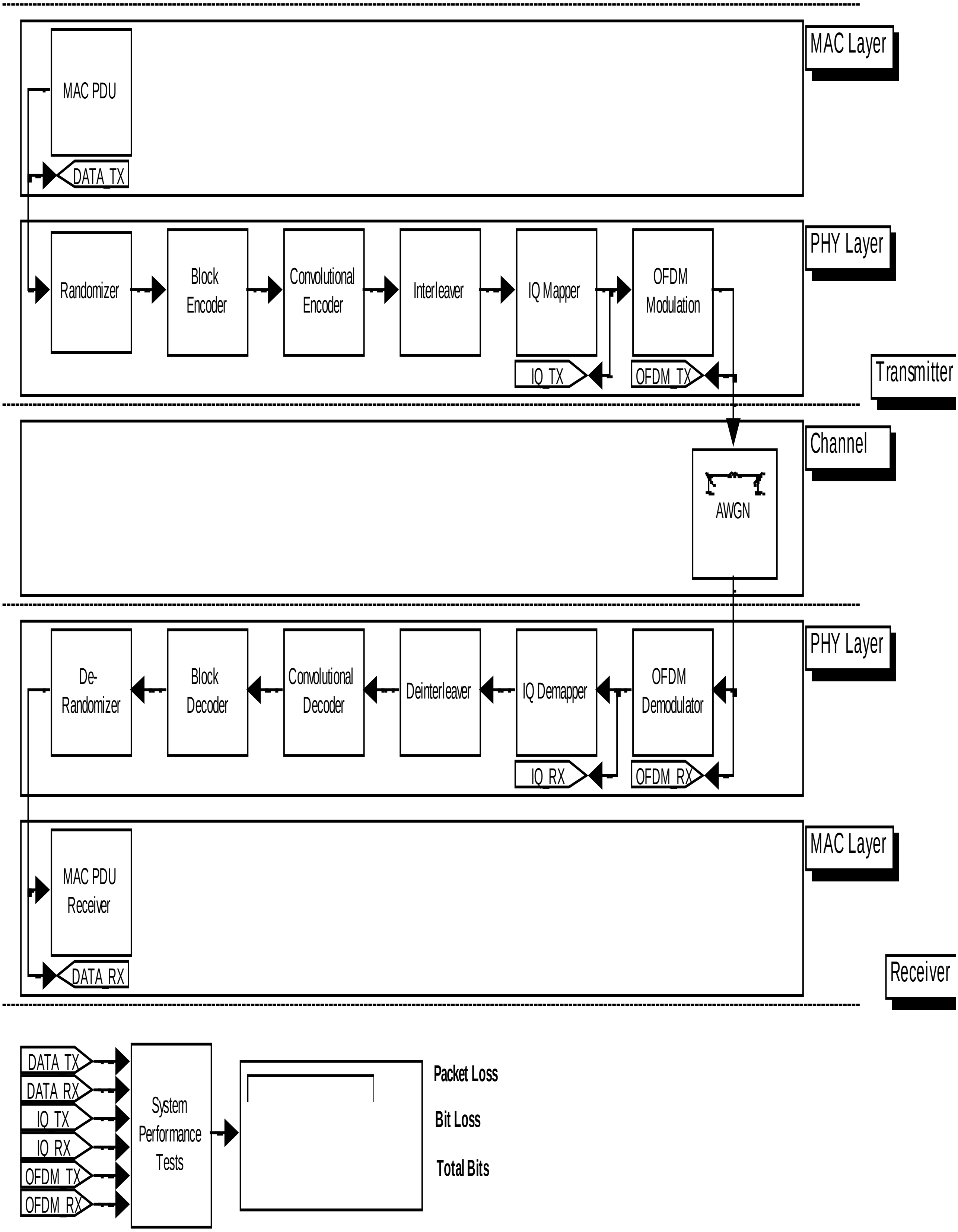

Fig.4.6. SIMULINK Model for WiMAX

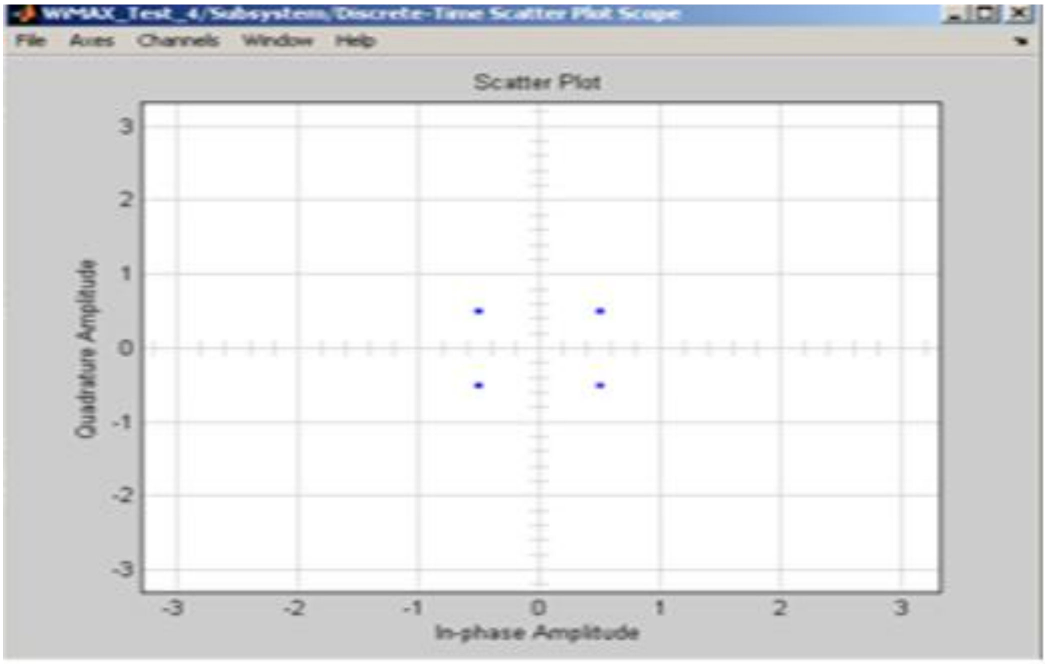

Fig.4. 7 (a). Transmitted Signal Constellation of WiMAX

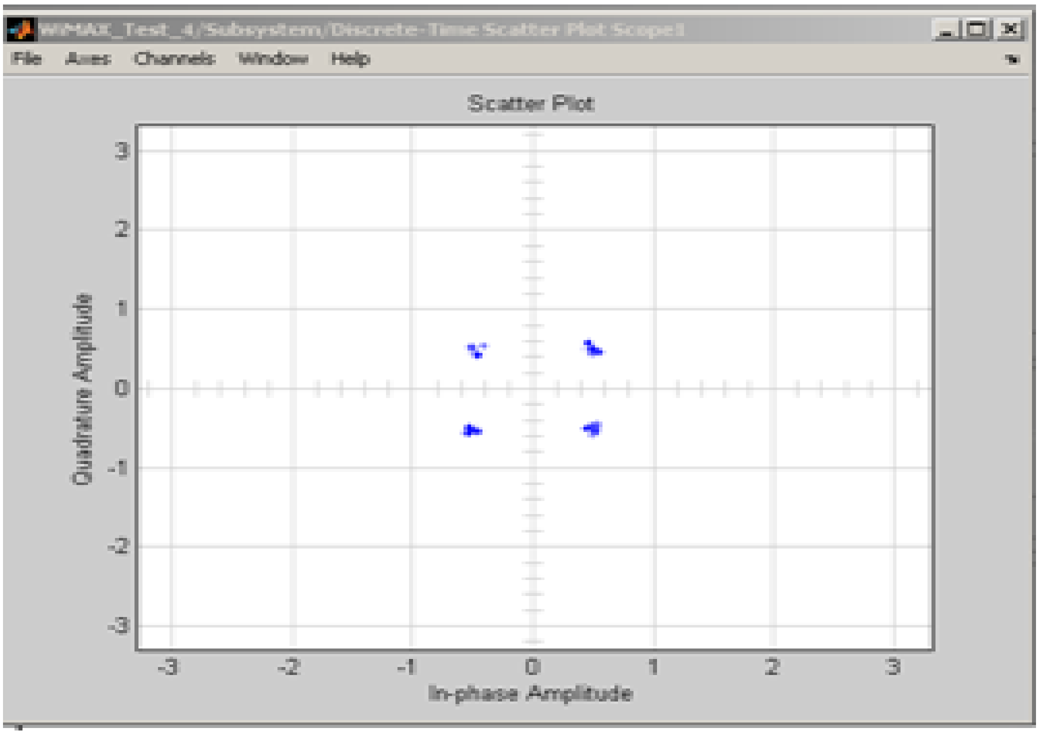

Fig.4. 7 (b). Received Signal Constellation of WiMAX

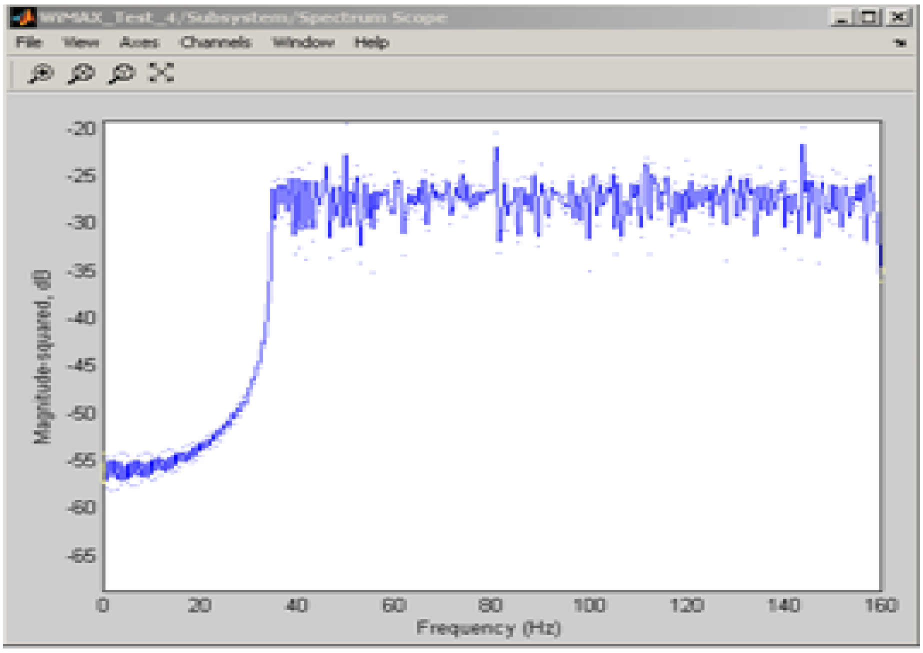

Fig.4. 7 (c). Transmitted Power Spectrum of WiMAX

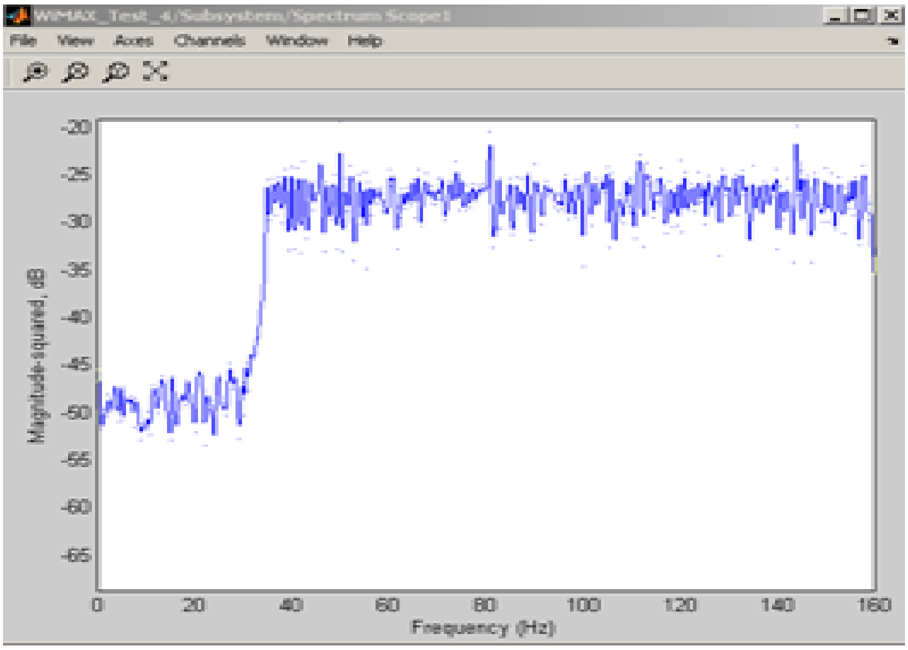

Fig.4. 7 (d). Received power Spectrum of of WiMAX

Fig.4.7. On-line Simulation of WiMAX

4.3 TRUETIME SIMULATION TOOL

TrueTime is a MATLAB/SIMULINK-constructed platform which was considered to simulate the chronological performance of multi-tasking real-time kernels comprising controller errands. The true-time model setting provides two-model blocks; a computer block and a network block as shown in the Figure 4-8. The blocks are adjustable stage, MATLAB S-functions written in C++ and discrete functions. The true-time computer (Kernel) block implements manipulator defined errands and interrupt processors. The TrueTime network block broadcasts information between computer nodes according to a selected network model. Computer and network blocks are event-driven with the implementation determined together by external and internal measures. The block inputs are supposed to be discrete-time signals, except the signals linked to the Analogue-to-Digital Converters (ADC) of the computer block, which can be continuous-time signals. The timetable and observer signals specify the distribution of shared resources throughout the simulation [160].

4.3.1 Computer (Kernel) Block

The TrueTime computer block simulates a processor node using a broad actual kernel, A/D and Digital-to-Analogue (D/A) converters, and network interfaces. The block is organised through an initialisation scenario. The scenario may be parameterised, allowing a similar scenario to be employed for numerous nodes. The TrueTime computer block provides diverse preventive scheduling systems, for instance; static-priority scheduling and initial-target-major scheduling. It is also executable to identify a custom scheduling strategy. The TrueTime computer block is shown in Figure 4-9.

4.3.2 Wireless Network Block

The TrueTime network block simulates the physical layer and the MAC layer of different local-area networks. The brands of networks provided are Carrier Sense Multiple Access with Collision Avoidance (CSMA/CD) (Ethernet), Carrier Sense Multiple Access with Arbitration on Message Priority (CSMA/AMP) Controller-Area Network (CAN), Frequency Division Multiple Access (FDMA), Time Division Multiple Access (TDMA), Switched Ethernet and Round Robin. TrueTime wireless network blocks are supported WLAN (WI-FI), ZigBee (802.15.4), and WMAN (WiMAX). The blocks simply simulate the scheduling, probable collisions or disturbance, and the point-to-point/ propagate transmissions as shown in Figure 4-10. The network blocks are mostly constructed through their block information flow. Shared factors to all kinds of networks are the data rate, the minimum frame size, and the network interface delay. For wireless network there are amounts of additional factors that can be identified. Such as, for the wireless networks it is possible to identify the transmit power, the receiver signal threshold, the path loss exponent (or a distinct path loss function), the ACK timeout, the retry limit, and the error coding threshold [161].

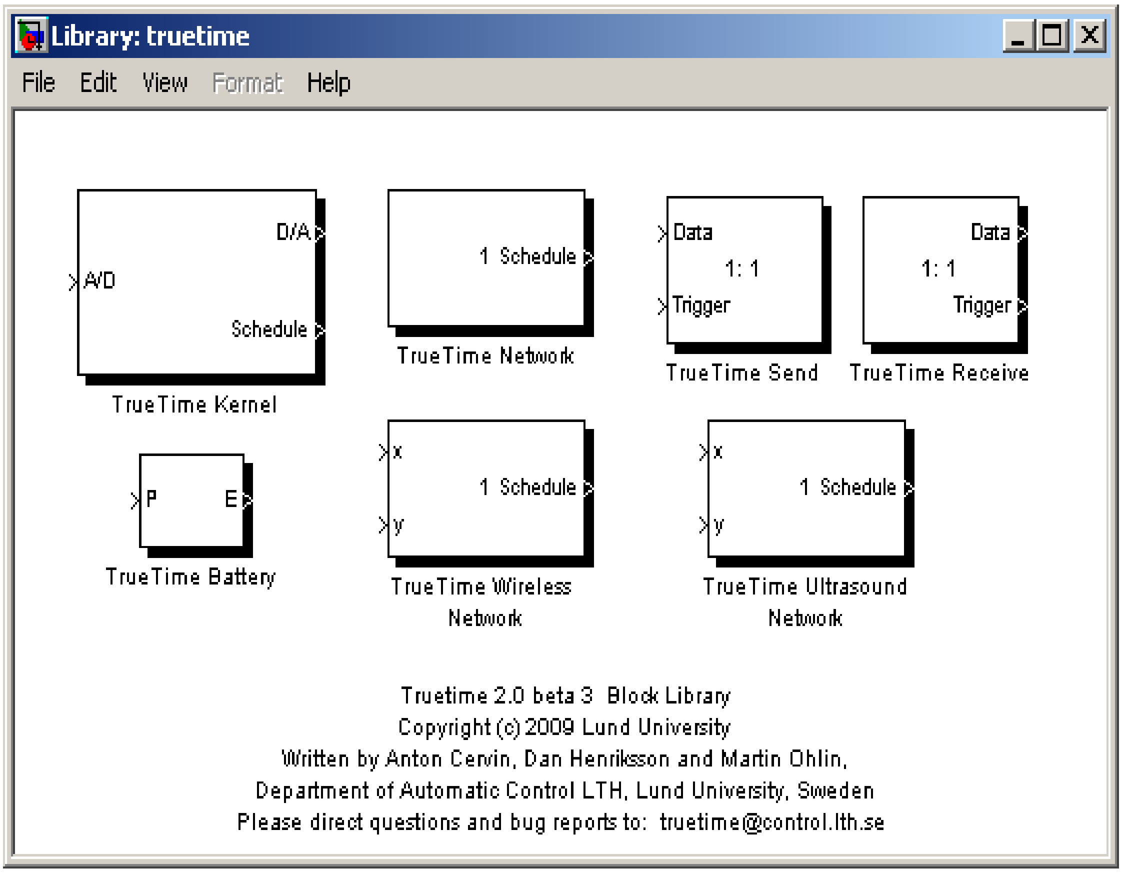

Truetime 2.0 beta 3 Block Library
Copyright (c) 2009 Lund University
Written by Anton Cervin, Dan Henriksson and Martin Ohlin,
Department of Automatic Control LTH, Lund University, Sweden
Please direct questions and bug reports to: truetime@control.lth.se

Fig.4.8. The TrueTime Block Library

This thesis, proposes an integrated control method, and network protocol. In addition, the effects of wireless network time delay and packet dropout on the performance and stability of the system are studied. When studying the effects of time-varying delays, we are not mainly interested in the fact that the delay may be increasing due to interfering network traffic, instead we want to know how that delay affects the system and how to optimally compensate for it. From our perspective, TrueTime seems to be more useful for studying the effects of resource allocation in the kernel or bandwidth usage on a small-scale, WLAN and WMAN simulations for which TrueTime offers extreme flexibility and precision is easily integrated with SIMULINK's ability to easily model complicated plant dynamics in continuous time. In the following section, the mathematical model for the photovoltaic system is derived [162].

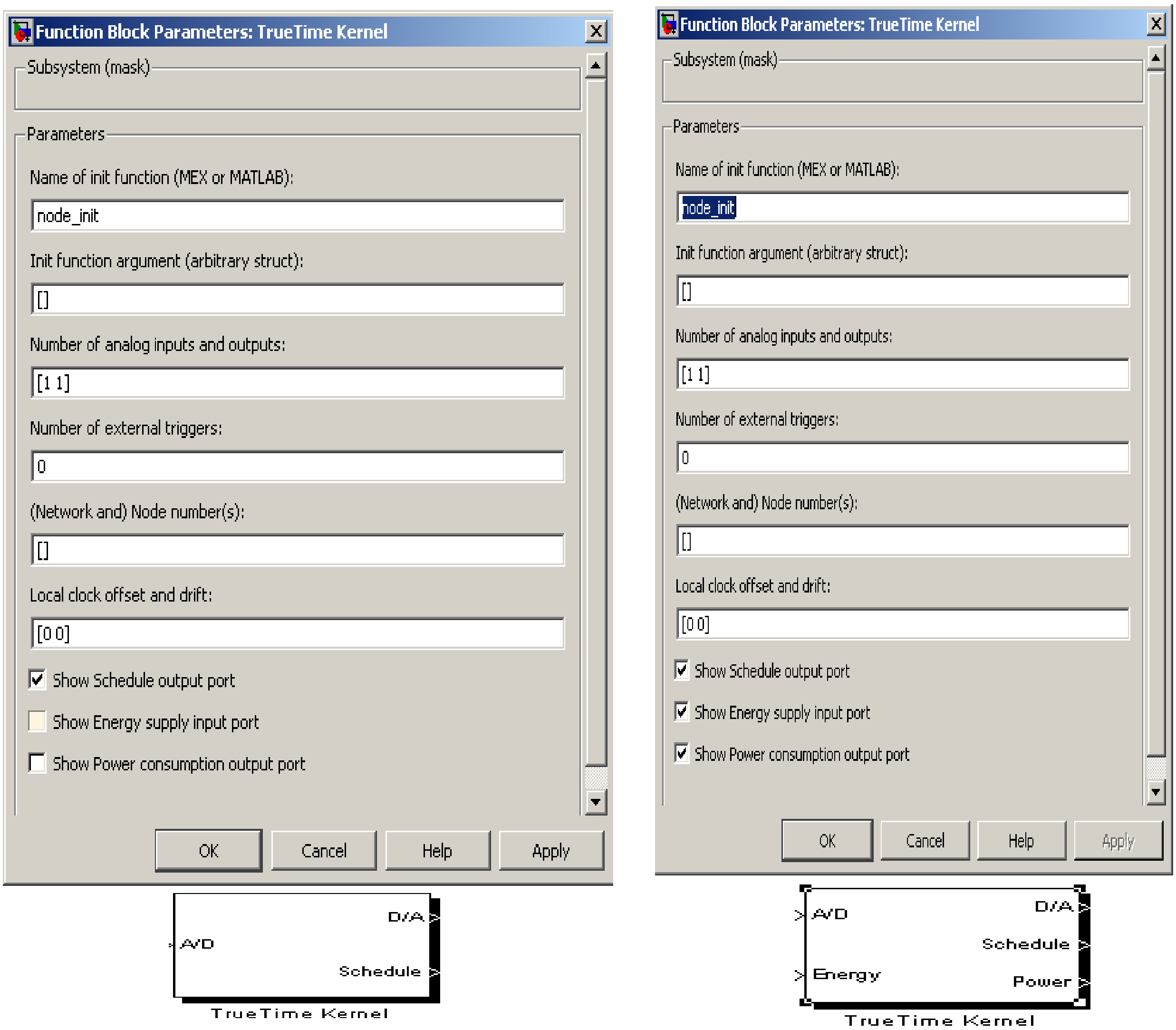

Function Block Parameters: TrueTime Kernel

Subsystem (mask)

Parameters

Name of init function (MEX or MATLAB): node_init

Init function argument (arbitrary struct): []

Number of analog inputs and outputs: [1 1]

Number of external triggers: 0

(Network and) Node number(s): []

Local clock offset and drift: [0 0]

☑ Show Schedule output port

☐ Show Energy supply input port

☐ Show Power consumption output port

Function Block Parameters: TrueTime Kernel

Subsystem (mask)

Parameters

Name of init function (MEX or MATLAB): node_init

Init function argument (arbitrary struct): []

Number of analog inputs and outputs: [1 1]

Number of external triggers: 0

(Network and) Node number(s): []

Local clock offset and drift: [0 0]

☑ Show Schedule output port

☑ Show Energy supply input port

☑ Show Power consumption output port

Fig.4.9. The Computer (Kernel) Block

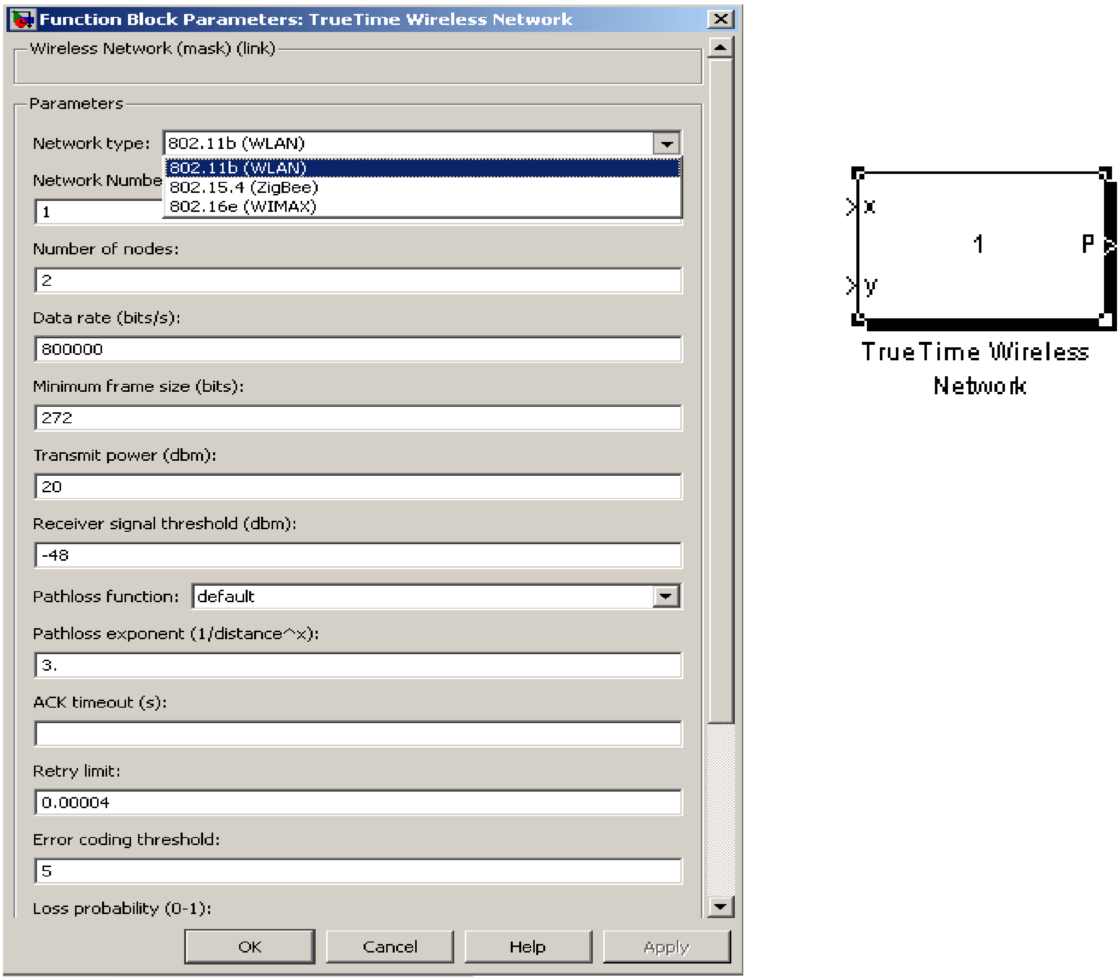

Function Block Parameters: TrueTime Wireless Network

Wireless Network (mask) (link)

Parameters

Network type: 802.11b (WLAN)

802.11b (WLAN)
802.15.4 (ZigBee)
802.16e (WIMAX)

Network Numbe: 1

Number of nodes: 2

Data rate (bits/s): 800000

Minimum frame size (bits): 272

Transmit power (dbm): 20

Receiver signal threshold (dbm): -48

Pathloss function: default

Pathloss exponent (1/distance^x): 3.

ACK timeout (s):

Retry limit: 0.00004

Error coding threshold: 5

Loss probability (0-1):

Fig.4.10. Network Block and TrueTime Wireless Network Block

4.4 MODELLING OF THE PHOTOVOLTAIC (PV) SYSTEM

The use of equivalent electric circuits makes it possible to model characteristics of a PV cell. The same modelling technique is also applicable for modelling a PV module. There are two key parameters frequently used to characterize a PV cell. Shorting together the terminals of the cell, the photon generated current will flow out of the cell as a short circuit current Isc., thus, Is = Isc. When there is no connection to the PV cell open-circuit, the photon created current is shunted internally by the intrinsic p-n junction diode. This gives the open circuit voltage Voc. The PV module or cell manufacturers usually provide the values of these parameters in their datasheets [163].

The simplest model of a PV cell equivalent circuit consists of an ideal current source in parallel with an ideal diode. The current source represents the current generated by photons often denoted as I_{ph}, and its output is constant under constant temperature and constant incident radiation of light. The PV panel is usually represented by the single exponential model or the double exponential model. The single exponential model is shown in Figure 4-11. The current is expressed in terms of voltage, current and temperature as shown in equation (4-1) [164].

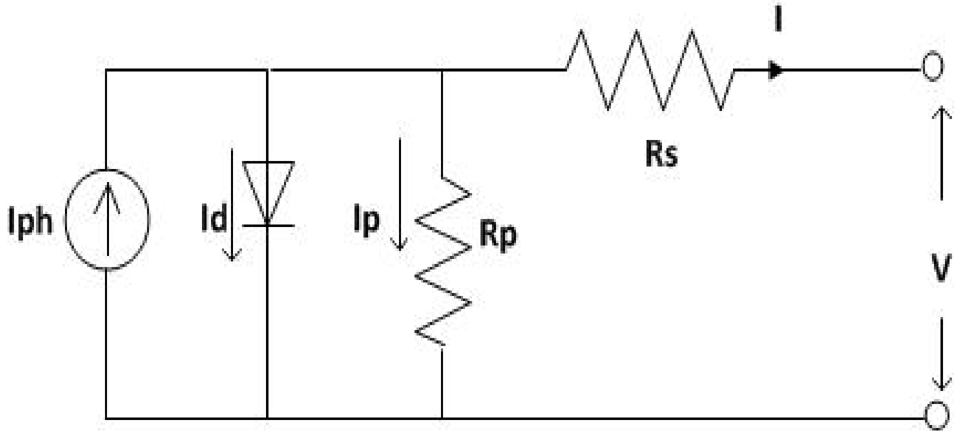

Fig.4.11. Equivalent Circuit of a Photocell

$$\boldsymbol{I = I_{ph} - I_o\left(e^{\frac{V+IR_S}{V_T}} - 1\right) \ldots\ldots\ldots (4-1)}$$

Where, I_{ph}: the photo generated current; I_o: the dark saturation current; R_s: cell series resistance; R_p: the cell (shunt) resistance; $V_T = \frac{KT}{q}$ representing the thermal potential (25mV at 20 ° C); q: the electronic charge, 1.6 × 10 – 19 C; k: the Boltzmann's constant, 1.38 × 10 – 23 J/K; and T: the ambient temperature, in Kelvin.

4.4.1 Battery Modelling

Several electrical equivalent circuits of a battery are establishing in the literature [165]. The Thevenins equivalent circuit is one of the most basic circuits used to study the transient behavior of a battery. This circuit is illustrated in Figure 4-12. It uses a R_{series} *and RC* parallel network ($R_{transient} and R_{transient}$) to calculate the response of the battery to transient load events at a particular state of charge by assuming a constant open circuit voltage.

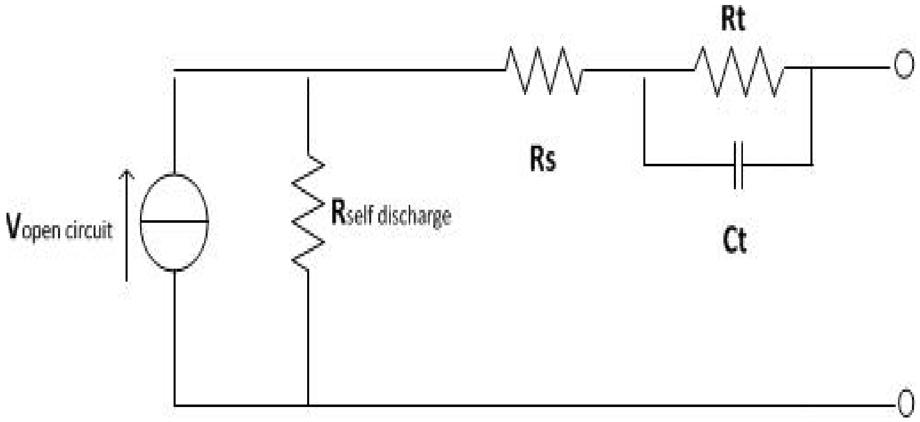

Fig.4.12. Thevenins Equivalent Circuit for the Battery Circuit

The structure of the hybrid sources of Figure 4-13 consists of a PV panel. The resistive load represents the street lighting and wireless networks, the capacitor represents a DC bus. Further, the battery is connected to the capacitor via a DC-DC current bidirectional convertor of solar panels is done with a PV panel and battery as shown in Figure 4-14.

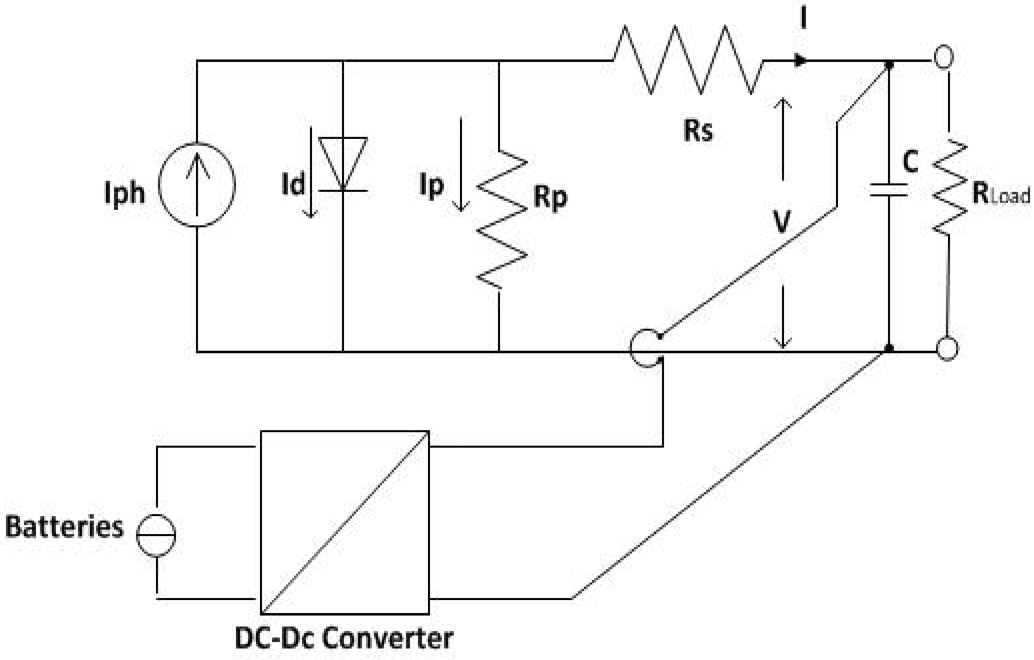

Fig.4.13. . Hybrid Structure of PV and Battery Sources

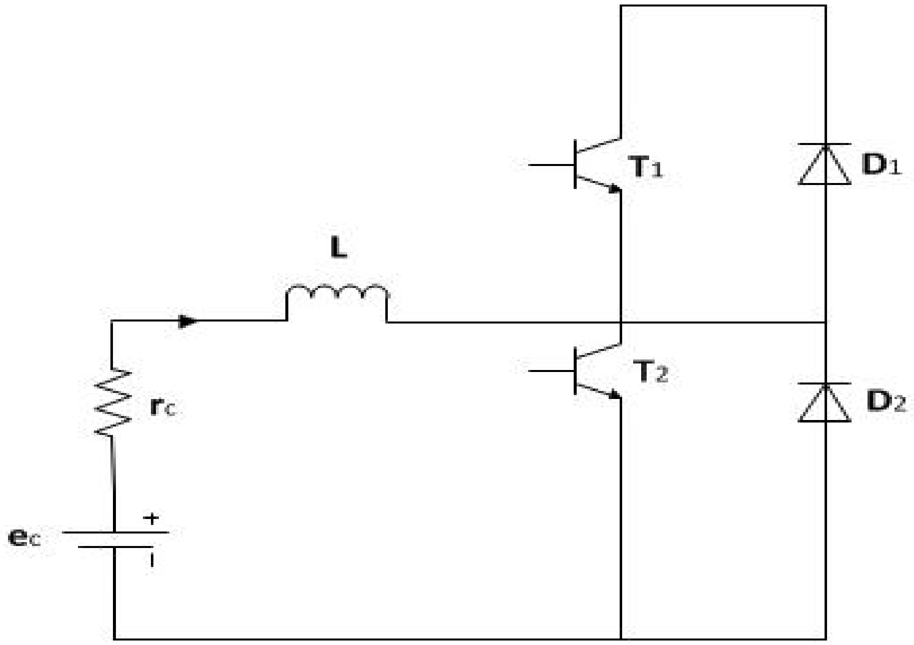

Fig.4.14. Structure of Battery and Converter

The following state vector of the whole system is chosen [166]:

$$\boldsymbol{X = [V\ ib]^T}$$

$$\begin{cases} \dot{x}_1 = \dfrac{1}{c}\left[\mu\, x_2 + I_{ph} - I_s(e^{Ax_1} - 1) - \dfrac{x_1}{R_p} - \dfrac{x_1}{R_{Load}}\right] \\ \dot{x}_2 = \dfrac{1}{L}[-\mu x_1 + e_c - r_c x_2] \end{cases} \quad \ldots\ldots\ldots(4-2)$$

With $\mu = 1 - u_c$ and$A = \frac{q}{KT} > 0$.

Where, μ is DC-DC converter.

4.4.2 PV Simulation Analysis

For lighting conditions and temperature data, the characteristics of current voltage and power voltage *P=f(v)* shows an operating point at maximum power. The proposed PV V-I and V-P characteristics figures are simulated with the MATLAB/SIMULINK model. Figures 4-15 and 4-16 illustrate the effect of illumination on the characteristic current voltage and power voltage respectively. The photo generated current is nearly proportional to the light or luminous flux. The I_{ph} created in photocell is proportional to the surface of the junction subjected to sunlight [167]. In general, this thesis presents a simple and efficient PV modelling experiment. It models each element and simulates them using MATLAB/SIMULINK. The result demonstrates that the PV model using the equivalent circuit in reasonable complexity presents a good match to the real PV module.

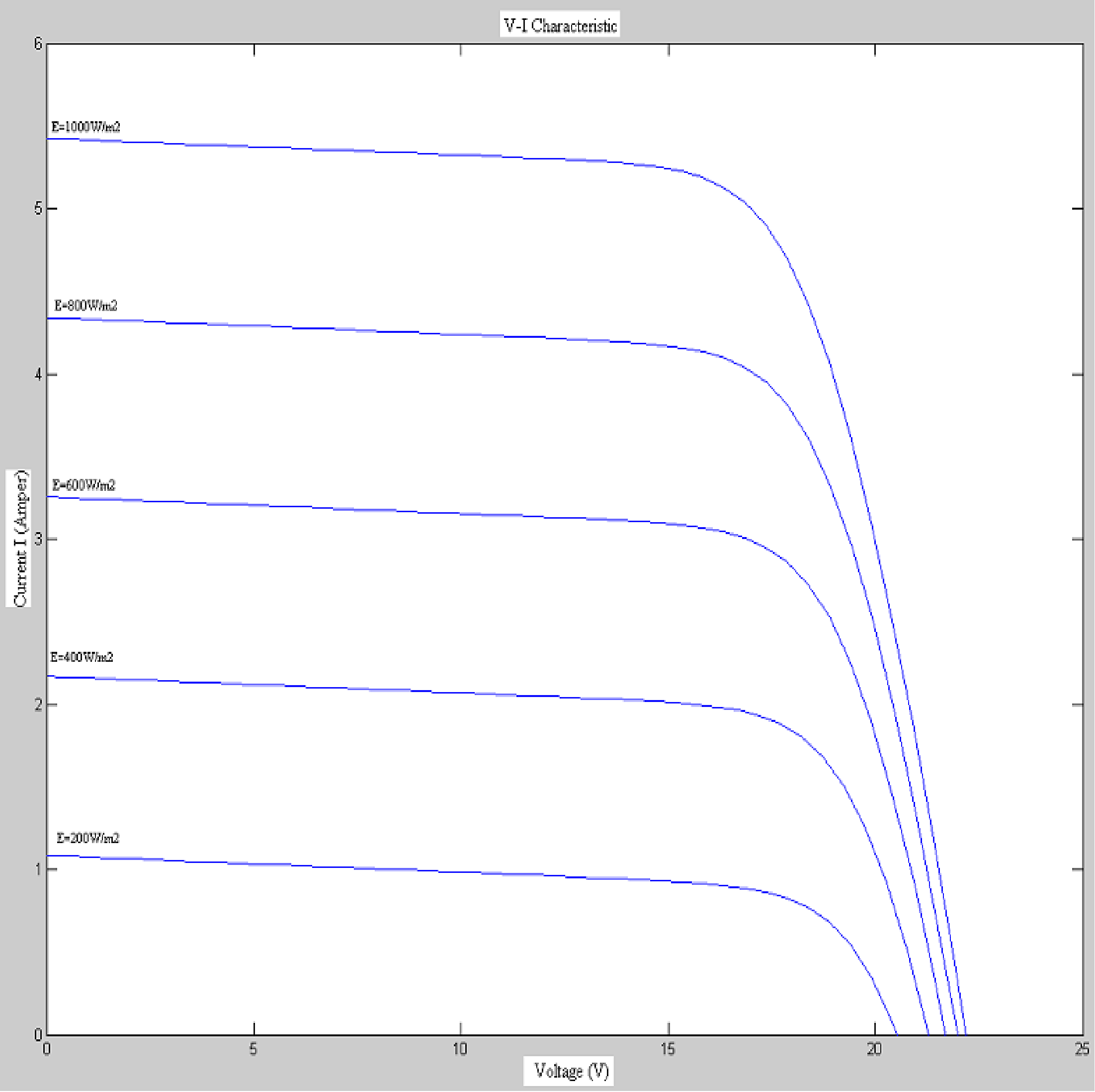

Fig.4.15. Illumination Effect on the Current-Voltage Characteristic

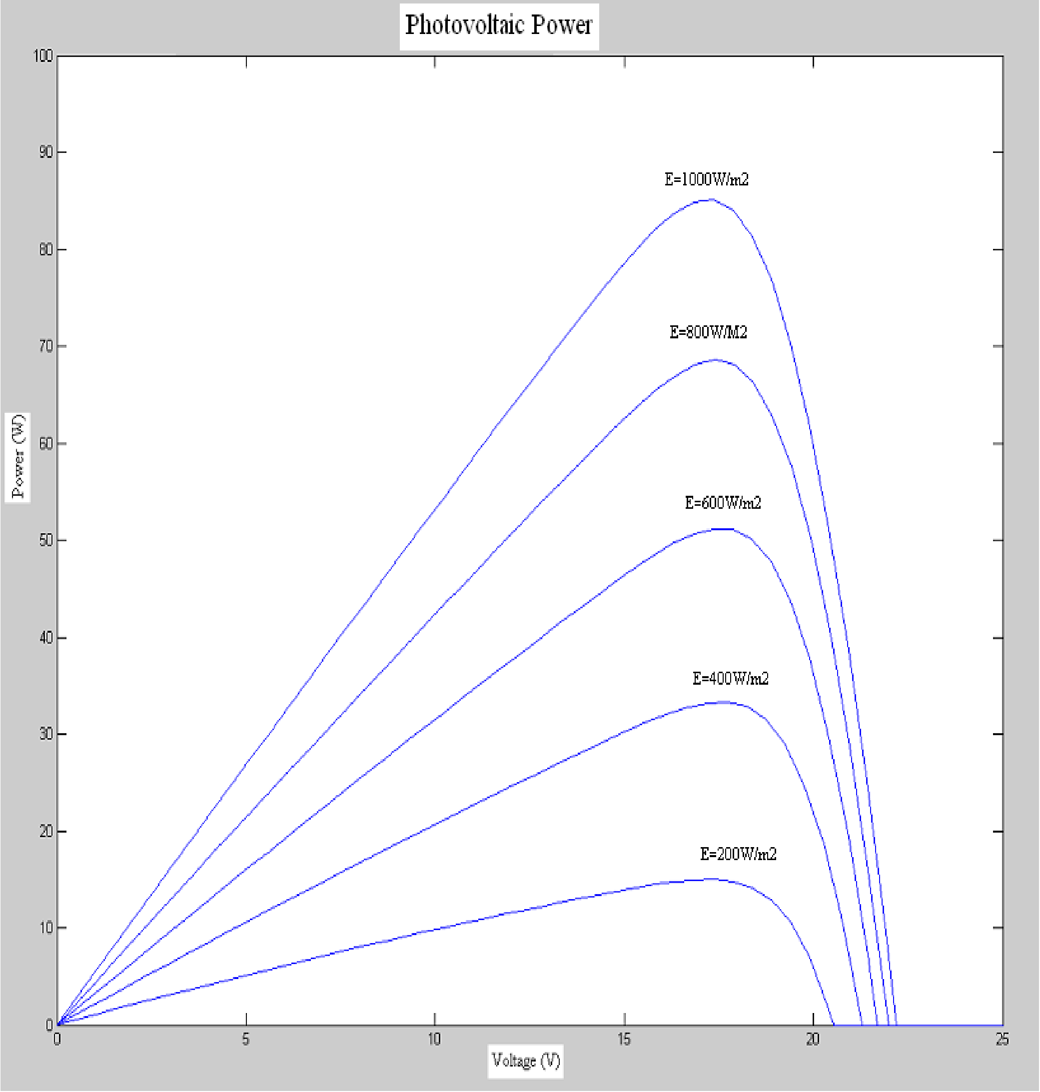

Fig.4.16. Illumination Effect on the Power-Voltage Characteristic

4.5 CHAPTER SUMMARY

The model constructed in this thesis demonstrates the significance of modelling a system to understand its functionality. Investigations can be carried out on the model to calculate the performance index. Components of the system can be experienced against a defined standard, IEEE 802.11b/IEEE 802.16e in this case, to prove the complete working of the component itself and the system as a whole. The same model can be used to implement RMPC and NNPC methods. A MATLAB simulation was carried out in order to analyse baseband processing of the proposed IEEE 802.11b & IEEE802.16e physical layer. A novel description of the standards of the IEEE 802.16e PHY and working experience with TrueTime tools was obtained.

In this thesis, a modeling principle of DC hybrid source systems composed of a photovoltaic source and battery have been presented. The state space model is given for the whole structure. Considering the chosen scenario, energy supplied by the battery is recovered by PV during periods of illumination.

CHAPTER 5 ..

RMPC DESIGN FOR SWNCS IN PRESENCE OF NETWORK TIME DELAY AND PACKET DROPOUT

5.1 INTRODUCTION

With the rapid development of wireless network methods, the combination of wireless network into control systems has attracted much concentration lately. The introduction of wireless network causes several problems, for example wireless network time delays, packet dropouts. It is recognised that the wireless network time delays and packet dropouts can degrade the system performance or even cause instability in feedback control systems. Thus, how to treat the wireless network time delays and packet dropouts has been the centre of much attention. In addition, the wireless network time delays are distinct from and more difficult than the conventional constant time delays because of the time-varying attribute of wireless networks. Different methods have been proposed in previous work for the controller design taking into accounts the wireless network time delays and packet dropouts. The robust control problem is able to deal with the problem of system parameter uncertainty, and also be applied to the typical problem of perturbation input control [68-70].

This thesis a SWNCS is designed with specific communications and control parameters using True-Time simulator tools. Investigated robust controllers will be able to estimate and remove the effect of delay times and packet dropouts that occurs in the SWNCS. This can be achieved by the design and optimisation of a suitable RMPC. The controller will be able to enhance the SWNCS QoS by removing the effect of the delay which occurs in the forward and feedback channels of the SWNCS. The delay time will be modeled as a Markovian chain which forms regular Linear Matrix Inequalities LMIs with unbounded limitations and it is assumed to obtain the RMPC. Further work will be carried out towards adding IEEE802.16e as another wireless network in the TrueTime Simulink library. Finally, work will be done to simulate the power consumption in SWNCS with/without a power control scheme.

5.2 FORMULATION OF SWNCS

In this chapter, the modelling procedure of SWNCSs will be introduced. The subsequent assumptions will be employed during this thesis, before proceeding to the modelling procedure. The sensor is clock-driven and the states of the plant are sampled periodically. The controller and actuator are event-driven and the control action is computed when new sensor information reaches the controller. The control action is applied to the plant as soon as new controller information reaches the actuator.

5.2.1 Physical Plant Model

Suppose the SWNCS is as shown in Figure 5-1, which has a physical plant based on a complete state vector for the PV system calculated and presented in the previous chapter. A PV system that is considered as a discrete-time system is given by the following system of equations:

$$\boldsymbol{x(k+1) = Ax(k) + Bu(k-\tau_k^{ca})} \ldots\ldots\ldots (\boldsymbol{5-1a})$$

$$\boldsymbol{y(k) = Cx(k)} \ldots\ldots\ldots (\boldsymbol{5-1b})$$

Where, $x(k)$ is the state vector, $u(k)$ is the control input, $y(k)$ is the output A, B, C are system matrices with appropriate dimension and τ_k^{ca} represents random delay from controller-to-actuator.

Suppose that the predictive signal $y_p(k)$ is generated by the following system

$$\boldsymbol{x_p(k+1) = A_p x_p(k) + B_p r(k)} \ldots\ldots\ldots (\boldsymbol{5-2a})$$

$$\boldsymbol{y_p(k+1) = C_p x_p(k)} \ldots\ldots\ldots (\boldsymbol{5-2b})$$

Where $x_p(k)$ is the predictive state, $y_p(k)$ has the same dimension as $y(k)$ and $r(k)$ is the reference input. A_p, B_p and C_p are constant matrices with appropriate dimensions. It is assumed that both $x(k)$ and $x_p(k)$ are real time calculable and the calculation of $x(k)$ and $x_p(k)$ is sent with a single packet.

5.2.2 Stochastic Time Delay Model

Both τ_k^{sc} and τ_k^{ca} are modeled as two homogenous Markov chains that have values in ***$\mathcal{M}$= {0, 1,…., τ_k^{sc}}* and** $\mathbb{N}$=*{0,1,……, τ_k^{ca}}*. The transition probability matrices are $\boldsymbol{\Lambda = [\lambda_{ij}]}$ **and** $\boldsymbol{\pi = [\pi_{rs}]}$. That means τ_k^{sc} jumps from mode *i* to *j* and τ_k^{ca} jumps from mode *r* to *s* with probabilities λ_{ij} and π_{rs}, which are summarized by:

$$\boldsymbol{\lambda_{ij} = Pr(\tau^{sc}_{k+1} = j|\tau^{sc}_{k} = i)} \qquad \boldsymbol{\pi_{rs} = Pr(\tau^{ca}_{k+1} = s|\tau^{ca}_{k} = r)}$$

Through the constraints $\lambda_{ij}, \pi_{rs} \geq 0$ and,

$$\boldsymbol{\sum_{j=0}^{\tau^{sc}_k} \lambda_{ij} = 1} \qquad \boldsymbol{\sum_{s=0}^{\tau^{ca}_k} \pi_{rs} = 1} \qquad \textbf{For all } \boldsymbol{j \in \mathcal{M}} \textbf{ and } \boldsymbol{s \in \mathbb{N}}$$

Where τ^{sc}_k is the stochastic delay from the sensor-to-controller.

It is noted that the Markov chain model has integrated the time delay and packet dropout procedures in wireless networks at the same time, as analysed in the following proof [168].

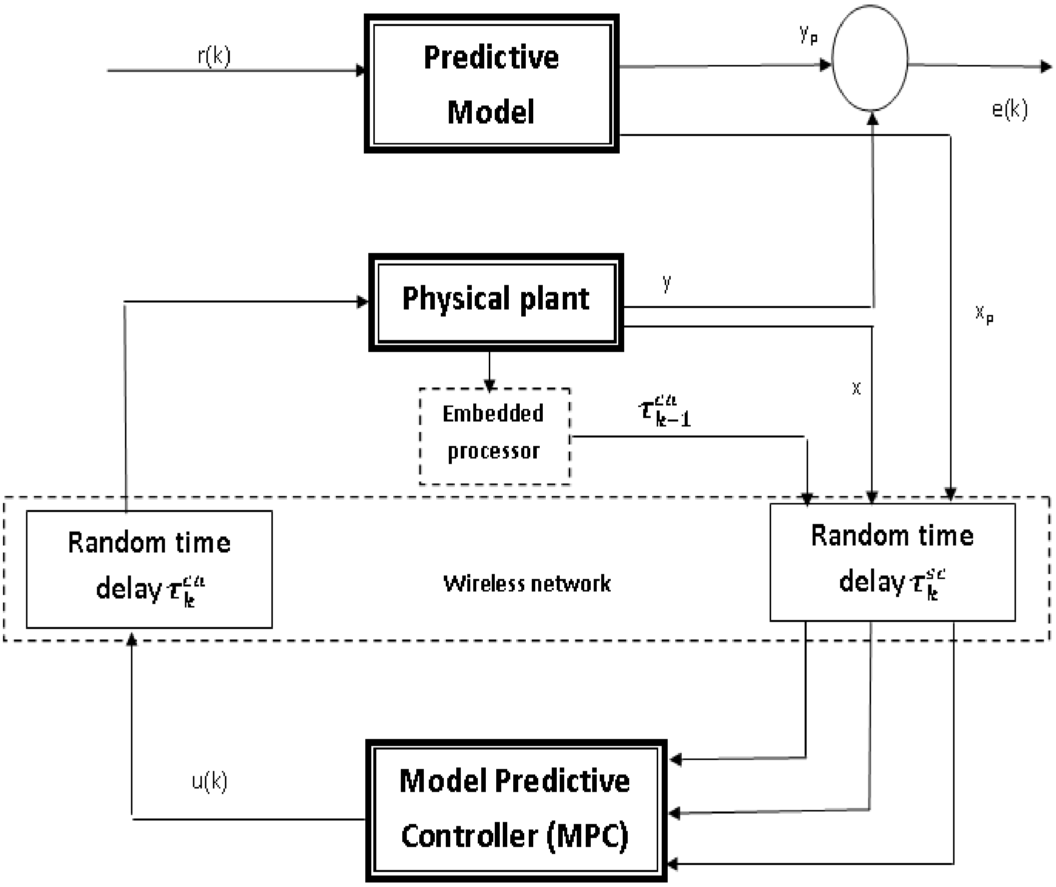

Fig.5.1. Wireless Network Control System Diagram

Supposition: the controller will for all time utilise the most current data. Therefore, we have $x(k - \tau^{sc}_k)$ at step k. However, there is no new data arriving at step $k + 1$. Hence, data could be missing or there is a longer time delay. Then as a minimum, have $x(k - \tau^{sc}_k)$ available for the feedback control system. So in this model of the physical plant in Figure 5-1, the stochastic time delay τ^{sc}_k can increase at most by 1 each step, and the constraint.

$$\mathbf{Pr}(\boldsymbol{\tau^{sc}_{k+1} > \tau^{sc}_k + 1}) = \mathbf{0}$$

However, the stochastic time delay τ^{sc}_k can reduce as many steps as possible. To decrease stochastic time delay of τ^{sc}_k models packet dropouts in the wireless network, assumes that no previous data exists if we have newer data coming simultaneously. Thus, the structured transition probability matrix is:

$$\begin{bmatrix} \lambda_{00} & \lambda_{01} & \mathbf{0} & \mathbf{0} & \cdots & \mathbf{0} \\ \lambda_{10} & \lambda_{11} & \lambda_{12} & \mathbf{0} & \cdots & \mathbf{0} \\ \vdots & \vdots & \vdots & \vdots & \ddots & \vdots \\ \vdots & \vdots & \vdots & \vdots & \vdots & \lambda_{\mathcal{M}\tau_{k-1}^{sc},\mathcal{M}\tau_{k}^{sc}} \\ \lambda_{\mathcal{M}0} & \lambda_{\mathcal{M}1} & \lambda_{\mathcal{M}2} & \lambda_{\mathcal{M}3} & \cdots & \lambda_{\mathcal{M}\tau_{k}^{sc},\mathcal{M}\tau_{k}^{sc}} \end{bmatrix} \dots\dots\dots(\mathbf{5-3})$$

Each row describes the transition probabilities from fixed state to all states. The diagonal elements are the probabilities of data coming in chain with equal delays, while the elements above the diagonal are the probabilities of meeting longer delays. Further, the elements below the diagonals designate packet dropouts or disordering previous data. Figure 5-2 illustrates a four state transition diagram with such construction, which obviously demonstrates that we can jump from i=0 to j=1 and from r=1 to r=0. However, we can jump directly from r=0 to r=2 or r=3. Therefore, the stochastic time delays τ_k^{sc} and τ_k^{ca} in the Markovian chains actually counting the packet dropouts technique.

In the next section, the full state feedback controller is designed at present time k, where the stochastic time delay from sensor-to-controller channel τ_k^{sc} can be obtained using the sampling time technique. The stochastic time delay from controller-to-actuator channel can be obtained by the controller at present time k.

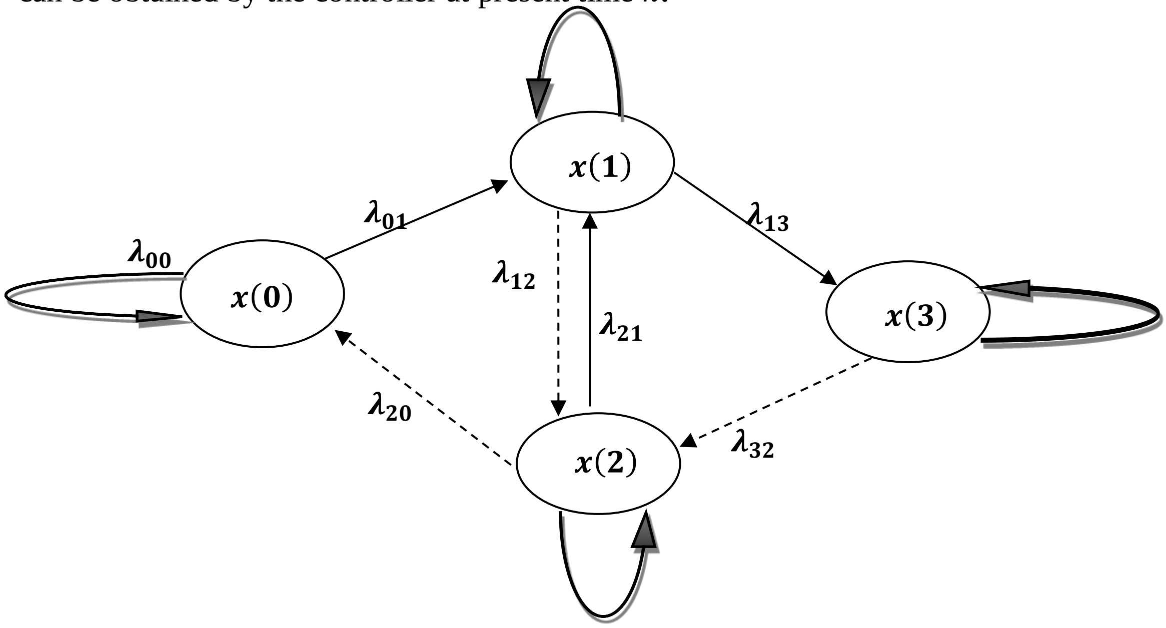

Fig. 5.2. Markovian Jump States of the Packet Dropout Sequence

5.2.3 Full State Feedback Controller Model

In any WNCS, the delay information is important for controller design. The controller designed at recent time k and stochastic time delay at a node can be described by the following steps:

1. The stochastic time delay τ_k^{sc} can be achieved using the time sampling techniques. Since at recent time k the stochastic time delay τ_k^{sc} can be achieved by comparing the recent time and the time-sampling of sensor data received [169].
2. The embedded processor measures the stochastic time delay $\tau_k^{ca}-1$.
3. Referring to the stochastic time delay in sensor-to-controller channel, the $\tau_{k-\tau_k^{sc}-1}^{ca}$ can be achieve by the controller at recent time *k*. However, this data cannot be received by the controller instantly, because it needs to be sent through the wireless network from the sensor-to-controller channel. So, if the time delays τ_k^{sc} exist, the data of $\tau_{k-\tau_k^{sc}-1}^{ca}$ at time *k* would be identified at the controller node [170], the two mode-dependent full state feedback controllers are to be designed by MPC.

$$\boldsymbol{u(k)=K_1\left(\tau_k^{sc},\tau_{k-\tau_k^{sc}-1}^{ca}\right)x_p(k-\tau_k^{sc})+K_2\left(\tau_k^{sc},\tau_{k-\tau_k^{sc}-1}^{ca}\right)x(k-\tau_k^{sc})}\ \ldots\ldots(\mathbf{5-4})$$

where, K_1 & K_2 are full state feedback controller gains

From system (5-1) and (5-2) and referring to the stochastic time delay τ_k^{ca}, the following model is obtained:

$$\boldsymbol{x(k+1)=\widetilde{A}X(k)+\widetilde{B}u(k-\tau_k^{ca})+\tilde{J}r(k)}\ \ldots\ldots\ldots(\mathbf{5-5a})$$

$$\boldsymbol{e(k)=\widetilde{C}X(k)}\ \ldots\ldots\ldots(\mathbf{5-5b})$$

where,

$$\boldsymbol{X(k)=[x_r(k)^T\ x(k)^T]}\qquad \boldsymbol{\widetilde{A}=\begin{bmatrix}A_r & 0\\ 0 & A\end{bmatrix}}\qquad \boldsymbol{\widetilde{B}=\begin{bmatrix}0\\ B\end{bmatrix}}\qquad \boldsymbol{\tilde{J}=\begin{bmatrix}B_r\\ 0\end{bmatrix}}\qquad \boldsymbol{\widetilde{C}=[-C_r\ C]}$$

Furthermore, if the states increase the state variables become:

$$\boldsymbol{\xi(k)=[X(k)^T\ X(k-1)^T\ \ldots X(k-\tau_k^{sc})^T\ U(k-1)^T\ U(k-2)^T\ \ldots U(k-\tau_k^{ca})^T]^T}\ \ldots\ldots\ldots(\mathbf{5-6})$$

The SWNCS is achieved:

$$\boldsymbol{\xi(k+1) = \bar{A}\left(\tau_k^{sc}, \tau_{k-\tau_k^{sc}-1}^{ca}, \tau_k^{ca}\right)\xi(k) + \bar{J}r(k)} \dots\dots\dots (\mathbf{5-7}\boldsymbol{a})$$

$$\boldsymbol{e(k) = \bar{C}\xi(k)} \dots\dots\dots (\mathbf{5-7}\boldsymbol{b})$$

Where,

$$\boldsymbol{K = \left[k_1\left(\tau_k^{sc}, \tau_{k-\tau_k^{sc}-1}^{ca}\right)\ k_2\left(\tau_k^{sc}, \tau_{k-\tau_k^{sc}-1}^{ca}\right)\right]}, \qquad \boldsymbol{\bar{A}} = \begin{bmatrix} \boldsymbol{A} & \mathbf{0} & \boldsymbol{\tilde{B}k} & \mathbf{0} & \mathbf{0} & \mathbf{0} & \dots & \mathbf{0} \\ \boldsymbol{I} & \mathbf{0} & \dots & \mathbf{0} & \mathbf{0} & \mathbf{0} & \dots & \mathbf{0} \\ \mathbf{0} & \boldsymbol{I} & \ddots & \mathbf{0} & \mathbf{0} & \mathbf{0} & \ddots & \mathbf{0} \\ \mathbf{0} & \mathbf{0} & \ddots & \mathbf{0} & \mathbf{0} & \mathbf{0} & \ddots & \mathbf{0} \\ \mathbf{0} & \mathbf{0} & \boldsymbol{k} & \mathbf{0} & \mathbf{0} & \mathbf{0} & \mathbf{0} & \mathbf{0} \\ \mathbf{0} & \mathbf{0} & \dots & \mathbf{0} & \boldsymbol{I} & \mathbf{0} & \dots & \mathbf{0} \\ \mathbf{0} & \mathbf{0} & \ddots & \mathbf{0} & \mathbf{0} & \boldsymbol{I} & \ddots & \mathbf{0} \\ \mathbf{0} & \mathbf{0} & \dots & \mathbf{0} & \mathbf{0} & \mathbf{0} & \ddots & \mathbf{0} \end{bmatrix},$$

$$\boldsymbol{\bar{J} = [\tilde{J}\ 0 \dots 0\ 0\ 0 \dots 0]^T} \qquad \boldsymbol{\bar{C} = \left[\tilde{C}\ 0 \dots 0\ 0\ 0 \dots 0\right]^T}$$

At each sampling time k, the controller design scheme can be expressed as follows:

Step1 measure the state $\boldsymbol{x(k)}$

Step2 calculate the state feedback gains controller $\boldsymbol{k_1\left(\tau_k^{sc}, \tau_{k-\tau_k^{sc}-1}^{ca}\right)}$ and $\boldsymbol{k_2\left(\tau_k^{sc}, \tau_{k-\tau_k^{sc}-1}^{ca}\right)}$ in (5-4)

Step3 implement the first control law $U(k|k)$ that is

$$\begin{aligned} \boldsymbol{U(k+m|k)} &= \boldsymbol{U(k|k)} \\ &= \boldsymbol{k_1\left(\tau_{k+m}^{sc}, \tau_{k+m-\tau_{k+m}^{sc}-1}^{ca}\right)x_p(k-\tau_{k+m}^{sc})} \\ &\quad + \boldsymbol{k_2\left(\tau_{k+m}^{sc}, \tau_{k+m-\tau_{k+m}^{sc}-1}^{ca}\right)x(k-\tau_{k+m}^{sc})} \dots\dots\dots (\mathbf{5-8}) \end{aligned}$$

By substituting the control signal given in system (5-8), the resulting SWNCS in system (5-7) becomes

$$\begin{cases} \boldsymbol{\xi(k+1) = \bar{A}\left(\tau_k^{sc}, \tau_{k-\tau_k^{sc}-1}^{ca}, \tau_k^{ca}\right)\xi(k) + \bar{J}r(k)} \\ \qquad\qquad \boldsymbol{e(k) = \bar{C}\xi(k)} \\ \qquad\qquad \boldsymbol{\|u(k)\|_2 \le u_{max}} \end{cases} \dots\dots\dots (\mathbf{5-9})$$

In the following section, the MPC full state feedback controller will be derived based on the Lyapunov method [171-172].

5.3 MAIN RESULTS

In this section, the MPC for full state feedback controller of system (5-9) are first specified, and then the sufficient and necessary conditions in terms of LMIs with non-convex constraints for RMPC are derived.

5.3.1 MPC Design

A solid on-line control approach which iteratively calculates locally optimal control signals by resolving an optimisation problem over a real-time horizon is called MPC [173]**.** To resolve the controller problem by using the MPC approach is to discover the technique to solve the optimisation problem by calculating the full state feedback controller gain.

The following presents the MPC for full state feedback controller based on the Lyapunov method. Consider the following min-max infinite horizon predictive cost function relating to the system (5-8)

$$\min_{\boldsymbol{U(k+i|k)_{i=0,1,\dots,\tau_k^{sc}}}} \max_{\boldsymbol{[A,B,A_p]\in\Omega}} \boldsymbol{J_\infty(k)} \dots\dots\dots (\boldsymbol{5-10})$$

$$\boldsymbol{J_\infty(k)} \\ = \sum_{\boldsymbol{m=0}}^{\infty} \boldsymbol{E\{X^T(k+m|k)Q_iX(k+m|k)+U^T(k+m|k)RU(k+m|k)|K_k\}}$$

Where, E[.] indicates the expectation, $X(k+m|k)$ indicates the predictive value of state at time k, $U(k+m|k)$ indicates the prediction of the control signal at time k, $Q_i > 0$ & $R > 0$ are the weighting symmetric matrices.

$K_k = \sigma\{x_o, r_o, \dots\dots\dots\dots.., x_k, r_k\}$ is σ algebra created by $\{(x_l, r_l) \quad 0 \le l \le k\}$

$\Omega = \mathrm{co}\{[A_1, A_{1p}, B_1] \dots\dots\dots\dots [A_l, A_{lp}, B_l]\}$ is a polytope

Create the subsequent Lyapunov function

$$\boldsymbol{V(x(k),r(k)) = x^T(k)p_{rk}(k) + \sum_{j=1}^{\tau_k^{sc}} x^T(k-j)sx(k-j) + \sum_{j=1}^{\tau_k^{sc}} x^T(k-j)K_{rk}^T Tx(k-j)} \dots\dots\dots (\boldsymbol{5-11})$$

Where, $s > 0$ &$T > 0$ are the constant matrices, and $p_{rk} > 0$ are dependents on the mode $r_k (r_k \in s)$

to resolve the optimisation (5-10), the unlimited horizon optimisation problem must be converted to a limited horizon optimisation problem by establishing the subsequent inequality [174].

$$\boldsymbol{E\{V(x\big((k+m+1)\big|k,r_k\big)(-V(x(k+m|k),r_k)|K_k)\}}$$
$$\boldsymbol{\leq -E\{x^T(k+m|k)Q_i x(k+m|k)}$$
$$\boldsymbol{+\, u^T(k+m|k)Ru(k+m|k)|K_k} \dots\dots\dots \boldsymbol{(5-12)}$$

where,

$$\boldsymbol{U(k+m|k) = k_1\left(\tau^{sc}_{k+m}, \tau^{ca}_{k+m-\tau^{sc}_{k+m}-1}\middle|k\right) x_p(k-\tau^{sc}_{k+m})}$$
$$\boldsymbol{+\, k_2\left(\left(\tau^{sc}_{k+m}, \tau^{ca}_{k+m-\tau^{sc}_{k+m}-1}\right) x(k-\tau^{sc}_{k+m})|k\right) x(k-\tau^{sc}_{k+m})}$$

For the performance index $J_\infty(k)$ to be limited, we must have $x(\infty|k) = 0$ therefore, we obtain

$$\boldsymbol{E\{V(x(\infty|k), r_k)\} = 0}$$

Addition to both sides of equation (5-10) from m=0 to m=∞ we get:

$$\boldsymbol{\max_{[A,A_p,B]\in\Omega} J_\infty(k) \leq V(x(k), r_k)} \dots\dots\dots \boldsymbol{(5-13)}$$

Subsequently, the optimisation problem of equation (5-10) above can be converted to the optimisation of $V(x(k), r_k)$. Assuming that there exists a positive integer γ and satisfies:

$$\boldsymbol{\min_{u(k+i|k)i=0,1,\dots,n-1} \max_{[A,A_p,B]\in\Omega} J_\infty(k) \leq minV(x(k), r_k) \leq \gamma} \dots\dots\dots \boldsymbol{(5-14)}$$

Then, we obtain

$$\boldsymbol{X^T(k)p_iX(k)}$$
$$\boldsymbol{+\sum_{j=1}^{\tau^{ca}_k} X^T(k-j)SX(k-j)}$$
$$\boldsymbol{+\sum_{j=1}^{\tau^{sc}_k} X^T(k-j)K_j^T TK_j X(k-j) \leq \gamma} \dots\dots\dots \boldsymbol{(5-15)}$$

In following section, the major consequences of the RMPC algorithm based on the solution of a set of LMIs are specified.

5.3.2 RMPC Design based on LMIs Approach

The main idea of the LMI approach is that at each time moment, an LMI optimisation problem such as the Lyapunov function, different to traditional linear or quadratic programs, is resolved. This integrates input and output constraints and a description of the plant uncertainty, and guarantees certain robustness properties [175].

Theorem (5-1)

For the Multi Jump Linear System (MJLS) uncertain system (5-9) with stochastic time delay, let the states of the system be measured. Then there exists a state feedback controller as in (5-8) can be calculated as:

$$\boldsymbol{k_i = e(k)_i Q_i^{-1}}$$

Both (5-12) and (5-14) there exists a finite $\boldsymbol{Q_i > 0}$ $\boldsymbol{w > 0}$ $\boldsymbol{e(k)_i > 0}$
Such that the following holds:

$$\min_{Q,W,X,e(k)_i} \gamma \ldots\ldots\ldots (5-16)$$

$$\begin{bmatrix} Q_i & 0 & 0 & Q_iA^T & Q_i & e_i^T(k) & Q_i\sqrt{Q} & 0 \\ 0 & w & 0 & wA_p^T & 0 & 0 & 0 & 0 \\ 0 & 0 & x & xB^T & 0 & 0 & 0 & \sqrt{R} \\ AQ_i & A_pw & Bx & Q_i & 0 & 0 & 0 & 0 \\ Q_i & 0 & 0 & 0 & w & 0 & 0 & 0 \\ e_i(k) & 0 & 0 & 0 & 0 & x & 0 & 0 \\ \sqrt{Q}Q_i & 0 & 0 & 0 & 0 & 0 & \gamma I & 0 \\ 0 & 0 & \sqrt{R} & 0 & 0 & 0 & 0 & \gamma I \end{bmatrix} > 0 \ldots\ldots\ldots (5-17)$$

$$\begin{bmatrix} U_{max}^2 & e(k)_i \\ e(k)_i^T & Q_i \end{bmatrix} > 0 \ldots\ldots\ldots (5-18)$$

$$\begin{bmatrix} \mathbf{1} & X^T(k) & X^T(k-1) & \cdots & X^T(k-\tau_k^{ca}) & X^T(k-1) & \ldots & X^T(k-\tau_k^{sc}) \\ * & Q_i & \mathbf{0} & \ldots & \mathbf{0} & \mathbf{0} & \ldots & \mathbf{0} \\ * & * & w & \ddots & \mathbf{0} & \mathbf{0} & \ldots & \mathbf{0} \\ \vdots & \vdots & \ddots & \ddots & \ddots & \vdots & \vdots & \vdots \\ * & * & * & * & w & \mathbf{0} & \mathbf{0} & \mathbf{0} \\ * & * & * & * & * & Q_i & \mathbf{0} & \mathbf{0} \\ \vdots & \vdots & \vdots & \vdots & \vdots & \ddots & \ddots & \vdots \\ * & * & * & \ldots & * & * & * & Q_i \end{bmatrix}$$

$$> \mathbf{0} \ldots\ldots\ldots (\mathbf{5-19})$$

Proof

Relating the feedback control systems (5-8) and (5-12) is equivalent to the subsequent inequality:

$$\begin{bmatrix} A^T p_i A - p_i + S + Q + K_i^T T K_i & A^T p_i A_p & A^T p_i B \\ A^T p_i A & A_p^T p_i A - S & A_p^T p^T p_i B \\ B^T p_i A & B^T p_i A_p & B^T p_i B + R - T \end{bmatrix} < \mathbf{0} \ldots\ldots\ldots (\mathbf{5-20})$$

Using Schur's complement, it is corresponding to:

$$\begin{bmatrix} p_i - S - Q - K_i^T T K_i & \mathbf{0} & \mathbf{0} & A^T \\ \mathbf{0} & S & \mathbf{0} & A_p^T \\ \mathbf{0} & \mathbf{0} & T - R & B^T \\ A & A_p & B & p_i^{-1} \end{bmatrix} > \mathbf{0} \ldots\ldots\ldots (\mathbf{5-21})$$

where, $Q_i = \gamma p_i^{-1}$ $\quad w = \gamma S^{-1}$ $\quad X = \gamma T^{-1}$

Before and after multiplying both sides of (5-19) by $diag\{Q_i, I, I, I\}$, use Schur's complement and relate with the description of A,A_p, B we get (5-18). As a result of (5-15), we get:

$$\begin{bmatrix} Q_i & \mathrm{e(k)}_\mathrm{i}^\mathrm{T} \\ \mathrm{e(k)}_\mathrm{i} & X \end{bmatrix} > 0$$

If the above is satisfied

$$Q_i - \mathrm{e(k)}_\mathrm{i}^\mathrm{T} \gamma \mathrm{T} \mathrm{e(k)}_\mathrm{i} > \mathbf{0} \ldots\ldots\ldots (\mathbf{5-22})$$

Note that $\mathrm{e(k)_i} = \mathrm{K_i} Q_i$ where, $Q_i = Q_i Q^{-1} Q_i$ we obtain:

$$\boldsymbol{K_i^T T K_i < \gamma Q_i^{-1}} \ldots\ldots\ldots (\mathbf{5-23})$$

Therefore,

$$\sum_{j=1}^{\tau_k^{sc}} \boldsymbol{X^T(k-j) K_j^T T K_j X(k-j)} < \sum_{j=1}^{\tau_k^{sc}} \boldsymbol{X^T(k-j) \gamma Q_i^{-1} X(k-j)} \ldots\ldots\ldots (\mathbf{5-24})$$

Using Schur's complement to obtain (5-19), combining (5-12) and (5-15), we obtain:

$$\boldsymbol{X^T(k+m-j|k) K_j^T T K_j X(k+m-j|k) \le \gamma} \ldots\ldots\ldots (\mathbf{5-25})$$

Subsequently,

$$\boldsymbol{X^T(k+m|k) p_i X(k+m|k) \le \gamma} \ldots\ldots\ldots (\mathbf{5-26})$$

And therefore,

$$\max_{[\boldsymbol{A},\boldsymbol{A_p},\boldsymbol{B}]\in\boldsymbol{\Omega}} \boldsymbol{X^T(k+m|k) Q_i^{-1} X(k+m|k) \le 1} \ldots\ldots\ldots (\mathbf{5-27})$$

So, the predictive states of an uncertain system create an invariant system=$\{Z | Z^T \boldsymbol{Q_i^{-1} Z \le 1}\}$. Then, resolving the input constraint based on the invariant system:

$$\begin{aligned} &\max_{\boldsymbol{m\ge0}} \|\boldsymbol{U(k+m|k)}\|_2 \\ &\quad = \max_{\boldsymbol{m\ge0}} \left\|\mathbf{e(k)_i} \boldsymbol{Q_i^{-1} X(k+m|k)}\right\|_2 \\ &\quad \le \max_{\boldsymbol{Z\in}} \left\|\mathbf{e(k)_i} \boldsymbol{Q_i^{-1} Z}\right\|_2 = \boldsymbol{\lambda_{max}}(\boldsymbol{Q_i^{-1/2}} \mathbf{e(k)_i^T e(k)_i} \boldsymbol{Q_i^{-1/2}}) \ldots\ldots\ldots (\mathbf{5} \\ &\quad \mathbf{-28}) \end{aligned}$$

Subsequently, the input constraint is transformed to:

$$\boldsymbol{Q_i^{-1/2}} \mathbf{e(k)_i^T e(k)_i} \boldsymbol{Q_i^{-1/2} \le U_{max}^2 I} \ldots\ldots\ldots (\mathbf{5-29})$$

And we can get (5-18) by Schur's complement. Finally, the minimisation problem is as follows:

$$\min_{\boldsymbol{Q_i, e(k)_i, w, X}} \boldsymbol{\gamma} \ldots\ldots\ldots (\mathbf{5-30})$$

This completes the proof

Theorem (5-2)

Any feasible solution of the optimisation in theorem (5-1) at sampling time k is also feasible for all sampling time t>k.

Proof

Let us assume the optimisation problem (5-10) is feasible at sampling time k. The only LMI in the problem that depends on the measured state $x(k|k) = x(k)$ is the constraint (5-19). Therefore, to prove this theorem, we need only to prove that inequality (5-19) is feasible for all the future measured states:

$$\boldsymbol{x(k+m|k+m) = x(k+m) \qquad for\, m > 0}$$

From (5-12), we obtain that the Lyapunov function $V(x(k), r_k)$ is decreasing, it follows that:

$$\boldsymbol{E\{V(x((k+m+1), r_k)|k) < E\{V(x((k), r_k)|k) \ldots\ldots\ldots (5-31)}$$

Therefore,

$$\boldsymbol{E\{V(x((k+1), r_k)|k) < E\{V(x((k), r_k)|k) < \gamma \ldots\ldots\ldots (5-32)}$$

Due to $x(k|k) = x(k)$, associated with system (5-8), obtain

$$\boldsymbol{x(k+1|k) = x(k+1|k+1) \ldots\ldots\ldots (5-33)}$$

At sampling time k+1, we denote $X^{k+1}, P^{k+1}_{rk+1}, Q^{k+1}_i, W^{k+1}, e(k)^{k+1}_i$ as the optimal solution of (5-14) and $X^k, P^k_{rk}, W^k, Q^k_i$ are the feasible solution of (5-16). Therefore, obtain:

$$\boldsymbol{E\{V(x((k+1)|k+1, r_k+1)|k) < E\{V(x((k+1|k), r_k)|k) < \gamma \ldots\ldots\ldots (5-34)}$$

This shows that the optimisation problem is feasible at time k+1, k+2, k+3,….. and it is feasible at all sampling time t>k.

This completes the proof

5.4 NUMERICAL EXAMPLE AND SIMULATION RESULTS

To demonstrate the confirmation of the results obtained previously, we consider the following numerical example, where the discrete-time physical plant with sampling time T_s=0.01 sec parameters are described as follows.

$$\boldsymbol{x(k+1) = \begin{bmatrix} 1.0123 & 0.0502 \\ 0.4920 & 1.0123 \end{bmatrix} X(k) + \begin{bmatrix} 0.0125 \\ 0.5020 \end{bmatrix} u(k-\tau^{ca}_k) + \begin{bmatrix} 0.1 \\ 0.1 \end{bmatrix} r(k)}$$

$$\boldsymbol{e(k) = [1 \quad 0]X(k)}$$

The discrete time system is unstable, due to the presence of the stochastic time delay in the system. Given the norm bounded uncertainty matrices

$$\boldsymbol{Q_1 = \begin{bmatrix} 0.01 \\ 0.5 \end{bmatrix} \qquad R_1 = [0.2 \quad 0.1] \qquad R_2 = 0.1}$$

The stochastic time delays involved in WNCS are assumed below:

$$\boldsymbol{\tau_k^{sc} \in \{0,1,2\} \qquad and \qquad \tau_k^{ca} \in \{0,1\}}$$

The transition probability matrices are also assumed as:

$$\boldsymbol{\Lambda = \begin{bmatrix} 0.5 & 0.5 & 0 \\ 0.3 & 0.6 & 0.1 \\ 0.3 & 0.6 & 0.1 \end{bmatrix} \qquad \pi = \begin{bmatrix} 0.2 & 0.8 \\ 0.5 & 0.5 \end{bmatrix}}$$

The initial distribution for $(\tau_0^{sc}, \tau_{0-\tau_0^{sc}-1}^{ca})$ is assumed for $\alpha(i,r) = \frac{1}{6}$ for each $i \in \mathcal{M}$ and $r \in \mathbb{N}, \gamma$ is set to be 2. The reference signal is assumed to be:

$$\boldsymbol{r(k) = \begin{cases} 1 & 1 \le k \le 10 \\ -1 & 21 \le k \le 30 \\ 0 & otherwise \end{cases}}$$

The equivalent controller gains $k_1\left(\tau_k^{sc}, \tau_{k-\tau_k^{sc}-1}^{ca}\right)$, $k_2\left(\tau_k^{sc}, \tau_{k-\tau_k^{sc}-1}^{ca}\right)$ is

$$k_1(0,0) = \begin{bmatrix} 0.6381 & -0.2795 \\ 1.5862 & 0.1193 \end{bmatrix} \qquad k_2(0,0) = \begin{bmatrix} 0.5321 & -0.2102 \\ 0.8723 & 0.1352 \end{bmatrix}$$

$$k_1(0,1) = \begin{bmatrix} 0.4230 & -0.1787 \\ 0.9434 & 0.4008 \end{bmatrix} \qquad k_2(0,0) = \begin{bmatrix} 0.3342 & -0.2310 \\ 0.7602 & 0.3052 \end{bmatrix}$$

$$k_1(1,0) = \begin{bmatrix} 0.4791 & -0.3242 \\ 0.8619 & 0.4258 \end{bmatrix} \qquad k_2(0,0) = \begin{bmatrix} 0.3321 & -0.2021 \\ 0.6793 & 0.2534 \end{bmatrix}$$

$$k_1(1,1) = \begin{bmatrix} 0.5538 & -0.3507 \\ 1.0446 & 0.3477 \end{bmatrix} \qquad k_2(0,0) = \begin{bmatrix} 0.4287 & -0.1142 \\ 0.7623 & 0.2806 \end{bmatrix}$$

$$k_1(2,0) = \begin{bmatrix} 1.0795 & -0.3557 \\ 0.6227 & 0.3569 \end{bmatrix} \qquad k_2(0,0) = \begin{bmatrix} 0.7996 & -0.2011 \\ 0.4103 & 0.1352 \end{bmatrix}$$

$$k_1(2,1) = \begin{bmatrix} 0.9886 & -0.3332 \\ 0.6021 & 0.4222 \end{bmatrix} \qquad k_2(0,0) = \begin{bmatrix} 0.5256 & -0.3206 \\ 0.5783 & 0.2341 \end{bmatrix}$$

The minimum value of $\|V(k)_3\|_2 = 0.31$ can be achieved by using system (5-23) since the value of $\|V(k)_3\|_2 = 0.31 < \gamma$=2. The RMPC is therefore solved under this framework of LMIs. The SWNCS output is maintained near to zero in spite of the uncertain parameters such as physical plant disturbance, wireless network stochastic delay and packet dropout. Table 5-1 demonstrates the performance parameters of the SWNCS obtained when RMPC techniques are used. Chapter 7 uses NNPC to remove the effect of stochastic time delay and packet dropout occurring in the SWNCS and to compute the performance parameters. Comparison is then made of the simulation results and performance parameters of SWNCS when employing RMPC and NNPC.

Table 5.1. Performance Parameters of SWNCS with WI-FI and WiMAX Wireless Network

Performance Parameters	RMPC Technique with WI-FI wireless network	RMPC Technique with WiMAX wireless network
Maximum Overshoot	0.32	0.45
Settling Time (sec.)	0.24	0.33
Steady State error	$4x10^{-5}$	$6x10^{-4}$

5.5 CONSTRUCTING SWNCS IN TRUETIME SIMULATION TOOLS

The stages required to construct a wireless networked control application in TrueTime will be studied in the model in Figure 5-1, in which 2 nodes are linked to a wireless network, data rate (80 kbits/sec.), minimum frame size (272 bits), transmit power (30dbm), error coding threshold (0.03), loss probability (0) and receiver signal threshold (-48dbm). The sampler (sensor) node samples the process output periodically and transmits the measurement values to the RMPC node over the wireless network. The arrival of sensor information data to the RMPC node generates a task that calculates a new control action. The control action is then transmitted to the Zero-order-hold ZOH (actuator) node, where it is sent to the process.

The subsequent management and control demonstration and network schedule using WI-FI and WiMAX is presented in Figures 5-3 and 5-4 respectively. The schedule of stochastic time delay demonstrates that the network load is very high. Figure 5-5 illustrates the output response and the control signal of the SWNCS when Wi-Fi and WiMAX are employed as wireless networks. Figure 5-6 shows the schedule of stochastic time delay at the computer node when Wi-Fi and WiMAX are used. Furthermore, the schedule of stochastic time delay at wireless networks to each Wi-Fi and WiMAX network are shown in Figure 5-7 [176].

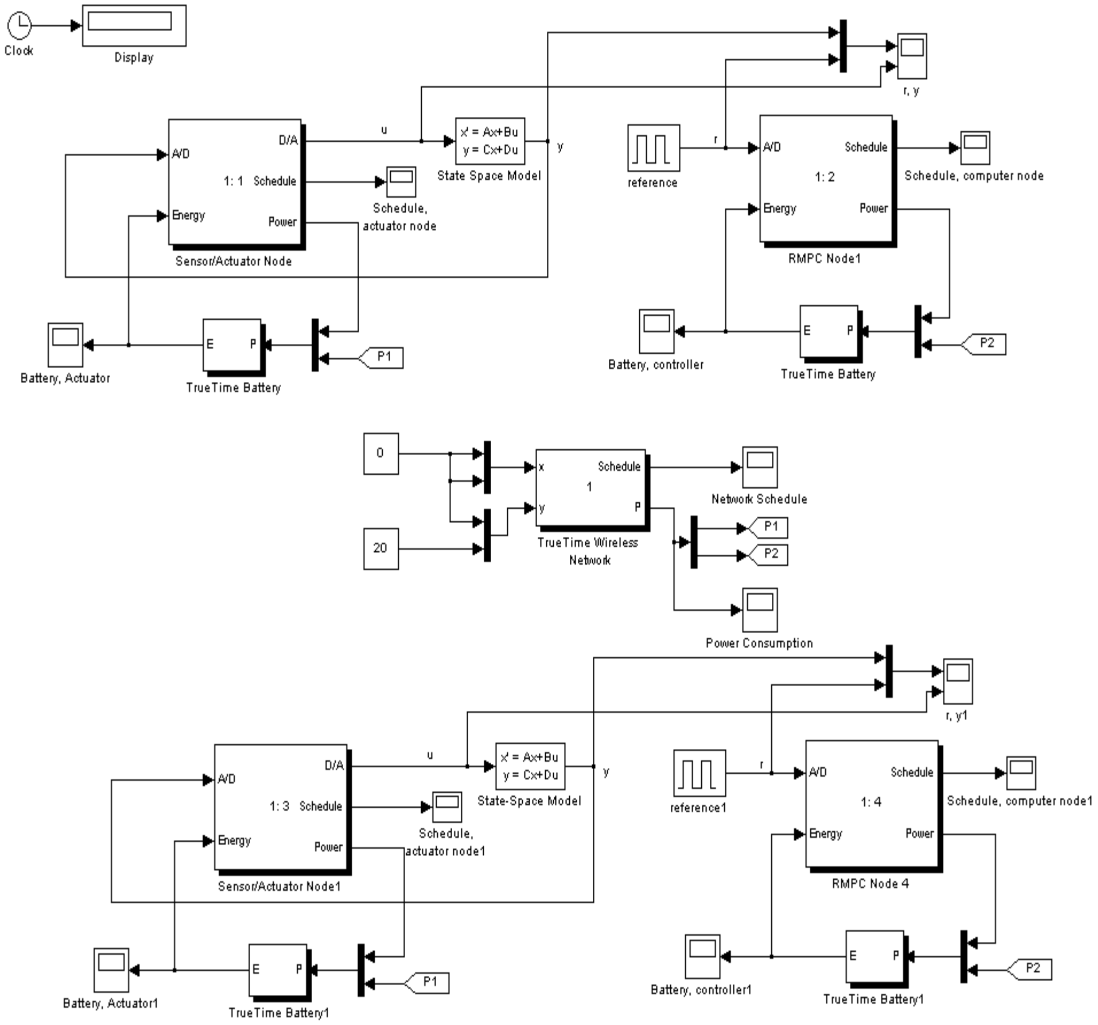

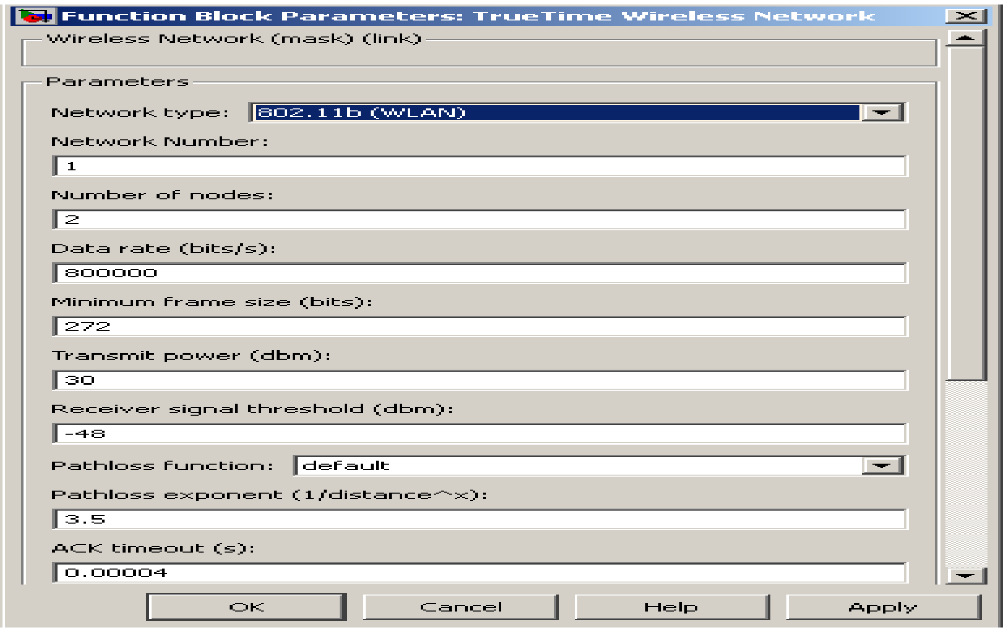
Function Block Parameters: TrueTime Wireless Network

Wireless Network (mask) (link)

Parameters

Network type: 802.11b (WLAN)

Network Number: 1

Number of nodes: 2

Data rate (bits/s): 800000

Minimum frame size (bits): 272

Transmit power (dbm): 30

Receiver signal threshold (dbm): -48

Pathloss function: default

Pathloss exponent (1/distance^x): 3.5

ACK timeout (s): 0.00004

Fig.5.3. SWNCS with Computer Nodes and WI-FI Wireless Network Node

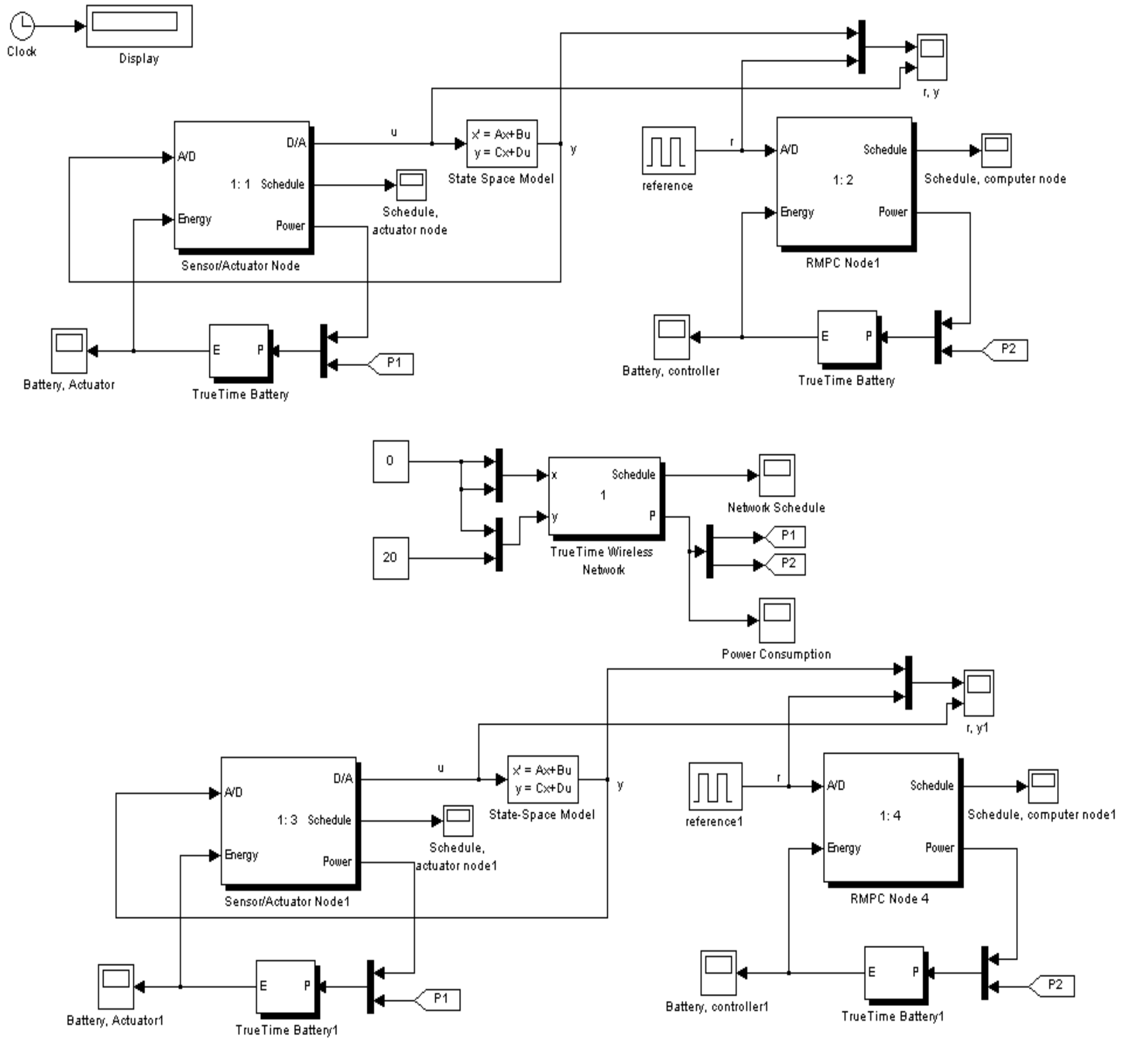

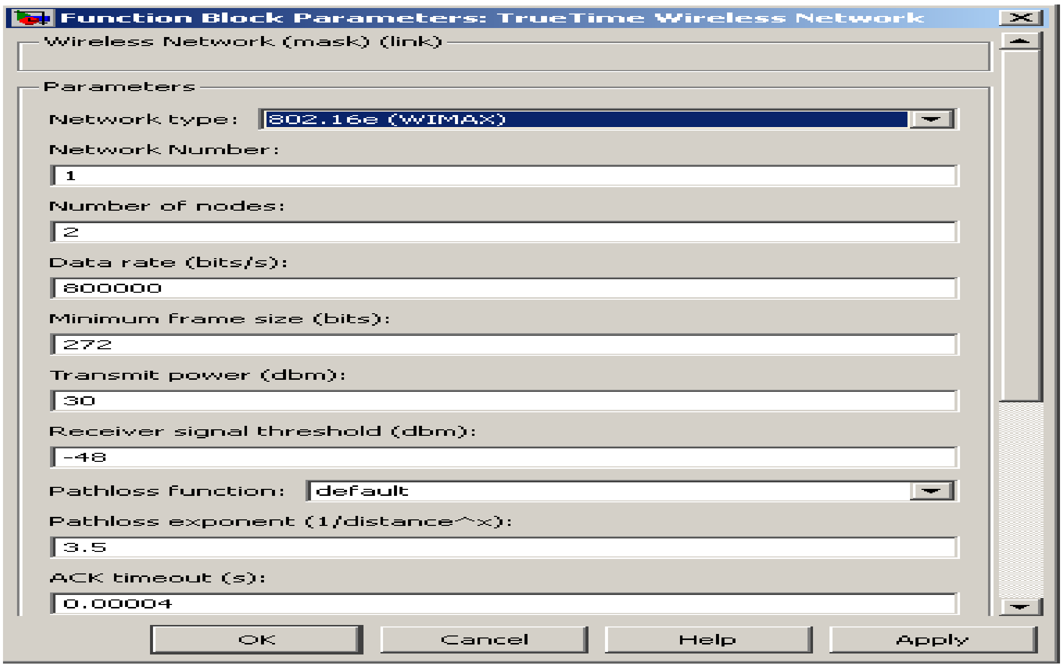
Function Block Parameters: TrueTime Wireless Network

Wireless Network (mask) (link)

Parameters

Network type: 802.16e (WIMAX)

Network Number:
1

Number of nodes:
2

Data rate (bits/s):
800000

Minimum frame size (bits):
272

Transmit power (dbm):
30

Receiver signal threshold (dbm):
-48

Pathloss function: default

Pathloss exponent (1/distance^x):
3.5

ACK timeout (s):
0.00004

Fig.5.4. SWNCS with Computer Nodes and WiMAX Wireless Network Node

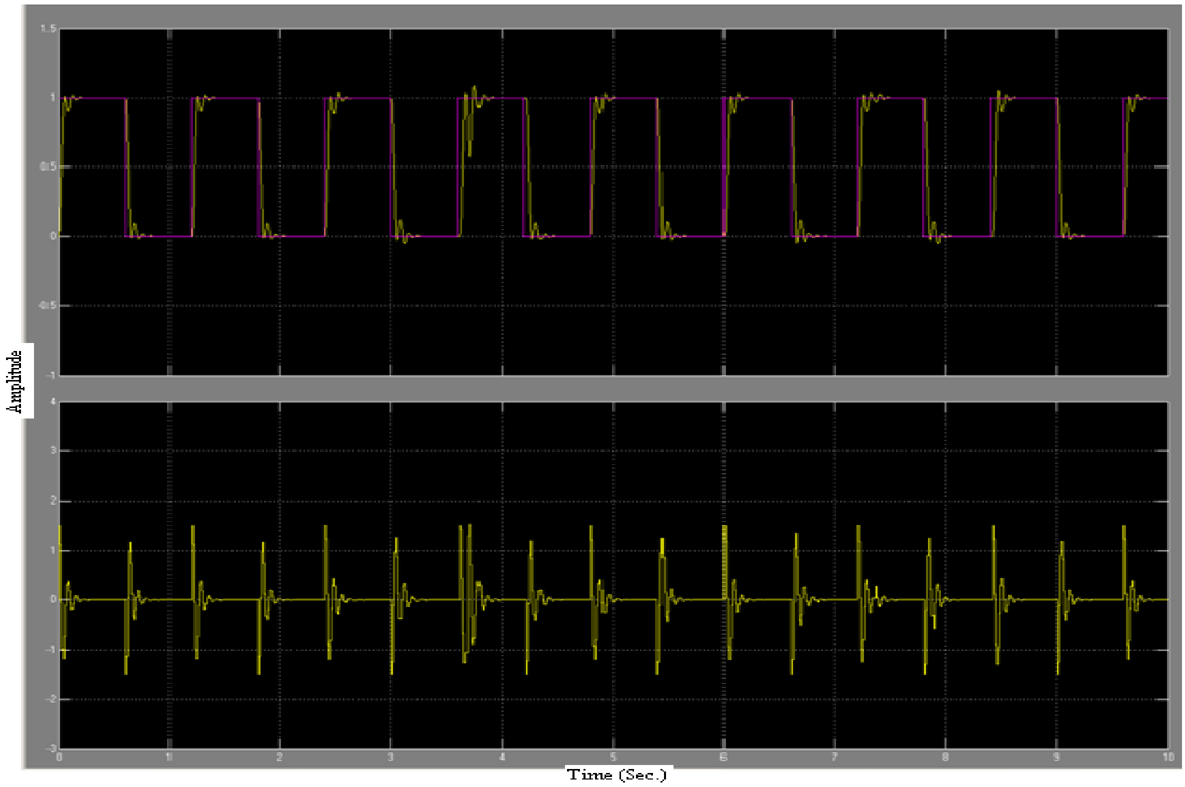

Wi-Fi Wireless Network

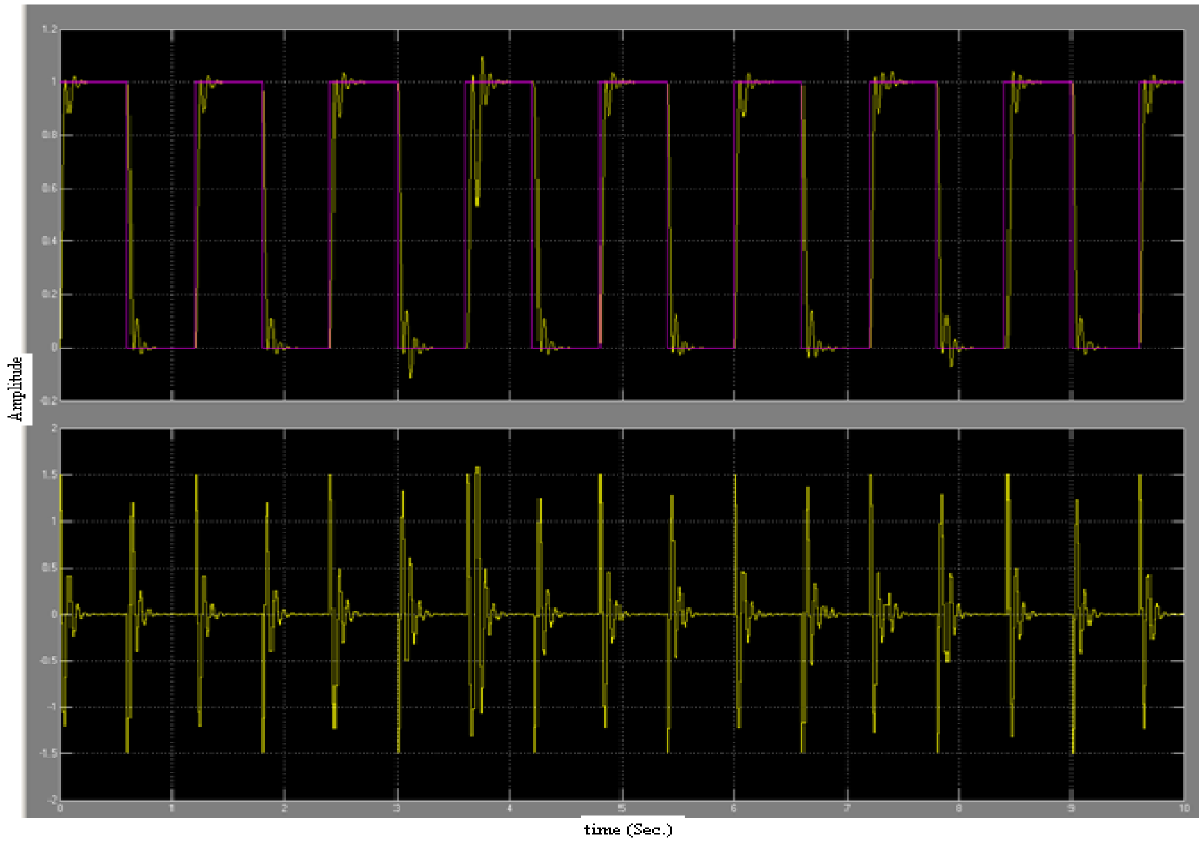

WiMAX Wireless Network

Fig.5.5. **Output Response for the SWNCS (Wi-Fi & WiMAX) Wireless Network**

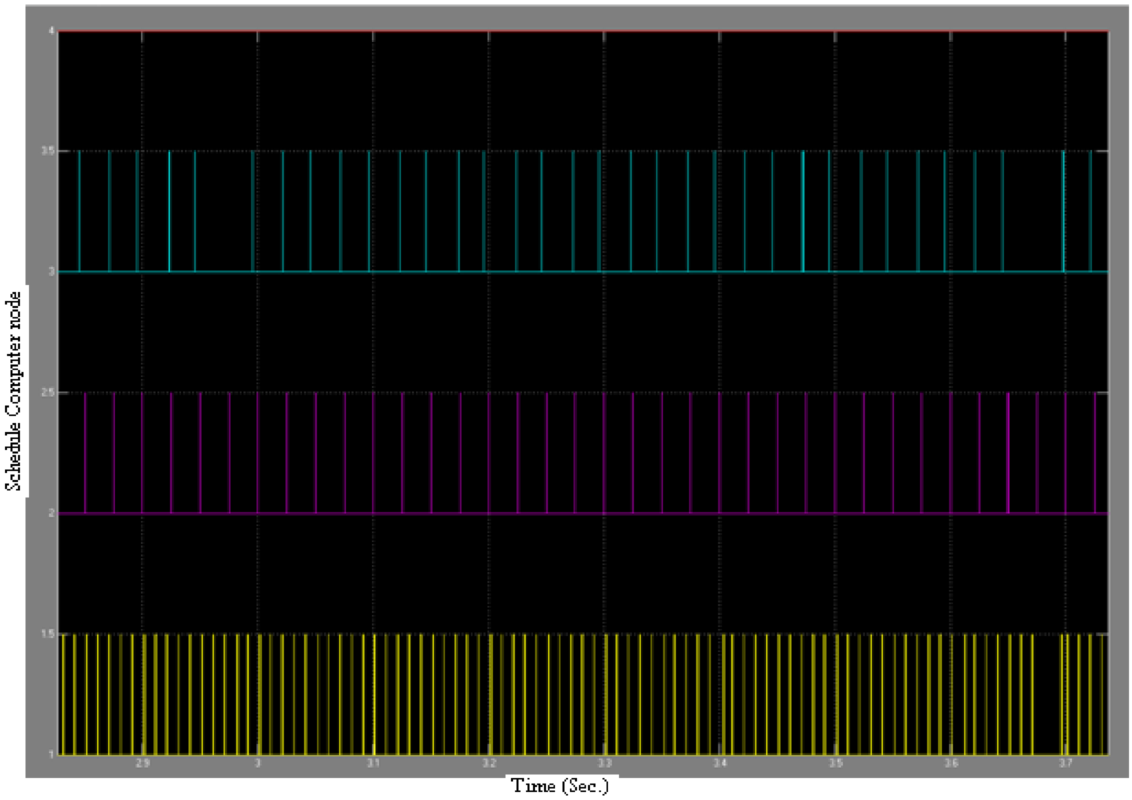

Wi-Fi Wireless Network

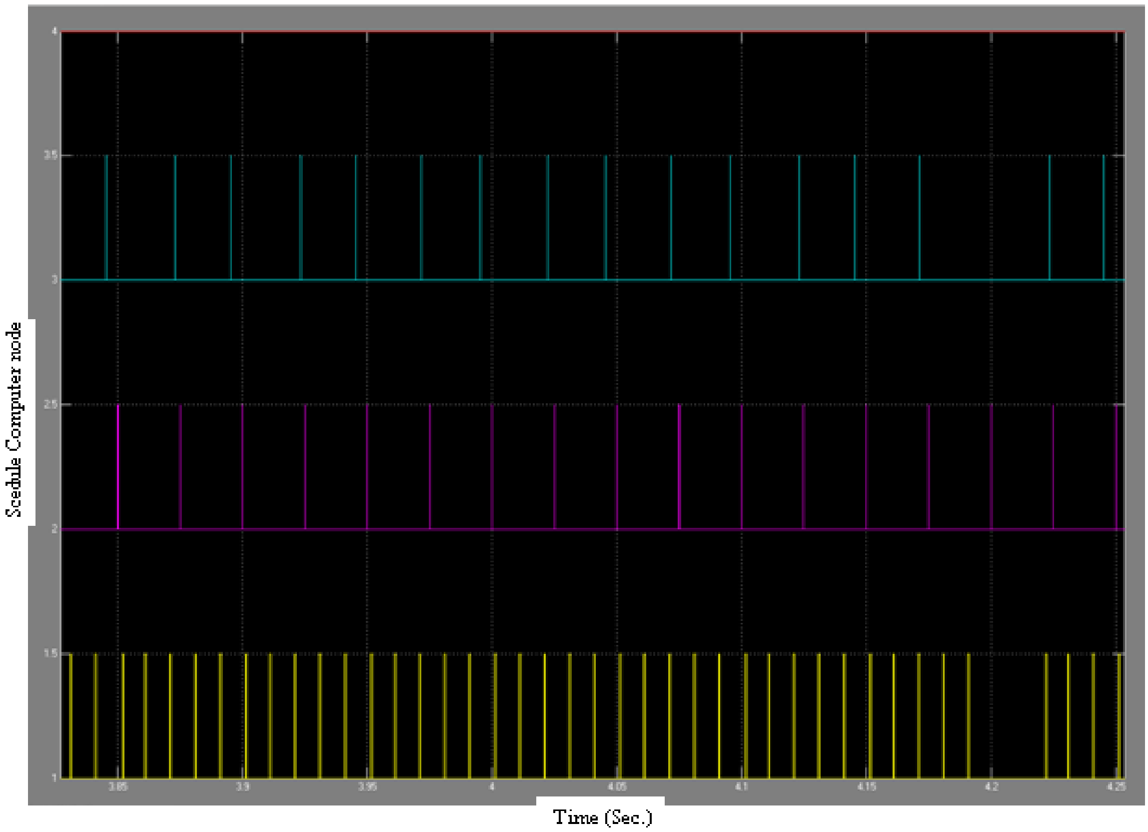

WiMAX Wireless Network

Fig.5.6. Schedule at Computer Node

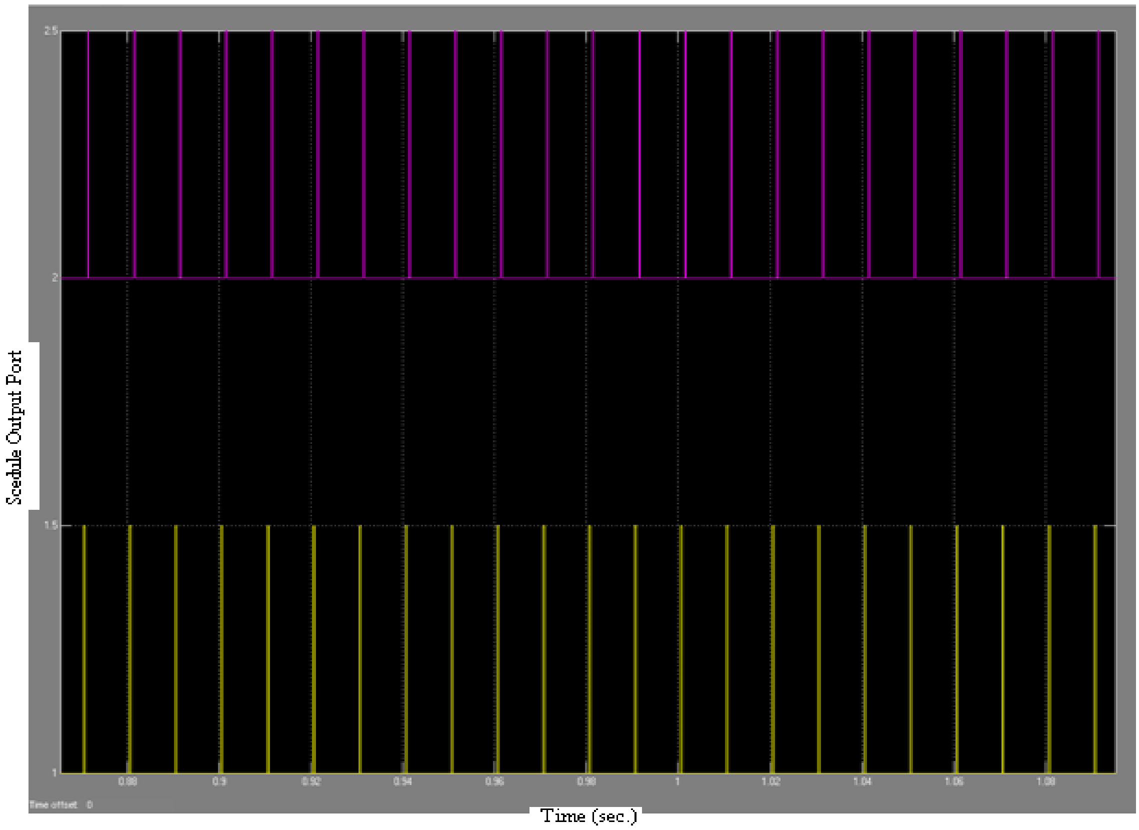

Wi-Fi Wireless Network

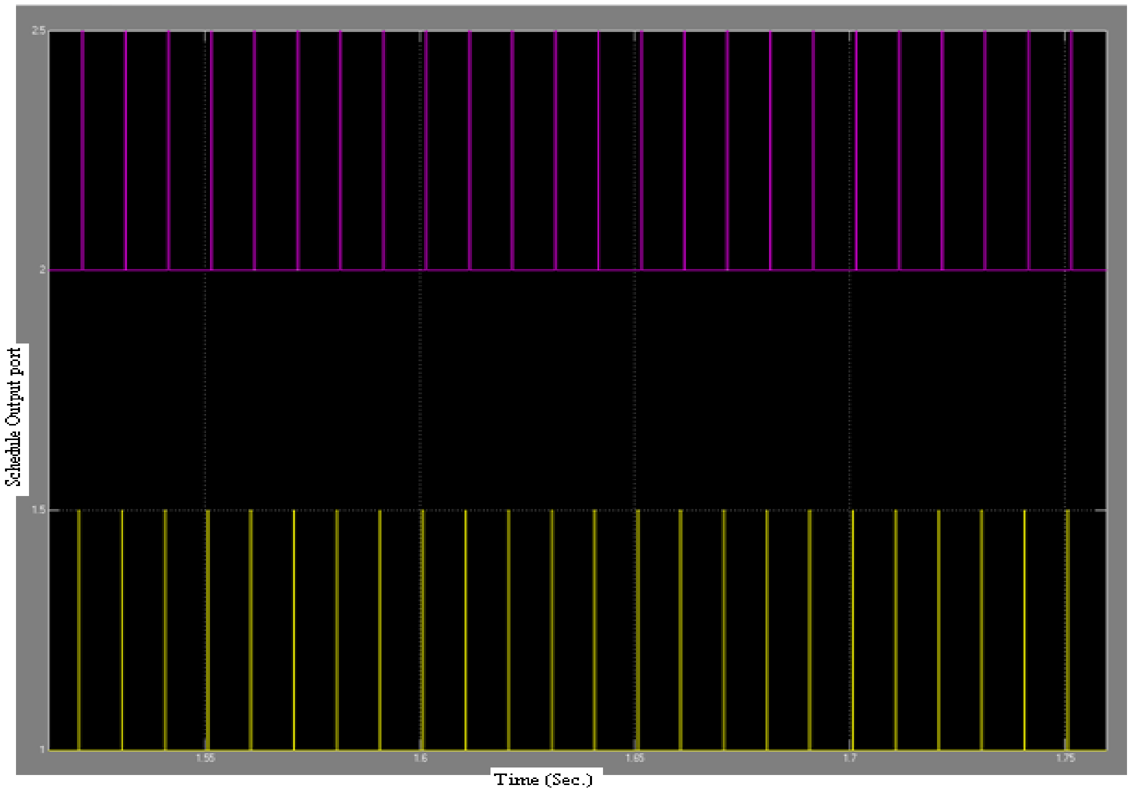

WiMAX Wireless Network

Fig.5.7. Schedule at Wireless Network Node

5.6 SIMULATION OF POWER CONSUMPTION IN SWNCS

The model in Figure 5-3 has four nodes located 20m apart when using Wi-Fi or 1000m apart when using WiMAX; each represented by TrueTime blocks. A time-driven sensor node samples the process periodically and transmits the samples over wireless network (Wi-Fi/WiMAX) to the event-driven controller node. The controller node computes the control signal and transmits the result back to the event-driven actuator node. The SWNCS connection is at the same time subject to a simple power control system. The power control signal running in all nodes (sensor, controller and actuator) periodically transmit out ping messages to the other nodes to test the channel transmission as follows:

- If the replay is received, the channel is assumed to be good and the transmission power is lowered.
- If no replay is received, then the transmission power is significantly increased until it saturates or replay is received again.

SWNCS power consumption can be summarised as:

Step1: run a first simulation with power control scheme in the controller node. Figures 5-8 and 5-9 demonstrate the battery levels in the controller and actuator nodes, respectively. Figure 5-10 illustrates the power consumption in the wireless network (Wi-Fi/WiMAX). Note the following issues:

1. Power is not activated until 4 second has elapsed.
2. The measured values sometimes diverge more than common from the desired values. This divergence is caused by the fact that it is possible to lose several consecutive sensor value readings when using simple power control in the nodes.

Step2: switch off the power control system in the controller node. This is done commenting out the creation of the signal power controller in the controller node. Run the simulation again and now note that the power drain is constant in the controller node. This causes the battery to run out of energy, and the control is lost as shown in Figures 5-11 and 5-12. The power consumption at wireless network (Wi-Fi/WiMAX) is illustrated in Figure 5-13.

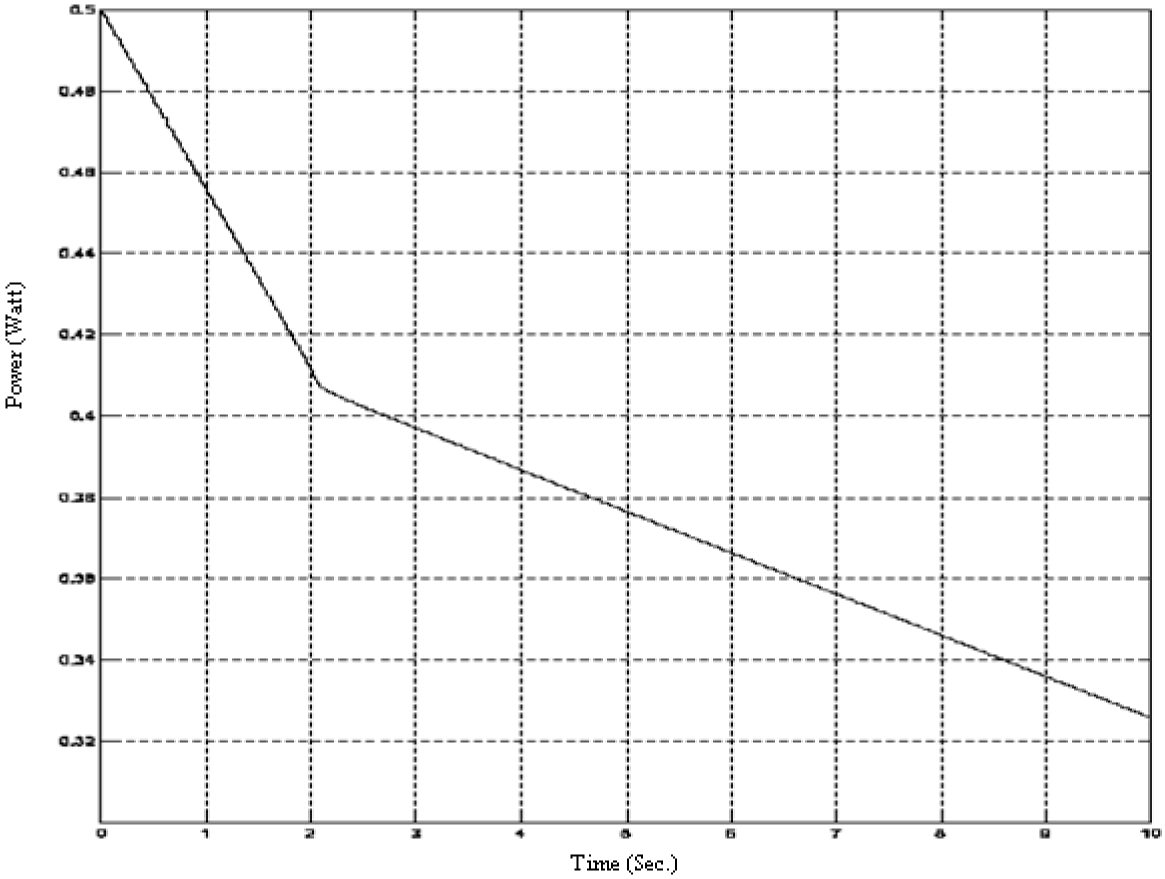

Fig.5.8. Battery Level at Controller Node

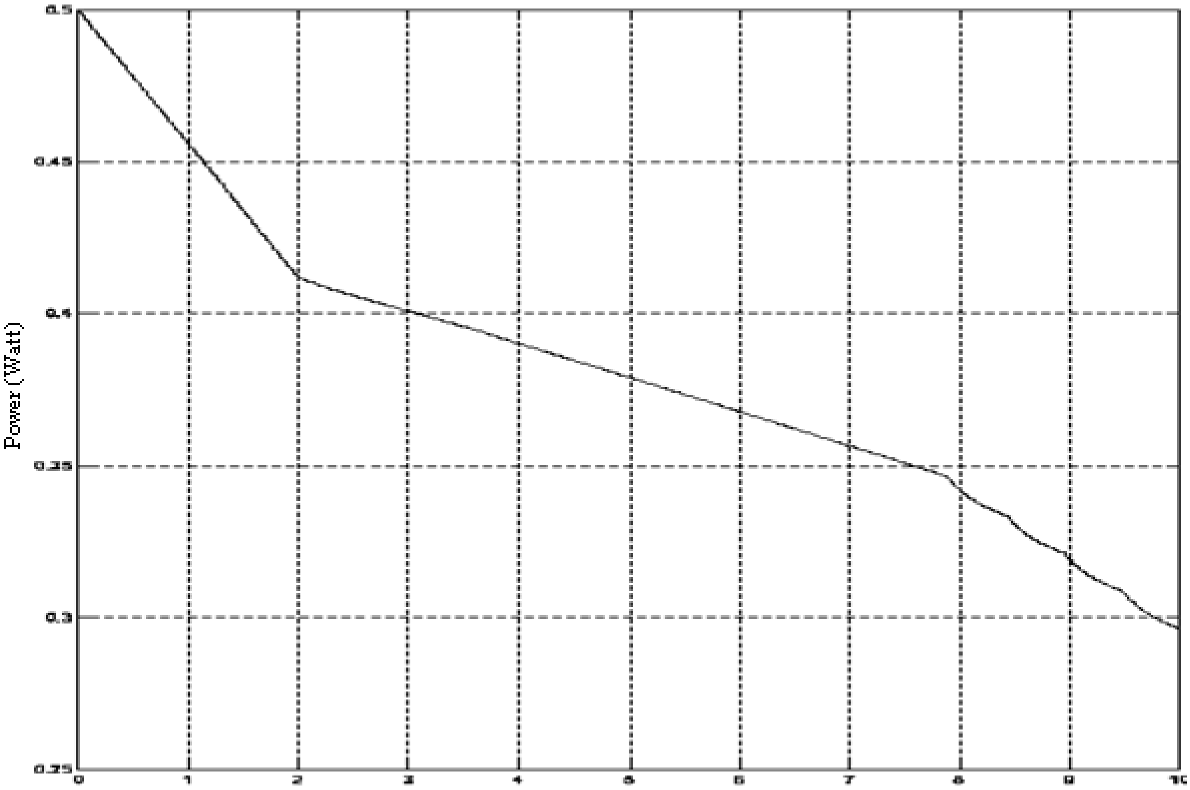

Fig.5.9. Battery Level at Actuator Node

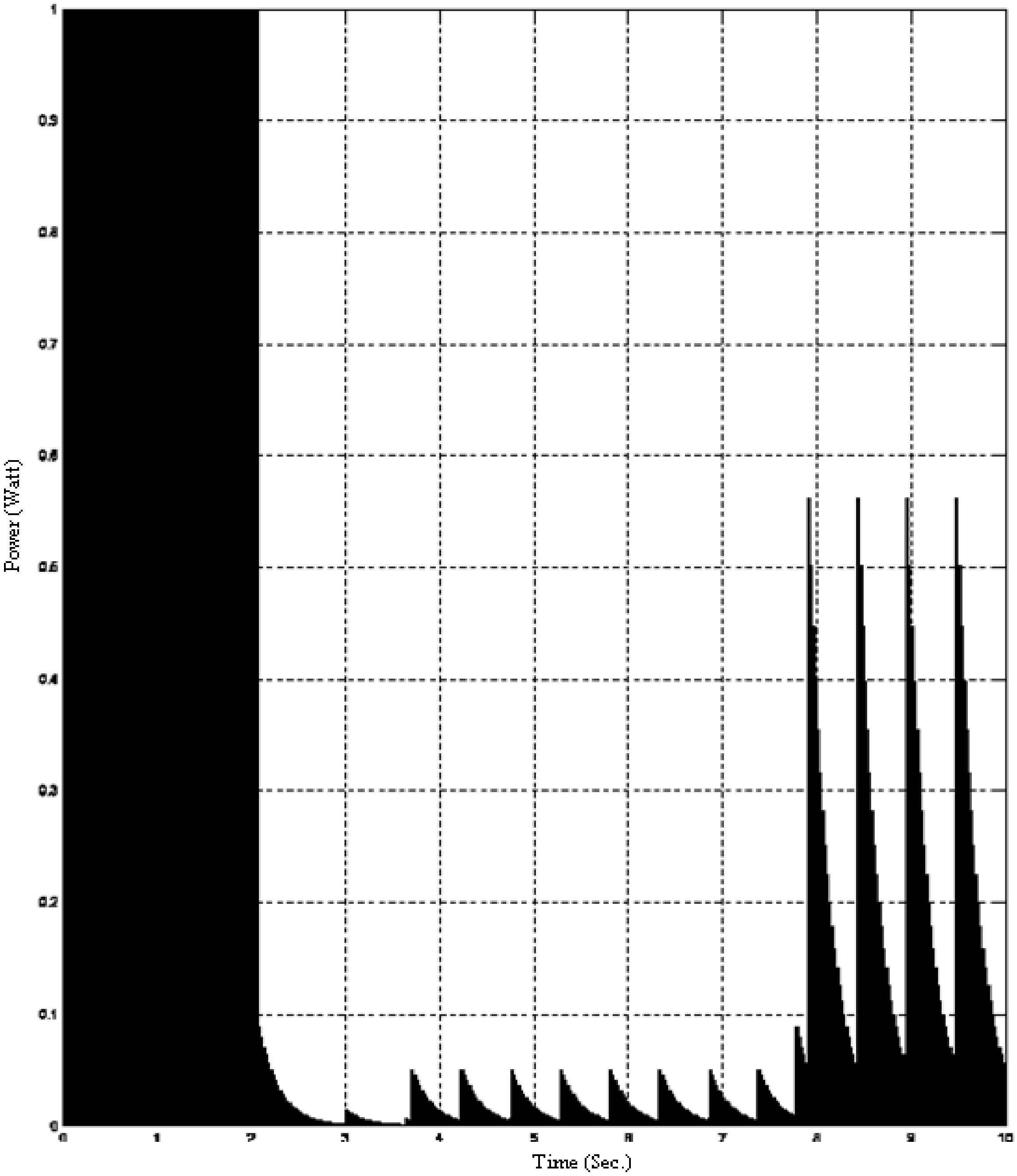

Fig.5.10. Power Consumption at Wireless Network

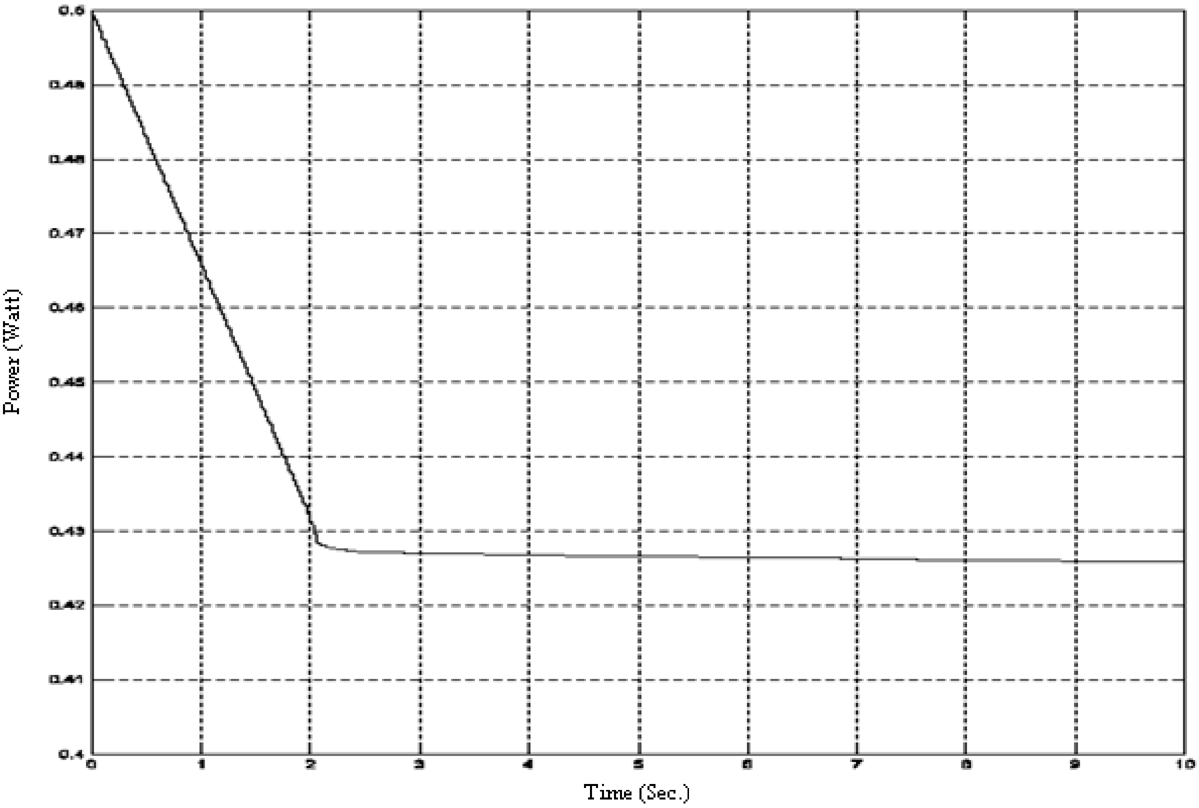

Fig.5.11. Battery Level at Controller Node (without Power Control System)

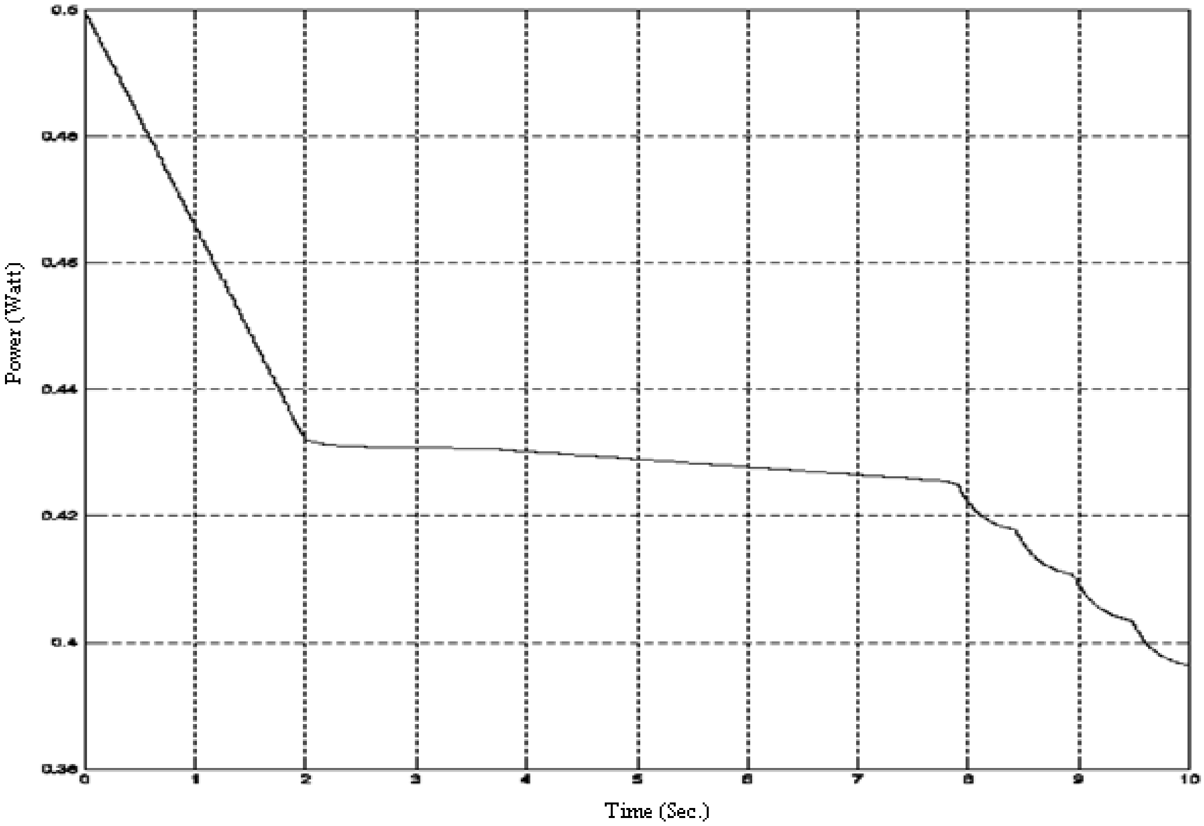

Fig.5.12. Battery Level at Actuator node (without Power Control System)

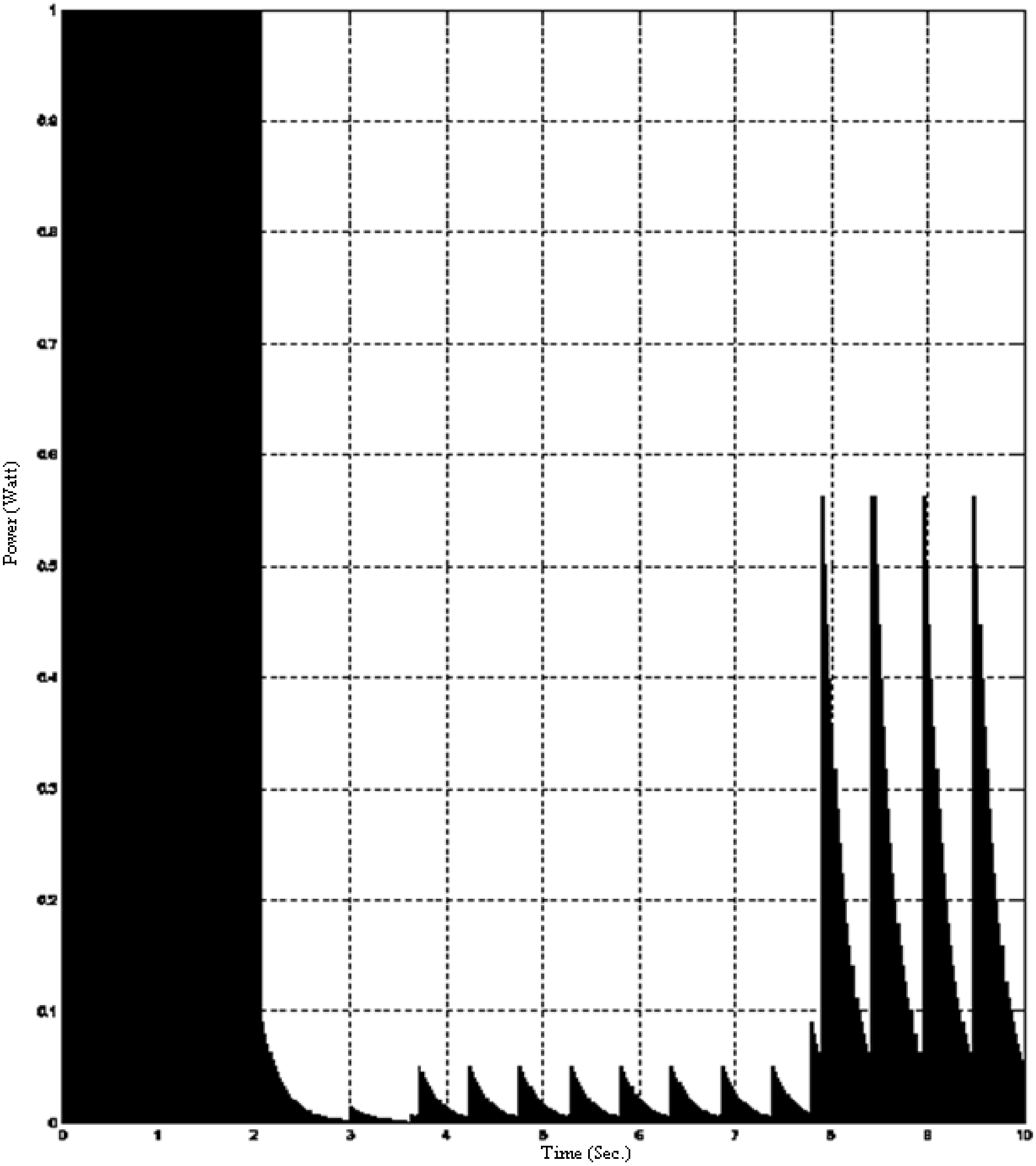

Fig.5.13. Power Consumption at Wireless Network (without Power Control System)

5.7 CHAPTER SUMMARY

In this chapter, RMPC has been investigated to enhance the QoS of the SWNCS by removing the effect of the stochastic time delay and packet dropouts occurring in the SWNCS. The network time delays and packet dropouts of the SWNCS are considered as stochastic variables controlled by a Markov chain. A discrete-time Markovian Jump Linear System (MJLS) with norm unbounded time delay is presented to model the SWNCSs. Based on the SWNCS model, the RMPC based on full state feedback controller can be solved under the framework of LMIs. SWNCS has been implemented with specific communications and control parameters using TrueTime simulator tools. A SWNCS with TrueTime simulation tools has been constructed to illustrate the efficiency of the proposed techniques.

The main contribution of this chapter is that both the sensor-to-controller $\tau_k^{sc}$and controller-to-actuator τ_k^{ca}wireless network time delays and packet dropouts have been considered. Furthermore, these delays are regarded as input delays and are handled in the scope of perturbation attenuation. Finally, the numerical example and simulation results have adjusted the robust controller gain according to the wireless network performance QoS. Validation of the results has been carried out by use of a numerical model and through simulation studies.

CHAPTER 6 ..

ROBUST STABILITY ANALYSIS OF SWNCS WITH STOCHASTIC NETWORK TIME DELAYS AND PACKET DROPOUT BASED ON H_∞ AND H_2 NORMS

6.1 INTRODUCTION

A basic performance requirement for any feedback control system is its ability to preserve the stability of the closed loop. By closed-loop stability, we denote the stability of uncertain parameters such as stochastic network time delays and packet dropout in physical plant model, rather than just the stability of the nominal linear finite dimensional model employed to characterize the physical plant model. With the framework of the controller design, nominal properties concern the characteristics of model when the model of controlled procedure is assumed to duplicate real procedure behaviour. Alternatively, robustness properties refer to those of a system in the presence of physical plant model divergence. Clearly, the significant stage of robust control design is to guarantee that the controller will stabilise the model of the process employed to design the controller and that it will realise the required performance [123-126].

In this chapter, the stability and stabilization problems of SWNCSs with stochastic network time delay and packet dropout are investigated. The physical plant considered here is a linear discrete-time system. The communication constraints comprise stochastic time delay and packet dropout, which usually appear in a wireless networked environment. Our aim is to design a RMPC such that the resulting SWNCS is robustly stable. A new model of SWNCS is created with time delay and packet loss components. The RMPC (a full state feedback controller) can be constructed by using the Lyapunov functional method. Both sensor-to-controller and controller-to-actuator time delays of the SWNCS are considered as stochastic variables controlled by a Markov chain. Sufficient conditions for the robust stability based on $H_\infty \& H_2$ norms of the SWNCSs are suggested in terms of LMI, and they are shown to be less conservative via an illustrative example. Numerical examples are presented to demonstrate the utility of the improved assumption. The following section derives the conditions for robust (stochastic) stability.

6.2 ROBUST (STOCHASTIC) STABILITY

In this chapter, the robust (stochastic) stability structure is used to investigate the robustness of discrete-time MJLSs in closed-loop with stabilizing RMPCs. In many applications the significance of these issues cannot be overstated, since nominally stabilising controllers are always affected by disturbances and uncertainties when applied in practice. However, the network time delay and packet dropout that occur in SWNCS are considered as uncertainty parameters. In Chapter 5, representations of the model set are given in terms of a nominal model (5-9), and control signal in system (5-4)

Definition 1 (robust stability)

The system (5-9) has robust stability with $r(k) = 0 \quad for\ k \geq 0$ if for all finite $\xi_o = \xi(0)$ initial modes $\tau_o^{sc} = \tau(0) \in \mathcal{M} and\ \tau^{ca}_{-\tau_o^{sc}-1} \in \mathbb{N}$ there exists, a finite $w > 0$ such that the following holds [125, 170].

$$\boldsymbol{E} = \sum_{\boldsymbol{k}=\boldsymbol{0}}^{\infty} \|\boldsymbol{\xi}(\boldsymbol{k})\|_2 | \boldsymbol{\xi}_{\boldsymbol{o}}, \boldsymbol{\tau}_{\boldsymbol{o}}^{\boldsymbol{sc}}, \boldsymbol{\tau}^{\boldsymbol{ca}}_{-\boldsymbol{\tau}_{\boldsymbol{o}}^{\boldsymbol{sc}}-\boldsymbol{1}} \leq \boldsymbol{\xi}_{\boldsymbol{o}}^{\boldsymbol{T}} \boldsymbol{w} \boldsymbol{\xi}_{\boldsymbol{o}} \ldots\ldots\ldots (\boldsymbol{6}-\boldsymbol{1})$$

Lemma (1)

The transition probability matrices for the multi-step delay mode jump can be written as follows:

$$\tau_k^{sc} = j \qquad\qquad \tau_k^{ca} = s1 \qquad\qquad \tau^{ca}_{k-\tau_k^{sc}-1} = s2$$

Proposition 1

These three probability transition matrices are:

$$\boldsymbol{\tau}_{\boldsymbol{k}}^{\boldsymbol{sc}} \rightarrow \boldsymbol{\tau}_{\boldsymbol{k}+\boldsymbol{1}}^{\boldsymbol{sc}} : \boldsymbol{\Lambda}$$

$$\boldsymbol{\tau}^{\boldsymbol{ca}}_{\boldsymbol{k}-\boldsymbol{\tau}_{\boldsymbol{k}}^{\boldsymbol{sc}}-\boldsymbol{1}} \rightarrow \boldsymbol{\tau}^{\boldsymbol{ca}}_{\boldsymbol{k}-\boldsymbol{j}} : \boldsymbol{\pi}^{\boldsymbol{1}+\boldsymbol{i}-\boldsymbol{j}}$$

$$\boldsymbol{\tau}^{\boldsymbol{ca}}_{\boldsymbol{k}-\boldsymbol{j}} \rightarrow \boldsymbol{\tau}_{\boldsymbol{k}}^{\boldsymbol{ca}} : \boldsymbol{\pi}^{\boldsymbol{j}}$$

Proposition 2

An interesting property obtained from theorem 3 is monotonically increasing behaviour of the following Lyapunov system:

$$\boldsymbol{E}\left\{\boldsymbol{x}(\boldsymbol{t})^{\boldsymbol{T}} \boldsymbol{Q}\left(\boldsymbol{\tau}_{\boldsymbol{k}}^{\boldsymbol{sc}}, \boldsymbol{\tau}^{\boldsymbol{ca}}_{\boldsymbol{k}-\boldsymbol{\tau}_{\boldsymbol{k}}^{\boldsymbol{sc}}-\boldsymbol{1}}\right) \boldsymbol{x}(\boldsymbol{k}) \middle| \boldsymbol{x}_{\boldsymbol{t}}, \boldsymbol{\tau}_{\boldsymbol{t}}^{\boldsymbol{sc}}, \boldsymbol{\tau}^{\boldsymbol{ca}}_{\boldsymbol{t}-\boldsymbol{\tau}_{\boldsymbol{t}}^{\boldsymbol{sc}}-\boldsymbol{1}}\right\} = \boldsymbol{0}\ \boldsymbol{for\ all}\ \ \boldsymbol{t} \leq \boldsymbol{k}_{\boldsymbol{1}} \leq \boldsymbol{k}$$

Theorem 3 (condition for robust stability)

Under the proposed control signal in system (5-4), the resulting feedback control system (5-9) is robustly stable if and only if there exist symmetric $P(i,r) > 0$ such that the following matrix inequality holds for all $i,j \in \mathcal{M}\ and\ r, s_1 and\ s_2 \in \mathbb{N}$.

$$-\boldsymbol{P}(\boldsymbol{i},\boldsymbol{r})+\sum_{\boldsymbol{j}=0}^{\tau_k^{sc}}\sum_{\boldsymbol{s1}=0}^{\tau_k^{ca}}\sum_{\boldsymbol{s2}=0}^{\tau_k^{ca}}\boldsymbol{\lambda_{ij}\pi_{rs2}^{1+i-j}\pi_{s2s1}^{j}\bar{A}(i,r,s1)^{T}XP(j,s2)\bar{A}(i,r,s1)}$$

$$< 0 \dots\dots\dots (6-2)$$

Proof

The closed-loop system in (5-9) constructs the Lyapunov function

$$\boldsymbol{V(x(k),k) = x(k)^{T}P\left(\tau_k^{sc},\tau_{k-\tau_k^{sc}-1}^{ca}\right)x(k)}$$

Then

$$\boldsymbol{E}\{\Delta(\boldsymbol{V(x(k),k)})\} = \boldsymbol{E}\{\Delta(\boldsymbol{V(x(k+1),k+1)}) - (\boldsymbol{V(x(k),k)})\}$$

$$= \boldsymbol{E}\left\{\boldsymbol{x(k+1)^{T}P\left(\tau_k^{sc},\tau_{k-\tau_k^{sc}-1}^{ca}\right)x(k+1)}\,\middle|\,\boldsymbol{x_k,\tau_k^{sc} = i,\tau_{k-\tau_k^{sc}-1}^{ca}}\right.$$

$$\left.= \boldsymbol{r}\right\}\dots\dots\dots(\boldsymbol{6-3})$$

To evaluate the first term in (6-3), we want to apply the probability transition matrices based on Lemma 1

$$\boldsymbol{\tau_k^{sc}\xrightarrow{yields}\tau_{k+1}^{sc},\quad \tau_{k-\tau_k^{sc}-1}^{ca}\xrightarrow{yields}\tau_{k-j}^{ca},\qquad and\tau_{k-j}^{ca}\xrightarrow{yields}\tau_k^{ca}}$$

According to Proposition 1(6-3) can be evaluated as:

$$\boldsymbol{E}\{\Delta(\boldsymbol{V(x(k),k)})\}$$

$$= \boldsymbol{x(k)^{T}}\left\{\sum_{\boldsymbol{j}=0}^{\tau_k^{sc}}\sum_{\boldsymbol{s1}=0}^{\tau_k^{ca}}\sum_{\boldsymbol{s2}=0}^{\tau_k^{ca}}\boldsymbol{\lambda_{ij}\pi_{rs2}^{1+i-j}\pi_{s2s1}^{j}\ X[\bar{A}}\right.$$

$$+ \boldsymbol{\bar{B}k(i,s1,r)\bar{C}(i)]^{T}P(j,s2)X\,[\bar{A}+\bar{B}k(i,s1,r)\bar{C}(i)]}$$

$$\left.- \boldsymbol{P(i,r)}\right\}\boldsymbol{x(k)}\dots\dots\dots(\boldsymbol{6-4})$$

Therefore, if P(i,r)<0, then

$$\boldsymbol{E}\{\Delta(\boldsymbol{V(x(k),k)})\} = \boldsymbol{x(k)^{T}P(i,r)x(k)} \le -\boldsymbol{\lambda_{min}}(-\boldsymbol{P(i,r)})\boldsymbol{x(k)^{T}x(k)}$$

$$\le -\boldsymbol{\beta}\|\boldsymbol{x(k)}\|_2\dots\dots\dots(\boldsymbol{6-5})$$

Where $\boldsymbol{\beta} = \boldsymbol{inf}\left\{\boldsymbol{\lambda_{min}}\left(-\boldsymbol{P}(\boldsymbol{i},\boldsymbol{r})\right)\right\} > 0$

From (6-2) we can see that for any $T \geq 1$

$$\boldsymbol{E}\{\boldsymbol{V}(\boldsymbol{x}(\boldsymbol{T}+\mathbf{1}),\boldsymbol{T}+\mathbf{1})\} - \boldsymbol{E}\{\boldsymbol{V}(\boldsymbol{x}_{\mathbf{0}},\mathbf{0})\} \leq -\boldsymbol{\beta}\boldsymbol{E}\left\{\sum_{\boldsymbol{t}=\mathbf{0}}^{\boldsymbol{T}}\|\boldsymbol{x}(\boldsymbol{t})\|_{\mathbf{2}}\right\}$$

Furthermore,

$$\boldsymbol{E}\left\{\sum_{\boldsymbol{t}=\mathbf{0}}^{\boldsymbol{T}}\|\boldsymbol{x}(\boldsymbol{t})\|_{\mathbf{2}}\right\} \leq \frac{\mathbf{1}}{\boldsymbol{\beta}}(\boldsymbol{E}\{\boldsymbol{V}(\boldsymbol{x}_{\mathbf{0}},\mathbf{0})\} - \boldsymbol{E}\{\boldsymbol{V}(\boldsymbol{x}(\boldsymbol{T}+\mathbf{1}),\boldsymbol{T}+\mathbf{1})\}) \leq \frac{\mathbf{1}}{\boldsymbol{\beta}}\boldsymbol{E}\{\boldsymbol{V}(\boldsymbol{x}_{\mathbf{0}},\mathbf{0})\}$$

$$= \frac{\mathbf{1}}{\boldsymbol{\beta}}\boldsymbol{x}(\mathbf{0})^{\boldsymbol{T}}\boldsymbol{P}(\boldsymbol{i}(\mathbf{0}),\boldsymbol{r}(\mathbf{0}))\boldsymbol{x}(\mathbf{0})$$

We want to show that if the system in (5-9) is robustly stable, then there exists symmetric $P(i,r) > 0$ such that (6-2) holds.

It suffices to prove that for any bounded and symmetric $Q = (\tau_k^{sc}, \tau_{k-\tau_k^{sc}-1}^{ca}) > 0$ there exists a set of $P\left(\tau_k^{sc}, \tau_{k-\tau_k^{sc}-1}^{ca}\right)$ such that:

$$\sum_{\boldsymbol{j}=\mathbf{0}}^{\boldsymbol{\tau_k^{sc}}}\sum_{\boldsymbol{s1}=\mathbf{0}}^{\boldsymbol{\tau_k^{ca}}}\sum_{\boldsymbol{s2}=\mathbf{0}}^{\boldsymbol{\tau_k^{ca}}}\boldsymbol{\lambda_{ij}}\boldsymbol{\pi}_{\boldsymbol{rs2}}^{\mathbf{1}+\boldsymbol{i}-\boldsymbol{j}}\boldsymbol{\pi}_{\boldsymbol{s2s1}}^{\boldsymbol{j}}\,\boldsymbol{X}[\overline{\boldsymbol{A}}+\overline{\boldsymbol{B}}\boldsymbol{k}(\boldsymbol{i},\boldsymbol{s1},\boldsymbol{r})\overline{\boldsymbol{C}}(\boldsymbol{i})]^{\boldsymbol{T}}\boldsymbol{P}(\boldsymbol{j},\boldsymbol{s2})\boldsymbol{X}\,[\overline{\boldsymbol{A}}+\overline{\boldsymbol{B}}\boldsymbol{k}(\boldsymbol{i},\boldsymbol{s1},\boldsymbol{r})\overline{\boldsymbol{C}}(\boldsymbol{i})]$$

$$-\,\boldsymbol{P}(\boldsymbol{i},\boldsymbol{r}) = -\boldsymbol{Q}(\boldsymbol{i},\boldsymbol{r})$$

We define

$$\boldsymbol{x}(\boldsymbol{k})^{\boldsymbol{T}}\tilde{P}\left(T-t,\boldsymbol{\tau_t^{sc}},\boldsymbol{\tau_{t-\tau_t^{sc}-1}^{ca}}\right)\boldsymbol{x}(\boldsymbol{t}) \triangleq \sum\left\{\boldsymbol{x}(\boldsymbol{t})^{\boldsymbol{T}}\boldsymbol{Q}\left(\tau_k^{sc},\tau_{k-\tau_k^{sc}-1}^{ca}\right)\boldsymbol{x}(\boldsymbol{k})\,\middle|\,\boldsymbol{x_t},\tau_t^{sc},\tau_{t-\tau_t^{sc}-1}^{ca}\right\}$$

Assuming that $\boldsymbol{x}(\boldsymbol{k}) \neq \mathbf{0}$**,** since

$$\boldsymbol{Q}\left(\tau_k^{sc},\tau_{k-\tau_k^{sc}-1}^{ca}\right) > 0,$$

as T increases

$\boldsymbol{x}(\boldsymbol{k})^{\boldsymbol{T}}\widetilde{\boldsymbol{P}}\left(\boldsymbol{T}-\boldsymbol{t},\boldsymbol{\tau_t^{sc}},\boldsymbol{\tau_{t-\tau_t^{sc}-1}^{ca}}\right)\boldsymbol{x}(\boldsymbol{t})$ is monotonically increasing.

From (6-2), $x(k)^T\tilde{P}\left(T-t,\tau_t^{sc},\tau_{t-\tau_t^{sc}-1}^{ca},\right)x(t)$ is upper bounded. Furthermore, its limit exists and can be expressed as:

$\boldsymbol{x}(\boldsymbol{k})^{\boldsymbol{T}}\boldsymbol{P}(\boldsymbol{i},\boldsymbol{r})\boldsymbol{x}(\boldsymbol{k}) \triangleq \mathbf{lim}_{\boldsymbol{T}\to\infty}\,\boldsymbol{x}(\boldsymbol{k})^{\boldsymbol{T}}\widetilde{\boldsymbol{P}}(\boldsymbol{T}-\boldsymbol{t},\boldsymbol{i},\boldsymbol{r})\boldsymbol{x}(\boldsymbol{t})$

$$x(k)^T P(i,r)x(k)$$

$$\triangleq \lim_{T\to\infty} E\left\{\sum_{k=t}^{T} x(t)^T Q\left(\tau_k^{sc},\tau_{k-\tau_k^{sc}-1}^{ca}\right)x(k)\,\middle|\, x_t,\tau_t^{sc}=i,\tau_{t-\tau_t^{sc}-1}^{ca}\right.$$

$$\left.= r\right\}\ldots\ldots\ldots(6-6)$$

Since this is valid for any $x(k)$, we have

$$P(i,r)=\lim_{T\to\infty} x(k)^T \widetilde{P}(T-t,i,r)x(t)\ldots\ldots\ldots(6-7)$$

From (6-7) we obtain $P(i,r)>0$ since $Q\left(\tau_k^{sc},\tau_{k-\tau_k^{sc}-1}^{ca}\right)>0$ consider

$$E=\left\{x(t)^T\widetilde{P}(T-t,i,r)x(t)-x(t+1)^T\widetilde{P}(T-t,i,r)x(t+1)|x_t,i,r\right\}\ldots\ldots\ldots(6-8)$$

By using Proposition 2, the second term in (6-8) can be evaluated as:

$$E=x(t+1)^T\widetilde{P}(T-t,i,r)x(t+1)|x_t,i,r$$

$$=x(t)^T\left\{\sum_{j=0}^{\tau_k^{sc}}\sum_{s1=0}^{\tau_k^{ca}}\sum_{s2=0}^{\tau_k^{ca}}\lambda_{ij}\pi_{rs2}^{1+i-j}\pi_{s2s1}^{j}\,X[\bar{A}\right.$$

$$\left.+\bar{B}k(i,s1,r)\bar{C}(i)]^T P(j,s2)X\,[\bar{A}+\bar{B}k(i,s1,r)\bar{C}(i)]\right\}x(t)\ldots\ldots\ldots(6-9)$$

Substituting (6-9) into (6-8) gives rise to

$$x(t)^T\widetilde{P}(T-t,i,r)$$

$$-\sum_{j=0}^{\tau_k^{sc}}\sum_{s1=0}^{\tau_k^{ca}}\sum_{s2=0}^{\tau_k^{ca}}\lambda_{ij}\pi_{rs2}^{1+i-j}\pi_{s2s1}^{j}\,X[\bar{A}+\bar{B}k(i,s1,r)\bar{C}(i)]^T P(j,s2)X\,[\bar{A}$$

$$+\bar{B}k(i,s1,r)\bar{C}(i)]Xx(t)=x(t)^T Q(i,r)x(t)\ldots\ldots\ldots(6-10)$$

Letting $T\to\infty$ in (6-10), we get (6-2).

This completes of the proof

6.3 MAIN RESULTS

In this section, the robust stability based on H_∞ and H_2 norms are analysed.

6.3.1 Robust Stability Based H_∞ Norm

The classical H_∞ for linear-time-invariant systems can be interpreted as a measure of robust stability that represents the worst-case performance degradation of any bounded disturbance.

Definition 2 (robust stability based on H_∞ Norm)

System (5-9) is said to be robustly stable based on H_∞ Norm if: $H_\infty < \gamma$ and

$$\left\|\boldsymbol{H}_{\boldsymbol{e}(\boldsymbol{k})\boldsymbol{r}(\boldsymbol{k})}\right\|_\infty = \underset{\boldsymbol{\tau}_{\mathbf{0}}^{\boldsymbol{sc}} \in \boldsymbol{\mathcal{M}}}{\boldsymbol{Sup}} \;\; \underset{\boldsymbol{\tau}_{-\boldsymbol{\tau}_{\mathbf{0}}^{\boldsymbol{sc}}-\mathbf{1}}^{\boldsymbol{ca}} \in \mathbb{N}}{\boldsymbol{Sup}} \;\; \underset{\boldsymbol{r}(\boldsymbol{k}) \in \boldsymbol{l}_{\mathbf{2}(\mathbf{0},\infty)}}{\boldsymbol{Sup}} \frac{\|\boldsymbol{e}(\boldsymbol{k})\|_{\mathbf{2}}}{\|\boldsymbol{r}(\boldsymbol{k})\|_{\mathbf{2}}} < \boldsymbol{\gamma} \ldots\ldots\ldots (\mathbf{6}-\mathbf{11})$$

6.3.2 Robust Stability Based H_2 Norm

In this section, the definition of H_2 norm for a closed-loop system in (5-8) is proposed. The necessary and sufficient condition of H_2 norm for robust stability is analysed in terms of LMIs with unbounded constraint.

Definition 3 classical definition H_2 norm for Linear Time Invariant (LTI) system

The Proposed closed-loop system in (5-9) is a stable discrete-time LTI system, and then control signal in (5-8) must be re-written as:

$$\boldsymbol{\xi}(\boldsymbol{k}+\mathbf{1}) = \overline{\boldsymbol{A}}\left(\boldsymbol{\tau}_{\boldsymbol{k}}^{\boldsymbol{sc}} = \mathbf{0}, \boldsymbol{\tau}_{\boldsymbol{k}-\boldsymbol{\tau}_{\boldsymbol{k}}^{\boldsymbol{sc}}-\mathbf{1}}^{\boldsymbol{ca}} = \mathbf{0}, \boldsymbol{\tau}_{\boldsymbol{k}}^{\boldsymbol{ca}} = \mathbf{0}\right)\boldsymbol{\xi}(\boldsymbol{k}) + \bar{\boldsymbol{J}}\boldsymbol{r}(\boldsymbol{k}) \ldots\ldots\ldots (\mathbf{6}-\mathbf{12}\boldsymbol{a})$$

$$\boldsymbol{e}(\boldsymbol{k}) = \overline{\boldsymbol{C}}\boldsymbol{\xi}(\boldsymbol{k}) \ldots\ldots\ldots (\mathbf{6}-\mathbf{12}\boldsymbol{b})$$

The classical H_2 norm has the following time-domain understanding; the l_2 norm of the output equals the H_2 norm of the system if the input is unit impulse [177].

Definition 4 (H_2 norm for MJLS)

Consider the closed-loop MJLS in (5-9) with initial condition $x(0) = 0$. The definition of H_2 norm of system (5-8) with initial condition $x(0) = 0$ is given by [178].

$$\left\|\boldsymbol{H}_{\boldsymbol{e}(\boldsymbol{k})\boldsymbol{r}(\boldsymbol{k})}\right\|_{\mathbf{2}}^{\mathbf{2}} = \sum_{\boldsymbol{s}=\mathbf{1}}^{\boldsymbol{l}}\sum_{\boldsymbol{j}=\mathbf{1}}^{\boldsymbol{N}}\left\|\boldsymbol{e}(\boldsymbol{k})_{\boldsymbol{s},\boldsymbol{j}}\right\|_{\mathbf{2}}^{\mathbf{2}} \ldots\ldots\ldots (\mathbf{6}-\mathbf{13})$$

where $k > 0, \{e(k)_1, \ldots\ldots, e(k)_r\}$ forms a basis for $C^r and\, j$ number of states.

Definition 5 (general definition of the H_2 norm)

The closed-loop system in (5-9) is a special discrete-time MJLS. Therefore, the definition of H_2 norm in definitions 3 and 4 are not suitable for this system. The general definition for H_2 norm of system (5-5) is:

$$\left\|H_{e(k)r(k)}\right\|_2^2 = \sum_{s=1}^{l}\sum_{i_0=0}^{\tau_k^{sc}}\sum_{r_0=0}^{\tau_k^{ca}} \alpha(i_0, r_0) \sum_{k=1}^{\infty} E\left\{\left\|e_{s,i_0,r_0}(k)\right\|_2^2\right\} \ldots\ldots\ldots (6-14)$$

Where $e_{s,i_0,r_0}(k)$ is the output sequence of system (5-9)

When:

1. The input sequence is given by $r = \{r(0), r(1), \ldots\ldots\}, r(0) = e_s, r(k) = 0, k > 0$
2. $\tau_k^{sc} = i_0$
3. $\tau_{k-\tau_k^{sc}-1}^{ca} = r_0$
4. The initial distribution for $(\tau_0^{sc}, \tau_{0-\tau_0^{sc}-1}^{ca})$ is given by $\alpha(i_0, r_0)$ where $i_0 \in \mathcal{M}, r_0 \in \mathbb{N}$ and $\sum i_0 \in \mathcal{M}, r_0 \in \mathbb{N}^{\alpha(i_0,r_0)} = 1$

Theorem 4 (relation between the H_2 norm and state-space model of MJLS)

The H_2 norm of the system (5-9) can be calculated as follows:

$$\left\|H_{e(k)r(k)}\right\|_2^2 =$$
$$\sum_{i_0=0}^{\tau_k^{sc}}\sum_{r_0=0}^{\tau_k^{ca}}\sum_{j_0=0}^{\tau_k^{sc}}\sum_{so2=0}^{\tau_k^{ca}} \alpha(i_0, r_0)\lambda_{i0j0}\pi_{r_oso2}^{1+i_0-j_0} tr\{\bar{J}^T S(j_0, s_{o2})\bar{J}\} \ldots\ldots\ldots (6-15)$$

Where, $S(j_0, s_{o2}) > 0$ provides the solution obtained from the following discrete-time system

$$S(i,r) = \sum_{j=0}^{\tau_k^{sc}}\sum_{s_1=0}^{\tau_k^{ca}}\sum_{s_2=0}^{\tau_k^{sc}} \lambda_{ij}\pi_{rs_2}^{1+i-j}\pi_{s_2s_1}^{j}\bar{A}^T S(j, s_2)\bar{A}(i, r, s_1) + \bar{C}^T\bar{C} \ldots\ldots\ldots (6-16)$$

Proof

Suppose that $e(k)$ is an impulse response of system (5-9). Then for $k \geq 1$ and corresponding system (6-16), we have

$$E[e(k)^T e(k)] = E\{\xi(k)^T\bar{C}^T\bar{C}\xi(k)\} =$$
$$E\left\{\xi(k)^T\left[S(i,r) - \sum_{j=0}^{\tau_k^{sc}}\sum_{s_1=0}^{\tau_k^{ca}}\sum_{s_2=0}^{\tau_k^{sc}} \lambda_{ij}\pi_{rs_2}^{1+i-j}\pi_{s_2s_1}^{j}\bar{A}^T S(j, s_2)\bar{A}(i, r, s_1)\right]\xi(k)\right\} \ldots\ldots\ldots (6-17)$$

$$= \boldsymbol{E}\{\boldsymbol{\xi}(\boldsymbol{k})^{\boldsymbol{T}}\boldsymbol{S}(\boldsymbol{i},\boldsymbol{r})\boldsymbol{\xi}(\boldsymbol{k})\}$$

$$- \boldsymbol{E}\left\{\sum_{\boldsymbol{j}=\boldsymbol{0}}^{\boldsymbol{\tau}_{\boldsymbol{k}}^{\boldsymbol{sc}}}\sum_{\boldsymbol{s}_{\boldsymbol{1}}=\boldsymbol{0}}^{\boldsymbol{\tau}_{\boldsymbol{k}}^{\boldsymbol{ca}}}\sum_{\boldsymbol{s}_{\boldsymbol{2}}=\boldsymbol{0}}^{\boldsymbol{\tau}_{\boldsymbol{k}}^{\boldsymbol{sc}}}\boldsymbol{\lambda}_{\boldsymbol{ij}}\boldsymbol{\pi}_{\boldsymbol{rs}_{\boldsymbol{2}}}^{\boldsymbol{1}+\boldsymbol{i}-\boldsymbol{j}}\boldsymbol{\pi}_{\boldsymbol{s}_{\boldsymbol{2}}\boldsymbol{s}_{\boldsymbol{1}}}^{\boldsymbol{j}}\boldsymbol{\xi}(\boldsymbol{k})^{\boldsymbol{T}}\overline{\boldsymbol{A}}^{\boldsymbol{T}}(\boldsymbol{i},\boldsymbol{r},\boldsymbol{s}_{\boldsymbol{1}})\boldsymbol{S}(\boldsymbol{j},\boldsymbol{s}_{\boldsymbol{2}})\overline{\boldsymbol{A}}(\boldsymbol{i},\boldsymbol{r},\boldsymbol{s}_{\boldsymbol{1}})\overline{\boldsymbol{A}}(\boldsymbol{i},\boldsymbol{r},\boldsymbol{s}_{\boldsymbol{1}})\boldsymbol{\xi}(\boldsymbol{k})\right\} \ldots\ldots\ldots (\boldsymbol{6} - \boldsymbol{18})$$

Note that the second term of equation (6-18) is the mathematical expectation of $\xi(k+1)^T S(\tau_{k+1}^{sc}, \tau_k^{ca} - \tau_{k+1}^{sc})\xi(k+1)$ based on the information of the previous step $\xi(k),\ \tau_k^{sc}\ and\ \tau_{k-\tau_k^{sc}-1}^{ca}$.

Based on lemma 1 [179], if the transition probability matrix from

$\boldsymbol{\tau}_{\boldsymbol{k}-\boldsymbol{1}}^{\boldsymbol{ca}} \to \boldsymbol{\tau}_{\boldsymbol{k}}^{\boldsymbol{ca}} : \boldsymbol{\pi},$

Then the transition probability matrix from

$$\boldsymbol{\tau}_{\boldsymbol{k}}^{\boldsymbol{ca}} - \boldsymbol{\tau}_{\boldsymbol{k}+\boldsymbol{1}}^{\boldsymbol{sc}} \to \boldsymbol{\tau}_{\boldsymbol{k}}^{\boldsymbol{ca}} : \boldsymbol{\pi}^{\boldsymbol{\tau}_{\boldsymbol{k}}^{\boldsymbol{sc}}+\boldsymbol{1}}$$

This is still a transition probability matrix of a Markov chain. Specifically, when$\tau_k^{sc} + 1 = 0$, the transition probability matrix is

$$\boldsymbol{\pi}^{\boldsymbol{\tau}_{\boldsymbol{k}}^{\boldsymbol{sc}}+\boldsymbol{1}} = \boldsymbol{\pi}^{\boldsymbol{0}} = \boldsymbol{I}$$

Define $\boldsymbol{\tau}_{\boldsymbol{k}+\boldsymbol{1}}^{\boldsymbol{sc}} = \boldsymbol{j} \qquad \boldsymbol{\tau}_{\boldsymbol{k}}^{\boldsymbol{ca}} = \boldsymbol{s}_{\boldsymbol{1}} \qquad \boldsymbol{\tau}_{\boldsymbol{k}-\boldsymbol{\tau}_{\boldsymbol{k}}^{\boldsymbol{sc}}-\boldsymbol{1}}^{\boldsymbol{ca}} = \boldsymbol{s}_{\boldsymbol{2}}$

the probability transition matrices for

$$\boldsymbol{\tau}_{\boldsymbol{k}}^{\boldsymbol{sc}} \to \boldsymbol{\tau}_{\boldsymbol{k}+\boldsymbol{1}}^{\boldsymbol{sc}}$$

$$\boldsymbol{\tau}_{\boldsymbol{k}-\boldsymbol{i}-\boldsymbol{1}}^{\boldsymbol{ca}} \to \boldsymbol{\tau}_{\boldsymbol{k}-\boldsymbol{j}}^{\boldsymbol{ca}}$$

$$\boldsymbol{\tau}_{\boldsymbol{k}-\boldsymbol{j}}^{\boldsymbol{ca}} \to \boldsymbol{\tau}_{\boldsymbol{k}}^{\boldsymbol{ca}}$$

As evaluate the second term in equation (6-18). According to lemma 1, these probability matrices are

$$\boldsymbol{\tau}_{\boldsymbol{k}}^{\boldsymbol{sc}} \to \boldsymbol{\tau}_{\boldsymbol{k}+\boldsymbol{1}}^{\boldsymbol{sc}} = \boldsymbol{\Lambda}$$

$$\boldsymbol{\tau}_{\boldsymbol{k}-\boldsymbol{i}-\boldsymbol{1}}^{\boldsymbol{ca}} \to \boldsymbol{\tau}_{\boldsymbol{k}-\boldsymbol{j}}^{\boldsymbol{ca}} = \boldsymbol{\pi}^{\boldsymbol{1}+\boldsymbol{i}-\boldsymbol{j}}$$

$$\boldsymbol{\tau}_{\boldsymbol{k}-\boldsymbol{j}}^{\boldsymbol{ca}} \to \boldsymbol{\tau}_{\boldsymbol{k}}^{\boldsymbol{ca}} = \boldsymbol{\pi}^{\boldsymbol{j}}$$

Then

$$\boldsymbol{E}\{\boldsymbol{\xi}(\boldsymbol{k}+\boldsymbol{1})^{\boldsymbol{T}}\boldsymbol{S}(\boldsymbol{\tau}_{\boldsymbol{k}+\boldsymbol{1}}^{\boldsymbol{sc}}, \boldsymbol{\tau}_{\boldsymbol{k}-\boldsymbol{i}+\boldsymbol{1}}^{\boldsymbol{ca}})\boldsymbol{\xi}(\boldsymbol{k}+\boldsymbol{1})\}$$

$$= \sum_{\boldsymbol{j}=\boldsymbol{0}}^{\boldsymbol{\tau}_{\boldsymbol{k}}^{\boldsymbol{sc}}}\sum_{\boldsymbol{s}_{\boldsymbol{1}}=\boldsymbol{0}}^{\boldsymbol{\tau}_{\boldsymbol{k}}^{\boldsymbol{ca}}}\sum_{\boldsymbol{s}_{\boldsymbol{2}}=\boldsymbol{0}}^{\boldsymbol{\tau}_{\boldsymbol{k}}^{\boldsymbol{sc}}}\boldsymbol{\lambda}_{\boldsymbol{ij}}\boldsymbol{\pi}_{\boldsymbol{rs}_{\boldsymbol{2}}}^{\boldsymbol{1}+\boldsymbol{i}-\boldsymbol{j}}\boldsymbol{\pi}_{\boldsymbol{s}_{\boldsymbol{2}}\boldsymbol{s}_{\boldsymbol{1}}}^{\boldsymbol{j}}\boldsymbol{\xi}(\boldsymbol{k})^{\boldsymbol{T}}\overline{\boldsymbol{A}}^{\boldsymbol{T}}(\boldsymbol{i},\boldsymbol{r},\boldsymbol{s}_{\boldsymbol{1}})\boldsymbol{S}(\boldsymbol{j},\boldsymbol{s}_{\boldsymbol{2}})\overline{\boldsymbol{A}}(\boldsymbol{i},\boldsymbol{r},\boldsymbol{s}_{\boldsymbol{1}})\boldsymbol{\xi}(\boldsymbol{k})$$

Furthermore, equation (6-17) can be re-written as:

$$\boldsymbol{E[e(k)^T\, e(k)]}$$
$$\boldsymbol{= E[\xi(k)^T S(\tau_k^{sc}, \tau_{k-i-1}^{ca})\xi(k)]}$$
$$\boldsymbol{- E[\xi(k+1)^T S(\tau_{k+1}^{sc}, \tau_{k-i+1}^{ca})\xi(k+1)]} \ldots\ldots\ldots \boldsymbol{(6-19)}$$

Notice that,

$S(i, r)$ in equation (6-16) satisfies the inequalities (6-2). Therefore, the closed-loop system in (5-8) is robustly stable, recalling that

$$\boldsymbol{E(\|\xi(k)\|)^2 \to 0 \qquad as\ k \to \infty}$$

Taking the sum of equation (6-19) from 1 to ∞, we obtain

$$\boldsymbol{\textstyle\sum_{k=1}^{\infty} E\left\{\|e_{s,io,ro}(k)\|_2^2\right\} |\tau_0^{sc}, \tau_{0-\tau_0^{sc}-1}^{ca} = E\left\{\xi(1)^T S\left(\tau_1^{sc}, \tau_{-\tau_1^{sc}}^{ca}\right) \xi(1) |\tau_0^{sc}, \tau_{0-\tau_0^{sc}-1}^{ca}\right\} =}$$

$$\boldsymbol{E\left\{e_s^T \bar{J}^T S(\tau_1^{sc}, \tau_{-\tau_1^{sc}}^{ca}) \bar{J} e_s\right\} = \textstyle\sum_{j0}^{\tau_k^{sc}} \sum_{s02=0}^{\tau_k^{ca}} \lambda_{i0jo} \pi_{r0so2}^{1+i0-j0} \{e_s^T \bar{J}^T S(j_0, s_{02}) \bar{J} e_s\}}$$

Where, $j_0 = \tau_1^{sc}$ and $s_{02} = \tau_1^{sc}, \tau_{-\tau_1^{sc}}^{ca}$

Then considering the distribution of initial states, we have

$$\boldsymbol{\|H_{e(k)r(k)}\|_2^2 = \sum_{s=1}^{l} \sum_{i_0=0}^{\tau_k^{sc}} \sum_{r_0=0}^{\tau_k^{ca}} \alpha(i_0, r_0) \sum_{k=1}^{\infty} E\left\{\|e_{s,i_0,r_0}(k)\|_2^2\right\}}$$
$$\boldsymbol{= \sum_{i_0=0}^{\tau_k^{sc}} \sum_{r_0=0}^{\tau_k^{ca}} \sum_{j_0=0}^{\tau_k^{sc}} \sum_{so2=0}^{\tau_k^{ca}} \alpha(i_0, r_0) \lambda_{i0j0} \pi_{r_o so2}^{1+i_0-j_0} tr\{\bar{J}^T S(j_0, s_{o2}) \bar{J}\}}$$

This completes the proof

<u>Theorem 5</u> (Robust Stability based H_2 norm)

Under the control signal system (5-4), the closed-loop system in (5-8) is robustly stable and $\|H_{e(k)r(k)}\|_2 < \beta$ if and only if there exist matrices $K(i, r)$ and symmetric matrices $\bar{X}(j, s_2) > 0, P(i, r) > 0$ satisfying the following inequalities with unbounded constraints.

$$\boldsymbol{\sum_{i_0=0}^{\tau_k^{sc}} \sum_{r_0=0}^{\tau_k^{ca}} \sum_{j_0=0}^{\tau_k^{sc}} \sum_{so2=0}^{\tau_k^{ca}} \alpha(i_0, r_0) \lambda_{i0j0} \prod_{r_o so2}^{1+i_0-j_0} tr\{\bar{J}^T S(j_0, s_{o2}) \bar{J}\} < \beta^2} \ldots\ldots\ldots \boldsymbol{(6-20)}$$

$$\begin{bmatrix} \boldsymbol{-P(i,r) + \overline{C}^T \overline{C}} & \boldsymbol{V(i,r)^T} \\ \boldsymbol{V(i,r)} & \boldsymbol{-X(i,r)} \end{bmatrix} < 0 \ldots\ldots\ldots \boldsymbol{(6-21)}$$

$$\boldsymbol{\bar{X}(j, s_2) P(j, s_2) = I} \ldots\ldots\ldots \boldsymbol{(6-22)}$$

$$V(i,r) = \left[V_o^T(i,r)\ \ V_1^T(i,r) \ldots\ldots V_{\tau_k^{sc}}^T(i,r)\right]^T,$$

$$V_j(i,r) = \left[V_{j,o}^T(i,r)\ \ V_{j,1}^T(i,r) \ldots\ldots V_{j,\tau_k^{ca}}^T(i,r)\right]^T$$

$$V_{j,s_2}(i,r) = \begin{bmatrix} \sqrt{\left(\lambda_{ij}\pi_{rs_2}^{1+i-j}\pi_{s_2 0}^{j}\right)} & \overline{A}(i,r,0) \\ \sqrt{\left(\lambda_{ij}\pi_{rs_2}^{1+i-j}\pi_{s_2 1}^{j}\right)} & \overline{A}(i,r,1) \\ \vdots & \vdots \\ \sqrt{\left(\lambda_{ij}\pi_{rs_2}^{1+i-j}\pi_{s_2\tau_k^{ca}}^{j}\right)} & \overline{A}(i,r,\tau_k^{ca}) \end{bmatrix}$$

$$X(i,r) = diag\left\{x_0(i,r)\ \ x_1(i,r) \ldots\ldots x_{\tau_k^{sc}}(i,r)\right\}$$

$$X_j(i,r) = diag\left\{x_{j,0}(i,r)x_{j,1}(i,r) \ldots\ldots x_{j,\tau_k^{ca}}(i,r)\right\}$$

$$X_{j,s_2}(i,r) = diag\{\overline{x}(j,s_2)\overline{x}(j,s_2) \ldots\ldots \overline{x}(j,s_2)\}$$

Proof

From Schur's complement and considering equation (6-22), the inequality (6-21) is equivalent to

$$\sum_{j=0}^{\tau_k^{sc}}\sum_{s_1=0}^{\tau_k^{ca}}\sum_{s_2=0}^{\tau_k^{sc}} \lambda_{ij}\pi_{rs_2}^{1+i-j}\pi_{s_2 s_1}^{j}\overline{A}^T(i,r,s_1)P(j,s_2)\overline{A}(i,r,s_1) + \overline{C}^T\overline{C} - P(i,r) < 0 \ldots\ldots\ldots(6-23)$$

It is easy to obtain that the inequality (6-23) implies the inequality (6-2), hence, system (5-9) is robustly stable.

$$\begin{aligned} &E\left\{\xi(k+1)^T P\left(\tau_{k+1}^{sc},\tau_{k-\tau_{k+1}^{ca}}^{sc}\right)\xi(k+1)\right\} \\ &= E\Big\{\xi(k+1)^T\overline{A}\left(\tau_{k+1}^{sc},\tau_{k-\tau_{k-1}^{ca}}^{sc},\tau_k^{ca}\right)^T P\left(\tau_{k+1}^{sc},\tau_{k-\tau_{k+1}^{ca}}^{sc}\right)\overline{A}\left(\tau_{k+1}^{sc},\tau_{k-\tau_{k-1}^{ca}}^{sc},\tau_k^{ca}\right)\xi(k)\Big\} \\ &+E\left\{r(k)^T\overline{J}^T P\left(\tau_{k+1}^{sc},\tau_{k-\tau_{k+1}^{ca}}^{sc}\right)\overline{A}\left(\tau_{k+1}^{sc},\tau_{k-\tau_{k-1}^{ca}}^{sc},\tau_k^{ca}\right)\xi(k)\right\} \\ &+E\left\{\xi(k)^T\overline{A}\left(\tau_{k+1}^{sc},\tau_{k-\tau_{k-1}^{ca}}^{sc},\tau_k^{ca}\right)P\left(\tau_{k+1}^{sc},\tau_{k-\tau_{k+1}^{ca}}^{sc}\right)\overline{J}r(k)\right\} \\ &+E\left\{r(k)^T\overline{J}^T P\left(\tau_{k+1}^{sc},\tau_{k-\tau_{k+1}^{ca}}^{sc}\right)\overline{J}r(k)\right\} \\ &< E\left\{\xi(k)^T\left[P\left(\tau_{k+1}^{sc},\tau_{k-\tau_{k-1}^{ca}}^{sc}\right) - \overline{C}^T\overline{C} - \frac{1}{\beta^2}P(i,r)\overline{J}\overline{J}^T P(i,r)\right]\xi(k)\right\} \\ &+E\left\{r(k)^T\overline{J}^T P\left(\tau_{k+1}^{sc},\tau_{k-\tau_{k+1}^{ca}}^{sc}\right)\overline{A}\left(\tau_{k+1}^{sc},\tau_{k-\tau_{k-1}^{ca}}^{sc},\tau_k^{ca}\right)\xi(k)\right\} \end{aligned}$$

$$+E\left\{\xi(k)^T\bar{A}\left(\tau^{sc}_{k+1},\tau^{sc}_{k-\tau^{ca}_{k-1}},\tau^{ca}_{k}\right)P\left(\tau^{sc}_{k+1},\tau^{sc}_{k-\tau^{ca}_{k+1}}\right)r(k)\right\}$$

$$+E\left\{r(k)^T\bar{J}^TP\left(\tau^{sc}_{k+1},\tau^{sc}_{k-\tau^{ca}_{k+1}}\right)\bar{J}r(k)\right\}\dots\dots\dots(6-24)$$

So that

$$\left\|\sqrt{P\left(\tau^{sc}_{k+1},\tau^{sc}_{k-\tau^{ca}_{k+1}}\right)}\,\xi(k+1)\right\|_2^2-\left\|\sqrt{P\left(\tau^{sc}_{k+1},\tau^{sc}_{k-\tau^{ca}_{k+1}}\right)}\,\xi(k)\right\|_2^2+\|e(k)\|_2^2$$

$$<-\frac{1}{\beta^2}\left\|\bar{J}^TP\left(\tau^{sc}_{k+1},\tau^{sc}_{k-\tau^{ca}_{k-1}}\right)\xi(k)\right\|_2^2$$

$$+E\left\{r(k)^T\bar{J}^TP\left(\tau^{sc}_{k+1},\tau^{sc}_{k-\tau^{ca}_{k+1}}\right)\bar{A}\left(\tau^{sc}_{k+1},\tau^{sc}_{k-\tau^{ca}_{k-1}},\tau^{ca}_{k}\right)\xi(k)\right\}$$

$$+E\left\{\xi(k)^T\bar{A}\left(\tau^{sc}_{k+1},\tau^{sc}_{k-\tau^{ca}_{k-1}},\tau^{ca}_{k}\right)^TP\left(\tau^{sc}_{k+1},\tau^{sc}_{k-\tau^{ca}_{k+1}}\right)\bar{J}r(k)\right\}$$

$$+E\left\{r(k)^T\bar{J}^TP\left(\tau^{sc}_{k+1},\tau^{sc}_{k-\tau^{ca}_{k+1}}\right)\bar{J}r(k)\right\}$$

$$=-\frac{1}{\beta^2}\left\|\bar{J}^TP\left(\tau^{sc}_{k+1},\tau^{sc}_{k-\tau^{ca}_{k-1}}\right)\xi(k)\right\|_2^2+\frac{1}{\beta^2}\left\|\bar{J}^TP\left(\tau^{sc}_{k+1},\tau^{sc}_{k-\tau^{ca}_{k+1}}\right)\xi(k+1)\right\|_2^2$$

$$-\frac{1}{\beta^2}\left\|\bar{J}^TP\left(\tau^{sc}_{k+1},\tau^{sc}_{k-\tau^{ca}_{k+1}}\right)\xi(k+1)\right\|_2^2$$

$$+2E\left\{r(k)^T\bar{J}^TP\left(\tau^{sc}_{k+1},\tau^{sc}_{k-\tau^{ca}_{k+1}}\right)\left[\bar{A}\left(\tau^{sc}_{k+1},\tau^{sc}_{k-\tau^{ca}_{k-1}},\tau^{ca}_{k}\right)\xi(k)+\bar{J}r(k)\right]\right\}$$

$$-E\left\{r(k)^T\bar{J}^TP\left(\tau^{sc}_{k+1},\tau^{sc}_{k-\tau^{ca}_{k+1}}\right)\bar{J}r(k)\right\}\dots\dots\dots(6-25)$$

Thus

$$\left\|\sqrt{P\left(\tau^{sc}_{k+1},\tau^{sc}_{k-\tau^{ca}_{k+1}}\right)}\,\xi(k+1)\right\|_2^2-\left\|\sqrt{P\left(\tau^{sc}_{k+1},\tau^{sc}_{k-\tau^{ca}_{k-1}}\right)}\,\xi(k)\right\|_2^2$$

$$+\|e(k)\|_2^2-\frac{1}{\beta^2}\left\|\bar{J}^TP\left(\tau^{sc}_{k+1},\tau^{sc}_{k-\tau^{ca}_{k+1}}\right)\xi(k+1)\right\|_2^2$$

$$+\frac{1}{\beta^2}\left\|\bar{J}^TP\left(\tau^{sc}_{k+1},\tau^{sc}_{k-\tau^{ca}_{k-1}}\right)\xi(k)\right\|_2^2<-\frac{1}{\beta^2}\left\|\bar{J}^TP\left(\tau^{sc}_{k+1},\tau^{sc}_{k-\tau^{ca}_{k+1}}\right)\xi(k+1)\right\|_2^2$$

$$+2E\left\{r(k)^T\bar{J}^TP\left(\tau^{sc}_{k+1},\tau^{sc}_{k-\tau^{ca}_{k+1}}\right)\xi(k+1)-\beta^2\|r(k)\|_2^2\right\}$$

$$+E\left\{r(k)^T\left[\beta^2I-\bar{J}^TP\left(\tau^{sc}_{k+1},\tau^{sc}_{k-\tau^{ca}_{k+1}}\right)\bar{J}\right]r(k)\right\}$$

$$=-\left\|\frac{1}{\beta}\bar{J}P\left(\tau^{sc}_{k+1},\tau^{sc}_{k-\tau^{ca}_{k+1}}\right)\xi(k+1)-\beta r(k)\right\|_2^2$$

$$+E\left\{r(k)^T\left[\beta^2I-\bar{J}^TP\left(\tau^{sc}_{k+1},\tau^{sc}_{k-\tau^{ca}_{k+1}}\right)\bar{J}\right]r(k)\right\}$$

$$\le E\left\{r(k)^T\left[\beta^2I-\bar{J}^TP\left(\tau^{sc}_{k+1},\tau^{sc}_{k-\tau^{ca}_{k+1}}\right)\bar{J}\right]r(k)\right\}$$

Taking the sum from$k=0\ to\ \infty$, and recalling that $X(0)=0,\|X(k)\|_2\rightarrow 0\ as\ k\rightarrow\infty$

$$\|\boldsymbol{e(k)}\|_2^2 \le \boldsymbol{E}\left\{\boldsymbol{r(k)^T}\left[\boldsymbol{\beta^2 I - \bar{J}^T P}\left(\boldsymbol{\tau_{k+1}^{sc}, \tau_{k-\tau_{k+1}^{ca}}^{sc}}\right)\boldsymbol{\bar{J}}\right]\boldsymbol{r(k)}\right\} = \boldsymbol{\beta^2(1-V)}\|\boldsymbol{r(K)}\|_2^2$$
$$\le \boldsymbol{\beta^2}\|\boldsymbol{r(K)}\|_2^2$$

Where, $V \in \left(0, \frac{1}{\beta^2}\sum_{i=0}^{\tau_k^{sc}}\sum_{j=0}^{\tau_k^{ca}} tr(\bar{J}^T P(i,r)\bar{J})\right)$

For $P(i,r) > S(i,r)$

Then

$$\left\|\boldsymbol{H_{e(k)r(k)}}\right\|_2^2 = \sum_{i=0}^{\tau_k^{sc}}\sum_{j=0}^{\tau_k^{ca}}\sum_{j=0}^{\tau_k^{sc}}\sum_{s_1}^{\tau_k^{ca}} \boldsymbol{\alpha(i,r)\lambda_{ij}} \prod_{rs_1}^{1+i-j}\{\boldsymbol{\bar{J}^T S(i,s_1)\bar{J}}\}$$
$$\le \sum_{i=0}^{\tau_k^{sc}}\sum_{j=0}^{\tau_k^{ca}}\sum_{j=0}^{\tau_k^{sc}}\sum_{s_1}^{\tau_k^{ca}} \boldsymbol{\alpha(i,r)\lambda_{ij}} \prod_{rs_1}^{1+i-j} \boldsymbol{tr}\{\boldsymbol{\bar{J}^T S(i,s_1)\bar{J}}\}$$

Furthermore, by comparing (6-4), (6-5) and (6-23) as well as considering the decreasing property for the solution $P(i,r)$ in theorem 1, the theorem can be readily verified

This completes the proof

6.4 PRODUCT REDUCTION ALGORITHM (PRA)

The aim is to design the full state feedback controller (5-4) such that the H_2 norm of system (5-5) is minimised. This can be achieved by using the LMI technique, the H_2 norm output tracking control problem is transformed to the condition of a set of LMIs with unbounded constraints. The conditions (6-20, 6-21, and 6-22) contain a set of LMIs (6-20, 6-21) and unbounded constraints (6-22). This can be solved by PRA. The PRA is the best numerical implementation method for the system using the LMI solver algorithm [180]. Starting from $i_0 \in \mathcal{M}\ and\ r_0 \in \mathbb{N}$ that verify (6-21), iterate the following step until convergence.

Step 1 Define linear function

$$\boldsymbol{F_k}\{[\boldsymbol{P(i,r)} + \boldsymbol{\bar{C}^T\bar{C}}]\boldsymbol{X(i,r)}\}$$
$$= \boldsymbol{trace}\left\{[\boldsymbol{P_k(i,r)} + \boldsymbol{\bar{C}^T\bar{C}X(i,r)}] + \left[[\boldsymbol{P(i,r)} + \boldsymbol{\bar{C}^T\bar{C}X_k(i,r)}]\right]\right\} \ldots\ldots\ldots(\boldsymbol{6-24})$$

Step 2 Solve for

$P_{k+1}(i,r), X_{k+1}(i,r)$ the bounded programming problem

$$\min_{i\in\mathcal{M}, r\in\mathbb{N}}\left\{\boldsymbol{F_k}[\boldsymbol{P(i,r)} + \boldsymbol{\bar{C}^T\bar{C}}]\boldsymbol{X(i,r)}: \begin{bmatrix} -\boldsymbol{P(i,r)} + \boldsymbol{\bar{C}^T\bar{C}} & \boldsymbol{V(i,r)^T} \\ \boldsymbol{V(i,r)} & -\boldsymbol{X(i,r)} \end{bmatrix} \ge \boldsymbol{0}\right\} \ldots\ldots\ldots(\boldsymbol{6-25})$$

Step 3 main aspect of this method

The most interesting aspect of this method is the additional constraint

$$\boldsymbol{trace\{\bar{J}^T S(j_0, s_{o2})\bar{J}\} < \beta^2} \dots\dots\dots \mathbf{(6-26)}$$

<u>Step 4 feasible solution of problem</u>

Fixed β can be easily incorporated into the feasible set of problem (6-25) as

$$\boldsymbol{trace\{\bar{J}^T S(j, s_{o2})\bar{J}\}} < \beta \dots\dots\dots (6-27)$$

<u>Properties of the PRA</u>

The PRA present the following properties:

1. $2n \leq F_{k+1} \leq F_k$ for n={1,2,3,…,}
2. $F_\infty(P_\infty, X_\infty) = 2n$ if and only if $P_\infty X_\infty = I$

<u>Theorem 6</u> (H_2 norm for output tracking control problem)

The H_2 output tracking control problem is equivalent to the following optimisation problem

$$\min_{\boldsymbol{K(i,r)P(i,r)\bar{X}(j,s_2)}} \boldsymbol{\beta} \dots\dots\dots \mathbf{(6-28)}$$

It is worth noting that general definitions of H_2 norm are one of several possible methods to formulate the H_2 norm output tracking control problem as repeated convex programming problems based on theorem 4.

6.5 ILLUSTRATIVE EXAMPLES

In this section, a numerical example and simulations are given to demonstrate the efficiency of the proposed techniques. Let us consider the following discrete-time system:

$$\boldsymbol{x(k+1) = \begin{bmatrix} 1.0123 & 0.0502 & 0.68802 \\ 0.9876 & 0.00567 & 0.1426 \\ 0.4920 & 1.0123 & 1.0034 \end{bmatrix} X(k) + \begin{bmatrix} 0.0125 \\ 0.5020 \\ 0.0786 \end{bmatrix} u(k - \tau_k^{ca}) + \begin{bmatrix} 0.1 \\ 0.1 \\ 0.1 \end{bmatrix} r(k)}$$

$$\boldsymbol{e(k) = [1 \quad 0 \quad 0] X(k)}$$

The discrete time system is unstable because the Eigen values of the system matrix are 1.8993, $0.061 \mp 0.591j$, due to the presence of the stochastic time delay in the system. Given the norm bounded uncertainty matrices

$$\boldsymbol{Q_1} = \begin{bmatrix} \mathbf{0.01} \\ \mathbf{0.5} \\ \mathbf{0.5} \end{bmatrix} \qquad \boldsymbol{R_1} = [\mathbf{0.2} \quad \mathbf{0.1} \quad \mathbf{0.3}] \qquad \boldsymbol{R_2} = \mathbf{0.1}$$

The stochastic time delays involved in WNCS are assumed below:

$$\boldsymbol{\tau_k^{sc}} \in \{\mathbf{0,1,2,3}\} \qquad \boldsymbol{and} \qquad \boldsymbol{\tau_k^{ca}} \in \{\mathbf{0,1,2}\}$$

The transition probability matrices are also assumed as:

$$\boldsymbol{\Lambda} = \begin{bmatrix} \mathbf{0.5} & \mathbf{0.5} & \mathbf{0} \\ \mathbf{0.3} & \mathbf{0.6} & \mathbf{0.1} \\ \mathbf{0.3} & \mathbf{0.6} & \mathbf{0.1} \\ \mathbf{0.3} & \mathbf{0.3} & \mathbf{0.1} \end{bmatrix} \qquad \boldsymbol{\pi} = \begin{bmatrix} \mathbf{0.2} & \mathbf{0.8} \\ \mathbf{0.5} & \mathbf{0.5} \\ \mathbf{0.3} & \mathbf{0.3} \end{bmatrix}$$

The initial distribution for stochastic time delay $(\tau_0^{sc}, \tau_{0-\tau_0^{sc}-1}^{ca})$ is assumed for $\alpha(i,r) = 0.1666$, γ is set to 3. The reference signal is assumed to be:

$$r(k) = \begin{cases} 1 & 1 \le k \le 20 \\ -1 & 31 \le k \le 40 \\ 0 & otherwise \end{cases}$$

6.5.1 Using H_∞ Norm

The equivalent controller gains $k_1\left(\tau_k^{sc}, \tau_{k-\tau_k^{sc}-1}^{ca}\right)$, $k_2\left(\tau_k^{sc}, \tau_{k-\tau_k^{sc}-1}^{ca}\right)$ in the presence of time delay and packet dropout for both sensor-to-controller and controller-to-actuator channels are:

$$\boldsymbol{k_1} = \begin{bmatrix} \mathbf{0.7861} & \mathbf{-0.4356} & \mathbf{0.8204} \\ \mathbf{2.7658} & \mathbf{0.2231} & \mathbf{1.2145} \\ \mathbf{1.5167} & \mathbf{0.8762} & \mathbf{0.5561} \end{bmatrix} \qquad \boldsymbol{k_2} = \begin{bmatrix} \mathbf{0.6581} & \mathbf{-0.5896} & \mathbf{1.7828} \\ \mathbf{3.3658} & \mathbf{0.5531} & \mathbf{4.0245} \\ \mathbf{2.8107} & \mathbf{0.6675} & \mathbf{0.5478} \end{bmatrix}$$

The frequency responses for the nominal SWNCS with 5 samples of uncertain parameters (network time delay and packet dropout) based on H_∞norm is plotted in Figure 6-1. Meanwhile, the frequency response plot of k_1 based on H_∞norm is illustrated in Figure 6-2.

The minimum value of $\|V(k)_4\|_2 = 0.765$ can be achieved by using system (5-20) since the value of $\|V(k)_4\|_2 = 0.765$. According to theorem 2 the stochastic time delay and packet dropout that maintains the SWNCS robust stability γ =3.

Calculating the H_∞ norm for the reference signal and output signal based on (6-10), we obtained the following $\|r(k)\|_2 = 6.4786$, $\|e(k)\|_2 = 3.5472$. These yields,

$$\frac{\|\boldsymbol{e(k)}\|_2}{\|\boldsymbol{r(k)}\|_2} = \frac{\mathbf{6.4786}}{\mathbf{3.5472}} = \mathbf{1.8265} < \gamma = 3.$$

SWNCS is robustly stable to modelled uncertainty. It can tolerate up to 142% of the modelled uncertainty. A destabilising combination of 142% of the modelled uncertainty exists, causing instability at 20.6 rad/s. Sensitivity with respect to uncertain parameters (network time delay and packet dropout) is 100%. Increasing uncertain parameters by 25% leads to a 25% decrease in the margin [181].

Then, the system has robust stability under these assumptions. From the simulation results, it can be viewed that the proposed robust stability based on H_∞ control method can achieve the control performance in the presence of uncertainty parameters such as stochastic time delay and packet dropouts. The robustness of the controller in closed-loop response of the nominal SWNCS and 5 perturbed based on H_∞ norms is shown in Figure 6-3. Finally, it can be seen that the SWNCS has good control performance although the rate of stochastic time delay is very high.

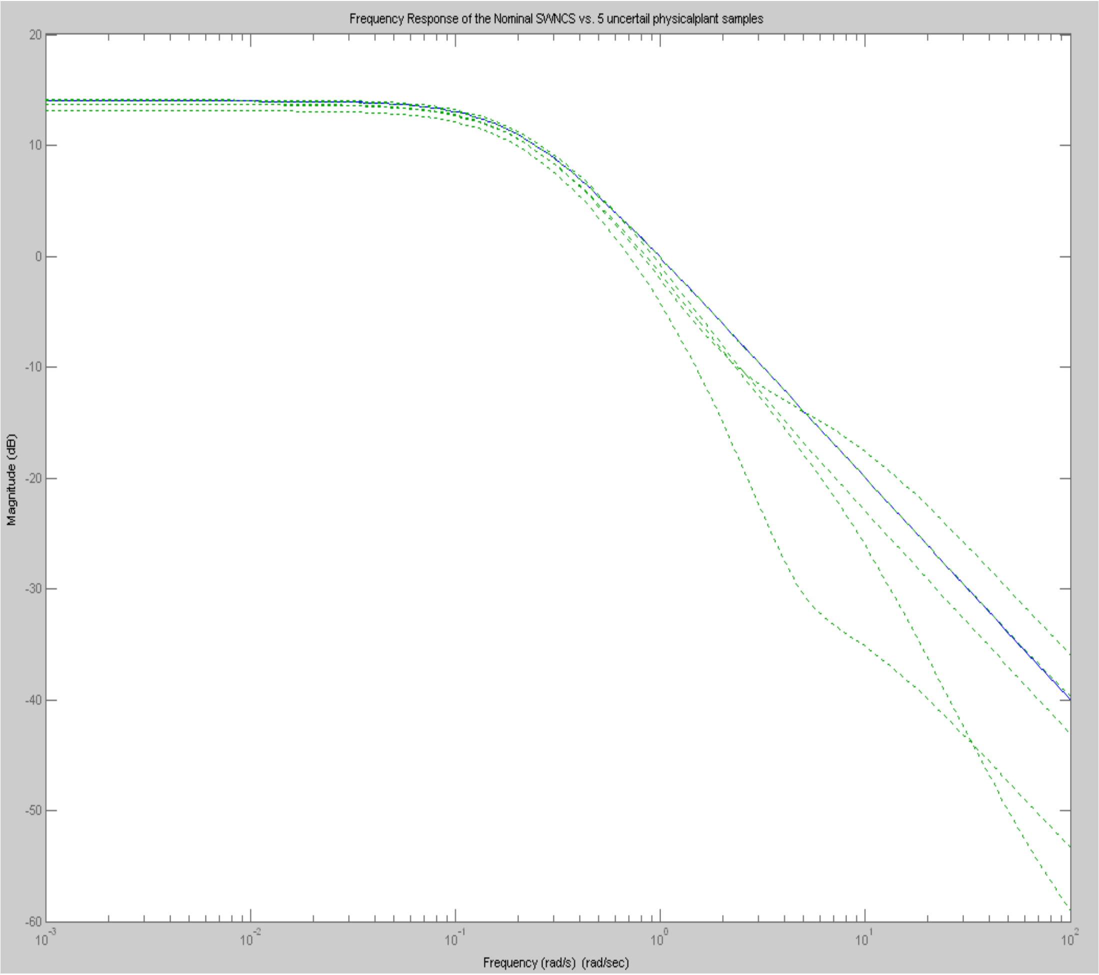

Fig.6.1. Frequency Response for Nominal SWNCS vs. Five Uncertain Physical Plant Samples Based H_∞ Norm

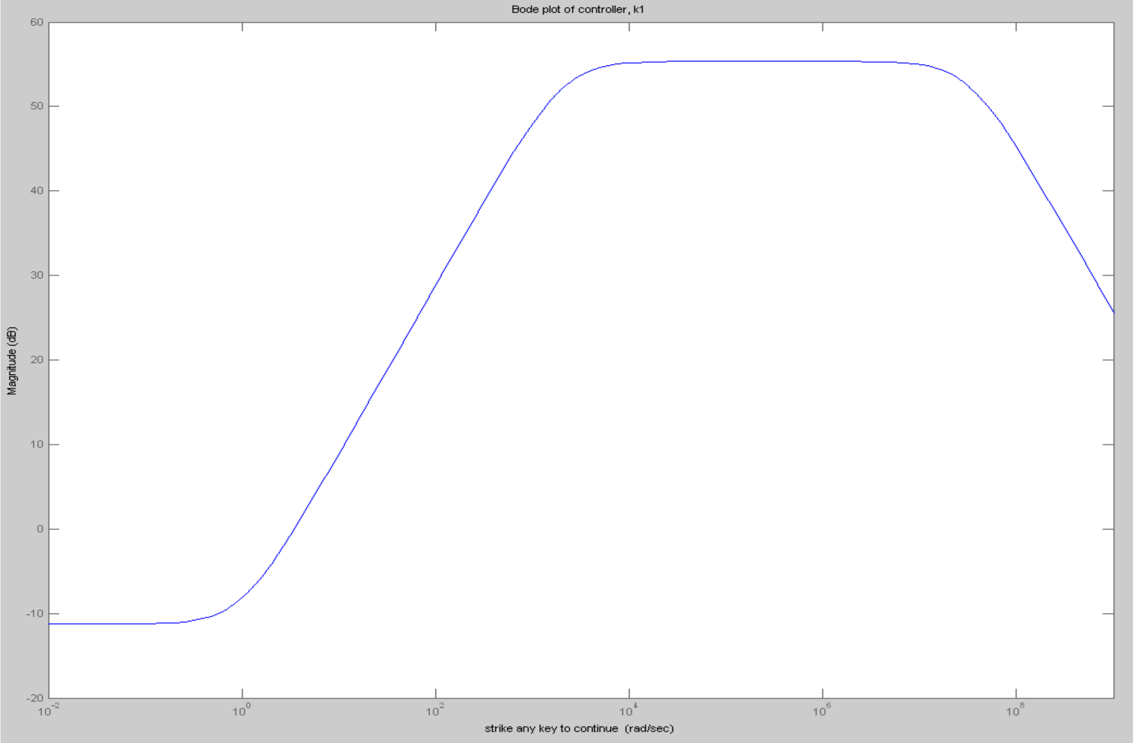

Fig.6.2. Bode Plot for Controller Gain k_1 based H_∞ Norm

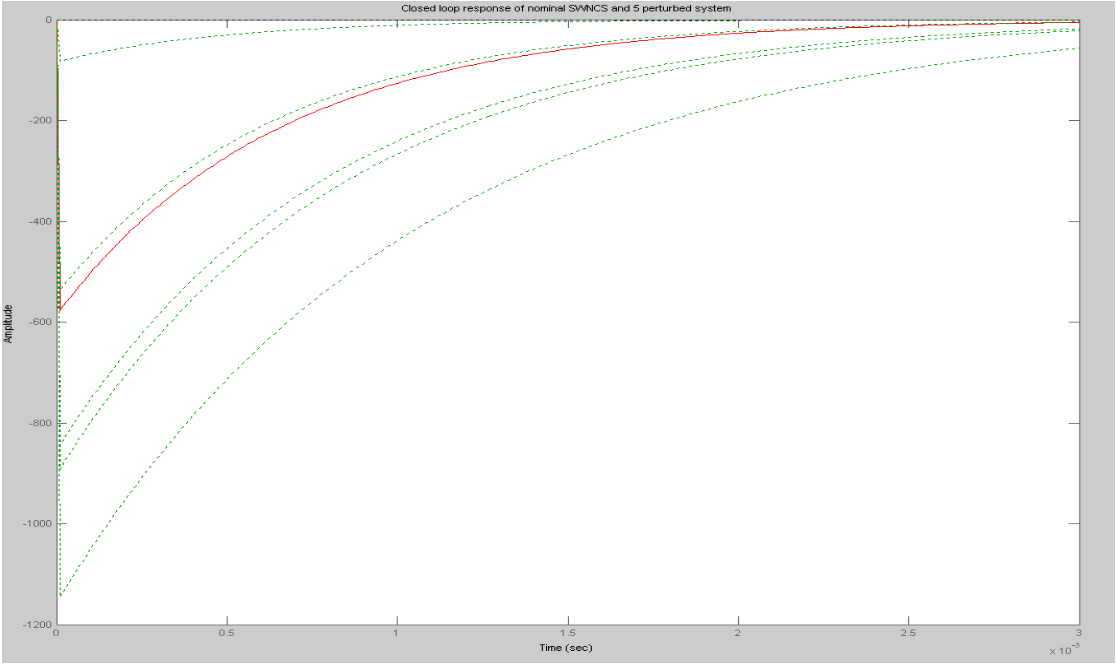

Fig.6.3. Robust Controller Closed Loop Response for Nominal SWNCS and 5 Perturbed System Based H_∞ Norm

6.5.2 Using H_2 Norm

The equivalent controller gains $k_1\left(\tau_k^{sc}, \tau_{k-\tau_k^{sc}-1}^{ca}\right)$, $k_2\left(\tau_k^{sc}, \tau_{k-\tau_k^{sc}-1}^{ca}\right)$ in the presence of time delay and packet dropout for both sensor-to-controller and controller-to-actuator channels are:

$$\boldsymbol{k_1} = \begin{bmatrix} \mathbf{0.8994} & \mathbf{-0.2578} & \mathbf{0.7426} \\ \mathbf{4.7896} & \mathbf{0.4843} & \mathbf{2.2246} \\ \mathbf{2.8931} & \mathbf{0.9541} & \mathbf{0.4477} \end{bmatrix} \qquad \boldsymbol{k_2} = \begin{bmatrix} \mathbf{1.0457} & \mathbf{-0.4296} & \mathbf{3.4472} \\ \mathbf{1.2821} & \mathbf{0.5686} & \mathbf{2.0735} \\ \mathbf{4.7842} & \mathbf{0.8892} & \mathbf{0.9427} \end{bmatrix}$$

The frequency responses for the nominal SWNCS with 5 samples of uncertain parameters (network time delay and packet dropout) based on H_2 norm are plotted in Figure 6-4. The frequency response plot of k_1 based on H_2 norm is illustrated in Figure 6-5.The minimum value of $||V(k)_4||_2^2 = 0.935$ can be calculated according to definition 5 and the result of the impulse response is$||V(k)_4||_2^2 = 0.935$.

According to theorem 2, the stochastic time delay and packet dropout that maintains the SWNCS robust stability γ =3. Calculating the H_2 norm for the reference and output signals based on (6-10), we achieve the following:

$$||\boldsymbol{r}(\boldsymbol{k})||_2^2 = \mathbf{2.456}, \; ||\boldsymbol{e}(\boldsymbol{k})||_2^2 = \mathbf{5.248}$$

These yields:

$$\frac{||\boldsymbol{e}(\boldsymbol{k})||_2^2}{||\boldsymbol{r}(\boldsymbol{k})||_2^2} = \frac{\mathbf{5.248}}{\mathbf{2.456}} = \mathbf{2.136} < \gamma \;= 3$$

The SWNCS system is robustly stable to modelled uncertainty. It can tolerate up to 86.23% of the modelled uncertainty. A destabilising combination of 86.23% of the modelled uncertainty exists, causing instability at 0.552 rad/s. Sensitivity with respect to uncertain parameters (network time delay and packet dropout) is 100%. Increasing uncertain parameters by 25% leads to a 25% decrease in the margin. Therefore, the following system has robust stability based H_2 norm. From the above simulation results, it is discovered that the system is stabilised and control performance is fulfilled in the presence of stochastic time delays and packet dropouts. The robustness of the controller in closed-loop response of the nominal SWNCS and 5 perturbed are shown in Figure 6-6. The SWNCS response based on H_∞ *and* H_2 norm are plotted in Figure 6-7. Finally, Figure 6-8 shows the robust stability analysis for the SWNCS in terms of H_∞ *and* H_2 norms [182].

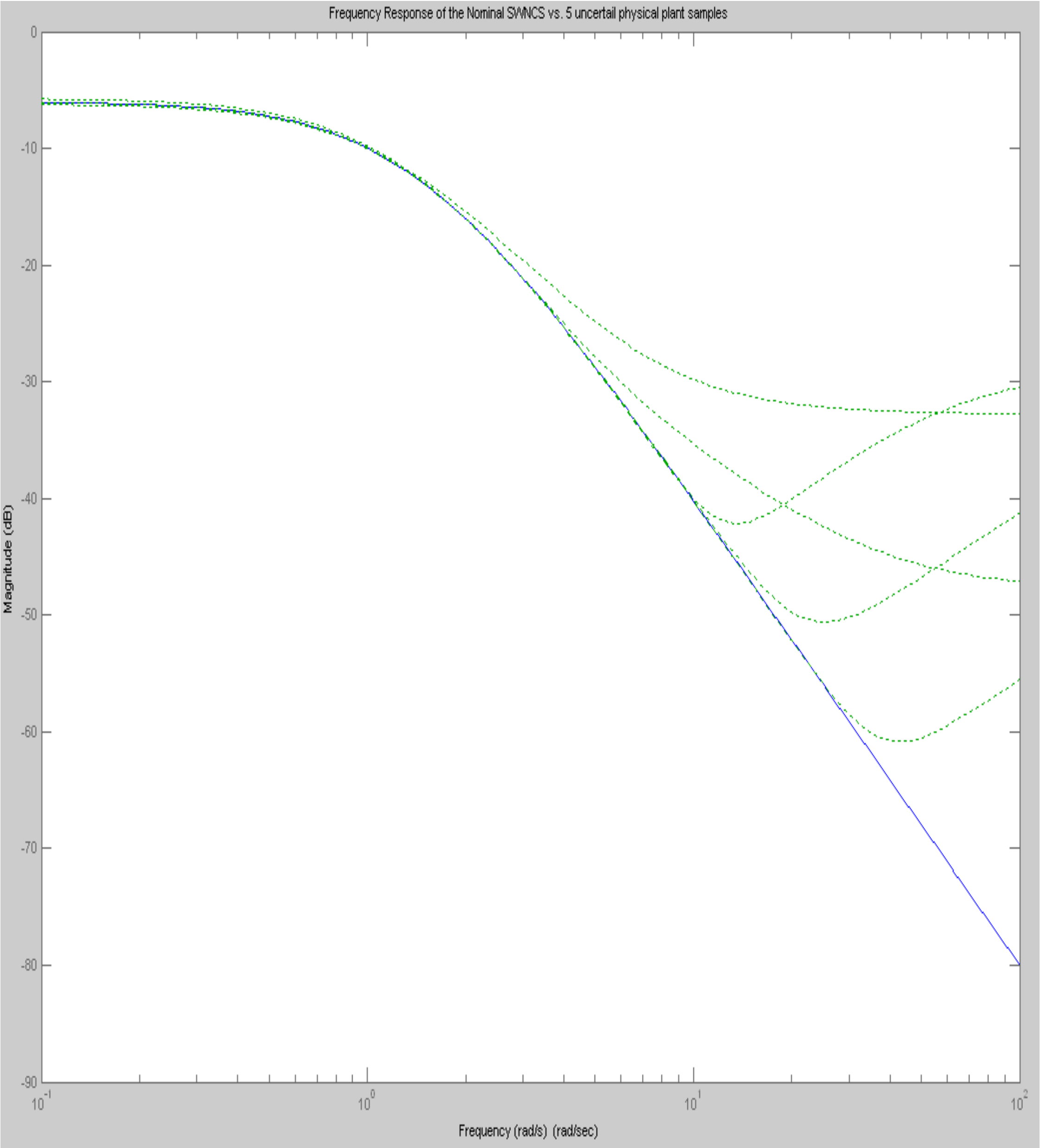

Fig.6.4. Frequency Response for Nominal SWNCS vs. Five Uncertain Physical Plant Samples Based H_2 Norm

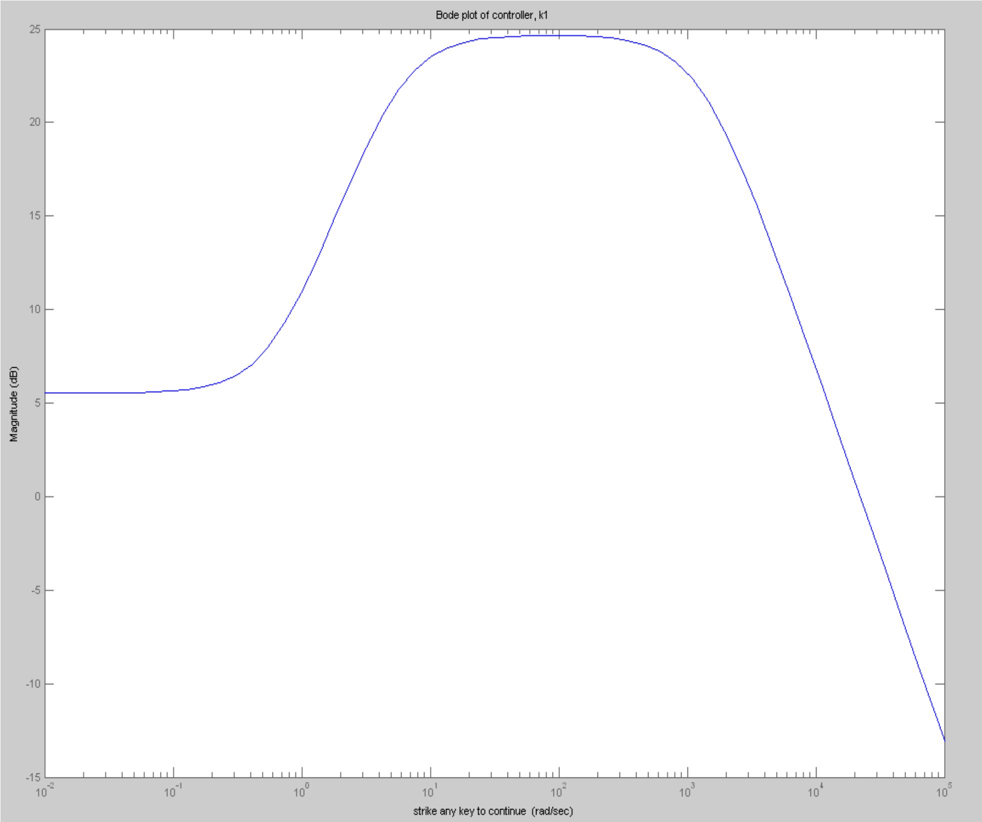

Fig.6.5. Bode Plot for Controller Gain k_1 Based H_2 Norm

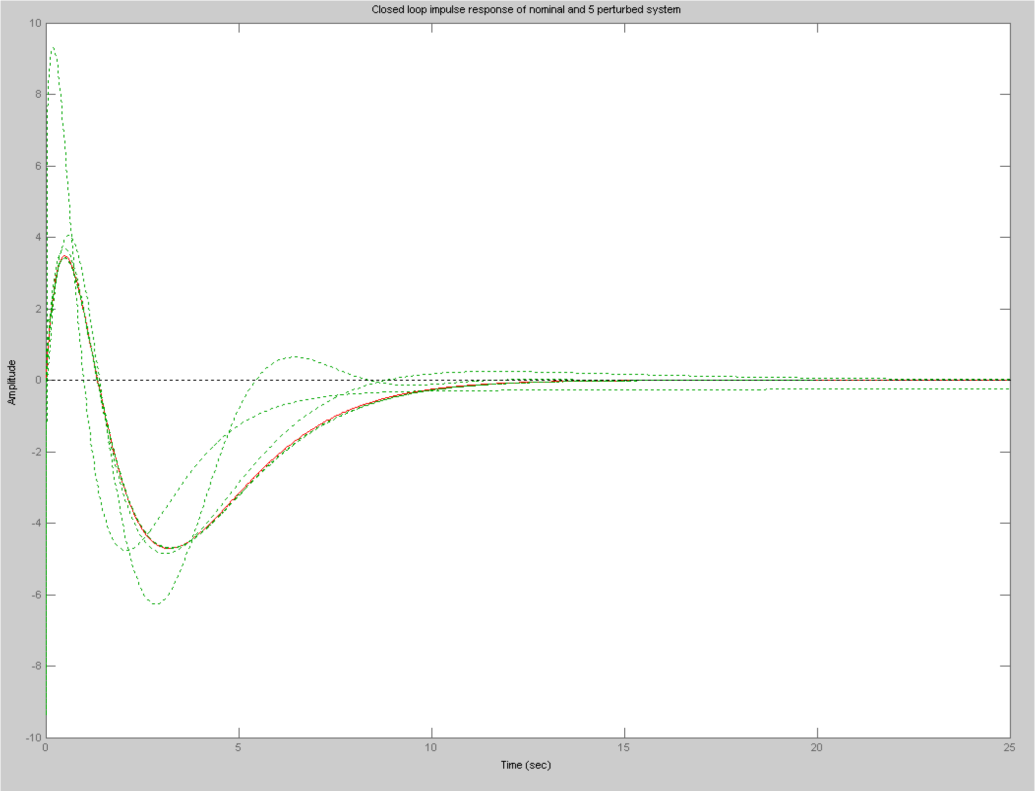

Fig.6.6. Robust Controller Closed Loop Response for Nominal SWNCS and 5 Perturbed System Based H_2 Norm

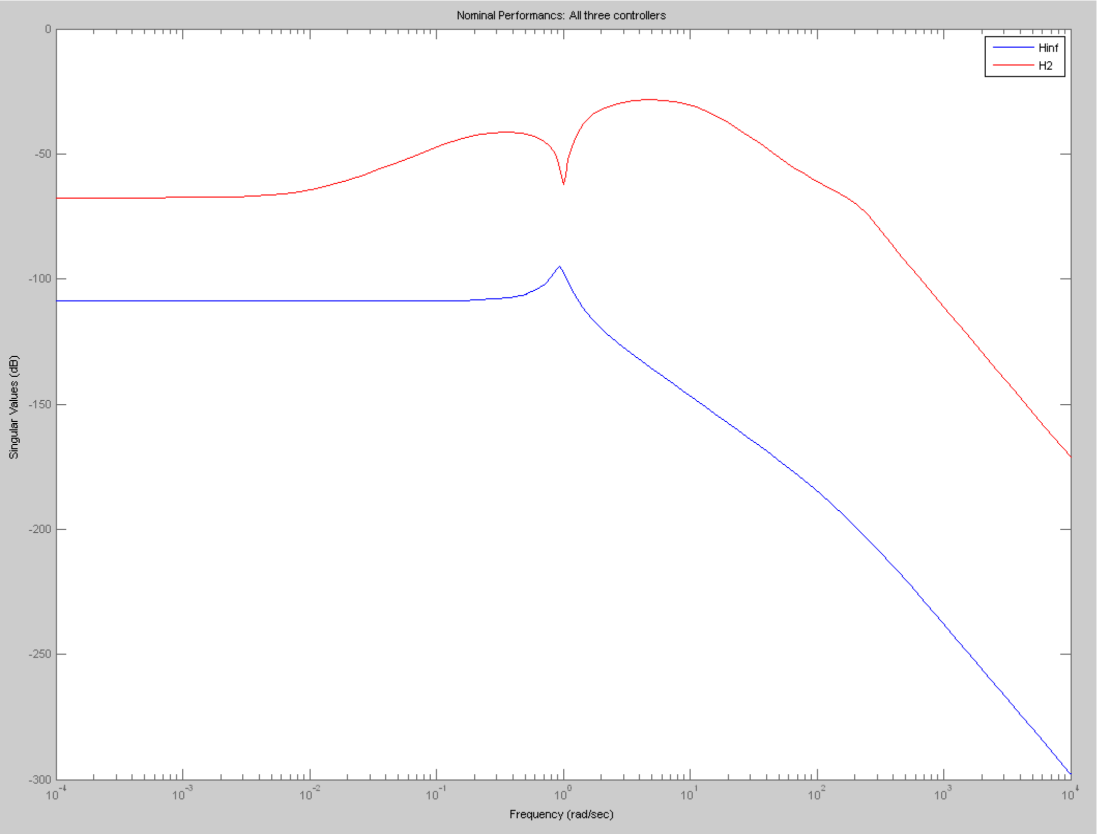

Fig.6.7. The SWNCS Response Based on H_∞ and H_2 Norm

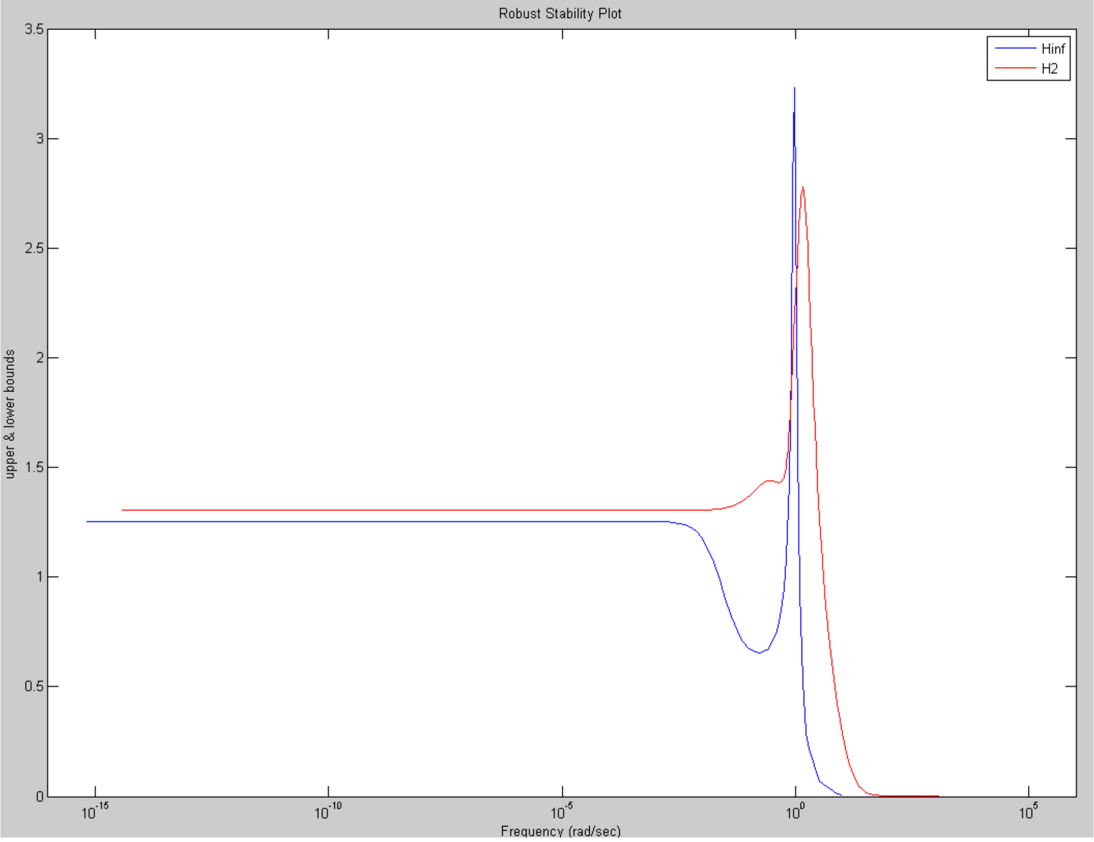

Fig.6.8. Robust Stability Analysis in Terms of H_∞ and H_2 Norms

6.6 CHAPTER SUMMARY

In the previous chapter, an efficient robust model for SWNCS through the stochastic time delay and packet dropout system approach was proposed. The RMPC technique for the SWNCS is obtained by solving set of the LMIs. Based on the SWNCS model, the RMPC can be designed using the Lyapunov functional method. Both sensor-to-controller τ_k^{sc} and controller-to-actuator τ_k^{ca} time delays of the SWNCS are considered as stochastic variables controlled by a Markov chain. A discrete-time Markovian Jump Linear System (MJLS) with norm bounded time delay is presented to model the SWNCSs.

In this chapter, a robust stability for uncertain parameter SWNCS has been proposed. The robust stability of the system has been confirmed using an approach based on H_∞ and H_2 norms criterion. To check this, sufficient conditions for stochastic stability based on H_∞ norm and stabilisation of the SWNCSs are derived via LMIs formulation. Use of the LMIs technique and utilising the data relating to the lower bound of variation of the SWNCS time delay has been shown by the numerical example to be effective. Robust stability analysis base on H_2 norm have been solved under the framework of LMIs. The condition is a set of LMIs with unbounded constraints, which are effectively solved by the PRA. Design examples have been presented to illustrate the effectiveness of the proposed methods.

CHAPTER 7 ..

NEURAL NETWORK PREDICTOR CONTROL (NNPC) FOR SWNCS WITH STOCHASTIC NETWORK TIME DELAY AND PACKET DROPOUT

7.1 INTRODUCTION

In the literature, it has been shown that Neural Networks (NNs) have the capability to estimate virtually any function of attention to any level of accuracy under the assumption that the neural network is presented with sufficiently many hidden units. Based on this capability, NNs have been applied extensively in time series predictions. The main problem that SWNCSs face is the network stochastic time delay, which can frequently degrade the performance of the SWNCS and even destabilise the system. Aiming at resolving this problem, a new modelling proposal for the SWNCSs, stimulated from a variable time sampling approach and applying predictive control techniques employing NN is presented in this chapter. The design demonstrates the construction of the predictive controller and the optimisation functions that are typically employed to update the control signal, then applies the NN method. Predictive control is characterised by achieving the prediction of future values via a model. Furthermore, based on the predicted values, on an optimisation function and on a control signal, the controller generates a future control signal. The predictive controller is characterised by calculating future control signals based on output values predicted by a model [88-89].

In this chapter, a new method is presented for SWNCS analysis and design based on TrueTime simulation tools by designing NNPC controller based MSE performance predictive criterion. SWNCS is designed with specific communications and control parameters using TrueTime simulator tools. A NNPC which is capable of estimating and removing the effect of the delay times that occurs in the SWNCS is introduced. This can be achieved by assuming that stochastic time delays occurring in forward and feedback channels are predicted using a BPNN and a learning algorithm which adopts an adaptive learning rate approach. The NNPC controller will be able to enhance the QoS of SWNCS by removing the effect of time delays which occur in the forward and feedback channels of the SWNCS.

7.2 PROBLEM FORMULATION

Suppose the SWNCS shown in Figure 7-1 has a physical plant that is modelled by the following system:

$$\boldsymbol{x(k+1) = Ax(k) + Bu(k - \tau_k^{ca})} \dots\dots\dots \boldsymbol{(7-1a)}$$

$$\boldsymbol{y(k) = Cx(k)} \dots\dots\dots \boldsymbol{(7-1b)}$$

Where x(k) is the state vector, u(k) is the control input, y(k) is the output A, B, C are system matrices with appropriate dimensions and τ_k^{ca} is a random delay from controller-to-actuator.

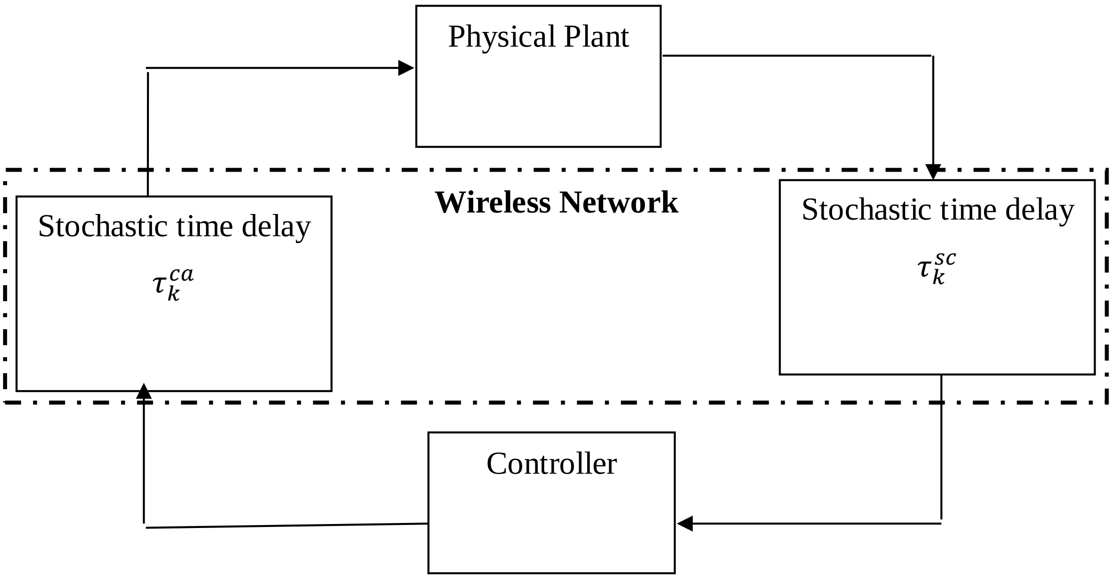

Fig.7.1. SWNCS Diagram

The target of this chapter is to design a NNPC based on BP controller with a learning algorithm adopting an adaptive learning rate approach such that the response of the closed SWNCS can follow a reference signal to get the required tracking control performance. Under the following assumptions:

- Controller and actuator are event-driven
- Sensor is time-driven
- τ_k^{sc}- stochastic time delay from sensor-to-controller
- τ_k^{ca}- stochastic time delay from controller-to-actuator

In any WNCS, the delay information is important for controller design. The controller designed at recent time k and stochastic time delay at a node can be described by the following steps:

1. The stochastic time delay τ_k^{sc} can be achieved using the time sampling techniques ince at recent time k the stochastic time delay τ_k^{sc} can be achieved by comparing the recent time and the sampling-time of sensor data received [96].
2. The embedded processor measures the stochastic time delay $\tau_k^{ca} - 1$.
3. The stochastic time delay in sensor-to-controller channel $\tau_{k-\tau_k^{sc}-1}^{ca}$can be achieved by the controller at recent time k. However, this data cannot be received by the controller instantly because it requires to be sent through the wireless network from the sensor-to-controller channel. So, if the time delays τ_k^{sc} exists, the data of $\tau_{k-\tau_k^{sc}-1}^{ca}$ at time k would be identified at the controller node [169], the two mode-dependent full state feedback controllers are to be designed by MPC.

$$\boldsymbol{u(k) = k_1\left(\tau_k^{sc}, \tau_{k-\tau_k^{sc}-1}^{ca}\right) x_p(k-\tau_k^{sc}) + k_2\left(\tau_k^{sc}, \tau_{k-\tau_k^{sc}-1}^{ca}\right) x(k-\tau_k^{sc}) \ldots\ldots\ldots(7-2)}$$

Referring to the stochastic time delay τ_k^{ca}, the following SWNCS model can be achieved

$$\boldsymbol{x(k+1) = \widetilde{A}X(k) + \widetilde{B}u(k-\tau_k^{ca}) + \tilde{J}r(k) \ldots\ldots\ldots(7-3a)}$$

$$\boldsymbol{y(k) = \widetilde{C}X(k) \ldots\ldots\ldots(7-3b)}$$

Where, $\boldsymbol{X(k)} = [\boldsymbol{x_r(k)^T\ x(k)^T}]$ $\qquad \boldsymbol{\widetilde{A}} = \begin{bmatrix} \boldsymbol{A_r} & \boldsymbol{0} \\ \boldsymbol{0} & \boldsymbol{A} \end{bmatrix}$

$\boldsymbol{\widetilde{B}} = \begin{bmatrix} \boldsymbol{0} \\ \boldsymbol{B} \end{bmatrix}$ $\qquad \boldsymbol{\tilde{J}} = \begin{bmatrix} \boldsymbol{B}_r \\ \boldsymbol{0} \end{bmatrix}$ $\qquad \boldsymbol{\widetilde{C}} = [-\boldsymbol{C_r}\ \boldsymbol{C}]$

7.2.1 Neural Network Predictive Control (NNPC)

The NNPC controller that is implemented using the MATLAB Neural Network Toolbox software employs a neural network model of a physical plant to predict future plant performance. The controller after that computes the control signal that will optimise plant performance over a specified future time horizon. This can be achieved by the following steps:

Step 1 in model predictive control is to establish the neural network SWNCS model (system identification).

Step 2 the SWNCS model is employed by the controller to predict future performance. In the following section we illustrate the system identification procedure. This is tracked by a description of the optimisation procedure.

7.2.2 System Identification

The first step of MPC is to train a NN to characterise the forward dynamics of the SWNC. The prediction error between the SWNCS output and the NN output is used as the NN training signal. The procedure is illustrated in Figure 7-2. The neural network model can be trained on-line in set mode using information collected from the operation of the SWNCS models. Further, Figure 7-3 presents the structure of the neural network SWNC model which uses previous inputs and previous plant outputs to predict future values of the plant output [170].

Choosing $y_p(t)$ as the input vector, $W^{1,1}$ as hidden layer weighting matrix, b^1 as hidden layer bias matrix, $W^{2,1}$ as output layer weighting matrix, b^2 as output layer bias matrix, a^1 as hidden layer output vector and $y_p(t+1)$ as output vector of the neural network , the following relations can be written :

$$\boldsymbol{a^1 = f\left(W^{1,1} e_p(t) + b^1\right) \ldots\ldots\ldots (7-4a)}$$

$$\boldsymbol{e_p(t+1) = f(W^{2,1} a^1 + b^2) \ldots\ldots\ldots. (7-4b)}$$

Where, $f(.)$ is a tangent hyperbolic function and is defined as:

$$\boldsymbol{f(x) = \frac{e^x - e^{-x}}{e^x + e^{-x}} \ldots\ldots\ldots (7-5a)}$$

$$\boldsymbol{\dot{f} = 1 - f^2(x) \ldots\ldots\ldots (7-5b)}$$

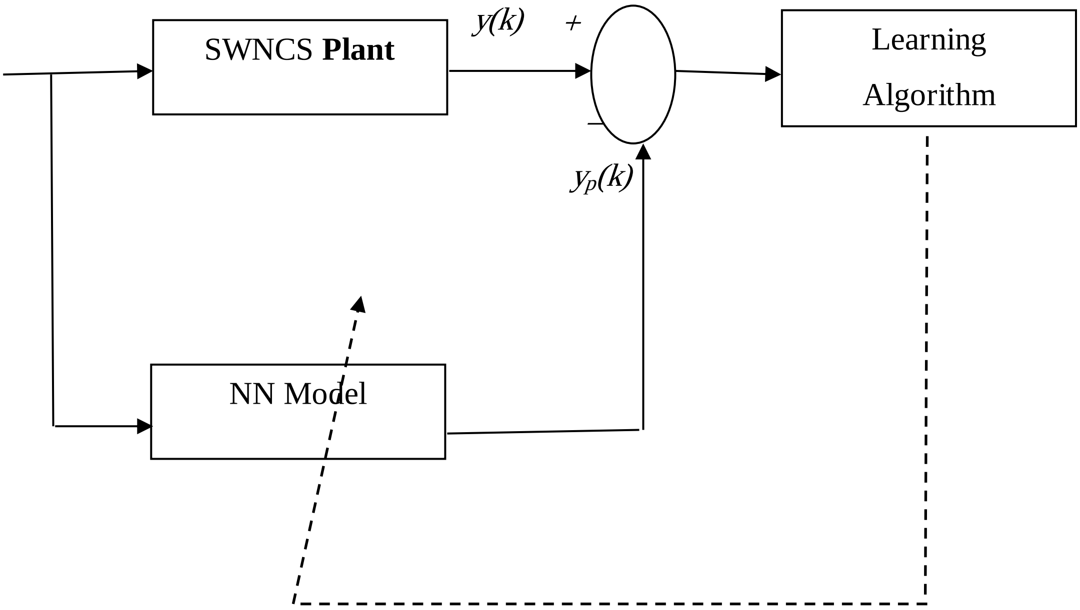

Fig.7.2. System Identification Diagram

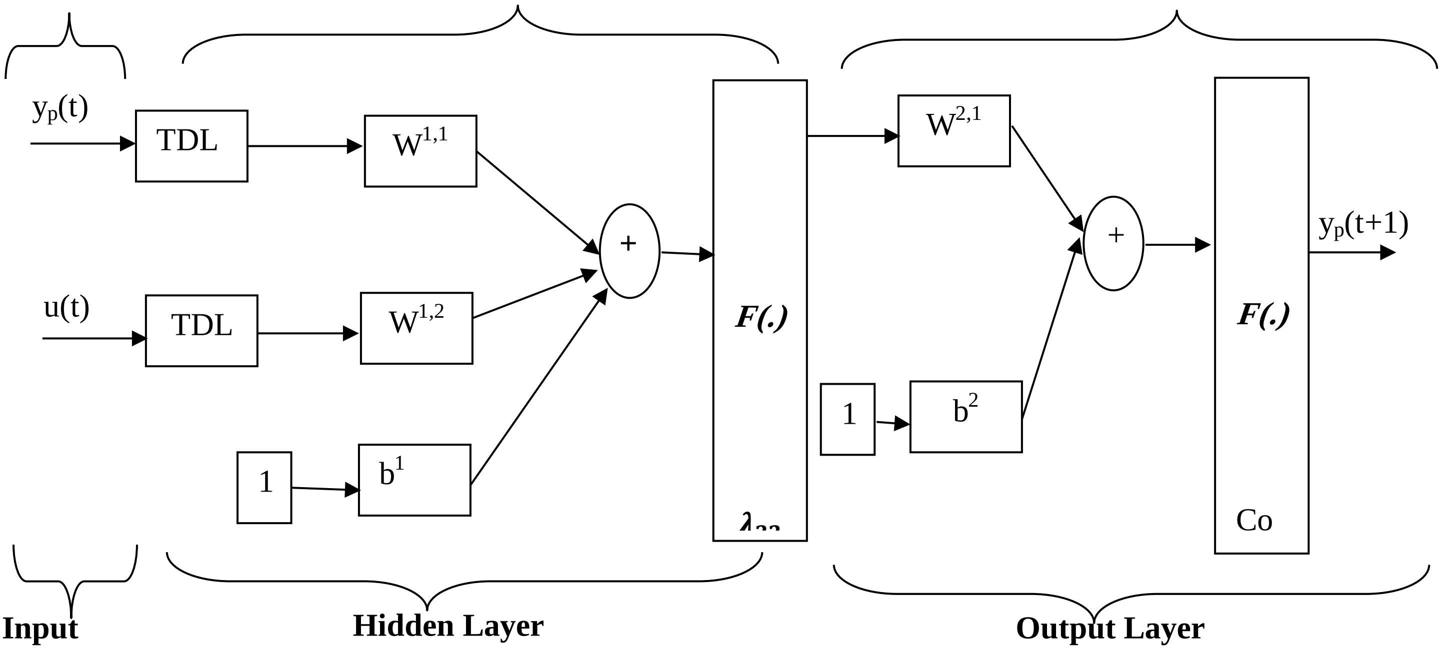

Fig.7.3. Neural Network Structure of SWNCS Model

7.2.3 The Back Propagation (BP) Training Algorithm

A stochastic gradient descent optimisation procedure minimises the MSE criterion in which the network weights are stimulated along the negative of the gradient of the MSE performance index. The term back-propagation refers to the mode in which the gradient is calculated for nonlinear multilayer networks. There are a number of variations on the basic algorithm that are based on other optimisation methods, such as conjugate gradient and Newton methods [97]. The BP mathematical approach is summarized as:

$$\boldsymbol{w_{ji}^{l}(k+1) = w_{ji}^{l}(k) - \lambda \frac{\delta F(k)}{\delta w_{ji}^{l}(k)}} \ldots\ldots\ldots (\mathbf{7-6a})$$

$$\boldsymbol{b_{j}^{l}(k+1) = b_{j}^{l}(k) - \rho \frac{\delta F(k)}{\delta b_{j}^{l}(k)}} \ldots\ldots\ldots (\mathbf{7-6b})$$

where, l is the layer number, $i = 1, 2, \ldots\ldots, \varepsilon_{l-1}$, and $j = 1,2, \ldots\ldots, \varepsilon_{l}$, $\lambda \; and \; \rho - are \; learning \; rates$

$F(k) = \frac{1}{\varepsilon_2}\sum_{j=1}^{\varepsilon_2} e_j^2(k)$ $\quad e_j(k) = t_j(k) - y_{pj}^2(k)$ $\; where \; t$ is the target vector and y_p is the output vector

$$\boldsymbol{\frac{\delta F(k)}{\delta x} = \begin{cases} -2e_j(k)a_i^1, & x = w_{ji}^2 \\ -2e_j(k), & x = b_j^2 \end{cases}} \ldots\ldots\ldots (\mathbf{7-7})$$

$$\boldsymbol{\frac{\delta F(k)}{\delta x} = \begin{cases} -2\left\{\left[\sum_{m=1}^{\varepsilon_2}\left(e_m(k)w_{mj}^2(k)\right)\left(1-a_j^1\right)^2\right]y_i(k)\right\}, x = w_{ji}^1 \\ -2\left\{\sum_{m=1}^{\varepsilon_2}\left(e_m(k)w_{mj}^2(k)\right)\left(1-a_j^1\right)^2\right\}, \quad x = b_j^1 \end{cases}} \ldots\ldots\ldots (\mathbf{7-8})$$

The BP training algorithm is summarised as follows:

- **Forward channel**

This channel can be known with subsequent equations

$$\boldsymbol{a^0 = y_p(k)} \ldots\ldots\ldots (\mathbf{7-9a})$$

$$\boldsymbol{a^{l+1}(k) = f^l\left(w^{l+1}a^l + b^{l+1}(k)\right), l = 1, 2} \ldots\ldots\ldots (\mathbf{7-9b})$$

- **Backward channel**

Sensitivity vectors are defined as follows:

$$\boldsymbol{\frac{\delta F(k)}{\delta\left(w^{l+1}a^l + b^{l+1}(k)\right)} \triangleq \delta^l(k), l = 1, 2} \ldots\ldots\ldots (\mathbf{7-10a})$$

$$\boldsymbol{\delta^{l}(k) = -2e(k) \ldots\ldots\ldots (7-10b)}$$

$$\boldsymbol{e(k) = t(k) - y_p^2(k) \ldots\ldots\ldots (7-10c)}$$

$$\boldsymbol{\delta^{1}(k) = diag\left[\dot{f}(w^{l+1}a^{l} + b^{l+1}(k)_1 \ldots \dot{f}(w^{l+1}a^{l} + b^{l+1}(k)_{\varepsilon_1}\right]\left(w^{2}(k)\right)^{T}\delta^{2}(k) \ldots\ldots\ldots (7-10d)}$$

- **Parameter regulation**

$$\boldsymbol{w^{l+1}(k+1) = w^{l+1}(k) - \lambda\delta^{l+1}(k)\left(a^{l}(k)\right)^{T} \ldots\ldots\ldots (7-11a)}$$

$$\boldsymbol{b^{l+1}(k+1) = b^{l+1}(k) - \rho\delta^{l+1}(k), l = 1,2 \ldots\ldots\ldots (7-11b)}$$

- **Stopping point**

For stopping the BP training algorithm, we can use the following MSE index. The MSE becomes less than a specified value in every epoch, that is, for all training patterns.

7.2.4 Model Predictive Control Technique

The Model predictive control technique can be illustrated as shown in Figure 4 where, the controller consists of the NN SWNCS model and the optimization block. The optimization block determines the values of $\bar{u}$ that minimises the performance index *J*, and then the optimal u is input to the SWNCS. The controller block is implemented in MATLAB/SIMULINK while the SWNCS block is implemented in TrueTime. The MPC method is based on the retreating horison technique. The NN model predicts the SWNCS response over a specified time horizon. The predictions are employed by a numerical optimisation plan to establish the control signal that minimises the subsequent performance index over the specified horizon [183].

$$\boldsymbol{J = \frac{1}{\varepsilon_2 N}\left\{\sum_{j=1}^{\varepsilon_2}[t(k+j) - y_M(k+j)]^2 + \partial\sum_{j=1}^{N}[\bar{u}(k+j-1) - \bar{u}(k+j-2)]^2\right\} \ldots\ldots\ldots (7-12)}$$

where, N- is the horizon over which the tracking error and the control increases are calculated, $\bar{u}$- is the variable provisional control signal, $\boldsymbol{y_M}$ is NN SWNCS model response, and ∂- establishes the part that the sum of the squares of control increases has on the performance index.

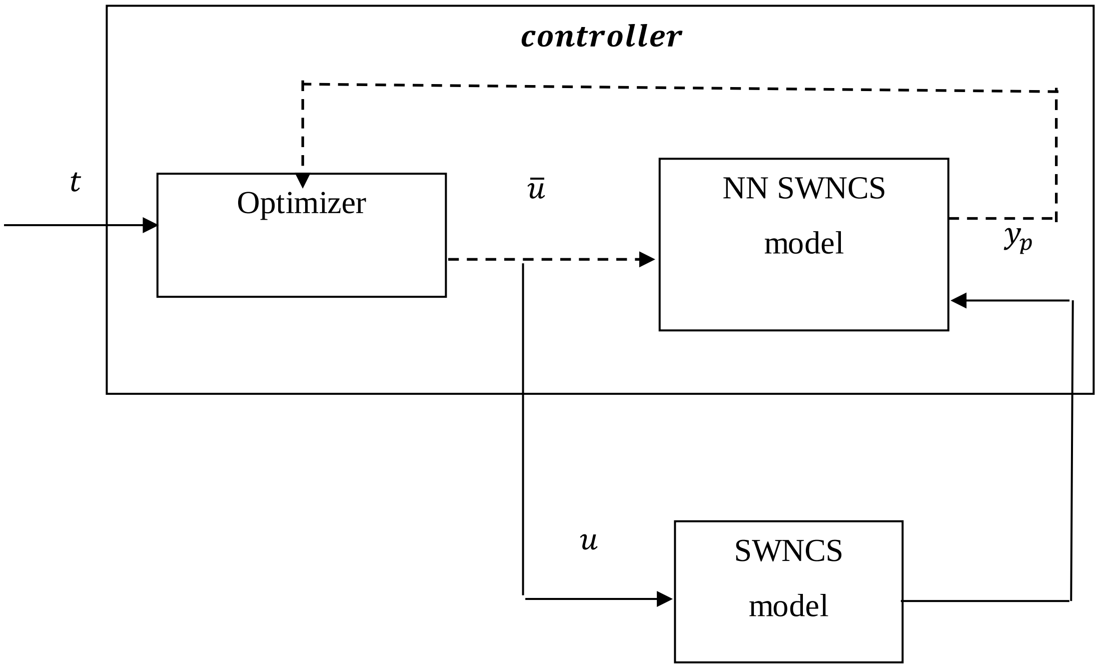

Fig.7.4. MPC Based NN Procedure

NN predictive controllers improve tracking performance by reducing the effect of time delays on SWNCS. The basic working principle of the NN predictive controller is to generate a sequence of control signals at each sample interval that optimise the control effort in order to track exactly the desired signal. The neural-network-based predictive control signal is obtained from minimising the predictive performance index equation (7-12) over the specified horizon as follows [89]:

$$\boldsymbol{u(k) = [u(k)\ u(k+1) \ldots\ldots u(k+N)]^T} \ldots\ldots\ldots \boldsymbol{(7-13)}$$

The control signal in (7-13) is found from optimisation of the performance index (7-12) based upon the gradient descent method, that is:

$$\begin{cases} \boldsymbol{u(k) = u(k-1) + \Delta u(k)} \\ \boldsymbol{u(k) = u(k-1) + \lambda \dfrac{\delta y_p^T(k)}{\delta u(k)}} \\ \boldsymbol{u(k) = u(k-1) + \lambda \bar{C}^T(k) e(k)} \end{cases} \ldots\ldots\ldots \boldsymbol{(7-14)}$$

where,

$$\boldsymbol{\bar{C}(k) = \frac{\delta y_p^T(k)}{\delta u(k)} = \begin{bmatrix} \dfrac{\delta y_p(k)}{\delta u(k)} & \dfrac{\delta y_p(k)}{\delta u(k+1)} & \cdots & \dfrac{\delta y_p(k)}{\delta u(k+N)} \\ \dfrac{\delta y_p(k+1)}{\delta u(k)} & \dfrac{\delta y_p(k+1)}{\delta u(k+1)} & \cdots & \dfrac{\delta y_p(k+1)}{\delta u(k+N)} \\ \vdots & \vdots & \ddots & \vdots \\ \dfrac{\delta y_p(k+N)}{\delta u(k)} & \dfrac{\delta y_p(k+N)}{\delta u(k+1)} & \cdots & \dfrac{\delta y_p(k+N)}{\delta u(k+N)} \end{bmatrix}}$$

Then the expression of the NNPC controller can be written in the following form

$$\boldsymbol{u(k) = u(k-1) + \lambda C^T e(k)} \ldots\ldots\ldots (\mathbf{7-15})$$

where,

$$\boldsymbol{C(k) = \left[\frac{\delta y_p(k)}{\delta u(k)} \ \frac{\delta y_p(k+1)}{\delta u(k)} \ \ldots\ldots \frac{\delta y_p(k+N)}{\delta u(k)}\right]^T}$$

7.2.5 Stochastic Network time Delay and Packet Dropout of SWNCS Architecture

The control signal sequence is started in the sensor and the real time of the controller is unknown without clock synchronization. Further, it is also not required in the proposed approach. Hence, at recent time k, the previous information of the physical plant before $k - \tau_k^{sc}$ is presented on the controller area as follows [91]:

$$\boldsymbol{\begin{bmatrix} y_p(k-\tau_k^{sc}) \\ y_p(k-\tau_k^{sc}-1) \\ \vdots \\ y_p(k-\tau_k^{sc}-N) \end{bmatrix}, \begin{bmatrix} u(k-\tau_k^{sc}-1) \\ u(k-\tau_k^{sc}-2) \\ \vdots \\ u(k-\tau_k^{sc}-N) \end{bmatrix}} \ldots\ldots\ldots (\mathbf{7-16})$$

Based on (7-13) and (7-16), the response predictions can be determined by the following equation:

$$\boldsymbol{y_p(k-\tau_k^{sc}+j|k-\tau_k^{sc}) = F\{y_p(k-\tau_k^{sc}+j-1|k-\tau_k^{sc}) \cdots y_p(k-\tau_k^{sc}+j-N|k-\tau_k^{sc}) \ \ u(k-\tau_k^{sc}+j) \cdots u(k-\tau_k^{sc}+j-N)\}} \ldots\ldots\ldots (\mathbf{7-17})$$

where,

$$\boldsymbol{y_p(k-\tau_k^{sc}+i|k-\tau_k^{sc}) = y_p(k-\tau_k^{sc}+i)}$$

Then, based on (7-13) and (7-16), the first control signal can be determined as:

$$\boldsymbol{u(k-\tau_k^{sc}|k-\tau_k^{sc}) = -\left[\sum_{i=1}^{N} C^T u(k-\tau_k^{sc}-i) + \sum_{i=0}^{N} y_p(k-\tau_k^{sc}-1-i|k-\tau_k^{sc})\right]} \ldots\ldots\ldots (\mathbf{7-18})$$

Thus, based on (7-18) and (7-17) the response predications and control signal predication are recursively determined as follows:

$$\boldsymbol{y_p(k-\tau_k^{sc}+j-1|k-\tau_k^{sc}) = F\begin{Bmatrix} y_p(k-\tau_k^{sc}+j-1|k-\tau_k^{sc})\cdots y_p(k-\tau_k^{sc}+j-N|k-\tau_k^{sc}) \\ u(k-\tau_k^{sc}+j-1|k-\tau_k^{sc})\cdots \\ u(k-\tau_k^{sc}+j-N|k-\tau_k^{sc}) \end{Bmatrix} \ldots\ldots\ldots(7-19)}$$

$$\boldsymbol{u(k-\tau_k^{sc}+j|k-\tau_k^{sc}) = -\left[\sum_{i=1}^{N} C^T u(k-\tau_k^{sc}+j-i|k-\tau_k^{sc}) + \sum_{i=0}^{N} y_p(k-\tau_k^{sc}+j-i-1|k-\tau_k^{sc})\right] \ldots\ldots\ldots(7-20)}$$

The sampling time at sensor node $\boldsymbol{k-\tau_k^{sc}}$ is set into an information packet with the control signal prediction sequence and transmitted to the actuator. Obviously, from system (7-20), we can generate control signal predictions as follows:

$$U(\boldsymbol{k-\tau_k^{sc}|k-\tau_k^{sc}}) = \begin{bmatrix} \boldsymbol{u(k-\tau_k^{sc}|k-\tau_k^{sc})} \\ \boldsymbol{u(k-\tau_k^{sc}+1|k-\tau_k^{sc})} \\ \vdots \\ \boldsymbol{u(k-\tau_k^{sc}+N|k-\tau_k^{sc})} \end{bmatrix} \ldots\ldots\ldots\boldsymbol{(7-21)}$$

Because the actuator is time-driven, the NNPC executes once at every sampling period regardless of whether the actuator collects new information packets or not. If no information packet is received, the content and sampling time of the actuator schedule remain invariant. When receiving new control signal prediction sequences, the actuator compares the sampling time of the new packets with that of the schedule, and then updates the schedule with the following rule:

$$\begin{cases} \boldsymbol{U(k)=\overline{U}(k)\ if\ new\ information\ packet\ recived} \\ \boldsymbol{U(k)=U(k-1)} \qquad\qquad \boldsymbol{otherwise} \end{cases}$$

Hence, the content of the schedule $U(k)$ is the newest control signal prediction sequence existing in the actuator node at time k, which can be expressed by:

$$\boldsymbol{U(k)} = \begin{bmatrix} \boldsymbol{u(k-\tau_k^{sc}-\tau_k^{ca}|k-\tau_k^{sc}-\tau_k^{ca})} \\ \boldsymbol{u(k-\tau_k^{sc}-\tau_k^{ca}+1|k-\tau_k^{sc}-\tau_k^{ca})} \\ \vdots \\ \boldsymbol{u(k-\tau_k^{sc}-\tau_k^{ca}+N|k-\tau_k^{sc}-\tau_k^{ca})} \end{bmatrix} \ldots\ldots\ldots\boldsymbol{(7-22)}$$

where, $k-\tau_k^{sc}-\tau_k^{ca}$ is the sampling time of the control signal predication sequence at the actuator node.

In order to remove or reduce the effect of the time delay that occurs in SWNCS, the NNPC chooses the proper control signal from (7-22) based on the forward and backward channel delays$(i.e.\ \tau_k^{sc}\ and\ \tau_k^{ca})$. Thus, the control signal input to the physical plant at time k will be

$$\boldsymbol{u(k) = u(k|k - \tau_k^{sc} - \tau_k^{ca})} \ldots\ldots\ldots (\mathbf{7-23})$$

7.3 NEUMERICAL EXAMPLE

In order to validate the effectiveness of the proposed method, the following numerical example is considered, where the parameters of the discrete-time physical plant with sampling time T$_s$=0.01 sec is described as follows:

$$\boldsymbol{x(k+1)} = \begin{bmatrix} \mathbf{1.0123} & \mathbf{0.0502} \\ \mathbf{0.4920} & \mathbf{1.0123} \end{bmatrix} \boldsymbol{X(k)} + \begin{bmatrix} \mathbf{0.0125} \\ \mathbf{0.5020} \end{bmatrix} \boldsymbol{u(k - \tau_k^{ca})} + \begin{bmatrix} \mathbf{0.1} \\ \mathbf{0.1} \end{bmatrix} \boldsymbol{r(k)}$$

$$\boldsymbol{y(k)} = [\mathbf{1} \quad \mathbf{0}]\boldsymbol{X(k)}$$

The NNPC model can be simulated in MATLAB/SIMULINK as shown in Figure 7-5, the block involves SWNCS in the TrueTime model, in which 2 nodes are linked to a wireless network as in Figure 7-6.

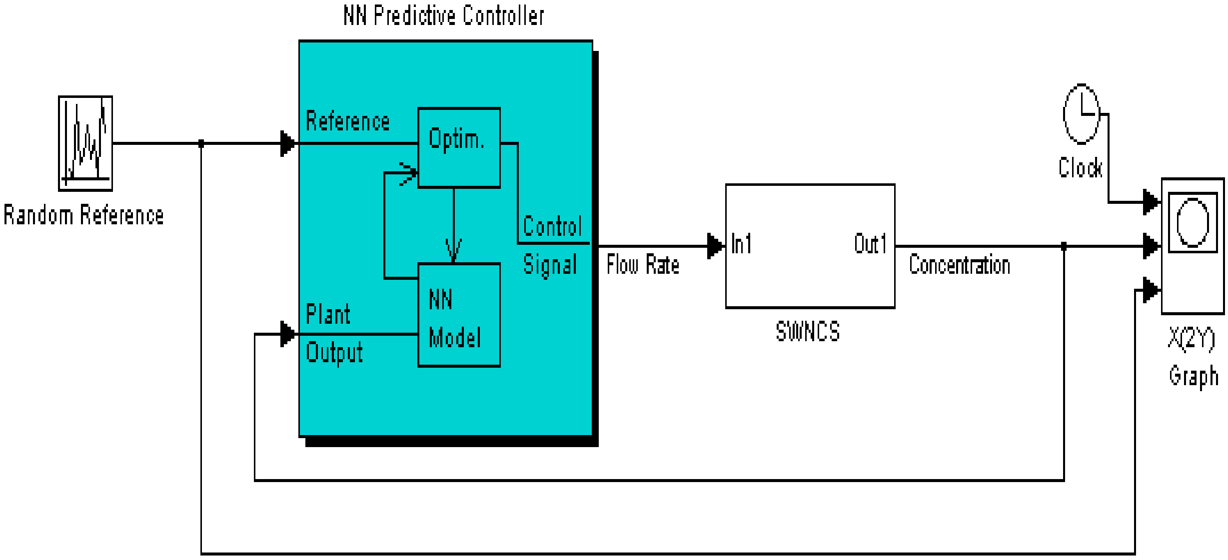

Fig.7.5. NNPC for SWNCS SIMULINK Model

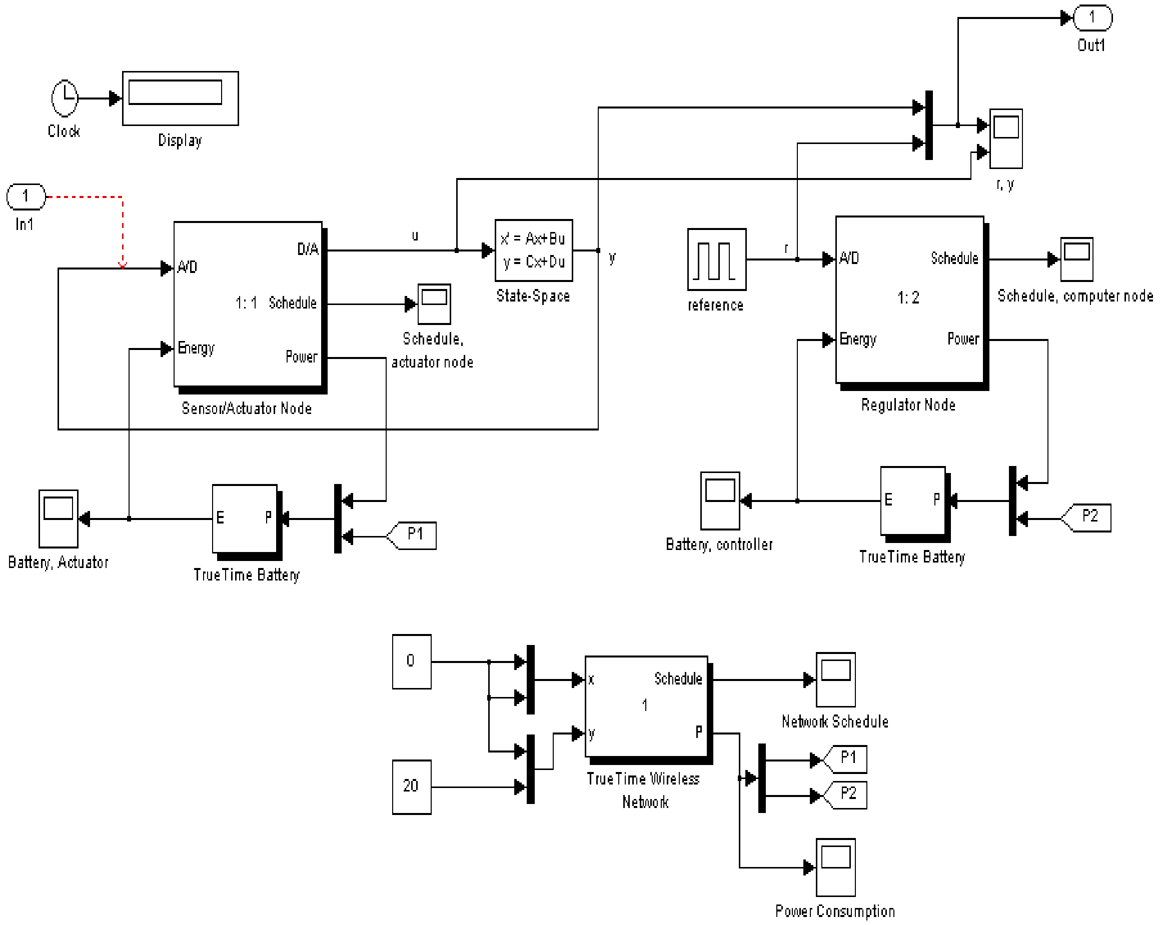

Fig.7.6. SWNCS Simulated in TrueTime

7.4 SIMULATION RESULTS

The simulated NNPC for the SWNCS is illustrated in Figure 7-7 with the following parameters: the cost horizon $N_2 = 7$, the control horizon $N_u = 4$, the control weighting factor $\sigma = 0.09$, search parameter $\alpha = 0.01$ and iteration per sample time$= 2$. When, plant identification in Figure 7-7 is selected, another window appears as shown in Figure 7-9. To design NNPC, the NN SWNCS model must be developed. The SWNCS model predicts future SWNCS responses. The optimisation algorithm employs these predictions to establish the control signal that optimise future performance. In this work, the SWNCS model has an input layer, a hidden layer and an output layer. The training function described in the BP training algorithm is used to train the NN SWNCS model with the following parameters:

1. Network architecture
    - Size of hidden layer=5, 7, and 10
    - Sampling interval=0.8 sec

2. Training data
   - Training sample=10000
   - Maximum interval value=50 sec
   - Minimum interval value=12 sec

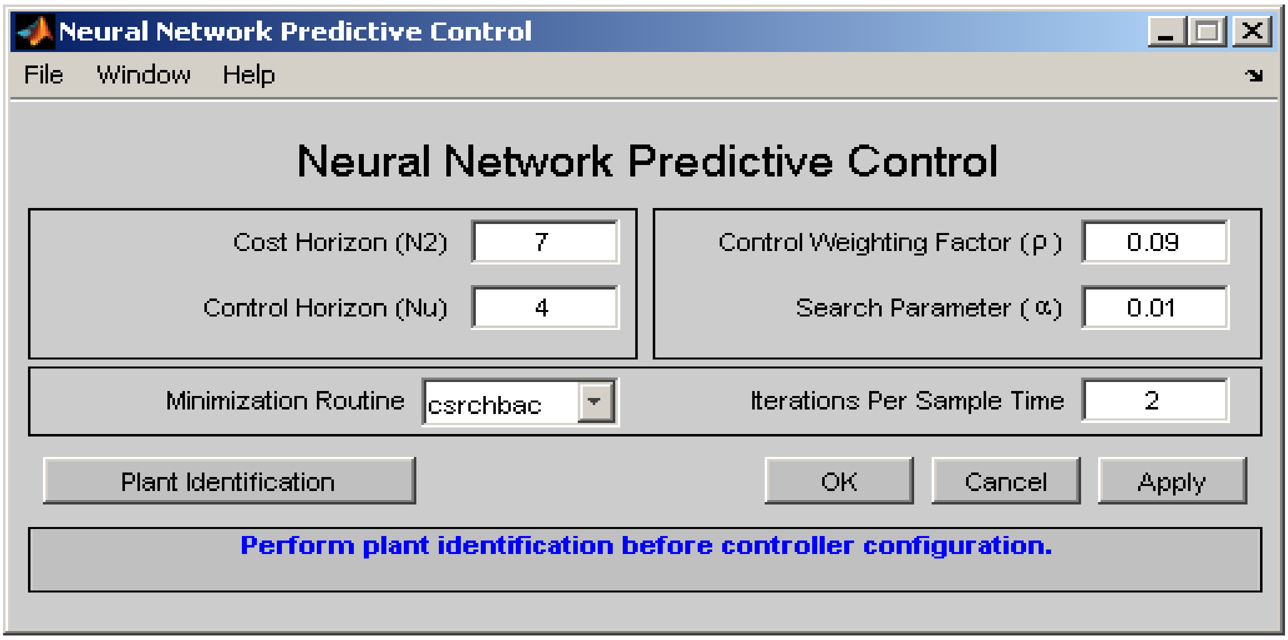

Neural Network Predictive Control

Cost Horizon (N2): 7

Control Horizon (Nu): 4

Control Weighting Factor (ρ): 0.09

Search Parameter (α): 0.01

Minimization Routine: csrchbac

Iterations Per Sample Time: 2

Perform plant identification before controller configuration.

Fig.7.7. NNPC Window

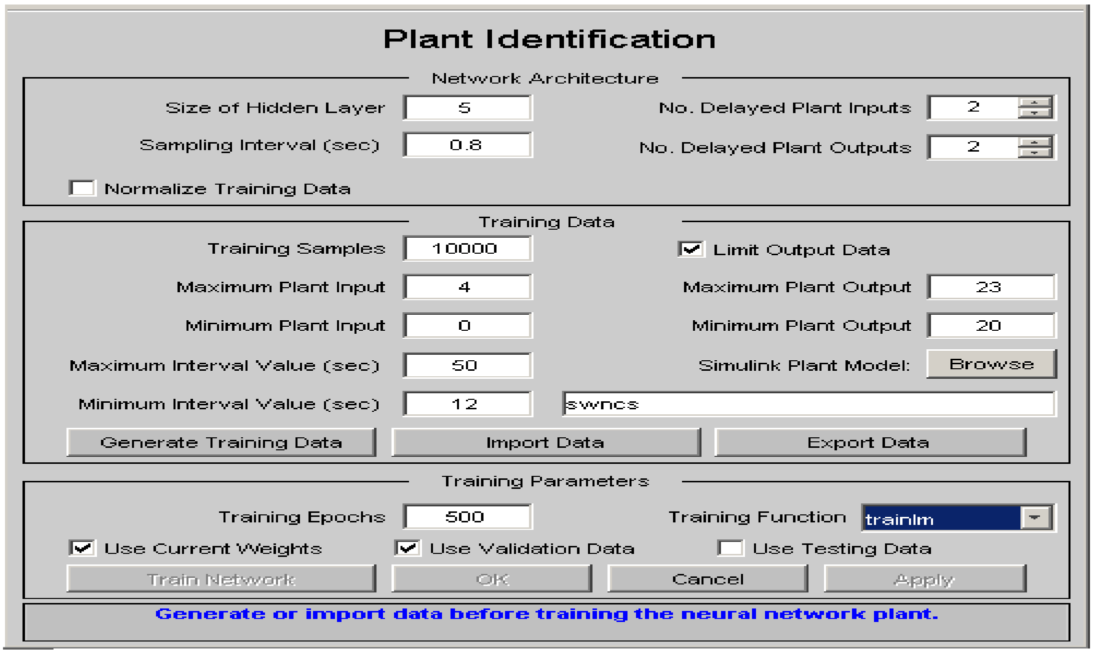

Plant Identification

Network Architecture

Size of Hidden Layer: 5

No. Delayed Plant Inputs: 2

Sampling Interval (sec): 0.8

No. Delayed Plant Outputs: 2

☐ Normalize Training Data

Training Data

Training Samples: 10000

☑ Limit Output Data

Maximum Plant Input: 4

Maximum Plant Output: 23

Minimum Plant Input: 0

Minimum Plant Output: 20

Maximum Interval Value (sec): 50

Simulink Plant Model: swncs

Minimum Interval Value (sec): 12

Training Parameters

Training Epochs: 500

Training Function: trainlm

☑ Use Current Weights ☑ Use Validation Data ☐ Use Testing Data

Generate or import data before training the neural network plant.

Fig.7.8. Plant Identification Window

Figure 7-9 illustrates the random training data for the SWNCS model. 10000 training samples will be generated before training the NN SWNCS model. Select *accept data* and then, select *train network* from plant identification window with the following training parameters (training Epochs=500 and training function=trainlm). After the training data is complete, the response of the resulting SWNCS model training data and validation training data is displayed as shown in Figures 7-10 and 7-11 respectively. Figure 12 demonstrates NN training parameters such as the performance in (a) and training state in (b).

The used NN training parameters like the size of hidden layer =5, 7, 10 are presented in Table 7-1 below. The SWNCS response when using the Wi-Fi as wireless network and the reference signal is shown in Figure 7-13. The SWNCS response when using WiMAX as wireless network is displayed in Figure 7-14. Figure 7-15 shows the schedule of stochastic time delay at the computer node when WI-FI and WiMAX are used. The schedule of stochastic time delay at wireless networks for both WI-FI and WIMAX networks are shown in Figure 7-16. The simulation responses in Figures 7-13 and 7-14 demonstrate the effectiveness of the proposed controller at the desired control performance, especially for SWNCS with Wi-Fi/ WiMAX wireless networks. The simulation results show that the proposed method is capable of controlling SWNCS with satisfactory tracking performance under stochastic wireless network delay. Table 7-2 demonstrates the performance parameters of the SWNCS obtained when using NNPC techniques [184].

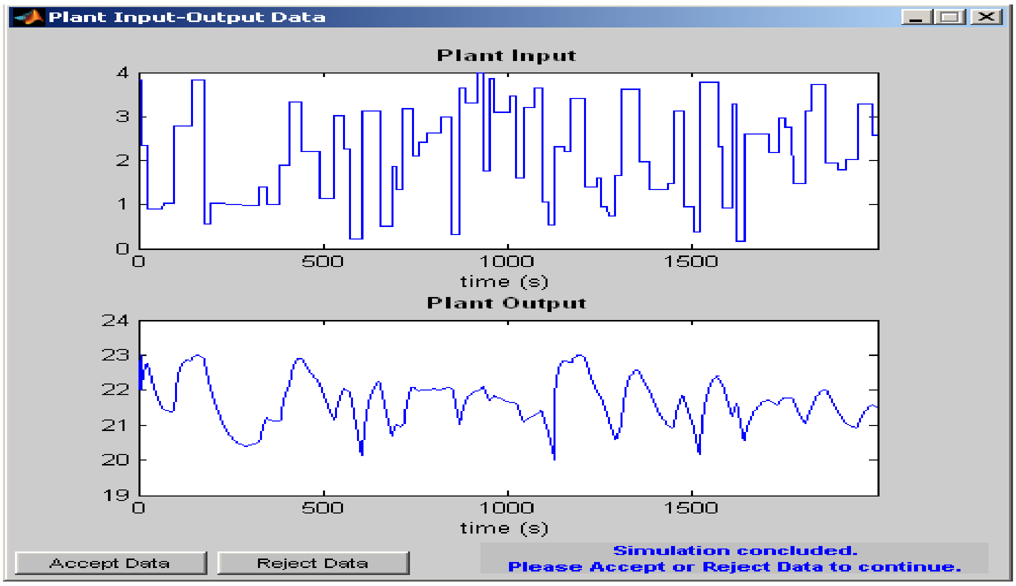

Simulation concluded.
Please Accept or Reject Data to continue.

Fig.7.9. Random Generated SWNCS Input/output Data

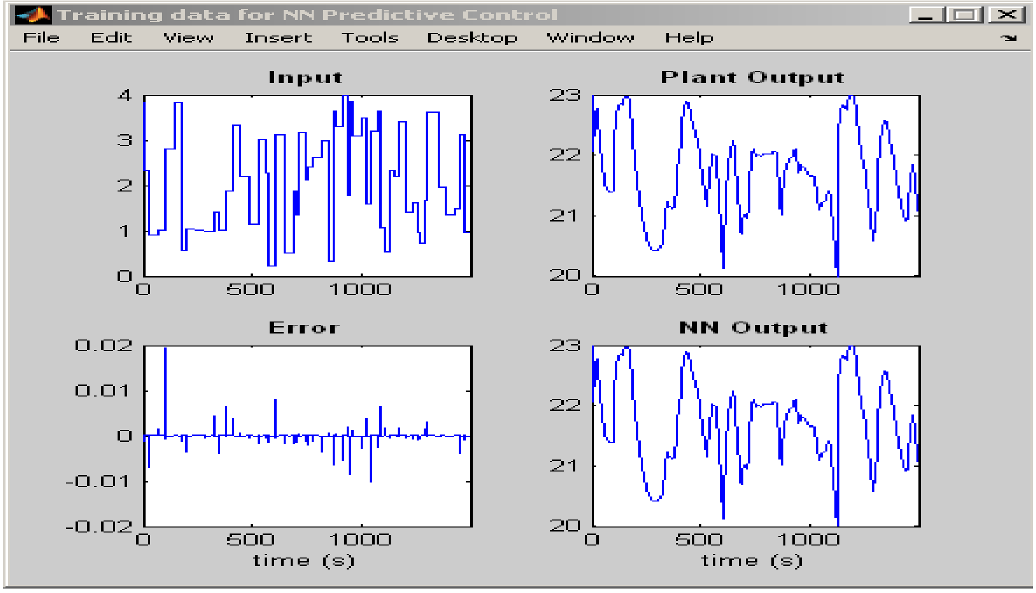

Fig.7.10. Training Data for SWNCS Model

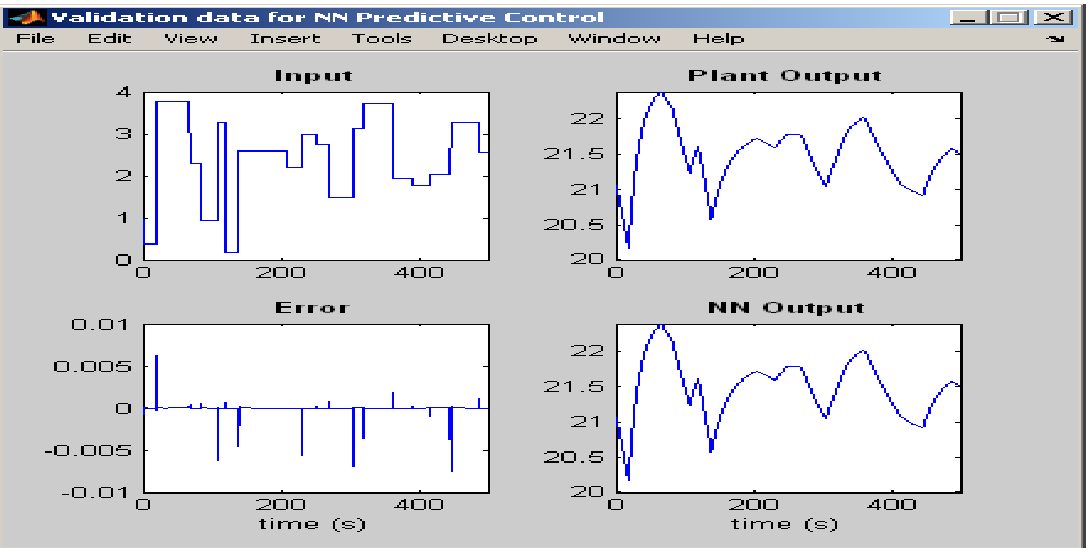

Fig.7.11. Validation Training Data for SWNCS Model

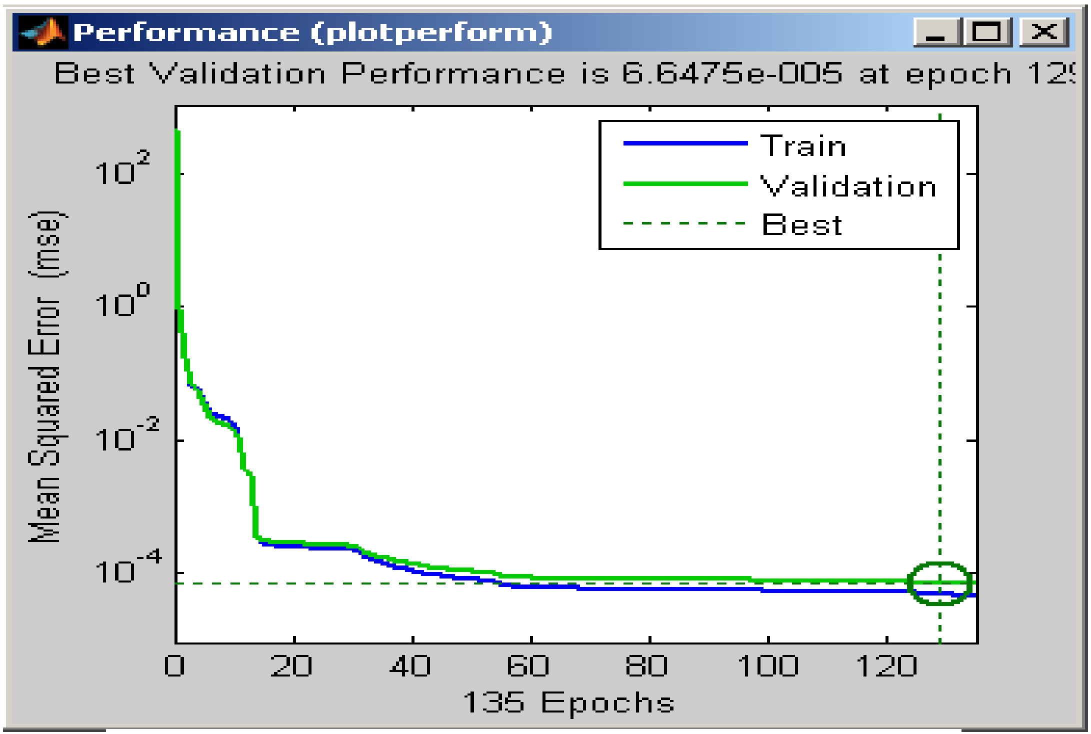

(A) Performance Plot

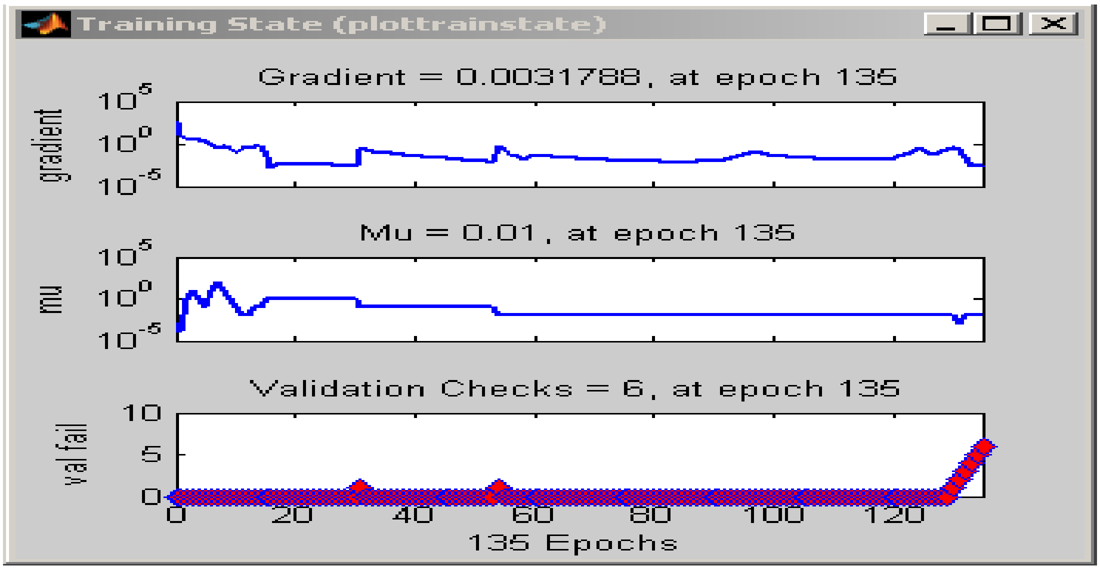

(B) Training State

Fig.7.12. NN Training Parameters

Table 7.1. NN Training Parameters

NN training parameters	*Size of hidden layer=5*	*Size of hidden layer=7*	*Size of hidden layer=10*
Epoch	**135 iterations**	**27 iterations**	**177 iterations**
Time	**0:00:05**	**0:00:01**	**0:00:14**
performance	**$4.70\ e^{-5}$**	**$9.9\ e^{-07}$**	**$7.09\ e^{-07}$**
Gradient	**0.00318**	**0.000641**	**0.000761**

Table 7.2. Performance Parameters of SWNCS with WI-FI and WiMAX Wireless Network

Performance Parameters	NNPC Technique with WI-FI wireless network	NNPC Technique with WiMAX wireless network
Maximum Overshoot	0.68	0.75
Settling Time (sec.)	0.37	0.41
Steady State error	$6x10^{-5}$	$7.4x10^{-4}$

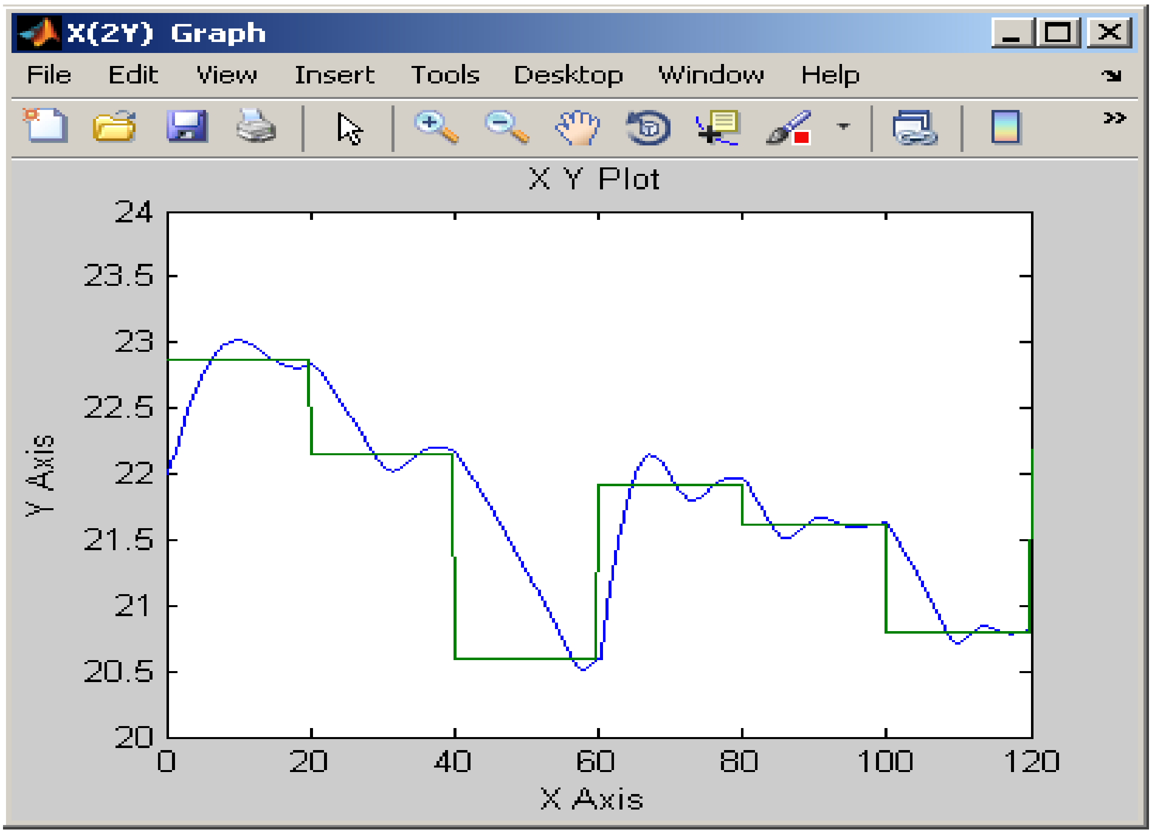

Fig.7.13. SWNCS Response with Wi-Fi Wireless Network

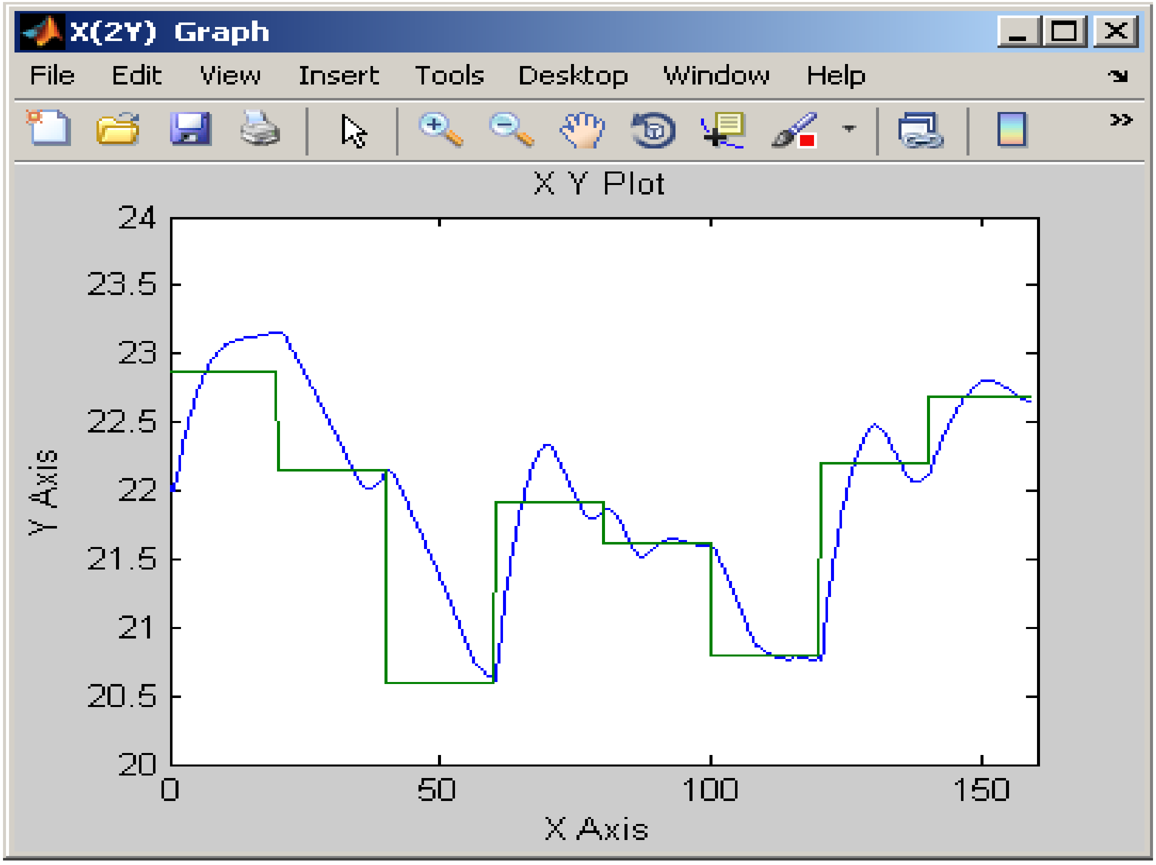

Fig.7.14. SWNCS Response with WiMAX Wireless Network

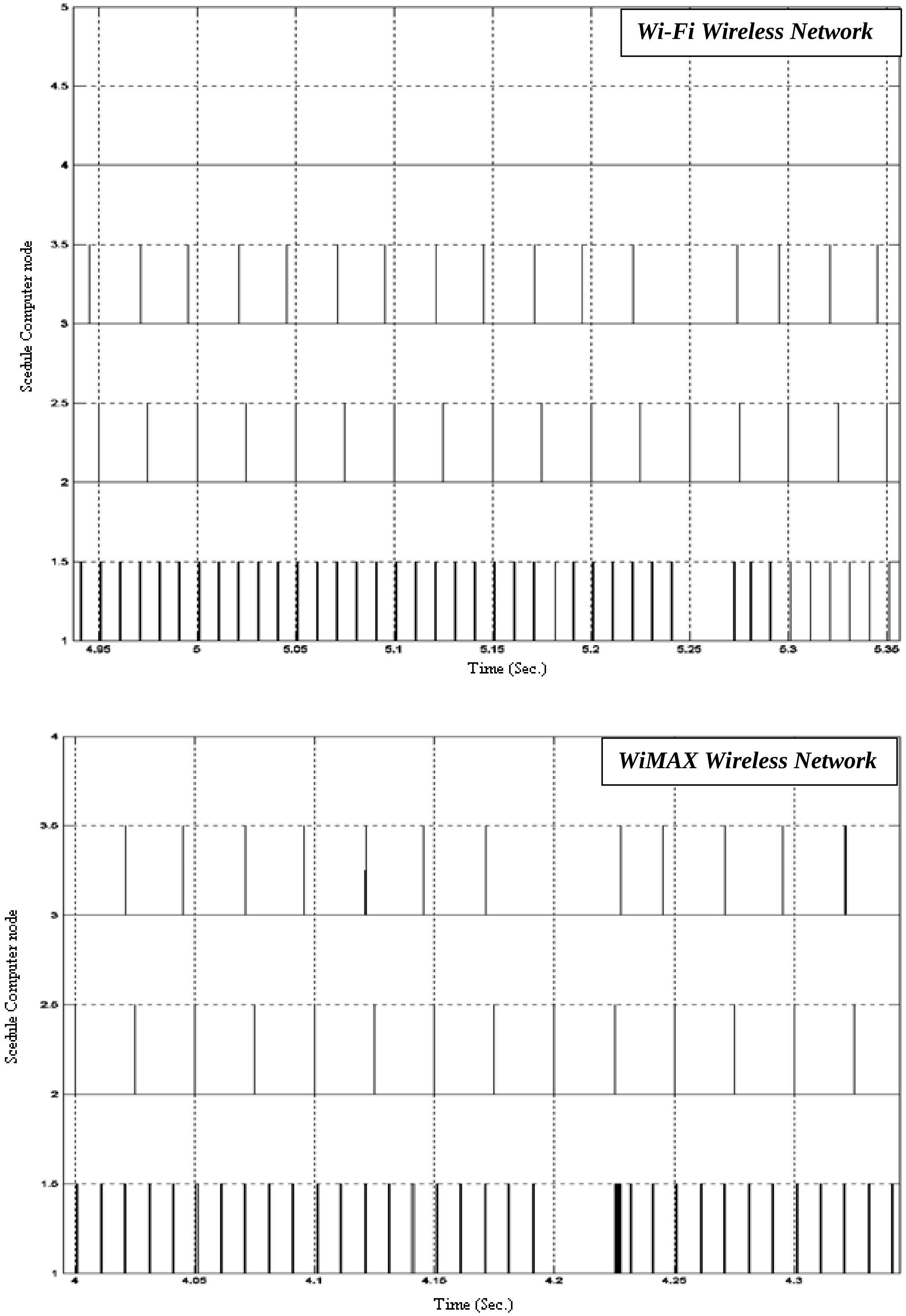

Fig.7.15. Schedule at Computer Node

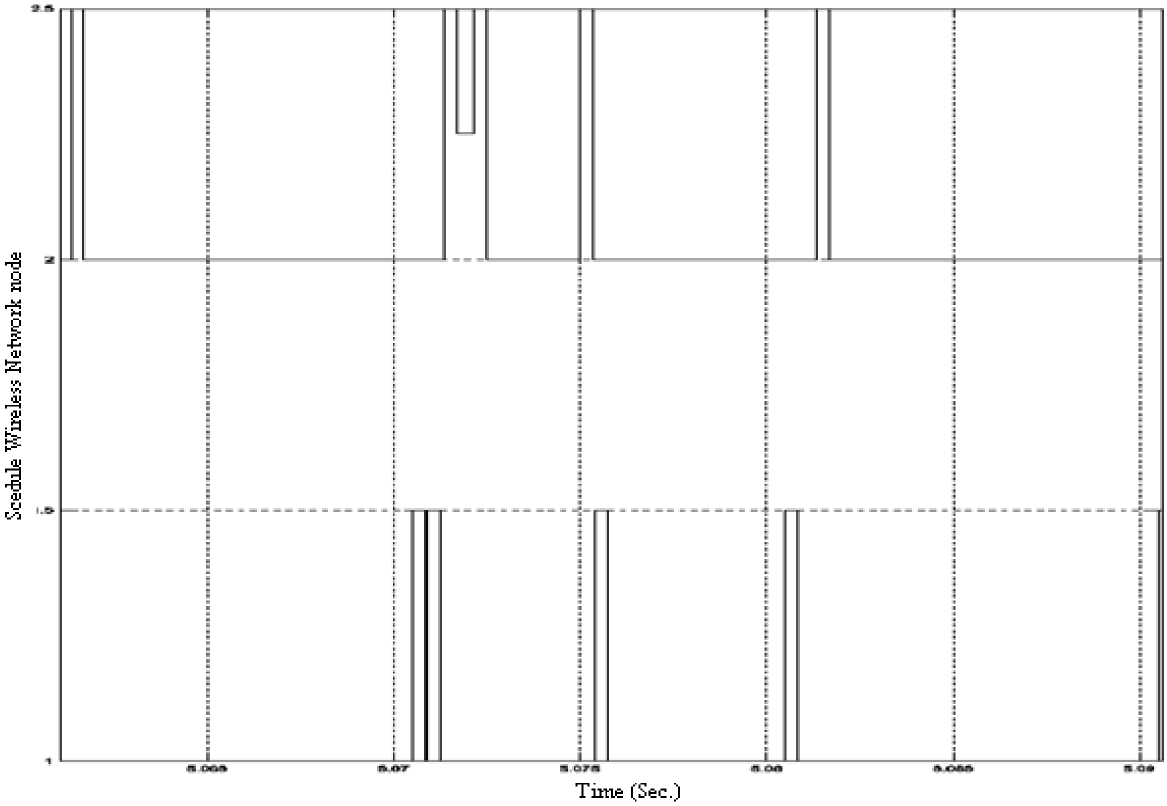

Wi-Fi Wireless Network

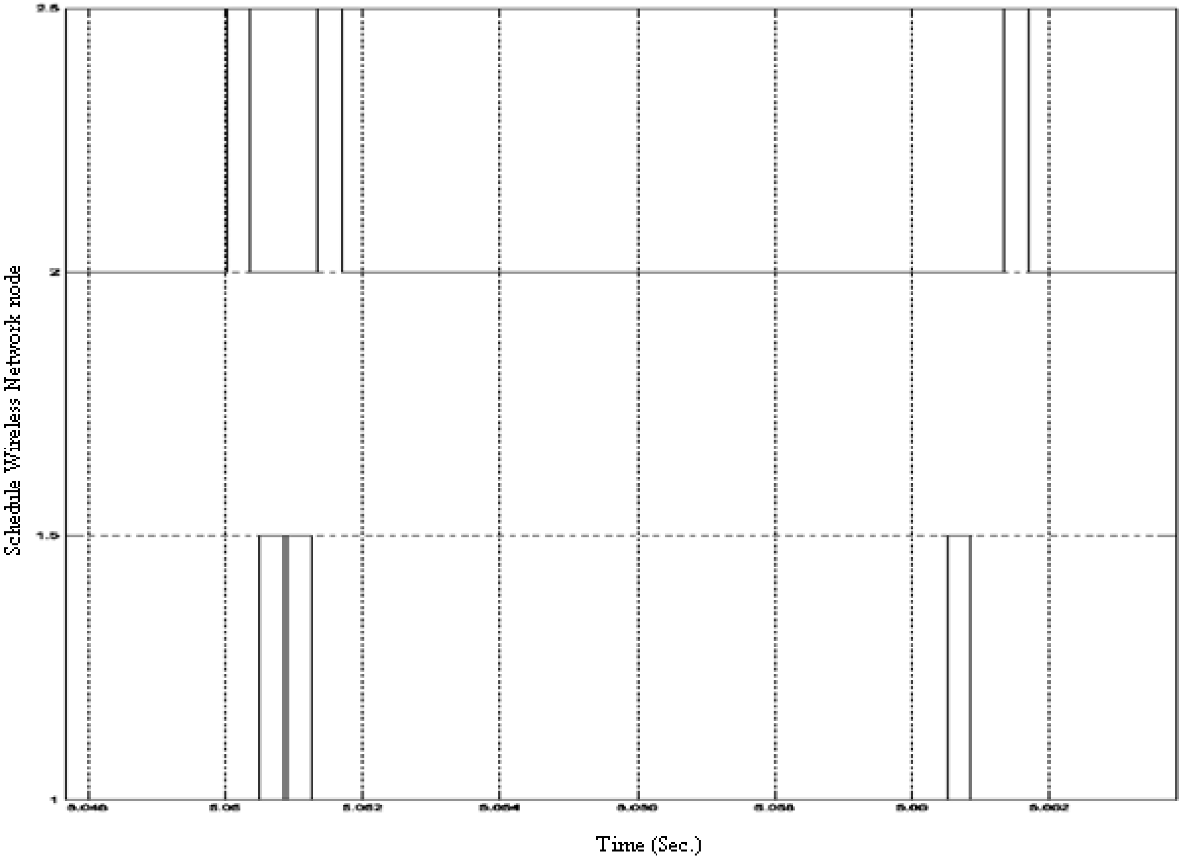

WiMAX Wireless Network

Fig.7.16. Schedule at Wireless Network Node

7.5 CHAPTER SUMMARY

In this chapter, the modelling schemes for SWNCSs have been analysed, and a new modelling method stimulated from the theory of variable sampling time has been introduced. In this method, the wireless network time delay was taken as the variable sampling time. The variable sampling time model was specified, where the wireless network time delay and packet dropout occurred in the system parameters. To avoid the effect of stochastic time delay existing in SWNCS, a methodology that employs NNPC to remove or reduce the effect of time delay in SWNCS and to employ the value modified by BPNN error predictive model to manage the SWNCS time delays has been presented.

The NNPC model is used to recursively calculate the output predictions and control signal predictions. To analyse the performance of the proposed scheme, a numerical simulation has been carried out. Due to the acceptable performance parameters that obtained in table 7.2, the simulation results have successfully illustrated the effectiveness of the proposed approach. NNPC simulations indicated that this new approach alleviated the effect of the wireless network time delay and packet dropout to the maximum extent and enhanced the performance of the control system. The performance parameters of the proposed method are acceptable when wireless network delay varies from the simulation. The method is also rapid and adaptable.

CHAPTER 8 ..

DISCUSSION AND REVIEW OF THE RESULTS

8.1 DISCUSSION

The work carried out in this thesis to investigate the RMPC design for SWNCS in order to control, manage and monitor. Recently, this type of system has been shown to be very effective in many application fields such as, broadband service, security and surveillance as well as street lighting and wireless sensor for measuring the weather; all powered by solar energy. In the following sections, work achieved for a SWNCS model, RMPC design, and robust stability of SWNCS and NNPC design are discussed.

8.1.1 SWNCS Model

One of the purposes of the SWNCS is to increase the ease of use of internet services to the centre of population and optimise the use of the street lighting control system. This SWNCS proposal requires financial support for the establishment of a solar-power system. The solar power system will address the following energy needs:

- Administrative centres: cybercafé, cashier, administration, computer rooms and a repair room as well as a high availability backup system for the Network Operation Centre.
- Street lighting: autonomous street lighting pylons.
- Tower: solar-powered wireless communication tower.
- Wireless Backbone: solar-powered radio repeaters to expand the wireless network backbone.

A SWNCS that offers wireless controller lighting, wireless communication over Wi-Fi and WiMAX networks, CCTV surveillance, and wireless sensor for measurement of the weather all controlled by RMPC and powered by solar energy is presented in this thesis. It offers the following outcomes:

- Enhances community safety (crime decrease) as it comprises observation.
- Introduces telephony, and internet admission for community instruction powered by solar energy.

- Street lighting leads to enhanced security and improved community and financial activity. Furthermore, it decreases accidents during night periods.

8.1.2 Design of RMPC

The SWNCS framework is employed in Chapter 4 to investigate the robustness of discrete-time state space systems in closed-loop with MPC. A strong warning is revealed by way of an example that RMPC can generate discrete-time MPC values that are not input-to-state Lyapunov functions. Therefore, one should be careful in drawing conclusions on robustness based on sets of LMIs solutions. The RMPC controller considers the effect of constraints (wireless network time delays and packet dropouts), although the disturbance disappears in reality. However, clear bounds on the evolution of the RMPC closed-loop system state are derived and full unbounded uncertainties are demonstrated for the closed-loop system. This method for calculating a terminal cost and full state-feedback controller such that the modified robust stabilisation conditions for RMPC are satisfied is presented in Chapter 6. These techniques use linear matrix Lyapunov cost inequality functions and norm inequalities for RMPC cost based LMIs. The RMPC design presents the following expected outcomes:

- This work has shown that by employing suitable model predictive approaches, the model predictive controller can be designed to be robust against challenges facing SWNCS, for example stochastic network time delays, time and packet dropouts. The associated robustness norms can be focused according to the action desires, such as, using RMPC for a definite jitter margin and the outcomes propose that enhancements are executable.
- The achieved RMPC system guarantees stochastic (robust) stability of the feedback control system and guaranteed performance index under contribution constraints in the total uncertainty field. At every sample period, the computation of the proposed RMPC system decreases to a result of an elementary mathematical statement.
- Because RMPC manages hard constraints in SWNCS such as, stochastic network time delays and packet dropout, it is industrially attractive and frequently applied.

8.1.3 Robust stability

Robust stability based on $H_\infty\ and\ H_2$ norms can be recognized for SWNCS via the new results derived in this thesis. General theorems on robust stability of RMPC are presented in Chapter 6. This theorem clearly allows for discrete-time system dynamics and MPC value functions and thus, can be directly applied to establish robust stability for MPC of SWNCSs. In chapter 6, new methods for computing a terminal cost that satisfies the developed stabilisation conditions are presented for the class of piecewise affine systems and MPC costs based on both $H_\infty\ and\ H_2$ norms. These methods also contribute to the field of LMIs in control, as for RMPC methods; the stabilisation conditions are expressed as an LMI. This approach can be employed for RMPC computation in stabilising MPC. The existing LMI methods for computing piecewise quadratic Lyapunov functions for SWNCSs cannot offer a solution to the RMPC stabilisation problem. Robust stability of SWNCS is obtained after calculation of RMPC, the conventional definition for H_2 norm has the following characteristic analysis:

- The l_2 norm of the output is equivalent to the H_2 norm of the system if the input is the unit impulse.
- The general definitions of H_2 norm for the closed-loop control system (5-8a and 8b) under the consideration in special MJLSs can be derived as shown in chapter 6.

8.1.4 Design of NNPC

Chapter 7 aims to address stochastic network time delay and packet dropouts in the SWNCS. A new approach is proposed which uses NNPC for the SWNCS. This approach can identify the controlled plant and adaptively adjusts weights of the controller. An output error prediction model is built using BPNN to handle the stochastic network time delay and packet dropout. The principle of this model is to revise the predictive output of NNPC model using predictive error signal. If the value of network time delay exceeds the upper limit, NNPC will immediately produce the control signals adopting the revised predictive output, and thus reducing the effect of network time delay and packet dropout on SWNCS performance. Simulation experiments have been conducted over Wi-Fi & WiMAX wireless networks which include both network time delay and packet dropout.

In chapter 7 a NNPC technique for a SWNCS is presented. A SWNCS model is created by using BPNN and a learning algorithm adopting an adaptive learning rate approach is used to identify the stochastic time delays in BPNN. The performance of the NNPC controller is based on minimisation of the MSE. It is shown that the NNPC technique results in good control performance in reducing and removing the effect of network time delay and packet dropout that occur in SWNCS. Then, the results are compared with the RMPC technique for SWNCS obtained previously as shown in Table 8.1.

Table 8.1. Performance Parameters for SWNCS when RMPC and NNPC Techniques are Used

Performance Parameters	RMPC		NNPC	
	Wi-Fi	WiMAX	Wi-Fi	WiMAX
Maximum Overshoot	0.32	0.45	0.68	0.75
Settling Time(sec.)	0.24	0.33	0.37	0.41
Steady State error	6x10-5	7.4x10-4	4x10-5	6x10-4

From the above table and according to performance parameters for SWNCS, we notice that the RMPC technique is better than the NNPC technique as follows:

Table 8.2. Performance Parameters Qualification for SWNCS

Performance Parameters	Wi-Fi	WiMAX
Maximum Over Shoot	30%	30%
Settling Time (Sec.)	13%	4%
Steady state Error	0.02%	0.14%

This thesis has presented a control problem that occurs when control loops are closed over a wireless communication network. The wireless communication network introduces wireless network time delays and packet dropouts in the control loop. The wireless network time delays and packet dropouts can have an influence on SWNCS stability and performance.

Stochastic wireless network time delays with probability distribution functions are controlled by a fundamental Markov chain. The model includes two homogenous Markov chains and has the attractive property of obtaining modelling of trends in the wireless network time delays and packet dropouts. The wireless network time delay and packet dropout models were verified by delay measurement experiments on two commercially used wireless networks; Wi-Fi and WiMAX. The simulations demonstrate that wireless network time delays are changing if the wireless network is loaded. The simulation results demonstrate that the model can be useful in modelling of wireless network time delays and packet dropouts.

To show the behaviour of the RMPC and NNPC techniques described in chapter 5 and chapter 7, the SWNCS is simulated with the resulting behaviour as in Figure 5-6, Figure 5-7, and Figure 5-8 based on RMPC technique. Control signals and output response for both Wi-Fi & WiMAX wireless networks are as shown in Figure 5-6. One can see that the system reaches the position set points (steady state) fast with high levels of accuracy i.e. low steady-state error. The tracking of the positive reference slope is quite good with very small overshoot. On the negative slope, however, the tracking is very bad. This phenomenon is due to the fact that the SWNCS can increase wireless network time delays. The SWNCS is simulated with the resulting behaviour as shown in Figure 7.13, Figure 7.14, Figure 7.15 and Figure 7.16 based on the NNPC technique. Output response for both Wi-Fi & WiMAX wireless networks are as in Figure 7.13 and Figure 7.14 respectively. In Figure 7.13 it can be seen that the SWNCS reaches the position set points fast and with high accuracy. The tracking of the positive reference slope is acceptable with small overshoot. On the negative slope however, the tracking is very bad. This phenomenon is due to the fact that the SWNCS can increase wireless network time delays. In contrast, it can be seen in Figure 7.14 that SWNCS reaches the position set points fast and with high accuracy. The tracking of the positive reference slope is quite good. However, the overshoot is more than that obtained in Figure 7.13. On the negative slope however, the tracking is very bad. This phenomenon is due to the fact that the SWNCS can increase wireless network time delays.

Robust stability of SWNCSs with uncertain parameters (stochastic wireless network time delays and packet dropouts) has been explicitly analysed in chapter 6. We analysed their robust stability based on $H_\infty \, and \, H_2$ norm techniques. The frequency responses for the nominal SWNCS with 5 samples of uncertain parameters based on H_∞ norm is plotted in Figure 6.1 and the robustness of the controller in closed-loop response of the nominal SWNCS and 5 perturbed based on H_∞ norms are shown in Figure 6.3. The frequency responses for the nominal SWNCS with 5 samples of uncertain parameters based on

H_2 norm are plotted in Figure 6.4 and the robustness of the controller in closed-loop response of the nominal SWNCS and 5 perturbed based on H_2 norms are shown in Figure 6.5. The SWNCS response based on H_∞ and H_2 norm are plotted in Figure 6.7 and Figure 6.8 which show the robust stability analysis for the SWNCS in terms of H_∞ and H_2 norms. In H_∞ norm analysis, uncertain SWNCS is not robustly stable to modelled uncertainty. It can tolerate up to 34% of the modelled uncertainty. A destabilising combination of 34% of the modelled uncertainty exists causing instability at 1.31 rad/sec. While in H_2 norm analysis, uncertain SWNCS is not robustly stable to modelled uncertainty. It can tolerate up to 104% of the modelled uncertainty. A destabilising combination of 104% of the modelled uncertainty exists causing instability at 1.03 rad/sec.

CHAPTER 9 ..

CONCLUSIONS AND FUTURE WORK

9.1 CONCULSIONS

This thesis proposes novel methodologies for stochastic wireless network time delays and packets dropout avoidance in SWNCS. Stability analysis, and fault estimation for a SWNCSs with stochastic wireless network time delays and packet dropouts in both sensor-to-controller and controller-to-actuator channels have been carried out. Models for such wireless network time delays and packet dropout effects are first developed by using Markov processes. Based on the mode-dependent full state feedback controller method for SWNCSs, the purpose of the designed RMPCs is to analyze and manage the SWNCS so that it improves the QoS for the SWNCS by removing the effect of the time delay that occurs in the SWNCS.

The MPC can be modeled using time delay as a Markovian Chain. The design of the MPC is based on a full state feedback controller. The RMPC is obtained by assuming regular form LMIs with unbounded limitations, and fault estimators are given in terms of the solvability of LMIs. The effectiveness and advantages of the proposed design methodologies are verified by numerical examples in each chapter. The simulation results show that the proposed design methodologies can achieve the prescribed performance requirement.

To clarify this approach, chapter 3 provides detail of the modeling procedure of SWNCSs used in this thesis. Chapter 4 demonstrates the mathematical model for each element in SWNC. Further the SWNCS simulation techniques based on TrueTime tools is carried out to validate the proposed control algorithm.

Chapter 5 presents the synthesis design procedure of a RMPC. In this chapter a RMPC is investigated to enhance the QoS of the SWNCS by removing the effect of the stochastic wireless network time delay and packet dropouts occurring in the SWNCS. The time delays of the SWNCS are considered as stochastic variables controlled by a Markov chain. A discrete-time Markovian jump system with norm unbounded time delay is presented to model the SWNCSs. Based on the SWNCS model, the RMPC based on full state feedback controller can be solved under the framework of LMIs. A SWNCS with specific communications and control parameters using TrueTime simulator tools has been implemented. A SWNCS is constructed with TrueTime simulation tools to illustrate the efficiency of the proposed techniques. The numerical example and simulation results have adjusted the robust controller gain according to the wireless network performance QoS. Validating the results has been carried out by a numerical model and simulation studies.

Chapter 6 presents the synthesis design procedure of a robust delay-dependent controller that guarantees robust stability based $H_\infty \: and \: H_2$ norms and a prescribed disturbance attenuation performance for the SWNCS. In This chapter an efficient robust model for SWNCS through the stochastic time delay and packet dropout system approach has been proposed. The network stochastic time delays were modeled as two Markovian chains in the closed-loop system. A discrete-time MJLS with norm bounded time delay has been presented to model the SWNCSs. Based on the SWNCS model, the RMPC (a full state feedback controller) can be constructed by using the Lyapunov functional method. The robust stability of the system is confirmed using an approach based on H_∞ and H_2 norms criteria. To check this, sufficient conditions for stochastic stability based on $H_\infty$and H_2 norms and stabilization of the fundamental systems are derived via LMIs formulation. LMIs technique and utilizing the data relating to the lower bound of variation of the SWNCS time delay have been shown by a numerical example to be effective.

Finally, in chapter 7, novel techniques have been proposed based on NNPC for reducing the effect of stochastic wireless network time delays and packet dropouts that occur in SWNCS. Prescribed disturbance attenuation performance for the SWNCSs is achieved. In this chapter a methodology that employs NNPC to remove or reduce the effect of time delay in SWNCS and to employ the value modified by BPNN error predictive model to manage the SWNCS time delays has been presented. The NNPC model is used to recursively calculate the output predictions and control signal predictions. To analyze the performance of the proposed scheme, a numerical simulation has been carried out. The simulation results have successfully illustrated the effectiveness of the proposed approach.

Consequently, this thesis provides an integrated approach for the design of SWNCSs and represents a valuable and significant contribution to the development of robust control theory and neural predictor controller techniques based SWNCSs.

The contributions of the thesis are summarized in Section 1.7. The main contributions are:

- Stochastic wireless network time delays and data packet dropouts in both the sensor-controller and controller-actuator channels are taken into account. Therefore, a mode-dependent full state feedback mode dependent controller has been designed and developed. Mutually, the control structure problems and stabilization are measured.
- Markovian processes are employed to model the stochastic wireless network time delays and data packet dropouts.
- A discrete-time MJLS with norm unbounded time delay is presented to model the SWNCSs. Sufficient conditions for stochastic stability based on $H_\infty \; and \; H_2$ norms and stabilization of the fundamental systems are derived via LMIs formulation.
- A SWNCS is constructed in a neural network based on NNPC.

9.2 FUTURE WORK

Generally, SWNCSs still remain an open field that requires extensive research. In this section, we discuss possible issues for future research which we consider would be valuable.

1. Measurement sampling and quantization affects is one of the necessary topics in the implementation of SWNCSs. In order to transmit a continuous-time signal via wireless network, the signal must be sampled, encoded to a digital format, transmitted via wireless network and the data must be decoded at the actuator node. In this method, the sampling and quantization are concerned. As the length of each packet is finite, there must be errors between the actual and quantization values. This sampling and quantization effect generates an additional layer of difficulty to the SWNCSs problems and needs further research attention.
2. Measurement bandwidth limitation affects is another essential issue in SWNCSs. The useful bandwidth of a SWNCS will depend on the physical bandwidth, efficiency of encoding the data into packets, and whether network time is wasted due to message collisions.
3. A new interesting consideration for future research work is relating to design of a Robust Model Reference Controller (RMRC) that can improve the

performance for SWNCS and guarantees stability against stochastic wireless time delays and packet dropouts.

4. Another technique to take into account for future work is to implement a mixed H_∞/H_2 controller to enhance performance for SWNCS and guarantee stability against stochastic wireless time delays and packet dropouts. This technique presents robustness and multi-objective problems. Mixed H_∞/H_2 techniques are an important example of a multi-objective design problem, where the feedback controller has to respond positively to several terms. It is worth noting that in H_∞/H_2 synthesis, the H_∞ controller channel is employed to improve the robustness of the design, while the H_2 controller channel guarantees high-quality performance of the system.
5. Other categories of uncertainties; for example temperature in the solar cell may be measured to cover more general systems.

References

[1] H. Chan and U. Äuner, "**Closed-loop control of systems over a communication network with queues,"** *International Journal of Control*, vol. 62, pp. 493-510, 1995.

[2] B. Etkin and L. D. Reid, "***Dynamics of Flight: Stability and Control"***. New York: Wiley, 1996.

[3] U. Äuner, G. Äoktas, H. Chan, J. Winkelman, M. Liubakka, and R. Krotolica, **"Automotive suspension control through a computer communication network"**, in *Proceedings of IEEE Conference on Control Applications*, pp. 895-900, 1992.

[4] K. Lee and R. Schneeman, **"Internet-based distributed measurement and control applications,"** *IEEE Instrumentation & Measurement Magazine*, vol. 2, pp. 23-27, 1999.

[5] J. Baruch and M. Cox, **"Remote control and robots: an Internet solution"**, *Computing & Control Engineering Journal*, vol. 7, pp. 39-45, 1996.

[6] A. Ray, **"Distributed data communication networks for real-time process control",** *Chem. Eng. Commun.*, vol. 65, pp 139-154, Mar. 1988.

[7] G. Kondraske, R. Volz, D. Johnson, D. Tesar, J. Trinkle, and C. Price, **"Network-based infrastructure for distributed remote operations and robotics research"**, *IEEE Transactions on Robotics and Automation*, vol. 9, pp. 702-704, 1993.

[8] M. Chow and T. Tipsuwan, **"Network-based control systems: A tutorial"**, in *Proceedings of 27th IEEE Annual Conference of the IEEE Industrial Electronics Society*, pp. 1593-1602, 2001.

[9] W. Zhang, M. Branicky, and S. Phillips, **"Stability of networked control systems,"** *IEEE Control System Magzine*, vol. 21, pp. 84-99, Feb. 2001.

[10] D. Hristu-Varsakelis and W. Levine (Editors), "***Handbook of Networked and Embedded Control Systems",*** *Springer*, *BirkhaÄuser Boston*, 2005.

[11] Y. Halevi and A. Ray, **"Integrated communication and control systems: Part I - Analysis,"** *Journal of Dynamic Systems, Measurement and Control*, vol. 110, pp. 367-373, 1988.

[12] G. Walsh, H. Ye, and L. Bushnell, **"Stability analysis of networked control systems"**, *IEEE Transactions on Control Systems Technology*, vol. 10, pp.438-446, 2002.

[13] I. Akyildiz, I. Kasimoglu, "**Wireless sensor and actor networks: research challenges*",*** *Ad Hoc Networks*, Vol. 2, pp. 351-367, 2004.

[14] J. Evans and C. Filsfils, ***Deploying IP and MPLS QoS for Multiservice Networks: Theory and Practice***. San Francisco, Calif.: Morgan Kaufmann, 2007.

[15] H. Lin; Y. Lin; W. Chang; R. Cheng; "**An Integrated WiMAX/WiFi Architecture with QoS Consistency over Broadband Wireless Networks**", *Consumer Communications and Networking Conference, 2009. CCNC 2009. 6th IEEE* , vol., no., pp.1-7, 10-13 Jan. 2009

[16] IEEE Std 802.16-2004, **"IEEE Standard for Local and Metropolitan Area Networks – Part 16: Air Interface for Fixed Broadband Wireless Access Systems"**, Oct. 2004.

[17] Wireless LAN Networking white paper, US Robotics, http://www.usr.com/download/whitepapers/wireless-wp.pdf.

[18] S. Dhawan. "**Analogy of Promising Wireless Technologies on Different Frequencies: Bluetooth, Wi-Fi, and WiMAX,"** Proc. *Wireless Broadband and Ultra Wideband Communications,* 2007.

[19] S. Jindal, A. Jindal, N. Gupta. **"Grouping WI-MAX, 3G and WI-FI for wireless broadband,"** en Proc, *First IEEE and IFIP International Conference in Central Asia,* 2005.

[20] A. Ian, W. Xudong, W. Weilin. **"Wireless Mesh Networks: A Survey",** *Computer Networks, Volume 47, Issue4*, pp. *445-487*, 15 March 2005.

[21] Y. Chen. **"Achieve User Authentication and Seamless Connectivity on Wi-Fi and WiMAX Interworked Wireless City,"** Proc. *Wireless and Optical Communication Networks*, pp. 1-5, 2007.

[22] F. Lin, "**Robust Control Design an Optimal Control Approach**", John Wiely & Sons, Ltd, Wayne State University, USA, 2007.

[23] W. Gu; P. Petkov; M. Konstawtinoo,"**Robust Control Design with MATLAB**", Springer-Varlage London Limited, 2005.

[24] Technology Report, "**Robust Control",** July 17, 2002, Measurement and Control Group, Eindhoven University of Technology: Eindhoven.

[25] M. Limebeer, "**LINEAR ROBUST CONTROL",** Pearson Education, Inc, 2004.

[26] A.Belton, "**Functional Analysis"**. Lectural Note, 2006.

[27] J. Doyle, B.Francic, "**Feedback Control System"**. 1990: Mac-Millan publishing Co.

[28] D. Ji, J. Park, W. Yoo and S. Won, “***Robust memory state feedback model predictive control for discrete-time uncertain state delayed systems”***. *Applied Mathematics and Computation*, 2009. 215: p. 2035-2044.

[29] V. Veselý, D. Rosinov’a and M. Foltin., “***Robust model predictive control design with input constraints”***. *The International Society of Automation. Published by Elsevier Ltd* ISA, 2010. 49: p. 114-120.

[30] A. Richards, J. How, “***Robust Model Predictive Control with Imperfect - Information”***. *Proceedings of the American Control Conference,* Portland, USA, June 8-10, 2005.

[31] F. Wang and L. Li,” **Control and Communication Synthesis in Networked Control Systems”,** *International Journal of Intelligent Control and Systems,* VOL. 13, NO. 2, June 2008, 81-88.

[32] Y. Tipsuwan and Y. Chow,” **Control Methodologies in Networked Control Systems”**, *Control Engineering Practice Vol. 11*, 2003.

[33] S. Mittal and A. S. Siddiqui**,” Networked Control System: Survey and Directions”**, *Journal of Engineering Research and Studies,* Vol.I/ Issue II/Oct.-Dec.,2010/35-50.

[34] S. Yanga and Y. Caob,” **Networked control systems and wireless sensor networks: theories and applications”,** *International Journal of Systems Science,* Vol. 39, No. 11, 14 July 2010, 1041–1044.

[35] Y. Millan, F. Vargas, F. Molano, E. Mojica, "**A Wireless Networked Control Systems review**", *Robotics Symposium, 2011 IEEE IX Latin American and IEEE Colombian Conference on Automatic Control and Industry Applications (LARC)* , vol., no., pp.1-6, 1-4 Oct. 2011.

[36] R. Gupta, C. Mo-Yuen, **"Networked Control System: Overview and Research Trends",** *Industrial Electronics, IEEE Transactions on*, vol.57, no.7, pp.2527-2535, July 2010.

[37] B.Ughanmi, C. Hugo and S. Ye Qiong,” **Case study of Wireless Networked Control System: CONECS and COWNECS platform”**, *2nd Workshop Supervision, Department of Safety and Security Systems - 3SGS'09*. 2009.

[38] Y. Zhao, G. Liu and D. Rees,” **Integrated predictive control and scheduling co-design for networked control systems”**, *IET Control Theory Appl*., 2008, 2, (1), pp. 7–15.

[39] P. Naghshtabrizi, J. Hespanha,” **Implementation Considerations For Wireless Networked Control Systems**”, *Wireless Network Based Control*, 2010.

[40] M. Kumar, A. Verma, and A. Srividya, “**Probabilistic modeling of network-induced delays in networked control systems”**. *International Journal of Applied Mathematics and Computer Science*, 5, 2009 43 – 54.

[41] F. Liu; Y. Yao, **"Modeling and analysis of networked control systems using hidden Markov models",** *Machine Learning and Cybernetics, 2005. Proceedings of 2005 International Conference on* , vol.2, no., pp.928-931 Vol. 2, 18-21 Aug. 2005.

[42] N. Vatanski, J. Georges, C. Aubrun, E. Rondeau and S. Jämsä-Jounela,” **Control Compensation Based on Upper Bound Delay in Networked Control Systems”,** *17th International Symposium on Mathematical Theory of Networks and Systems (MTNS)*, Japan, 2006.

[43] J. Li; X. Yanhong; Yu Haibin; Q. Zhang; , **"Modeling and control of networked control systems with bounded delay and packet disordering",** *Control and Decision Conference (CCDC), 2010 Chinese* , vol., no., pp.3122-3127, 26-28 May 2010.

[44] F. Yang, Z. Wang, Y. Hung, M. Gani ,” **H∞ Control for Networked Systems with Random Communication Delays”**, *IEEE Transactions on Automatic Control, 51(3): 511-518*. 2006.

[45] J. Chen, W. George, M. Adrian, G. William,” A **Model Predictive Approach to Wireless Networked Control”**, *Scanlon Proceedings of the UKACC International Conference on Control 2008, University of Manchester*, Sept. 2-4 2008.

[46] Z. Haitao, Z. Li, ”**Simulation of Networked Control System based on Smith Compensator and Single Neuron Incomplete Differential Forward PID”,** *Journal of Networks*, VOL. 6, NO. 12, Dec. 2011.

[47] T. Skeie, S. Johannessen, O. Holmeide, "**The road to an end-to-end deterministic Ethernet",** *Factory Communication Systems, 2002. 4th IEEE International Workshop on*, vol., no., pp. 3- 9, 2002.

[48] Y. Sun, S. Qin ,” **Stability of networked control systems with packet dropout: an average dwell time approach”**, *IET Control Theory Appl.*, Vol.5, Iss.1, pp.47-53, 2011.

[49] X. Dexiao, H. Xiaodong, H. He, W. Zhiquan, ”**Research on Robust Mean Square Stability of Networked Control Systems with Packet Dropout”**, *Journal of Systems Engineering and Electronics*, Vol. 21, No. 1, February 2010, pp.95–101.

[50] M. Yu; L. Wang; T. Chu; G. Xie, **"Stabilization of networked control systems with data packet dropout and network delays via switching system approach"**, *Decision and Control, 2004. CDC. 43rd IEEE Conference on*, vol.4, no., pp. 3539- 3544 Vol.4, 14-17 Dec. 2004.

[51] Y. Tian; D. Levy,” **Compensation for control packet dropout in networked control systems”**, *Information Sciences 178 (2008) 1263–1278*, 2008.

[52] H. Chang-Chun; Z. Ying; G. Xin-Ping,” **Modelling and Control for Wireless Networked Control System”**, *International Journal of Automation and Computing*, August 2011, 357-363.

[53] P. Seiler, R. Sengupta, "**An H_∞ approach to networked control**," *Automatic Control, IEEE Transactions on*, vol.50, no.3, pp. 356- 364, March 2005.

[54] M. Christopher, M. Iven, N. Mareels,” **Stability results for networked control systems subject to packet dropouts”,** *Proceedings of the 16th International Federation of Automatic Control IFAC World Congress*, 2005.

[55] J. Wu and T. Chen,” **Design of Networked Control Systems with Packet Dropouts”,** *IEEE Transactions on Automatic Control*, Vol. 52, NO. 7, July 2007.

[56] S. Mehrdad, C. Tongwen, L. Sirish,” **Optimal H_∞ Filtering in Networked Control Systems with Multiple Packet Dropouts”**, *Systems & Control Letters 57* (2008), 2008 696–702.

[57] M. Huang and S. Dey,” **Kalman Filtering with Markovian Packet Losses and Stability Criteria”,** *Proceedings of the 45th IEEE Conference on Decision & Control*, Manchester Grand Hyatt Hotel, San Diego, CA, USA, December 13-15, 2006.

[58] G. Vijay, H. Babak, M. Richard,” **Optimal LQG Control across Packet-Dropping Links”**, *Elsevier Science*, 16 November 2006.

[59] S. Van, F. Donkers; W. Heemels; N. van de Wouw,” **On Dropout Modelling for Stability Analysis of Networked Control Systems”**, *2010 American Control Conference Marriott Waterfront, Baltimore, MD, USA*, June 30-July 02, 2010.

[60] W. Yu-Long; Q. Han; X. Yu,” **Packet Dropout Separation-Based Networked Control Systems Quantitative Synthesis”,** *49th IEEE Conference on Decision and Control, Hilton Atlanta Hotel, Atlanta, GA, USA*, December 15-17, 2010.

[61] J. Liabc; Q. Zhangac; M. Cai,” **Modelling and robust stability of networked control systems with packet reordering and long delay”**, *International Journal of Control*, Vol. 82, No. 10, October 2009, 1773–1785.

[62] J. Wang; L. Dong; Y. Bai,” **State Feedback Controller Design for Exponential Stability of Networked Control System”**, *International Journal of Computer and Electrical Engineering*, Vol. 2, No.2, April, 2010 1793-8163.

[63] F. Hao; X. Zhao,” **Linear Matrix Inequality Approach to Static Output-Feedback Stabilisation of Discrete-Time Networked Control Systems”**, *IET Control Theory Appl.*, Vol. 4, Iss. 7, 2010 pp. 1211–1221.

[64] N. Xie; B. Xia;,"**Robust Fault Tolerant Controller Design for Uncertain Networked Control Systems with Fast-Varying Delay and Packet-Dropout",** *Wireless Communications Networking and Mobile Computing (WiCOM), 2010 6th International Conference on* , vol., no., pp.1-4, 23-25 Sept. 2010.

[65] O. Gabel and L. Litz,” **QoS-adaptive Control in NCS with Variable Delays and Packet Losses – A Heuristic Approach”**, *43rd IEEE Conference on Decision and Control Atlantis, Paradise Island, Bahamas,* December 14-17, 2004.

[66] F. Jin; H. Zhang,” ***H*∞ Control for Networked Control Systems under Communication Constraints”,** Third International Conference on Intelligent Networks and Intelligent Systems, 2010.

[67] A. Liu; L. Yu; W. Zhang,” **One-step receding horizon H∞ control for networked control systems with random delay and packet disordering”**, The International Society of Automation ISA Transaction. Published by Elsevier, 50 (2011) 44–52.

[68] D. Bernardini; M. Donkers; A. Bemporad; W. Heemels,” **A Model Predictive Control Approach for Stochastic Networked Control Systems”,** *2nd IFAC Workshop on Distributed, Estimation and Control in Networked Systems, 2010.*

[69] Z. Zhanshan; Z. Qun; Z. Jing, **"Robust Controller for Networked Control Systems Induced Noise and Long Transmission Delay",** *Networking, Sensing and Control, 2008. ICNSC2008. IEEE International Conference on*, vol., no., pp.859-863, 6-8 April 2008.

[70] G. Liu; J. Mux; D. Rees; S. Chai,” **Design and stability analysis of networked control systems with random communication time delay using the modified MPC”**, *International Journal of Control*, Vol. 79, No. 4, April 2006, 288–297.

[71] G. Liu; Y. Xia; J. Chen; D. Rees , **"Networked Predictive Control of Systems With Random Network Delays in Both Forward and Feedback Channels",** *Industrial Electronics, IEEE Transactions on* , vol.54, no.3, pp.1282-1297, June 2007.

[72] M. Kostas and J. Lygeros,” **A Simulation Based MPC Technique for Feedback Linearizable systems with Input Constraints”,** *49th IEEE Conference on Decision and Control,* Hilton Atlanta Hotel, Atlanta, GA, USA, December 15-17, 2010.

[73] X. Gang; Y. Shiming; Y. Li;, "**MPC-based computer network control strategy with stochastic time delay",** *Systems, Man and Cybernetics, 2003. IEEE International Conference on*, vol.4, no., pp. 3864- 3869 vol.4, 5-8 Oct. 2003.

[74] A. Ulusoy, O. Gurbuz, A. Onat, **"Wireless Model-Based Predictive Networked Control System Over Cooperative Wireless Network",** *Industrial Informatics, IEEE Transactions on* , vol.7, no.1, pp.41-51, Feb. 2011.

[75] J. Chen; W.George ; A. McKernan,” **Packet-based robust MPC for Wireless Networked Control using co-design”**, *2010 American Control Conference,* Marriott Waterfront, Baltimore, MD, USA, June 30-July 02, 2010.

[76] L. Xiao-Hua; L. Jian, "**Robust model predictive control for constrained networked control system",** *IT in Medicine & Education, 2009. ITIME '09. IEEE International Symposium on*, vol.1, no., pp.1225-1230, 14-16 Aug. 2009.

[77] D. Wang; S. Wu; S. Okubo,” **Design of The State Predictive Model Following Control System with Time–Delay”,** International Journal of Applied Mathematics and Computing, Vol. 19, No. 2, 2009 247–254.

[78] C. Peng and D. Yue,” **State Feedback Controller Design of Networked Control Systems with Parameter Uncertainty and State-Delay”**, *Asian Journal of Control,* Vol. 8, No. 4, pp. 385-392, December 2006.

[79] P. Varutti; B. Kern; T. Faulwasser; R. Findeisen,” **Event-based Model Predictive Control for Networked Control Systems”,** *Joint 48th IEEE Conference on Decision and Control and 28th Chinese Control Conference,* Shanghai, P.R. China, December 16-18, 2009.

[80] Z. Li; L. Wang; X. Lai; S. Xu,” **Stability of Constrained Model Predictive Control for Networked Control Systems with Data Packet Dropout”**, *Proceedings of the IEEE International Conference on Automation and Logistics,* Jinan, China, August 18 - 21, 2007.

[81] W. Yu-Long; Y. Guang-Hong,”H_∞**Controller Design for Networked Control Systems via Active Varying Sampling Period Method**”, *ACTA AUTOMATICA SINICA, 2007.*

[82] B. Tavassoli and P. Jabehdar Maralani,” **Robust Design of Networked Control Systems with Randomly Varying Delays and Packet Losses”,** *Proceedings of the 44th IEEE Conference on Decision and Control, and the European Control Conference 2005,* Seville, Spain, December 12-15, 2005.

[83] A. NASKALI; A. ONAT,” **Random Network Delay in Model Based Predictive Networked Control Systems”,** *Proceedings of the 6th WSEAS International Conference on Applied Computer Science*, Tenerife, Canary Islands, Spain, December 16-18, 2006.

[84] Z. Du; Q. Zhang; L. Liu,” **New Delay-Dependent Robust Stability of Discrete Singular Systems with Time-Varying Delay”**, *Asian Journal of Control,* Vol. 12, No. 6, pp. 1 12, November 2010.

[85] Y. Long Wang and G. Yang,” **State Feedback Control Synthesis for Networked Control Systems with Packet Dropout”**, *Asian Journal of Control,* Vol. 11, No. 1, pp. 49 58, January 2009.

[86] Y. and G. Yang,” **Network-Based $H\infty$ Control of Systems with Time-Varying Sampling Period”,** *International Journal of Innovative Computing, Information and Control,* Volume 6, Number 4, April 2010.

[87] L. Lu; L. Xie; W. Cai,” **$H2$ Controller Design for Networked Control Systems”**, *Asian Journal of Control,* Vol. 6, No. 1, pp. 88-96, March 2004.

[88] C. Lu; C. Tsai; C. Liu; Y. Charng,” **Neural-Network-Based Predictive Controller Design: an Application to Temperature Control of a Plastic Injection Molding Process”**, *Asian Journal of Control,* Vol. 12, No. 6, pp. 1 12, November 2010.

[89] T. Wang; L. Zhou; P. Han; Q. Zhang**,” Complete Compensation for Time Delay in Networked Control System Based on GPC and BP Neural Network”,** *Proceedings of Sixth International Conference on Machine Learning Cybernetics,* Hong Kong, 19-22 August 2007.

[90] N. Sadeghzadeh, A. Afshar, M. Menhaj, "**An MLP Neural Network for Time Delay Prediction in Networked Control Systems",** *Control and Decision Conference, 2008. CCDC 2008. Chinese,* vol., no., pp.5314-5318, 2-4 July 2008.

[91] J. Yi; Q. Wang; D. Zhao; T. Wen,” **BP Neural Network Prediction-Based Variable-Period Sampling Approach for Networked Control Systems”**, *Applied Mathematics and Computation 185,* (2007) 976–988.

[92] A. Antunes, F. Dias, A. Mota,"**A Neural Network Delay Compensator for Networked Control Systems",** *Emerging Technologies and Factory Automation, 2008. ETFA2008. IEEE International Conference on*, vol., no., pp.1271-1276, 15-18 Sept. 2008.

[93] W. Du; Feng Du, "**New Smith Predictor and Single Neural Adaptive Control for Wireless Networked Control Systems",** *Industrial Electronics and Applications, 2009. ICIEA2009. 4th IEEE Conference on*, vol., no., pp.1699-1703, 25-27 May 2009.

[94] K. Kara, M. Hadjili, K. Hemsas, T. Missoum, "**Predictive Control Using Neural Networks",** *Industrial Electronics, 2009. IECON '09, 35th Annual Conference of IEEE*, vol., no., pp.1702-1705, 3-5 Nov. 2009.

[95] F. Du; W. Du, "**Networked Control Systems with RBF Neural Network Control and New Smith Predictor",** *Industrial Electronics and Applications, 2009. ICIEA2009. 4th IEEE Conference on*, vol., no., pp.2744-2748, 25-27 May 2009.

[96] L. Schnitman and A. de Barros Fontes," **The Basic Ideas of Neural Predictive Control",** *Proceedings of the 7th Mediterranean Conference on Control and Automation (MED99) Haifa, Israel* - June 28-30, 1999.

[97] Z. Pang; G. Liu, "**Model-Based Recursive Networked Predictive Control",** *Systems Man and Cybernetics (SMC), 2010 IEEE International Conference on* , vol., no., pp.1665-1670, 10-13 Oct. 2010.

[98] L. Chao; W. Dongfeng; D. Ze; Han Pu;, "**Controller Design for Networked Control Systems Based on Neural Network Prediction",** *Information Science and Engineering (ICISE), 2010 2nd International Conference on* , vol., no., pp.1930-1933, 4-6 Dec. 2010.

[99] B. Sharmila; N. Devarajan**," Neuro-Fuzzy Controller for Networked DC Motor Control",** *European Journal of Scientific Research, ISSN 1450-216X Vol.56 No.2,* pp.219-228, 2011.

[100] G. Boggia, P. Camarda, L. Grieco, G. Zacheo, "**Toward Wireless Networked Control Systems: An Experimental Study on Real-Time Communications in 802.11 WLANs",** *Factory Communication Systems, 2008. WFCS2008. IEEE International Workshop on*, vol., no., pp.149-155, 21-23 May 2008.

[101] J. Colandairaj, G. Irwin, W. Scanlon, "**Wireless Networked Control Systems with QoS-Based Sampling",** *Control Theory & Applications, IET* , vol.1, no.1, pp.430-438, January 2007.

[102] B. Najet; Ye Qiong Song; E. Rondeau,” **Wireless Networked Control System using IEEE 802.15.4 with GTS”,** *2nd Junior Researcher Workshop on Real-Time Computing JRWRTC*, 2008.

[103] C. Jian; W. George, G. William, "**Experimental Characterisation and Analysis of Wireless Network Control Systems",** *Signals and Systems Conference, 208. (ISSC 2008), IET Irish*, vol., no., pp.238-243, 18-19 June 2008.

[104] C. Rafael; L. G´amez; Pau Mart; V. Manel; M. Josep ,” **Wireless Network Delay Estimation for Time-Sensitive Applications”,** *Research report ESAII-RR-06-12*, July 2006.

[105] T. Refaat, R. Daoud, H. Amer, E. Makled, "**Wi-Fi implementation of Wireless Networked Control Systems"**, *Networked Sensing Systems (INSS), 2010 Seventh International Conference on* , vol., no., pp.145-148, 15-18 June 2010.

[106] A. Ulusoy; A. Onat; O. Gurbuz,”**Wireless Model Based Predictive Networked Control System”**, *IEEE Transactions on Industrial Informatics*, 2010.

[107] C. Cheng; C. Lai; Bor-Chyun Wang; Pau-Lo Hsu; , "**The Time-Delay Effect of Multiple-Network Systems in NCS",** *SICE, 2007 Annual Conference* , vol., no., pp.929-934, 17-20 Sept. 2007.

[108] G. Nikolakopoulos; A. Panousopoulou,” **Experimental Controller Tuning and QoS Optimization of A Wireless Transmission Scheme for Real-Time Remote Control Applications”**, *Control Engineering Practice 16*, (2008) 333–346.

[109] J. Bai; C. Eyisi, Y. Xue; X. Koutsoukos, "**Dynamic Tuning Retransmission Limit of IEEE 802.11 MAC Protocol for Networked Control Systems",** *Green Computing and Communications (GreenCom), 2010 IEEE/ACM Int'l Conference on & Int'l Conference on Cyber, Physical and Social Computing (CPSCom)* , vol., no., pp.666-671, 18-20 Dec. 2010.

[110] A. Onat; T. Naskali; E. Parlakay; O. Mutluer,” **Control Over Imperfect Networks: Model-Based Predictive Networked Control Systems”**, *IEEE TRANSACTIONS ON INDUSTRIAL ELECTRONICS, VOL. 58, NO. 3,* MARCH 2011.

[111] Y. Li; G. Xinping; L. Xiaoyuan; Y. Caihong,” **The High Performance Controller Design for Networked Control Systems with Multi-packet Transmission”,** *Proceedings of the 27th Chinese Control Conference,* Kunming,Yunnan, China, July 16-18, 2008.

[112] H. Lin; Y. Lin; W. Chang; R. Cheng, "**An Integrated WiMAX/WiFi Architecture with QoS Consistency over Broadband Wireless Networks",** *Consumer Communications and Networking Conference, 2009. CCNC2009. 6th IEEE,* vol., no., pp.1-7, 10-13 Jan. 2009.

[113] S. Ibanez, R. Santos, V. Licea, A. Block, M. Ruiz, "**Hybrid Wi-Fi/WiMAX Network Routing Protocol",** *Electronics, Robotics and Automotive Mechanics Conference, 2008. CERMA '08,* vol., no., pp.87-92, Sept. 30 2008-Oct. 3 2008.

[114] S. Jindal, A. Jindal, N. Gupta, "**Grouping WI-MAX, 3G and WI-FI for Wireless Broadband",** *Internet, 2005.The First IEEE and IFIP International Conference in Central Asia on* , vol., no., pp. 5 pp., 26-29 Sept. 2005.

[115] C. Lai and P. Hsu," **Design of the Multiple-Rate Robust Controller for Wireless Networked Control Systems",** *International Conference on Control, Automation and Systems,* COEX, Seoul, Korea, Oct. 14-17, 2008.

[116] F. Zheng; J. Nelson, "**An $H\infty$ Approach to Congestion Controller Design for Wireless Access Networks",** *Wireless Communications and Networking Conference, 2006. WCNC2006. IEEE,* vol.1, no., pp.86-91, 3-6 April 2006.

[117] E. Witrant, P. Johansson, C. Fischione, K. Johansson, **"Predictive Control Over Wireless Multi-hop Networks",** *Control Applications, 2007. CCA2007. IEEE International Conference on,* vol., no., pp.1037-1042, 1-3 Oct. 2007.

[118] G. Pin and T. Parisini," **Networked Predictive Control of Uncertain Constrained Nonlinear Systems: Recursive Feasibility and Input-to-State Stability Analysis",** *IEEE TRANSACTIONS ON AUTOMATIC CONTROL,* VOL. 56, NO. 1, JANUARY 2011.

[119] S. Vardhan and R. Kumar,"**Simulations for Time Delay Compensation in Networked Control Systems"**, Multidisciplinary *Journals in Science and Technology, Journal of Selected Areas in Telecommunications (JSAT),* June Edition, 2011.

[120] G. Yafeng and L. Shaoyuan," **H∞ Control for Discrete-Time Systems with Limited Communication Channel",** *Proceedings of the 27th Chinese Control Conference,* Kunming, Yunnan, China, July 16–18, 2008.

[121] R. Fontaine and P. Laurencot," **Mathematical Model of the Maximum Throughput in Infrastructure Based Wireless Network",** *4th International Conference: Sciences of Electronic, Technologies of **I**nformation and **T**elecommunications,* TUNISIA, March 25-29, 2007.

[122] L. Wu; J. Lam; X. Yao; J. Xiong,” **Robust Guaranteed Cost Control of Discrete-Time Networked Control Systems”,** OPTIMAL CONTROL APPLICATIONS AND METHODS *Optim. Control Appl. Meth.* 2011; 32:95–112.

[123] D. Xie; D. Zhang; Z. Wang,” **Robust H∞ Fault-Tolerant Control for Uncertain Networked Control System with Two Additive Random Delays”,** *International Journal of Innovative Computing, Information and Control,* Volume 7, Number 1, January 2011.

[124] L. Figueredo, P. Santana, E. Alves, J. Ishihara, G. Borges, A. Bauchspiess, "**Robust Stability of Networked Control Systems",** *Control and Automation, 2009. ICCA2009. IEEE International Conference on*, vol., no., pp.1535-1540, 9-11 Dec. 2009.

[125] L. Zhang; Y. Shi; T. Chen; B. Huang,” **A New Method for Stabilization of Networked Control Systems with Random Delays [4]”**, *American Control Conference*, Portland, OR, USA, June 8-10, 2005.

[126] S. Ye-Guo and Q. Shi-Yin,” **Stability and Stabilization of Networked Control Systems with Bounded Packet Dropout”**, *ACTA AUTOMATICA SINICA,* Vol. 37, No. 1, January, 2011.

[127] X. Ge; X. Jiang; X. Zhang, "**A New Stability Criterion of Networked Control Systems,"** *Computer Technology and Development, 2009. ICCTD'09, International Conference on*, vol.2, no., pp.15-19, 13-15 Nov. 2009.

[128] X. Ge; X. Jiang, "**A new robust stability criterion of networked control systems",** *Intelligent Control and Automation (WCICA), 2010 8th World Congress on* , vol., no., pp.2855-2860, 7-9 July 2010.

[129] J. Li; S. Han; M. Zheng; H. Yu; Q. Zhang,” **State Feedback Control of Network-Based Systems with Packet Disordering”**, *Journal of Systems Engineering and Electronics,* Vol. 22, No. 2, April 2011, pp.306–313.

[130] A. Seuret, "**Stability analysis of networked control systems with asynchronous sampling and input delay"**, *American Control Conference (ACC), 2011* , vol., no., pp.533-538, June 29 2011-July 1 2011.

[131] L. Xie and L. Xie,” **Stability Analysis of Networked Sampled-Data Linear Systems with Markovian Packet Losses”,** *IEEE Transactions on Automatic Control,* VOL. 54, NO. 6, JUNE 2009.

[132] J. Ko; W. Lee; P. Park,” **Delayed System Approach to the Stability of Networked Control Systems”,** Proceedings of the International Multiconference of Engineers and Computer Sciences IMECS2011, Vol. II, Hong Kong, March16-18, 2011.

[133] M. Teddy CHENG,” **Robust Output Feedback Stabilization of Non-Linear Networked Systems via a Finite Data-Rate Communication Channel”,** *Journal of System Sciences Complex JSSC2011,* 24: 1–13, 2011.

[134] B. Azimi-Sadjadi, "**Stability of Networked Control Systems in the Presence of Packet Losses",** *Decision and Control, 2003. Proceeding 42nd IEEE Conference on*, vol.1, no., pp. 676- 681 Vol.1, 9-12 Dec. 2003.

[135] L. Dianting; L. Mingtao;, "**Delay-independence Stability Analysis of MIMO Networked Control Systems with State Feedback",** *Measuring Technology and Mechatronics Automation (ICMTMA), 2011 Third International Conference on*, vol.1, no., pp.846-848, 6-7 Jan. 2011.

[136] C. Peng; Y. Tian; D. Yue, "**Output Feedback Control of Discrete-Time Systems in Networked Environments"**, *Systems, Man and Cybernetics, Part A: Systems and Humans, IEEE Transactions on* , vol.41, no.1, pp.185-190, Jan. 2011.

[137] X. Jiang; Q. Han; S. Liu; A. Xue,” **A New $H\infty$ Stabilization Criterion for Networked Control Systems”,** *IEEE Transactions on Automatic Control*, VOL. 53, NO. 4, MAY 2008.

[138] Z. Wang; F. Yang; W. Daniel; X. Liu,” **Robust $H\infty$ Control for Networked Systems With Random Packet Losses”**, *IEEE Transactions on Systems, MAN, AND CYBERNETICS—PART B: CYBERNETICS,* VOL. 37, NO. 4, AUGUST 2007.

[139] T. Jia; Y. Niu; X. Wang,” **$H\infty$ Control for Networked Systems with Data Packet Dropout”**, *International Journal of Control, Automation, and Systems (2010) 8(2):198-203,* KIEE and Springer 2010.

[140] R. Wang; B. Wang; G. Liu; W. Wang; D. Rees,” **$H\infty$ Controller Design for Networked Predictive Control Systems Based on the Average Dwell-Time Approach”**, *IEEE Transactions on Circuits and Systems—II: EXPRESS BRIEFS,* VOL. 57, NO. 4, APRIL 2010.

[141] Y. Xia; G. Liu; D. Rees,**”H2 Control for Networked Control Systems in Presence of Random Networked Delay and Data Dropout”,** *proceedings of International Control Conference (ICC2006),* Glasgow, Scotland, United Kingdom, 30th August to 1st September 2006.

[142] W. Wang and F. Cai and F. Yang," **An *H*2 Approach for Networked Control Systems with Multiple Packet Dropouts",** *Proceedings of the 8th World Congress on Intelligent Control and Automation*, Jinan, China, July 6-9 2010.

[143] Green Power for Mobile: Charging Choices,"**Off-grid charging solution for mobile phones",** http://www.gsmworld.com/documents/charging_choices.pdf.2009.

[144] The Solar-Power Alternative in Broadband Wireless Networks**, " A Primer on the Uses of and Benefits of Solar Power in Outdoor Broadband Wireless Networks",** White paper**, www.proxim.com, 2007.**

[145] S.Ganapati and C. F. Schoepp, **"The Wireless City"**, IGI Global, 2009.

[146] City Council Study Session, Report Item 071706–2–Wireless Pilot Update (http://www.stlouispark.org/pdf/ July_17_2006.pdf).

[147] G.A. Torshizi, M. Niknam, "**Solar Energy in Telecommunications"**, *Bechtel Telecommunications Technical Journal*, pp 65 – 74, 2007.

[148] Outdoor LED Lighting - High Power LED Streetlights - LED Wall Washer Lights, **"LED Street Lights Model Lights SP90",** http://www.dmxledlights.com/OutdoorLighting/.

[149] E. Claudio, G. Pau, M. Roccetti, S. Ferretti, M. Gerla, "**Wireless Home Entertainment Centre: Reducing Last Hop Delays for Real-time Applications"**, *ACM International Conference Proceeding Series*, vol. 266, article no. 67, 2006.

[150] S. Xu, T. Saadawi, "Does **the IEEE 802.11 MAC protocol work well in multi-hop wireless ad-hoc networks"**, *IEEE Communications Magazine*, Pages 130-137, June 2001.

[151] T. Janevski and I. Petrov," **Cross-layer Analysis of Transport Control Protocols over IEEE 802.11 Wireless Networks",** *International Journal of Advanced Science and Technology,* Vol. 26, January 2011.

[152] P. Nikitin, O. Celebioglu, and V. Kukrer, "**TCP performance in mobile wireless environment: channel modelling and network simulation"**, *6th World Multiconference on Systemics, Cybernetics and Informatics*, Orlando, FL, July 2002.

[153] **"WiMAX and WiFi Wireless Mesh -- Friends or Foes",** *Mesh dynamics,* http://www.meshdynamics.com/documents/MDWImaxFriendOrFoe.pdf, March-13-2007.

[154] M. Portmann, A. Pirzada, "**Wireless Mesh Networks for Public Safety and Crisis Management Applications",** *Internet Computing, IEEE* , vol.12, no.1, pp.18-25, Jan.-Feb. 2008.

[155] M.Ohlin,”**Feedback Linux Scheduling and Simulation Tool for Wireless Control**”, Licentiate thesis, Departement of Automatic Control, Lund University, Sweden, 2006.

[156] Javvin, **http://www.javvin.com/wireless/BLER.html**, 2009.

[157] A.Cervin; D.H.a.M.O.,“**TRUETIME 2.0—Reference Manual**”, *Department of Automatic Control/Lund University*. February 2009.

[158] R. Flickenger,”**Building Wireless Community Network**”, *O’reilly Media, 0-596-00502-4, pages 182*, 2003.

[159] A. Roca, “**Implementation of a WiMAX Simulator in Simulink**”, *diploma thesis, Vienna*, February 2007.

[160] C. Anton; M. Ohlin; D. Henriksson, “**Simulation of Networked Control Systems Using TrueTime**”, *3rd International Workshop on Networked Control Systems: Tolerant to Faults*, Nancy, France, 2007.

[161] N. Song*,” **Wireless Networked Control System Using ZigBee/IEEE 802.15.4”,** 13th IFAC Symposium on Information Control Problems in Manufacturing*, Moscow: Russian Federation, 2009.

[162] W. Al-Azzawi, M. Al-Akaidi,” **Modeling and Simulation of Solar Wireless Network Control System Based on Robust Model Predictive Controller”,** *Proceeding 10th MESM Conference*, Al-Exandria, Egypt, 1-3 December, 2010.

[163] Masters; M. Gilbert, “**Renewable and Efficient Electric Power Systems**”, *John Wiley & Sons Ltd*, 2004.

[164] A. Keyhani; M. Marwali; Min Dai, "**Integration of Green and Renewable Energy in Electric Power Systems",** *John Wiley & Sons Ltd*, January 2010.

[165] M. Chen; A. Gabriel; Rincon-Mora, ”**Accurate Electrical Battery Model Capable of Predicting Runtime and I-V Performance**”, *IEEE transaction, Energy Convers*, Vol.21, No.2, 2006.

[166] M. Becherif; M. Y.Ayad; A. Aboubou, ”**Hybridization of Solar Panel and Batteries for Street Lighting by Passivity Based Control**”, *IEEE Energy Conference*, 2010.

[167] U. Boke, "**A simple model of photovoltaic module electric characteristics",** *Power Electronics and Applications, 2007 European Conference on* , vol., no., pp.1-8, 2-5 Sept. 2007.

[168] L. Xiao and A. Hassibi, “**Control with Random Communication Delays via a Discrete-Time Jump System Approach”,** *Proceedings of the American Control Conference*, Chicago, June 2000**.**

[169] D. Hristu-Varsakelis and W. Levine,**" Handbook of Networked and Embedded Control Systems",** *Dimitrios Hristu-Varsakelis, William S. Levine, editors,* Boston, 2005.

[170] Y. Shi and B. Yu," **Output Feedback Stabilization of Networked Control Systems with Random Delays Modelled by Markov Chains",** *IEEE Transactions on Automatic Control,* VOL. 54, NO. 7, JULY 2009.

[171] W. Al-Azzawi, M. Al-Akaidi," **SIMULATION METHODS FOR DELAYS AND PACKET DROPOUT AVOIDANCE IN SOLAR-POWER WIRELESS NETWORKS",** *Proceeding 11th MESM Conference, Amman, Jordon,* November 14-16, 2011.

[172] W. Al-Azzawi and M. Al-Akaidi," **Solar-Powered Wireless Network Control System Based on "TRUE-TIME" Simulator",** *Proceeding of 11th Salford Postgraduate Annual Research Conference,* University of Salford, UK, 8 and 9 June 2011

[173] H. Ding," **Robust Constrained Model Predictive Control by Linear Matrix Inequalities"**, *Final Report, St. Petersburg,* 2008.

[174] L. Zhilin; Z. Jun; Pei Run, "**Robust model predictive control of time-delay systems",** *Control Applications, 2003. CCA2003. Proceedings of 2003 IEEE Conference on,* vol.1, no., pp. 470- 473 vol.1, 23-25 June 2003.

[175] J. van den Boom and A. Stoorvogel, "**Model Predictive Control",** *DISC Course, Lecture Notes,* January 16, 2010.

[176] W. Al-Azzawi, M. Al-Akaidi," **Robust Model Predictive Controller for Solar Wireless Network Control System",** Journal of Intelligent Learning Systems and Applications (JILSA), 23 April 2012.paper under review.

[177] M. Corless, "**Introduction to Dynamic Systems",** *Network Mathematics Graduate Programmed, School of Aeronautics & Astronautics,* Purdue University, West Lafayette, Indiana, July 14, 2011.

[178] O. Costa; M. Fragoso; R. Marques, "**Discrete-Time Markov Jump Linear Systems",** *Springer-Verlage London Limited,* pages: 82-83, 2005.

[179] A. Goncalves; A. R. Fioravanti; M. Al-Radhawi; J. Geromel, " **H∞ State Feedback Control of Discrete-time Markov Jump Linear Systems through Linear Matrix Inequalities",** *Preprints of the 18th International Federation of Automatic Control (IFAC),* Milano (Italy) August 28 - September 2, 2011.

[180] J. Sheng; T. Chen; L. Shah, "**Optimal Filtering for Multi-rate Systems,"** *Circuits and Systems II: Express Briefs, IEEE Transactions on*, vol.52, no.4, pp. 228- 232, April 2005

[181] W. Al-Azzawi, M. Al-Akaidi, "**Robust Stability of Solar-Power Wireless Network Control System with Stochastic Time Delays Based on H_∞ Norm**", Taylor &Francis Group, International Journal of Systems Science, 13 March 2012.

[182] W. Al-Azzawi, M. Al-Akaidi," **Robust Stability of Solar-Power Wireless Network Control System with Stochastic Time Delays Based on H_2 Norm",** *Proceeding of 1st IET Wireless Sensor System Conference,* 18 - 19 June 2012 | RIBA, London, UK.

[183] http://www.doc.ic.ac.uk/~nd/surpise_96/journal/vol4/CS11/report.htm#theback-propagationalgorithm.

[184] W. Al-Azzawi, M. Al-Akaidi," **Solar Wireless Network System Based on Neural Network Predictive Control",** European Journal of Control, 3 May 2012.

Appendix A

ROBUST MODEL PREDICTIVE CONTROLLER

The system is linear-time invariant and demonstrated using the discrete-time state-space equation is

$$\boldsymbol{x(k+1) = Ax(k) + Bu(k) + w(k)} \text{………… } \textbf{(7-1)}$$

where w is unknown disturbance however limited, submitting

$$\forall \boldsymbol{k w(k)} \in \boldsymbol{W}$$

The target is to fulfil output constraints

$$\boldsymbol{y(k) = Cx(k) + Du(k)} \text{………… } \textbf{(7-2)}$$

$$\boldsymbol{y(k)} \in \boldsymbol{Y}$$

Though reducing the performance index

$$\boldsymbol{J = \sum_{k=0}^{\infty} l(u(k), x(k))} \text{………… } \textbf{(7-3)}$$

where *l*(·) is certain phase performance index. C and D are matrices with suitable dimensions, the set *Y* and the function *l*(·) are altogether selected through the user as portion of the job instruction.

Currently describe *P(x(k),Y,W)*, the (MPC) optimization preliminary from state *x(k)* with output constraint *Y* and unknown (bounded)disturbance *W*.

$$\boldsymbol{J^{*}(x(k), Y, W) = min_{u,x,y} \sum_{j=0}^{N} l\big(u(k+j|k), x(k+j|k)\big)} \qquad \forall \boldsymbol{j} \in \{\boldsymbol{0, 1, 2, \dots\dots, N}\} \text{………… } \textbf{(7-4)}$$

$$x(\boldsymbol{k+j+1|k}) = \boldsymbol{Ax(k+j|k) + Bu(k+j|k)} \text{………… } \textbf{(7-5)}$$

$$\boldsymbol{y(k+j|k) = Cx(k+j|k) + Du(k+j|k)} \text{………… } \textbf{(7-6)}$$

$$\boldsymbol{x(k|k) = x(k)} \text{………… } \textbf{(7-7)}$$

$$\boldsymbol{x(k+N+1|k)} \in \boldsymbol{X_F} \text{………… } \textbf{(7-8)}$$

$$\boldsymbol{y(k+j|k)} \in \boldsymbol{Y(j)} \text{………… } \textbf{(7-9)}$$

where the output and disturbance constraints for the strategy *Y(j)* are tautened for robustness utilizing the subsequent assumption

- $\boldsymbol{j} \in \{\boldsymbol{0, 1, 2, \dots\dots, N}\}$
- $\boldsymbol{Y(0) = Y}$
- $\boldsymbol{Y(j+1) = Y(j) \sim \big(C + Dk(j)\big) L(j) W}$
- $\boldsymbol{L(0) = I}$
- $\boldsymbol{L(j+1) = \big(A + Bk(j)\big) L(j)}$

The state feedback controller that stabilizes the system is

$$\boldsymbol{u(j) = K(j) x(j)}$$

The operator " $\sim$" means the Pontryagin alteration characterize as

$$\boldsymbol{A}\sim\boldsymbol{B}=\{(\boldsymbol{a}|\boldsymbol{a}+\boldsymbol{b}\in\boldsymbol{A}\ \forall\boldsymbol{b}\in\boldsymbol{B})\}$$

The concluding constraint condition is specified through

$$\boldsymbol{X_F}=\boldsymbol{\mathcal{R}}\sim\boldsymbol{L}(\boldsymbol{N})\boldsymbol{W}$$

where $\mathfrak{R}$ is a robust control constant acceptable condition namely there is a control law $k(x)$comforting the subsequent

- $\boldsymbol{Ax}+\boldsymbol{BK}(\boldsymbol{x})+\boldsymbol{L}(\boldsymbol{N})\boldsymbol{w}\ \in\boldsymbol{\mathfrak{R}}\ \ \boldsymbol{x}\in\boldsymbol{\mathfrak{R}},\quad \boldsymbol{w}\in\boldsymbol{W}$
- $\boldsymbol{Cx}+\boldsymbol{DK}(\boldsymbol{x})\ \in\boldsymbol{Y}(\boldsymbol{N})$

Appendix B

WI-FI/WIMAX PYSICAL LAYER PARAMETERS

The physical layer parameters simulation identification for WI-FI

- The data rate selected from (1, 2, 5.5, or 11) Mpbs.
- Packet size (1024)bytes
- Employ small introduction selection for (2, 5.5, or 11) Mpbs.
- Channels type (none, or Additive White Gaussian Noise (AWGN)
- Channels number from (1-11).
- Channel noise power for (AWGN) selection.

The physical layer parameters simulation identification for WIMAX

- Spectrum (10-66) GH_z.
- Data rate (32-134) Mpbs.
- Cannel band-width (20, 25, and 28) MH_z
- Modulation (2-PAM, 4-QAM, 16-QAM, and 64-QAM).

Appendix C

A MARKOVIAN CHAIN

Markov process that precedes values in a finite set with transition probabilities is

$$\boldsymbol{P((r_{k+1} = j|r_{k=i}) = q_{ij}}$$

The transition probabilities $\boldsymbol{q_{ij}}$, achieve, $\boldsymbol{q_{ij}} \geq \boldsymbol{0}$ for every $\boldsymbol{i, j} \in \boldsymbol{S}$ and

$$\sum_{\boldsymbol{j=1}}^{\boldsymbol{S}} \boldsymbol{q_{ij} = 1}$$

Present the Markov state probability distribution

$$\boldsymbol{\pi(k) = [\pi_1(k)\ \ \pi_2(k)\ \ \ldots\ldots\ldots\pi_s(k)]}$$

Where $\pi_i(k)$ is the possibility that the Markov chain state at time k is i. The possibility distribution for r_k is given by

$$\boldsymbol{\pi(k+1) = \pi(k)Q}$$

$$\boldsymbol{\pi(0) = \pi^0}$$

Where, $\boldsymbol{\pi^0}$ is the distribution for r_0.

A Markov chain is assumed to be governed if the transition matrix Q is an original matrix. An original matrix achieves $Q^k \gg 0$ for a positive integer $k, A \gg B$ means that the matrix elements fulfil $a_{ij} > b_{ij}$. That a Markov chain is governed resources that completely states will be executable to achieve in the future. If a Markov chain is original the fixed probability distribution $\pi^\infty = \lim_{k\to\infty} \pi(k)$ is given exclusively by

$$\boldsymbol{\pi^\infty = \pi^\infty Q}$$

Where, π^∞ is a probability distribution

Appendix D

Linear Matrix Inequality (LMI) Problem

LMI control toolbox that was developed by MATLAB provides modern tools for LMI based analysis and design of control systems. Furthermore, it offers a flexible and accessible to specify and solve general LMI problems.

Given an LMI$\boldsymbol{F}(\boldsymbol{x}) > 0$**,** the LMI problems is to find $\boldsymbol{x}$ **feasible** such that $\boldsymbol{F}(\boldsymbol{xfeasible}) > 0$ or determine that the LMI is infeasible.

As an example, consider the simultaneous Lyapunov stability problem. We are given $A_i \in \Re^{nxm}, i = 1, \dots, r,$ and need to find P satisfying the LMI:

$$\boldsymbol{P} > 0, \boldsymbol{A_i^T P} + \boldsymbol{PA_i} < 0, \quad i = 1, \dots, r \dots \dots \dots (D-1)$$

Or determine that no such P exists [22-24].

Appendix E

The Schur Complement

The Schur Complement is standard in LMI framework. The basic idea is as follows:

$$\begin{bmatrix} \boldsymbol{Q(x)_i} & \boldsymbol{e(x)_i} \\ \boldsymbol{e(x)_i^T} & \boldsymbol{X(x)_i} \end{bmatrix} > 0 \ldots\ldots\ldots (\boldsymbol{E-1})$$

Where, $Q(x)_i$, $e(x)_i$, and $X(x)_i$ are symmetric matrices depend on x, is equivalent to

$$\boldsymbol{e(x)_i} > 0\boldsymbol{,}\ \boldsymbol{Q(x)_i} - \boldsymbol{e(x)_i X(x)_i^{-1} e(x)_i^T} > 0 \ldots\ldots\ldots (\boldsymbol{E-2})$$

In the other words, the set of nonlinear inequalities (E-2) can be represented as the LMI (E-1).

Notation and Symboles

$(.)^{-1}$	**Matrix Inverse**
$(.)^{T}$	**Matrix Transpose**
$tr(.)$	**Matrix Trance**
$H_{\infty}(.)$	**Maximum Singular Value of matrix**
$\underline{H_{\infty}}(.)$	**Minimum Singular Value of matrix**
$\mathfrak{R}^{n}$	**The n-Dimensional Eucliden Space**
$\in$	**Belong to**
$\doteq$	**Defined as**
$\approx$	**Approximate to**
$\equiv$	**Equivalent to**
$\|\ldots.\|$	**Norm of the element**
$\|\ldots.$	**Restriction of function**
$diag\{\ldots.\}$	**Block-Diagonal matrix**
$\|.\|_{2}$	**Eucliden norm for vector induced 2-norm for matrices**
$E(.)$	**Mathematical expectation operator**